OPTIMUM DESIGN OF SOFC BASED POLYGENERATION SYSTEM FOR RESIDENTIAL AREA WITH VEHICLE CHARGING OR FUELING STATION

FARAH RAMADHANI

FACULTY OF ENGINEERING
UNIVERSITY OF MALAYA
KUALA LUMPUR

2019

OPTIMUM DESIGN OF SOFC BASED POLYGENERATION SYSTEM FOR RESIDENTIAL AREA WITH VEHICLE CHARGING OR FUELING STATION

FARAH RAMADHANI

THESIS SUBMITTED IN FULFILMENT OF THE REQUIREMENTS FOR THE DEGREE OF DOCTOR OF PHILOSOPHY

FACULTY OF ENGINEERING
UNIVERSITY OF MALAYA
KUALA LUMPUR

2019

UNIVERSITY OF MALAYA

ORIGINAL LITERARY WORK DECLARATION

Name of Candidate: FARAH RAMADHANI

Matric No: KHA150093

Name of Degree: Doctor of Philosophy (PhD)

Title of Thesis: Optimum design of SOFC based polygeneration system for residential area with vehicle charging or fueling station

Field of Study: Process System Engineering & Control

I do solemnly and sincerely declare that:

(1) I am the sole author/writer of this Work;
(2) This Work is original;
(3) Any use of any work in which copyright exists was done by way of fair dealing and for permitted purposes and any excerpt or extract from, or reference to or reproduction of any copyright work has been disclosed expressly and sufficiently and the title of the Work and its authorship have been acknowledged in this Work;
(4) I do not have any actual knowledge nor do I ought reasonably to know that the making of this work constitutes an infringement of any copyright work;
(5) I hereby assign all and every rights in the copyright to this Work to the University of Malaya ("UM"), who henceforth shall be owner of the copyright in this Work and that any reproduction or use in any form or by any means whatsoever is prohibited without the written consent of UM having been first had and obtained;
(6) I am fully aware that if in the course of making this Work I have infringed any copyright whether intentionally or otherwise, I may be subject to legal action or any other action as may be determined by UM.

Candidate's Signature Date:

Subscribed and solemnly declared before,

Witness's Signature Date:

Name:

Designation:

UNIVERSITI MALAYA
PERAKUAN KEASLIAN PENULISAN

Nama: FARAH RAMADHANI

No. Matrik: KHA150093

Nama Ijazah: Doktoral

Title of Thesis: Reka bentuk terbaik sistem polipenjanaan menggunakan SOFC untuk kawasan kediaman dengan stesen pengecasan atau pengisian bahan bakar kendaraan

Bidang Penyelidikan: Kejuruteraan proses sistem dan kawalan

Saya dengan sesungguhnya dan sebenarnya mengaku bahawa:

(1) Saya adalah satu-satunya pengarang/penulis Hasil Kerja ini;
(2) Hasil Kerja ini adalah asli;
(3) Apa-apa penggunaan mana-mana hasil kerja yang mengandungi hakcipta telah dilakukan secara urusan yang wajar dan bagi maksud yang dibenarkan dan apa-apa petikan, ekstrak, rujukan atau pengeluaran semula daripada atau kepada mana-mana hasil kerja yang mengandungi hakcipta telah dinyatakan dengan sejelasnya dan secukupnya dan satu pengiktirafan tajuk hasil kerja tersebut dan pengarang/penulisnya telah dilakukan di dalam Hasil Kerja ini;
(4) Saya tidak mempunyai apa-apa pengetahuan sebenar atau patut semunasabahnya tahu bahawa penghasilan Hasil Kerja ini melanggar suatu hakcipta hasil kerja yang lain;
(5) Saya dengan ini menyerahkan kesemua dan tiap-tiap hak yang terkandung di dalam hakcipta Hasil Kerja ini kepada Universiti Malaya ("UM") yang seterusnya mula dari sekarang adalah tuan punya kepada hakcipta di dalam Hasil Kerja ini dan apa-apa pengeluaran semula atau penggunaan dalam apa jua bentuk atau dengan apa juga cara sekalipun adalah dilarang tanpa terlebih dahulu mendapat kebenaran bertulis dari UM;
(6) Saya sedar sepenuhnya sekiranya dalam masa penghasilan Hasil Kerja ini saya telah melanggar suatu hakcipta hasil kerja yang lain sama ada dengan niat atau sebaliknya, saya boleh dikenakan tindakan undang-undang atau apa-apa tindakan lain sebagaimana yang diputuskan oleh UM.

Tandatangan Calon Tarikh:

Diperbuat dan sesungguhnya diakui di hadapan,

Tandatangan Saksi Tarikh:

Nama:

Jawatan

OPTIMUM DESIGN OF SOFC BASED POLYGENERATION SYSTEM FOR RESIDENTIAL AREA WITH VEHICLE CHARGING OR FUELING STATION

ABSTRACT

The residential sector is one of the energy consumers in the world generally, and in Malaysia, especially. Integrated energy supply which can simultaneously generate multi-energy types for fulfilling the demand of residential and vehicle users called polygeneration system is promising as the future and modern energy supply design. This study proposes a modern energy supply design for the residential area with considering stationary power and vehicle applications. The proposed system can generate electricity, hot water, and cooling system for the building. The system also provides power and hydrogen supplied to vehicle charging or fueling station in the private area. The polygeneration employs solid oxide fuel cell as a prime mover for heat and power generation. This study optimizes the design of polygeneration through four steps to overcome the deficiency in the system, increasing energy savings, cost savings and minimizing carbon emission generated from the system. The first step, four configurations of the proposed design based on grid connection and type of vehicle to be served was evaluated. Next, the reliability of polygeneration system was improved by adding renewable energy, a thermoelectric device, and energy storage to increase the efficiency of the system. The third step was to design the optimum operating strategy to increase the reliability and primary energy saving reduce the energy cost and carbon emission. The last step was to develop the optimum size for the system component by using evolutionary and swarm based optimization algorithm. The results in the first step revealed the advantages of the SOFC based polygeneration system over the conventional separated system with several improvements in energy saving, energy cost savings and carbon emission of about 36%, 50% and 33%, respectively. Amongst four configurations studied in the first step, the standalone polygeneration with electric vehicle becomes the optimum configuration chosen as it has high energy saving, energy cost saving, and a good emission reduction. This study also proved the effect of the hydrogen selling strategy in decreasing the energy cost of the polygeneration system by about 51% and improves the system to be more economically competitive against the conventional separated system. The results of the second step of this study confirmed that the polygeneration with added extra heat recovery system achieves the gains of reliability, efficiency, and energy saving by about 35.91%, 14.36%, and 11. 58%, respectively. The optimum operating strategy based on Fuzzy operation gives significant improvements on the efficiency, energy saving, and cost saving by about 4%, 112%, and 33% respectively compared to the conventional polygeneration. The optimal polygeneration capacity using genetic algorithm achieves improvements in primary energy saving, cost saving and carbon reduction by up to 65.1%, 42.4% and 62.6% respectively. It also confirms the stability of the optimizing process by running the optimization cycles in several times and attaining the deviation by about 2%.

Keywords: Solid oxide fuel cell, polygeneration, electric vehicle, hydrogen vehicle, residential application

REKA BENTUK TERBAIK SISTEM POLIPENJANAAN MENGGUNAKAN SOFC UNTUK KAWASAN KEDIAMAN DENGAN STESEN PENGECASAN ATAU PENGISIAN BAHAN BAKAR KENDARAAN

ABSTRAK

Sektor kediaman merupakan salah satu pengguna tenaga terbesar secara amnya di dunia dan terutamanya di Malaysia. Bekalan tenaga bersepadu yang boleh menghasilkan pelbagai jenis tenaga secara serentak untuk memenuhi permintaan pengguna kediaman dan kenderaan yang dipanggil sistem polipenjanaan adalah menjanjikan untuk masa depan dan reka bentuk bekalan tenaga moden. Kajian ini mencadangkan satu reka bentuk bekalan tenaga moden untuk kawasan kediaman dengan menimbangkan aplikasi pegun dan kenderaan. Sistem yang dicadangkan ini boleh menghasilkan sistem elektrik, air panas dan penyejukan untuk bangunan. Sistem ini juga boleh menyediakan kuasa dan hidrogen bekalan untuk stesen pengecasan kenderaan atau stesen minyak di kawasan swasta. Sistem polipenjanaan menggunakan sel bahan bakar oksida pepejal (SOFC) sebagai penggerak utama untuk penjanaan haba dan kuasa. Kajian ini mengoptimumkan reka bentuk sistem polipenjanaan melalui empat langkah untuk mengatasi kekurangan dalam sistem tersebut, meningkatkan penjimatan tenaga, kos tenaga dan mengurangkan pelepasan karbon yang dihasilkan dari sistem tersebut. Pertama, konfigurasi reka bentuk yang dicadangkan telah dinilai berdasarkan sambungan grid dan jenis kenderaan yang akan disampaikan. Seterusnya, kebolehpercayaan sistem polipenjanaan telah ditambahbaik dengan menanbah tenaga yang boleh diperbaharui, peranti thermoelektrik dan penyimpanan tenaga untuk meningkatkan sistem kecekapan. Fasa ketiga adalah untuk mereka strategi operasi yang optimum untuk mengurangkan penggunaan tenaga utama dan juga kos tenaga dan pelepasan karbon. Langkah terakhir adalah untuk menghasilkan saiz optimum untuk komponen sistem dengan menggunakan algoritma pengoptimuman berasaskan evolusi dan kawanan. Hasil penyelidikan dalam fasa pertama menunjukkan kelebihan sistem polipenjanaan berasaskan SOFC berbanding dengan sistem berpisahan konvensional dengan beberapa penambahbaikan dalam penjimatan tenaga, kos tenaga dan pelepasan karbon masing-masing sebanyak 36%, 50% dan 33%. Di antara empat konfigurasi yang dikaji dalam fasa pertama, polipenjanaan mandiri dengan kenderaan elektrik (EV) merupakan konfigurasi optimum yang dipilih kerana ia mempunyai penjimatan tenaga, kos tenaga yang tinggi dan pengurangan pelepasan yang baik. Kajian ini juga menunjukkan kesan strategi jualan hidrogen dalam mengurangkan kos tenaga sistem polipenjanaan sebanyak 51% dan menambahbaik sistem ekonomi untuk menjadi lebih berdaya saing dengan sistem berpisahan konvensional. Hasil kajian fasa kedua mengesahkan bahawa sistem polipenjanaan dengan sistem pemulihan haba tambahan boleh mencapai peningkatan kebolehpercayaan, kecekapan dan penjimantan tenaga sebanyak 35.91%, 14.36% and 11.58% masing-masing. Strategi operasi optimum berasaskan operasi Fuzzy memberikan peningkatan yang ketara dalam kecekapan, penjimatan tenaga dan kos sebanyak 4%, 112% dan 33% berbanding dengan sistem polipenjanaan yang tidak menggunakan Fuzzy sebagai strategi operasi. Kapasiti polipenjanaan yang optimum dengan menggunakan algoritma genetik mencapai penambahbaikan dalam penjimatan tenaga utama, kos dan pengurangan karbon sebanyak 65.1%, 42.4% dan 62.6% masing-masing. Ia juga mengesahkan kestabilan proses pengoptimuman dengan menjalankan beberapa kitaran pengoptimuman dan mencapai sisihan sebanyak kira-kira 2%.

Kata kunci: Sel bahan bakar oksida pepejal, polipenjanaan, kenderaan elektrik, kendaraan hidrogen, sektor kediaman

ACKNOWLEDGMENTS

This thesis is dedicated to my mother (Allahyarham) Hariati taher and my mother in-law Senidarwati, two great women who have inspired me to be a better woman, better mother and a better person.

My fullest praise and gratitude to Allah S.W.T. for the strength given to me to complete this thesis in my pursuit to fulfill the requirements for the Doctor of Philosophy. Firstly, I would express my sincere gratitude to my supervisor Prof. Ir. Dr. Mohammad Azlan Hussain and Prof. Ir. Dr. Hazlie Mokhlis for their valuable guidance, scholarly input, and consistent encouragement throughout my Ph.D. journey. Without their precious support it would not be possible for me to conduct this research. They always give me valuable suggestions, cheer me up and remind me not to waste my time and lower my quality to be a better student and researcher personally. I consider it as a great opportunity to conduct my doctorate program under their guidance and learn from their research expertise.

I am grateful to my college mate, my brothers and sisters in faith who are in companions with me through this Ph.D. journey. My special thanks to my precious family, my late mother and late father (may Allah bless them), my mother and father-in-law, my siblings and brother/sister-in-law for their support and sacrifices they all have made on my behalf. The last but not least, lovely thanks to my husband Oon Erixno and our baby boy for his companion throughout four years our marriage and three years my Ph.D. life. You are always being a friend in happiness, sadness, stressfulness, my senior, my college mate, and a person I want to rest my life with. I never forget the times when we were arguing something scientifically and laughing happily after all.

TABLE OF CONTENTS

LIST OF FIGURES

LIST OF TABLES

LIST OF SYMBOLS AND ABBREVIATIONS

á	:	Ohmic resistant constant
αg	:	Emission factor of the grid (gCO_2/kWh)
α		Seebeck coefficient (V/K)
a_1	:	Faraday efficiency parameter (mA/cm)
a_2	:	Faraday efficiency parameter (–)
A_{cell}	:	Cell area (m^2)
A_{col}	:	Wide area of the collector (m^2)
A_{pl}	:	The heating surface area (m^2)
A_{el}	:	Element cross-sectional area (m^2)
$\bar{C}_{pH2}$	:	The hydrogen gas average constant-pressure specific heat (J/mol.K)
$\bar{C}_{pO2}$	:	The oxygen gas average constant-pressure specific heat (J/mol.K)
$\bar{C}_{pN2}$	:	The nitrogen gas average constant-pressure specific heat (J/mol.K)
$\bar{C}_{pH2O}$	:	The water vapor average constant-pressure specific heat (J/mol.K)
C_{pi}	:	The ith gas average constant-pressure specific heat
C_{xw}	:	Specific heat of strong solution
C_{xs}	:	Specific heat of weak solution
COP_c	:	Coefficient of performance of the absorption chiller
C_s	:	Overall cost per unit component of the polygeneration
C_{inv}	:	Investment cost ($)
C_{om}	:	Operation and maintenance costs ($)
C_{init}	:	Initial cost ($)
COE	:	Cost of the energy

COE_{ref}	:	Cost of the energy of the reference system (CSS)
$CO_{2_{PS\_HV}}$	:	Carbon emission of the polygeneration with hydrogen vehicle power supply
$CO_{2_{PS\_EV}}$	:	Carbon emission of the polygeneration with electric vehicle power supply
CO_{2_ref}	:	Carbon emission of the reference system (CSS)
CS_S	:	Cost saving of the polygeneration system
c1	:	Cognitive learning of PSO
c2	:	Social learning of PSO
d_1	:	Temperature dependence of the saturation diode current
d_2	:	Temperature dependence of the ideal current source
d_3	:	Temperature dependence of the current loss
E_{cl}	:	Cell potential voltage (V)
$E_{0,cl}$	:	The reference potential of the cell
E_g	:	Band gap energy (W)
E_{H2}	:	Energy of hydrogen
E_{SOFC}	:	Electric energy generated by the SOFC
$E_{add,g}$	:	Electric energy imported from the grid
F	:	Faraday constant, 96,485 C/mol
fit	:	Fitness value of solution
F_{car}	:	Fuel consumption of the car
F_{SOFC}	:	Fuel consumption of the SOFC
F'	:	Collector efficiency factor
$gbest$	:	Global best particle in the iterations
H_{hw}	:	Heat generated by the heat exchager
H_{ac}	:	Heat generated by the absorption chiller
H_{H2}	:	Hydrogen energy generated by the electrolyzer

H_{st}	:	Heat stored in the hot storage tank
H_{ex}	:	The exhaust heat energy from the polygeneration system
$h_{x,std}$	:	The xth gas per mole at the standard pressure and temperature
h_x	:	The xth gas per mole enthalpy
H_l	:	Enthalpy of liquid water
h_{ex}	:	Heat transfer coefficient between the exhaust gas and the TEG modules
H_v	:	Enthalpy of water vapors
H_s	:	Enthalpy of strong solution
H_m	:	Enthalpy of medium solution
H_{wv}	:	Enthalpy of water vapour
H_{LHV}	:	The low heating value of hydrogen (kJ/mole)
H_2	:	Hydrogen
H_2O	:	Water
h_w	:	Heat transfer between the TEG modules and the water (W/m^{2}K)
i_{dens}	:	Electric current density (A/m^2)
i_{EL}	:	Eelectrolyzer current (A)
I_{fc}	:	Fuel cell current (A)
I_{ph}	:	Ideal current source (A)
I_d	:	Depletion zone in the single diode current (A)
I_{sh}	:	Current losses (A)
I_{TEG}	:	TEG current (A)
I_0	:	Current limit (A)
K	:	Thermal conductance (W/K)
K	:	Molar valve constant
K_B	:	Boltzmann-constant

K_{O_2}	:	Molar valve constant of oxygen
K_r	:	Molar vale constant of the fuel
$LPSP_e$	:	Loss of power supply probability of the electric generation
$LPSP_H$	:	Loss of power supply probability of the heat generation
$LPSP_c$	:	Loss of power supply probability of the cooling generation
$LPSP_{H2}$	:	Loss of power supply probability of the hydrogen generation
$LPSP_{poly,EV}$	:	Loss of power supply probability of the polygeneration with EV supply
$LPSP_{poly,HV}$	:	Loss of power supply probability of the polygeneration with HV supply
$m_s C_{ps}$	:	Stack solid mass-specific product (J/K)
m_{hex}	:	Mass fluid flowrate at the heat exchanger (kg/s)
M_{H2_Stored}	:	Hydrogen stored in the hydrogen storage tank
m_r	:	Refrigerant flowrate
m_s	:	Strong solution flowrate
m_w	:	Weak solution flowrate
m_m	:	Medium solution flowrate
N_{cell}	:	Number of cells
$N_{H_2O}^{in}$	:	Mole flowrate of water vapor enter the channel
$N_{O_2}^{in}$	:	Mole flowrate of oxygen gas enter the channel
$N_{H_2}^{in}$	:	Mole flowrate of hydrogen gas enter the channel
N_P	:	The parallel number of PVT panel
N_S	:	The series number of PVT panel
O_2	:	Oxygen
P	:	Power generated by the SOFC (W)
pbest	:	Best particle in a swarm
PEC_{ref}	:	Primary energy consumption of the reference system (CSS)

$PEC_{poly,bl}$	:	Primary energy consumption of the polygeneration with EV supply
$PEC_{poly,se}$	:	Primary energy consumption of the polygeneration with HV supply
P_{el}	:	Electrical power generated by the PVT (W)
$P_{el,d}$	:	Electric demand
$P_{H_2}^{ch}$	:	The partial pressure of the hydrogen
$P_{H_2O}^{ch}$	:	The partial pressure of the water vapors
$P_{O_2}^{ch}$	:	The partial pressure of the oxygen
PES_{sys}	:	Primary energy saving of the polygeneration system
P_{th}	:	Thermal generation of PVT
P_x	:	Partial pressure of specific x gases
q_x^{in}	:	Mole flowrate input (mol/s)
q_x^{r}	:	Mole flowrate reacted (mol/s)
Q_{HEX}	:	Heat generated in the heat exchanger
Q_c	:	Heat power generated in the condenser (W)
Q_{HG}	:	Heat power generated in the high-pressure generator (W)
Q_{LG}	:	Heat power generated in the low-pressure generator (W)
Q_A	:	Heat power generated in the absorber (W)
Q_E	:	Heat power generated in the evaporator (W)
$Q_{hw,d}$	:	Heat demand
Q_c	:	Cooling demand
Q_{in}	:	Heat power at the input TEG
r_s	:	Series resistance of the PVT panel
R	:	Universe gas constant (J/mol.K)
R_{TEG}	:	TEG resistance (Ω)
R_L	:	Load resistance (Ω)

SOC_{bat}	:	State of charge of the battery
t_{lg}	:	Low-pressure generator temperature (K)
t_{hg}	:	High-pressure generator temperature (K)
t_c	:	Condenser temperature (K)
t_e	:	Evaporator temperature (K)
t_a	:	Absorber temperature (K)
$t_{in,hex}$	:	Temperature of input at the heat exchanger (K)
$t_{in,lg}$	:	Temperature of input at the low-pressure generator (K)
$t_{in,a}$	:	Temperature of input at the absorber (K)
T	:	Temperature (K)
T_c^j	:	The junction temperature (K)
T_{cj}	:	TEG low side temperature (K)
T_{hj}	:	TEG high side temperature (K)
T_h	:	High site temperature (K)
T_c	:	Water temperature at the low side (K)
T_{EL}	:	Electrolyzer temperature (K)
T_{in}	:	Input temperature (K)
T_{fc}	:	Fuel cell temperature (K)
$T_{in,TES}$	:	Input temperature of the thermal energy storage
$T_{out,TES}$	:	Output temperature of the thermal energy storage
U_L	:	Overall convective heat loss of PVT collector
V_a	:	Anode volume
V_{cl}	:	Cell voltage (V)
V_{act}	:	Activation voltage (V)
V_C	:	Cell voltage (V)

V_T	:	Thermal potential of PVT (V)
V_{cell}	:	Cell voltage (V)
V_{ref}	:	Voltage at the reference condition (V)
V_{ohm}	:	Ohmic voltage (V)
V_{con}	:	Concentration voltage (V)
W	:	Unit energy generated by the polygeneration components
$W_{h2,elect}$	:	Hydrogen generated from the electrolyzer
$W_{h2,d}$	:	Hydrogen imported from the retail
W_p	:	Compressor power consumption (W)
X_A	:	Absorber concentration
X_{HG}	:	High-temperature generator solution
X_{LG}	:	Low-temperature generator solution
n_{H_2}	:	Total hydrogen production
η_b	:	Efficiency of the auxiliary boiler
η_f	:	Faraday efficiency
η_p	:	Compressor efficiency
η_{poly}	:	Polygeneration efficiency
η_g	:	Grid efficiency
η_{loss}	:	Energy loss from the thermal energy storage
β	:	Emission factor of the natural gas (gCO_2/kWh)
γ	:	Emission factor of conventional car (gCO_2/Kg_g)
λ	:	Thermal conductivity (W/mK)
ρ	:	Resistivity ($\mu\Omega m$)
μ_{el}	:	Fuzzy membership of electric load
μ_{evl}	:	Fuzzy membership of electric vehicle load

μ_{hvl}	:	Fuzzy membership of hydrogen vehicle load
μ_{socb}	:	Fuzzy membership of state of charge from the battery
μ_{cl}	:	Fuzzy membership of cooling load
μ_{pvt}	:	Fuzzy membership of photovoltaic thermal power
AFC	:	Alkaline fuel cell
AFR	:	Air to fuel ratio
ACO	:	Ant colony optimization
AGM	:	Absorbed glass mat
AHP	:	Analytic hierarchy process
AI	:	Artificial intelligence
ANN	:	Adaptive neural network
APU	:	Auxiliary power unit
ATCR	:	Annual total cost reduction
BES	:	Battery energy storage
BOP	:	Balance of plant
CC	:	Combustion chamber
CCHP	:	Combined cooling, heating and power
CER	:	Carbon dioxide emission reduction
CDE	:	Carbon dioxide emission
CHP	:	Combined heat and power
CI	:	Consistency index
COP	:	Coefficient of performance
CRF	:	Capital recovery factor
CS	:	Cost saving
CSS	:	Conventional separated system
DO	:	Design optimization

DOE	:	Department of Energy
DMFC	:	Direct methanol fuel cell
EDM	:	Electric demand management
EUF	:	Energy utilization factor
EV	:	Electric vehicle
FC	:	Fuel cell
FEL	:	Following electrical load
FEMS	:	Fuzzy energy management system
FL	:	Fuzzy logic
FTL	:	Following thermal load
FU	:	Fuel utilization
GA	:	Genetic algorithm
GHG	:	Greenhouse gas
GSHP	:	Ground source heat pump
GOM	:	Gross operation margin
GT	:	Gas turbine
HEV	:	Hybrid electric vehicle
HES	:	Hydrogen-based energy storage
HRES	:	Hybrid renewable energy system
HT	:	High temperature
HV	:	Hydrogen vehicle
HVAC	:	Heating, ventilation and air conditioning system
ICE	:	Internal combustion engine
IEMS	:	Intelligent energy management system
LA	:	Lead-Acid
LPSP	:	Loss probability of power supply

LT	:	Low temperature
MCFC	:	Molten carbonate
MD	:	Minimum distance
MP	:	Matching performance
MILP	:	Mixed-integer linear programming
MIDF	:	Malaysian industrial development finance
MIMO	:	Multi-input and multi-output
MISO	:	Multi-input and single output
MINLP	:	Mixed-integer non-linear programming
MOGA	:	Multi-objective genetic algorithm method
NEDO	:	New energy and industrial technology development organization
NRE	:	Non-renewable energy
NRPE	:	Non-renewable primary energy
NTRL	:	National Energy Technology Laboratory
NSGA II	:	Non-dominated solution genetic algorithm
OO	:	Operating optimization
ORC	:	Organic Rankine cycle
PAFC	:	Phosphoric acid fuel cell
PEC	:	Primary energy consumption
PES	:	Primary energy saving
PEMFC	:	Proton exchange membrane fuel cell
PGU	:	Power generation unit
PSO	:	Particle swarm optimization
PVT	:	Photovoltaic thermal
SA	:	Simulate annealing
SE	:	Stirling engine

SHS	:	Sensible heat storage
SO	:	Size optimization
SOFC	:	Solid oxide fuel cell
SOEC	:	Solid oxide electrolyzer cell
SP	:	Separated system
ST	:	Steam turbine
TEG	:	Thermoelectric generator
VRLA	:	Valve regulated lead acid
TDM	:	Thermal demand management
TS	:	Taboo search
TNB	:	Malaysian government Nasional Electricity Board
ZEBRA	:	Zeolite Battery Research Africa

LIST OF APPENDICES

CHAPTER 1: INTRODUCTION

1.1 Overview

Globally, the necessity of energy has been rapidly increasing from year to year and the growth of energy supply cannot equilibrate the demand requirements due to these increasing needs. For the last decades, conventional energy types such as fossil fuel and coal have become a tremendous energy source that has been consumed for electricity generation, heat, and cooling applications. However, these types of energy have caused several issues such as energy depletion, high energy cost and high air pollution in all applications related to public facility, industrial, residential and transportation.

As one of the energy consumers, most of residential applications have been adopting the conventional design for energy supply. The design utilized conventional energy sources to generate electricity and to fuel in heating, cooling, and vehicles components. The overwhelming consumption of this type of energy leads to spike of energy price, environmental pollution and creates frictions amongst some countries. Furthermore, the issue of climate changes that harms the environment must be considered seriously by improving the energy supply design into a modern, efficient and environmentally friendly form.

In Malaysia, the residential sector faces excessive electricity consumption issue from year to year. This sector consumed 14,365 GWh in 2006 or about 19% of the entire electricity consumption in Peninsular Malaysia (Saidur et al., 2006). The increase in energy consumption also occurred in ten years later based on the latest data from the Electricity Commission Board (Suruhanjaya Tenaga, 2016) which reported that the electricity usage from the residential sector has risen to 31,128 GWh or 21% of national energy consumption in 2016. The electricity and fuel are commonly consumed for five significant appliances such as cooking (45%), cooling (29%), lighting (8%), laundry and cleaning (7%) and others electronic devices (11%) (Kubota et al., 2011) for a typically terrace house.

Several modern technologies of energy supply such as integrated sources, multi-generations and smart grids concepts have been developed to cope with the massive energy loss occurring in the conventional energy generation. The designs come from the idea of integrating electricity and other energy types to improve the efficiency of the system. This integration between energy sources can generate two (cogeneration), three and more (trigeneration/polygeneration) energy types in a single operation. These systems are developed based on its necessity by preferences of users, the energy cost, and environmental matters and can achieve better performances in reducing primary energy consumption (PEC), system costs and air pollution issues.

For further development, integration of supply in the residential area should not focus on the stationary application only but also expanded to the automotive industries. The technology growth in the automotive sector explores the future of the transportation system, which is more efficient, technically advanced and environmentally friendly. Utilization of electric-based and hydrogen-based vehicles have been replacing conventional vehicles fueled by gasoline gradually. Development of those electrification vehicles has been promisingly growing since the last decade and on the commercialization stage to build fuel stations since 2015 (Eberle et al., 2012).

As one of advanced emerging energy sources, solid oxide fuel cells (SOFCs) have been implemented as the prime mover in energy generation system. Besides its high-quality of exhaust heat, SOFCs are flexible in regard to the hydroxide fuel and more resistant to Sulphur contents compared to the other fuel cell types (Akikur et al., 2015;

Tonekabonimoghadam et al., 2015). SOFC is categorized as purely renewable energy when it is fueled by pure hydrogen and half renewable energy when it is fed by natural gas. However, both are less harmful to the air compared to coals and fossil fuels. All these advantages make SOFC an ideal source as the prime mover in polygeneration systems.

Regarding this polygeneration system as a modern energy generation, this emerging concept needs a comprehensive design of the energy supply system. Further when integrating SOFC with other energy sources, these phases would maximize its design complexity. Moreover, since the energy requirement in the residential sector is increasing attractively, robust design of modern energy generation should be considered.

1.2 Problem statement

Polygeneration system is expected to be a promising technology of energy generation for public and private places such as in residential buildings. This system can enhance energy generation performance by producing more than one types of energy. Defining the prime mover and the auxiliary components can affect its overall efficiency, its design cost and environmental effects to the system. SOFC is an emerging prime mover technology for the polygeneration system which is more efficient, less noises, and environmentally friendly compared to combustion-based engines (Al Moussawi et al., 2016). Therefore, employing SOFC as the prime mover can enhance the overall efficiency of the polygeneration system and lessen the carbon emission effect to the environment.

Integrating SOFC to the polygeneration system means to deal with its high component cost and high-temperature operation. These issues can be handled by optimally designing the polygeneration system based on its optimum requirements. In the literature, design of the system based on the load requirement, climate changes of the area and the specific operation of the system revealed their superiority in energy planning (Facci & Ubertini, 2018; Rokni, 2018; Sigurjonsson & Clausen, 2018; Ullvius & Rokni, 2018). Modeling the system is the first step in optimally designing the polygeneration. The existing studies mostly used several module-based software types such as ANSYS (Calise et al., 2017d) and others applied mathematical-based modeling software such as MATLAB (Al Moussawi et al., 2017). Although several SOFC models have been developed for polygeneration systems, the formulation of the models was too specific. Those models were referred to the particular parameters, components and configurations used. To design the polygeneration system suitable for evaluation, management and optimization purposes, a simple yet comprehensive model should be considered to reduce the complexity of the system. The modeling process not only taking into account the prime mover but also the other components in the polygeneration system.

Furthermore, integrating the polygeneration system with vehicles power supply is a promising technology for residential applications, however there are only few studies focused on this design for management and optimization purposes. Several studies integrated cogeneration system with electric vehicle power supply in residential applications (Hiroaki, 2013; Tanaka et al., 2014; Vialetto et al., 2017; Wakui et al., 2012). Meanwhile, another study focused on the development of the polygeneration with hydrogen vehicle power supply (Fernandes et al., 2016). However, the energy generation used, system components, energy management and sizing attempts were designed for a particular case study and demand requirements. Moreover, all studies considered only either electric or hydrogen vehicles power supply that was integrated into the stationary system. Since different energy requirements, system components, and weather conditions were used in the existing studies, they presented different analyses on the optimal design and the evaluation results. Therefore, considering a specific study case, load profiles, climate changes and user behaviors in Malaysia, it is essential to evaluate the best configuration of the polygeneration design combined with vehicles power supply in the residential area considering vehicles supply and grid connection types.

Furthermore, high demands for heating and cooling in residential applications can reduce the reliability of the polygeneration system. Several existing studies tended to add an auxiliary boiler to the system to cope with this issue (Al Moussawi et al., 2017; Jing et al., 2017; Weber et al., 2006b; Zhao et al., 2015). However, utilizing a boiler leads to environmental issue due to carbon emission released by the fuel combustion process. Another approach is by generating power from renewable energy sources. Integrating a renewable energy source such as photovoltaic thermal to the polygeneration system has been proposed by Calise et al. (2017c). However, in a larger capacity, photovoltaic-thermal panels are initially costly. Therefore, an approach for combining the photovoltaic for recovering the heat production of the polygeneration system is needed to increase the efficiency and the reliability of the system.

Due to the high complexity of polygeneration components, designing an optimal system is challenging when considering its operation and component capacities. The existing studies are either considering optimal operating strategy or sizing the component based on the specific configuration design, criteria, weather condition, and energy requirements (Al Moussawi et al., 2017; Baghernejad et al., 2015; Hajabdollahi & Fu, 2017). Moreover, since more components considered in a polygeneration system, the complexity of the design increases. Therefore, a multi-objective, multi-parameter, and multi-level optimization mechanism is necessary to be proposed for this sophisticated design which generates a set of non-dominated solutions of the operating strategy and the component capacities. Therefore, conducting optimization for this system is vital as the final approach in designing an optimal polygeneration system.

Following the issues stated for the SOFC based polygeneration system, it is essential to design an optimal system to overcome the high investment cost of the components. Moreover, the proposed design is expected to have higher energy saving and more environmentally friendly compared to conventional separated system. In the end, the polygeneration system designed should overcome other issues such as energy loss and reduce its independence to the national grid. Therefore, the polygeneration system can be seen as an alternative power generation which can be developed not only for residential area in the capitol city but also in remote areas.

1.3 Objective

This thesis primarily aims to design an optimum polygeneration system employing SOFC as the prime mover. The design is evaluated through simulation studies and the following are its main objective satisfied during the course.

1. To develop a mathematical model of an SOFC based polygeneration system through zero-dimensional modeling.

2. To analyze different configurations of the SOFC based polygeneration system based on grid connectivity and vehicle types.

3. To maximize the reliability and energy saving of the SOFC based polygeneration system by combining heat recovery with photovoltaic and thermoelectric components.

4. To design an optimum operating strategy and size of polygeneration system based on the energy saving, cost saving, power loss and carbon emission of the system.

1.4 Research scope and contributions

The scope of this research is based on guard steps for energy supply design in the residential area. Firstly, four configurations of the SOFC based polygeneration system are studied based on the connection of grid and vehicle types. Next, the performance of the overall polygeneration system is improved by adding renewable energy sources and thermoelectric devices to maximize heat and electricity generations of the system.

Furthermore, an optimum operating strategy is developed using artificial intelligence method. Three fuzzy membership shapes based on demand profiles and sunlight irradiance are compared to optimize the operation strategy of the SOFC and the absorption chiller based on the demand requirements, photovoltaic power and battery condition. Lastly, optimal sizing the capacity of system components is conducted by using evolutionary-based and swarm-based optimization methods comparing their performances to overcome the energy, economic and environmental issues in the polygeneration system.

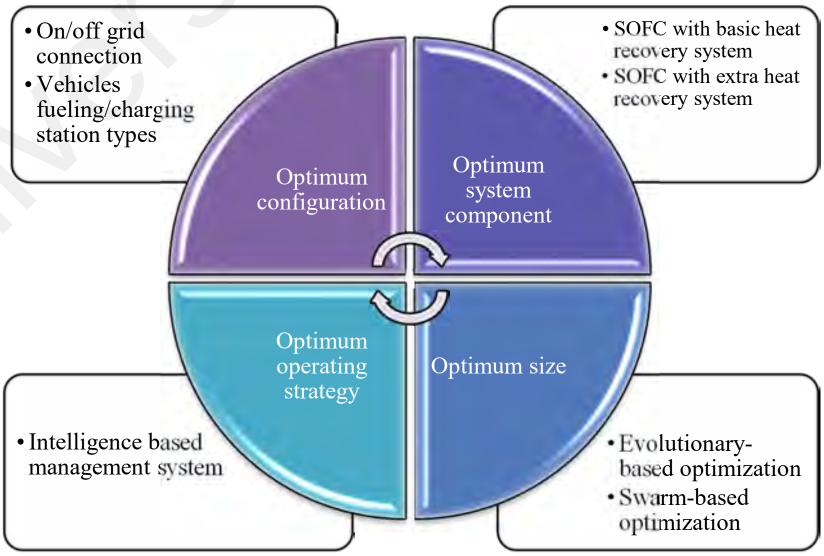

Figure 1.1: Research scope of this study

Moreover, this study has several contributions in gaining knowledges of energy generation system design especially for multi-purposes system such polygeneration. Analysis in the system integration between the polygeneration system and vehicles supply is also mentioned as a novel knowledge which is beneficial for future design of energy supply in residential applications. This integration has been researches only in the developed countries such as the UK, US, Japan and European countries. With taking into account Malaysia as the case study, this research is the first in this area which considers the climates, consumption profiles and house type in a tropical country. The comprehensive design resulted by this study could be favorable for the next developments and prototype stages before going to commercialization.

1.5 Thesis outline

The sequences for this study are explained as follows. Chapter 1 presents the introduction of this study which covers the background of this study, the problem statement, the objective of the research, the research scope and the outline of the thesis.

Chapter 2 provides the literature review of this study. This chapter discusses energy supply designs in residential applications. It also explains the current technologies in energy generation based on the number of energy types generated from the system. The overview of the polygeneration system and several applications of SOFC as the prime mover in power generation system are also provided. Furthermore, energy planning steps and optimization algorithm needed for the system are presented. Lastly, synthesis and analysis of the literature are summarized along with the summary of the chapter.

In Chapter 3, the methodology of this study is explained through four steps in energy planning for residential applications. The general working principal of the proposed SOFC based polygeneration system is presented. Residential load profiles including homes and vehicles energy consumptions are presented as the case study. Evaluation and optimization criteria are also explained through energy, economic and environmental aspects.

The development of the polygeneration system is explained in Chapter 4. It starts with the mathematical modeling of the polygeneration system. Mathematical modeling of the auxiliary components such as photovoltaics thermal, thermoelectric generators and battery storages are also designed. Parameter analysis of three crucial elements such as SOFC, absorption chiller and electrolyzer are explained. Lastly, discussion and summary of the findings are presented.

Chapter 5 presents the first and second stages of energy planning for the polygeneration design. Firstly, the evaluation of the polygeneration configuration is conducted, then improving the polygeneration components for the second. Configuration analysis is conducted based on energy, economic and environmental criteria. The study of performance is also conducted in a comparison between the polygeneration with basic heat recovery and the improved polygeneration with additional heat recovery. Discussion of the findings and summaries are presented in the last sub-section.

Chapter 6 provides the third and fourth of energy planning steps started by applying optimization of operating strategy and sizing the polygeneration components capacity. The design of operating strategy is explained using artificial intelligence-based energy management. Performance of operating strategy is analyzed through a comparison between three membership shapes of a multi-level fuzzy energy management strategy (FEMS). Moreover, optimal sizing of the system components is also proposed using evolutionary-based and swarm-based algorithms to find the best capacity considering multi-objective criteria. Sizing analysis is performed for six essential components in the polygeneration system namely SOFC, electrolyzer, absorption chiller, photovoltaic thermal, thermoelectric generator and battery storage. Discussion of findings and summaries are presented.

Chapter 7 presents the conclusions of the energy planning including achievements and contributions of the proposed polygeneration system. This chapter also provides possible future works that could be conducted.

CHAPTER 2: LITERATURE REVIEW

2.1 Introduction

This chapter presents a review of the SOFC based power generation system including the technologies in energy generation for residential application in conventional and modern perspectives. Several types of energy generation especially for residential such as single power, cogeneration, and polygeneration systems is also discussed along with several applications of solid oxide fuel cell (SOFC) as the prime mover in power generation systems. Focused on the integrated supply in stationary power and vehicle power supply, this chapter provides energy planning strategies in designing an SOFC based polygeneration system. The energy plan includes evaluation of the configurations, development of operating strategy and optimization of the components capacities in the polygeneration system. Lastly, synthesis and analysis of reviewed studies are explained to identify the gaps filled by this study and the summary of Chapter 2.

2.2 Energy supply technologies in residential applications

Residential users are one of the primary energy consumers that contribute to the effects of the greenhouse gas (GHG) emissions in the world. More than 40% of electricity and 21% of GHG radiation are produced from residential sectors (Department of Energy, 2015). The increase in energy consumption is predicted to be more than 67% in 2050 in line with the population growth, the number of households and new types of energy services (International Energy Agency, 2011) which affects the national energy generation, the cost of energy and carbon dioxide production.

From 1990 to 2009, the national energy consumption and carbon emission in Malaysia had increased by 210.7% and 235.6% respectively (Zaid et al., 2013). These issues will become worse in the future due to the lack of effective strategies in the Malaysian building sector. Therefore, several policies concerning energy generation and consumption should be made to reduce the greenhouse gas (GHG) emission of buildings and to increase the efficiency of the energy supply in Malaysia.

Several technologies of energy generation have been developed starting from the conventional stationary power to the integrated stationary power systems. To keep up to current and future trends, the integrated stationary power system can be further combined with automotive applications such as for vehicles charging and fueling systems in these residential areas.

2.2.1 Conventional separated power supply system

Conventional stationary power supplies are energy generation system which generates electricity from non-renewable sources and distributes to residential areas. By using conventional supplies, electronic devices, heating, cooling water and space for homes are powered by electricity from the national grid. The increase in electricity used can reduce the efficiency of overall delivery system since more losses occur through the distribution line from the grid. The efficiency of electricity generated by the grid is about 0.4% – 0.48% (Akikur et al., 2015), hence the more electricity is used the more primary energy sources is reduced and the energy cost increases. Moreover, conventional supplies also cause problem for the environment since the usage of non-renewable sources increases the greenhouse gas (GHG) emission in the air.

As depicted in Figure 2.1., conventional separated power supply in residential applications does not consist of electricity supply for electronic devices, heating and cooling but also fuel supply for gasoline vehicles. Conventional cars use gasoline as fuel which has a high energy cost and a high GHG emission. The gasoline car has an efficiency of 236.8 MJ per 100 kilometers which equals 20 km per liter or 30% from the fuel utilization (Dennehy et al., 2018; Wakui & Yokoyama, 2012). Moreover, vehicles fueled by gasoline generate 2.344 kilograms of carbon emission per liter which is harmful to the air (Wakui et al., 2012). Therefore, the utilization of petroleum products must be reduced or substituted by other primary sources such as natural gas, electricity or hydrogen.

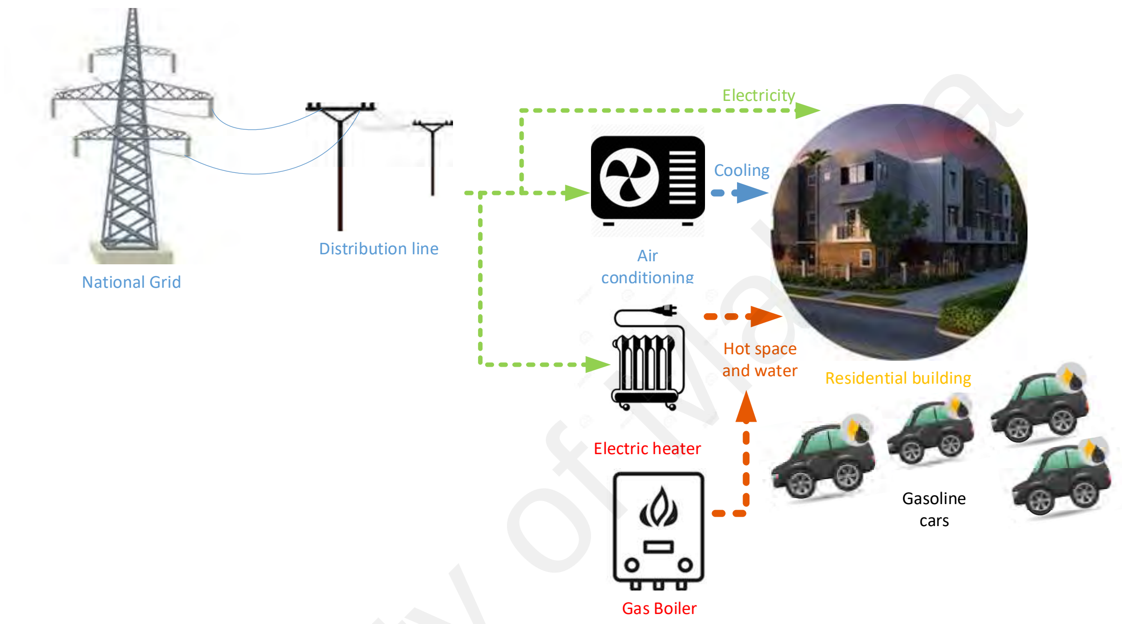

Figure 2.1: Conventional separated power supply and consumption for residential applications

2.2.2 Integrated stationary power supply system

To minimize dependency on main grid, integration of two or more power generation as a standalone or micro-grid system is essential. For small-scale application, 1kW to 2kW of independent power generation can supply a single house as standalone or connected to the national grid. As depicted in Figure 2.2, this integration will minimize power losses by shortening the distribution line and optimize the usage of electricity. For multi-family houses area or apartment buildings, a mini-grid power supply can be built from two or more integrated power generation consisting of non-renewable or renewable energies.

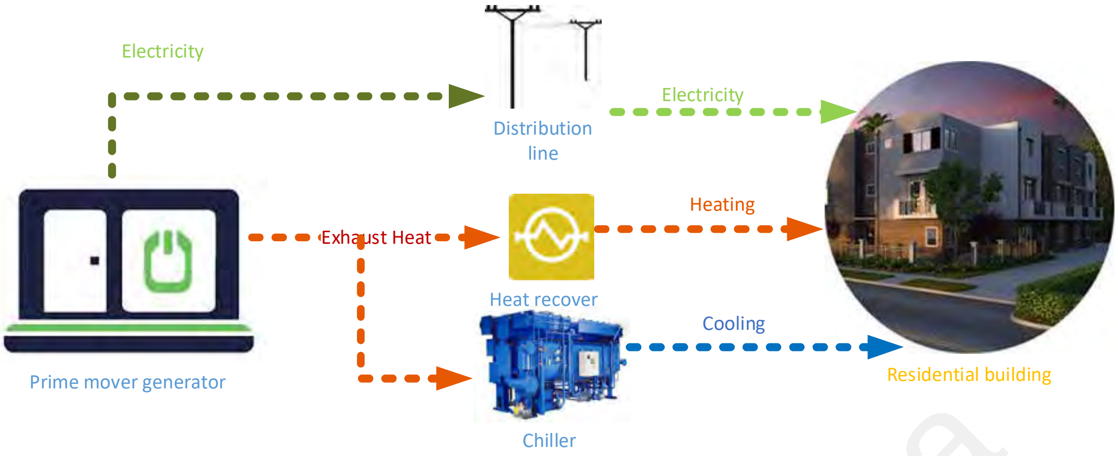

Figure 2.2: Integrated energy supply design for residential applications

Furthermore, the integrated energy supply does not provide electricity only but also heating and cooling supplies. In its structure, the system consists of a single or combined energy sources acting as a prime mover to generate electricity and heat simultaneously. The exhaust heat from the prime mover which is usually released to the air can be recovered to provide hot water and heating space for residential buildings which is called combined heat and power (CHP) or cogeneration system. For further applications, the CHP system can be evolved into combined cooling, heating and power (CCHP) or trigeneration system which provides three types of energy, i.e., electricity, heating and cooling. Trigeneration is formally categorized as polygeneration system since it generates more than two energy supplies from a single source or integrated primary energy sources. The polygeneration system can not only generate electricity, heat, and cooling but also produce fresh water, oxygen, hydrogen and other energy types. Section 2.3 presents the detail explanations of cogeneration and polygeneration systems.

2.2.3 Integrated stationary power and vehicle power supply system

Integrated stationary power and vehicle power supply could be promising in the current and future developments of energy generation design for residential uses. As depicted in Figure 2.3, the idea comes from the trend in transportation that focuses on electricity and hydrogen as fuels instead of gasoline for driving vehicles. Due to the development of electric and hydrogen cars in hybrid or pure fuel systems, the opportunity for developing a micro-scale or a mini private charging or fueling stations is promising. Private vehicle charging systems could be implemented for single and multi-family uses in the residential application. Meanwhile, fueling station systems could work with electrolyzer or combustion and purifier systems to produce hydrogen from non-renewable and renewable energy sources (Al-Zareer et al., 2018; Im-orb et al., 2018).

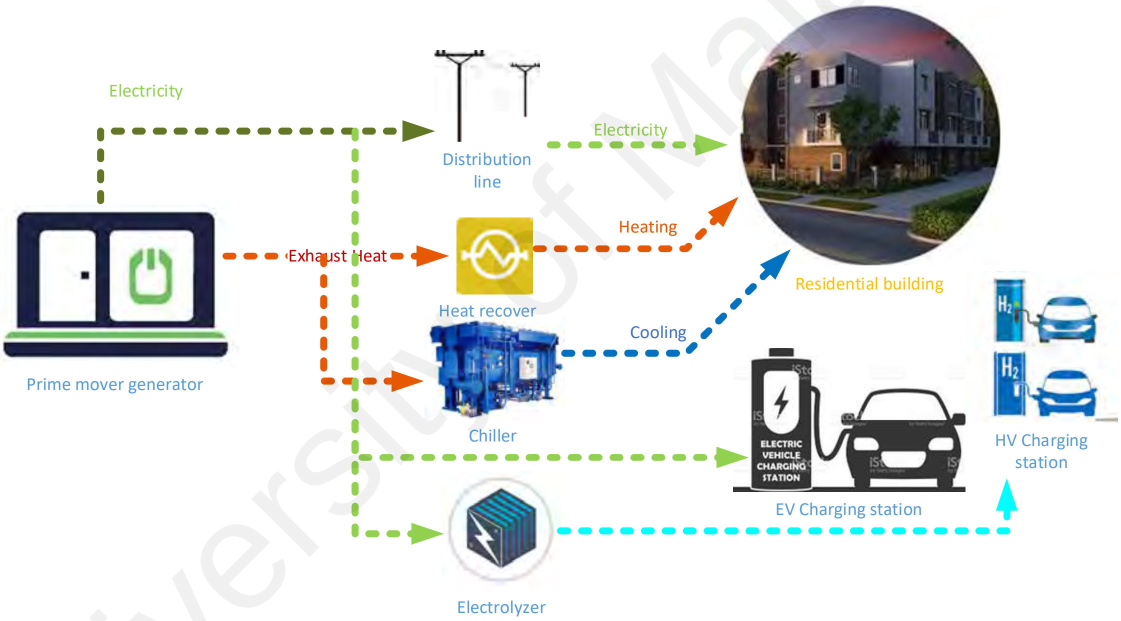

Figure 2.3: Integrated energy supply design with vehicle charging/fueling system for residential applications

Integrated stationary power and vehicle power supply can reduce PEC from non-renewable energy sources, increase the efficiency and minimize the power loss of the system. Moreover, by using renewable energy as prime mover, the integrated system can significantly reduce the GHG emission. Economically, the integrated system can also reduce the energy cost and be beneficial for long-term usage with a short payback period

(Jana et al., 2017). Therefore, the system should be well designed based on the requirements from the users.

2.3 Types of energy generation in residential applications

From the number of energies produced, energy generation system can be divided into single-power generator, cogeneration, and trigeneration or polygeneration systems. Single-power generator produces energy such as electricity, district heating or cooling in a separated system based on the user requirement. Meanwhile, the cogeneration system can generate two types of energy from sole or combined primary source. It could be electricity and heat water and space, cooling water and space, hydrogen or fresh water. On the other hand, polygeneration system can generate three or more energies from a single or integrated source. In certain applications, polygeneration could be a trigeneration or combined cooling, heating and power (CCHP) when the system produced three types of energy.

2.3.1 Single-power generation system

In stationary power applications, a single generator is used for generating electricity in standalone or grid-connected configurations. Several non-renewable energy sources have been used before as the prime mover such gas turbine, combustion engines and stirling engines. However, due to environmental and fuel efficiency issues, renewable energies are more popular and widely implemented for residential applications compared to non-renewable energy sources. Photovoltaics, wind turbine generators, geothermal and fuel cells are several types of favorable renewable energy sources which have been used as prime movers in power generation systems.

To improve the prime mover performance, several types of renewable and non-renewable energy sources could be integrated into a hybrid system. Hybrid SOFC-gas turbine was implemented by Jens Palsson (2000) for residential building using the prime mover size of 500 kW. Chachuat et al. (2005) developed an optimal design and operation of power generation system employing hybrid fuel cells as the prime mover. Dicks et al. (2000) also conducted a study of the hybrid SOFC and proton-exchange membrane fuel cell (PEMFC) for increasing system efficiency.

Another method to increase prime mover efficiency has been conducted by adding thermoelectric materials in the exhaust heat recovery line. Several studies revealed the increase of electricity production by attaching thermoelectric generators in the burner, air preheater or fuel preheater of the single-power generation system (Islam et al., 2017, 2018; Zhang et al., 2017a; Zhang et al., 2017b). For non-renewable energy sources, most of the prime mover types can be combined with thermoelectric generators to produce the auxiliary electricity. However, not all renewable energy sources are suitable for thermoelectric materials due to their low-temperature operation. Photovoltaics and fuel cells are some of the promising renewable energies which work well with thermoelectric materials, but due to heat quality and temperature limitations, the fuel cells work better than the photovoltaics.

Besides generating electric power, a single-power system can also produce heat or cooling using separated systems. Several district heating or cooling systems have been developed for multi-family in residential applications (Ameri & Besharati, 2016; Franco & Versace, 2017; Li et al., 2017b; Verrilli et al., 2016). The district heating or cooling system is produced by a single or hybrid prime mover which commonly uses combusting engines in heat generation. Udomsri et al. (2012) studied the performance of a district heating network for a multi-family residential area. A comprehensive analysis was also conducted regarding power-sharing mechanisms between district heating and combined heat and power systems for supplying to residential homes (Gładysz & Ziębik, 2013).

2.3.2 Cogeneration system

In several applications, especially for offices and residential, electricity is not the sole required energy. Other energies such as heating, cooling and purified water are also needed continuously. There are several types of energy that are mostly required for residential in areas such as electricity, hydrogen, fresh water and oxygen (Ahmadi, 2013). However, most office and residential buildings utilized separated system (SP) in generating electricity, heating and cooling energies to meet those requirements which caused inefficiency in energy usage and significantly raising the energy cost. Therefore, an integrated system which can cover more than one energy demand is desired to enhance the system efficiency, energy utilization and the energy cost.

Cogeneration system consists of a single or hybrid energy source as the prime mover that generates one or two types of primary power simultaneously and auxiliary components to recover the generated energy by the prime mover. In several applications, a cogeneration system is also equipped with storage devices such as hot water tank or battery. The storages are used to store excess energies generated by the system. By using this configuration, cogeneration can reach efficiency of up to 80% compared to the single-power generation system (Chen & Ni, 2014).

Combined heat and power (CHP) system is one of the most favorable types of cogeneration system which generates electricity and heat. The CHP is efficient since it does not require additional fuels to produce heat power as in the separated system. This system was the first energy generation commercialized for residential applications which had been successfully developed by several companies such as Hexis (Switzerland) and Ceres Power (UK), in partnership with British Gas and Ceramic Fuel Cells Ltd (Australia) (Irvine & Connor, 2012).

2.3.3 Polygeneration system

Even though the development of cogeneration systems has been successful, they could not fulfill the requirements in electricity, heat and cooling at the same time. Moreover, for the CHP system, when the heat requirement was lower than its production, the exhaust heat from the prime mover would be useless then reduces the overall efficiency of the system. Recent technology in the energy generation has developed polygeneration to overcome those issues. A polygeneration system can produce three or more types of energy simultaneously. The system consists of a single or hybrid energy source as the prime mover in providing one to three types of energy and several auxiliary components for generating more energy productions. Since the fuel is utilized optimally to generate more types of energy, polygeneration is more advanced than cogeneration and single-power generation systems.

Polygeneration systems are adapted to optimize the utilization of the exhaust energies from the prime mover and to optimize the fuel consumption. In polygeneration systems, by using similar amount of fuels, more energy types can be produced to satisfy more than two demands. For instance, it has better energy waste recovery as well as higher energy efficiency. In its applications, polygeneration systems are named by trigenerations when they produce three types of energy and quad generation when it generates four energy types.

Combined cooling, heating and power (CCHP) is one example of trigeneration systems which generates three types of energy simultaneously. As the essential energy types required in offices and residential applications, electricity, heat and cool powers should be generated sustainably. The CCHP system utilizes one or two energy sources as the prime mover to generate electricity and heat, then recovers the exhaust heat in producing cooling. In several systems, the cooling system uses chillers and refrigerators as part of the auxiliaries (Ciampi et al., 2014; Liu & Leong, 2006; Malico et al., 2009; Palmero-Marrero & Oliveira, 2011; Szega & Zymelka, 2017).

Several existing research topics in polygeneration revealed the performance of this system as the future promising energy generation to be applied for residential applications. Chen and Ni (2014) concluded that the trigeneration system is more efficient than the cogeneration system by taking a hotel building in Hong Kong as a case study. The study found the efficiency for the trigeneration and cogeneration systems were 93.86% and 84.02%, respectively. However, extra cost had to be incurred for the trigeneration system since it had an additional cooling device which caused a more extended payback period of about 4.3 years. Chitsaz et al. (2015) also reported that the trigeneration system achieved exergy efficiency of 46% which was higher by about 5% than the exergy efficiency for the single-power generation system. For residential applications, polygeneration proved to generate more productions such as hydrogen for vehicles, fresh water aside from electricity, heating and cooling for water and room (Calise et al., 2017d; Ghaem Sigarchian et al., 2018; Rokni, 2018; Sigurjonsson & Clausen, 2018). Therefore, implementation of the polygeneration systems which are integrated with vehicles power supplies are also promising for future residential buildings.

2.4 Overview of polygeneration system

A polygeneration system consists of two or more components acting as the prime mover and auxiliary elements such as heating, cooling, storages, hydrogen generators, purifying devices or other recovery components.

2.4.1 Prime movers

A prime mover is a component that generates energies as the end products by consuming coal, natural gas, oil and hydrogen. Different designs of polygeneration system result in different types of prime mover. Based on the literature, Jradi and Riffat (2014) divided the prime mover technologies into combustion-based technologies such as gas turbines, stirling engines, reciprocating engines and Rankine cycle engines and electro-chemical-based technologies such as fuel cells. Some of them are mature technology and have been commercialization such as reciprocating engines and gas turbines. However, some others such as organic Rankine cycle engines, Stirling engines and fuel cells are still under research stage. Table 2.1 presents the comparison of the prime mover technologies that have been implemented in polygeneration systems.

Amongst the prime mover types, internal combustion engines (ICEs) are the oldest technology which has been developed for single-power and multi-power generation systems. Due to its low efficiency (about 30%) and high investment cost, ICEs are suitable for the broader application in medium and large scales cogeneration and polygeneration systems (Badami et al., 2008). ICEs are powered by diesel, natural gas and gasoline as fuels and its waste heat can be recovered using the exhaust heat channel and jacket water cooling (Arteconi et al., 2009). The overall efficiency of combustion engines reaches about 80%, however, its noisy operation and high maintenances become the disadvantages of this technology. Furthermore, the engines also generate a large number of gases emissions such as nitrogen oxides and carbon dioxides which cause environmental issues which are restricted in residential applications (Badea et al., 2008).

Another type of prime mover which has mature technology is the gas turbine. Gas turbines in the polygeneration system generally consist of several parts such as generators, recuperators, a single shaft for connecting turbines, combustion chamber and compressors

(Arteconi et al., 2009). A gas turbine is operated by the Brayton thermodynamic principle and is usually fueled by natural gas, light fuel oil or diesel (Al Moussawi et al., 2016). The combustion gas turbines have been used since the 1930s for electricity generation purposes such as micro-scale polygeneration systems (Liu et al., 2014). For micro-scale applications, a micro-turbine is preferred rather than the general gas turbine. The micro-turbine has smaller capacity, faster response, compact design, low weight, lower noise and low maintenance compared to the general gas turbine (Sonar et al., 2014).

Table 2.1: Assessment and comparison between different polygeneration prime movers (Al Moussawi et al., 2016; Jradi & Riffat, 2014)

Prime movers	Reciprocating engines	Gas turbine	Stirling engines	Steam turbine	Rankine engines	Fuel cells
Advantages	Efficient part load performance High flexibility Short startup time required	Compact and flexible design Low maintenance level Moderate output heat temperature	Low noise and emission level Suitable for domestic application Possibility to run by renewables	Flexibility in fuel including renewable energy Long life cycle High overall efficiency Flexibility in fuel to heat ratio	High flexibility and simple design Low operation temperature and pressure Wide range fuel required	High electrical efficiency Low operation noise and emission High output temperature
Disadvantages	Large number of moving parts High mechanical vibration and noise	Inefficient part load performance Unsuitable for start/stop application	Long startup time High investment cost Limited adaptability	Bulky construction High initial cost Slow respond at partial load Slow start-up	Low efficiency Infrequent of research and commercialism in	High capital and investment cost Complex design
Capacity	Up to 75 MW	Up to 250 MW	Up to 55 kW	50kW to 100 MW	Up to 250 MW	Up to 2 MW
Electrical efficiency	25 – 45 %	18 – 36%	15 – 35%	10 – 37%	15 – 38%	37 – 60%
Overall efficiency	65 – 80%	65 – 75%	60 – 80%	60 – 80%	80%	55 – 80%
Life time (h)	20000 – 50000	5000 – 40000	10000 – 30000	50000 – 100000	30000 – 50000	10000 – 65000
Fuels used	Diesel, natural gas, propane	Natural gas, biogas, propane, distillated oil	Any fuel (natural gas and biofuels)	Any fuel (natural gas, biofuels and renewable energies)	Any fuel (natural gas and biofuels)	Hydrogen, natural gas, propane, methane

Table 2.1, continued

Prime movers	Reciprocating engines	Gas turbine	Stirling engines	Steam turbine	Rankine engines	Fuel cells
Electrical to thermal ratio	0.5 – 1	0.4 – 0.7	0.15 – 0.4	0.9 – 1.13	0.15 – 0.4	0.5 – 2
Waste heat temperature (°C)	80 – 200	120 – 350	Up to 85	Up to 85	Up to 100	Up to 1000
Thermal output (kJ/kWh)	3376 – 5908	3376 – 7174	-	-	1065 – 52753	1900 – 4431
Part load efficiency	High	Low	Moderate	Low	Moderate	Very high
Startup time	> 10 s	> 10 min	-	> 5 h	> 1 h	> 3 h
Noise level	High	Moderate	Moderate	Moderate	Low	Moderate
Investment cost ($/kWe)	340 -1600	450 – 1500	1300 – 2000	2000 - 32000	1000 – 2000	2500 – 3500
NOx emissions (Kg/MWh)	Up to 10	0.1 – 0.5	0.23	Fuel-dependent	Fuel-dependent	0.005 – 0.01
CO_2 emissions (Kg/MWh)	Up to 650	580 – 720	672	Fuel-dependent	Fuel-dependent	430 – 490

Beside the gas turbines, stirling engines (SE) are another typical type of prime mover. SE are external combustion engines which use a simple ambient pressure combustor to provide a constant source of heat to move a piston for doing work (Sonar et al., 2014). Different from ICEs which have limitations in the fuel flexibility and producing high noise, SEs are well known for its fuel flexibility and quiet operation. Other advantages of the engines are related to its long-life engine characteristic and low carbon generation as it could be fueled by biofuels besides natural gases. However, due to its limitations at lower power output compared to other combustion engines, high costs and not controllable, the engines become challenging to be implemented in the energy generation systems.

Steam turbines (ST) are one of the early developed technologies in the multi-purpose generators which have been used over 100 years ago (Al Moussawi et al., 2016). The turbines contain a mechanical device that uses an extraction of thermal energy from the pressured steam and convert the energy into rotary motions. ST has higher efficiency and lower energy cost compared to reciprocal engines, hence have been implemented for larger applications (Mago et al., 2010). The capacity of ST is up to 50kW for small power generation and up to 100 MWs for large power generations (ICF International Company, 2008). ST is implemented in large-scale systems especially for industrial applications. However, due to the limitation in efficiency during the part-load operation, the ST is not suitable for small-scale residential applications.

Besides, the rankine cycle is also generally used for polygeneration systems. A rankine cycle works with the principle of converting the heat into electricity. Similar to the steam turbine, the rankine cycle works using organic fluids instead of water (Al Moussawi et al., 2016). The organic liquids are preheated and the evaporated gas from the steam process is used to turn the engine which connects to the generator (NewEnCo, 2017). This technology received high attention since it has a low-cost investment, high safety, simplicity, durability and can be operated at lower levels of temperature and pressure (Jradi & Riffat, 2014). However, since the rankine cycle is still an emerging technology, it could face technical issues. Therefore, long-term research becomes necessary if needed to implement this technology for commercialization.

In recent applications, utilization of renewable energy sources such as wind, sunlight and geothermal are attractively developed as these sources are reliable and can be replenished continuously. Integrated photovoltaic in a cogeneration system was studied by Akikur et al. (2014) and they concluded that the overall cogeneration efficiency for standalone SOFC, PV-SOSE and PV-SOFC systems were 83.6%, 20% and 23% respectively. Anatone and Panone (2015) optimized the design and management of combined ICE-PV based CCHP system for a residential house. Boyaghchi and Heidarnejad (2015) also combined PV and ORC as the prime mover of a tri-generation system also for a residential house. Parameters analysis and optimization of operating conditions were performed to maximize both thermal and exergy efficiencies and minimize product cost rates.

Lastly, fuel cells (FCs) are also promising candidates as a prime mover in polygeneration systems. Fuel cells have similar characteristics to a battery in converting chemical primary sources into electrical energy through electrochemical reactions. The reactions occurring between hydrogen, oxygen and other oxidizing agents generate heat and water as the by-products and electricity as the primary product. This technology has been attracting much attention due to its environmentally friendly nature compared to the conventional generators which generated harmful gases as the by-products. FCs are commonly divided into six types based on the electrolyte characteristics namely proton exchange membrane fuel cell (PEMFC), direct methanol fuel cell (DMFC), alkaline fuel cell (AFC), phosphoric acid fuel cell (PAFC), molten carbonate fuel cell (MCFC), microbial fuel cell (MFC) and SOFC. Each type has the advantages and drawbacks which is presented in Table 2.2.

Amongst the fuel cell types, SOFC is the most favorable generator for power and heat energy supply applications and becomes attractive to be implemented in polygeneration systems. Generally, three essential components drive the SOFC operation namely balance of plant, SOFC stack and power conditioning unit (PCU) as depicted in Figure 2.4. The balance of plant extracts the hydrocarbon gases and the air into hydrogen through shifting and reforming reactions. The hydrogen, then, is reacted with the oxygen through a chemical reaction in the anode of the cell. The electricity generated is converted into alternate current (AC) power using the PCU. SOFC based trigeneration system that utilizes natural gas can reach higher system efficiency of up to 55% (Jradi & Riffat, 2014). Lately, a micro-scale cogeneration system has been successfully developed powered by a 4.6 kW Vaillant PEMFC and a 1 kW Sulzer Hexis SOFC (Bernard, 2008).

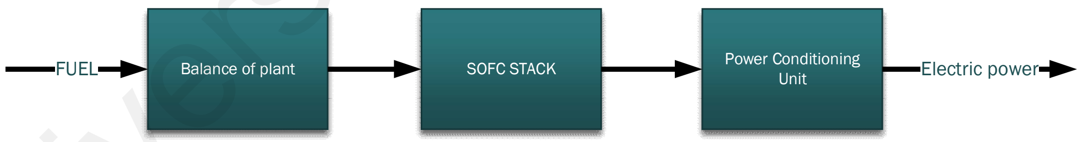

Figure 2.4: Diagram of SOFC system

Several research works have been conducted on polygeneration systems using SOFC as a prime mover. Perdikaris et al. (2010) designed a tri-generation system based on combined SOFC – solid oxide electrolyte cell (SOFC-SOEC) as the prime mover and energy storage for a standalone configuration. The proposed system claimed to have exergy and energy efficiencies of about 28.25% and 18.55% respectively. Kazempoor et al. (2011) conducted a performance analysis between a cogeneration and polygeneration systems employing SOFC as the prime mover for a residential house. It revealed the improved performance of the SOFC based trigeneration system by reducing non-renewable source as the primary energy and carbon dioxide equivalent values by about 66% and 35% respectively.

Performance analysis on several parameters of SOFC such as fuel cell cost, absorption chiller cost, auxiliary component cost, subsidiary, fuel cost and maintenance cost was conducted by Chen and Ni (2014). The study was performed under pessimistic and optimistic scenarios. The study found that the tri-generation system has a higher efficiency of 9.84% than the cogeneration system, yet it had a more extended payback period of about 5.7 years due to the additional auxiliary parts in meeting both heating and cooling demands. Sigurjonsson and Clausen (2018) developed a novel polygeneration system integrating biomass and reversible SOFC (RSOFC) to generate electricity, heat and bio-synthetic natural gas (SNG). This system reached efficiencies by about 46% and 69% respectively in relation to the produced electricity and syngas. Calise (2011) designed a polygeneration system combining SOFC and photovoltaic thermal (PVT) using a simulation-based software, TRNSYS. The results showed that the SOFC based polygeneration was profitable in the feed-in tariffs scenario as funded by their government. Almansa (2010) developed a polygeneration system based on SOFC fueled by biomass for residential applications, then study focus on waste management in protecting the environment and generating more energy.

Table 2.2: Comparison between different type of fuel cell (Ellamla et al., 2015; Elmer et al., 2015; US DOE Energy Efficiency and Renewable Energy, 2007)

Fuel cell type	PEMFC	AFC	DMFC	PAFC	MCFC	SOFC
Operating temp (°C)	30 - 100	90 - 100	50 - 100	160-220	600-700	500-1000
Electrical efficiency (%)	30-40	60	20 - 25	40-42	43-47	50-60
Energy conversion efficiency (heat and power) (%)	85-90	85	85	85-90	85	up to 90
Typical stack size	< 1kW–100kW	10kW – 100kW	Up to 1.5kW	50kW – 1MW (250kW module typical)	<1kW – 1MW (250kW module typical)	5kW – 3MW
Electrolyte	Solid polymeric membrane	Aqueous solution of potassium hydroxide soaked in a matrix	Solid organic polymer poly-perfluoro sulfonic acid	100% phosphoric acid stabilized in a Sic based matrix	Li2CO3/K2CO3 materials stabilized in an alumina-based matrix	Solid, stabilized zirconia ceramic matrix with free oxide ions
Fuels	Hydrocarbons or methanol	Pure hydrogen	Methanol	Natural gas	Natural gas, biogas, others	Natural gas or propane, hydrocarbons or methanol

Table 2.2, continued

Fuel cell type	PEMFC	AFC	DMFC	PAFC	MCFC	SOFC
Applications	Backup power, Portable power, DG, Transportation, Specialty vehicles	Military, Space, Backup power, Transportation	Consumer goods, Laptops, Mobile phones	Distributed generation (DG)	Electric utility, Distributed generation	Auxiliary power, Electric utility, Distributed generation
Advantages	Quick start up time, can vary output quickly, compact, no corrosive fluid used	Wider range of stable materials allows lower cost components, Low temperature, Quick start-up	High energy storage, no reforming needed, Easy storage and transport	High cogeneration efficiency	High efficiency, scalable, fuel flexible	High temperature enables internal reforming, no liquid electrolyte used, useful high temperature output can be used for other applications, no purity H2 needed (low price fuel)
Disadvantages	Expensive platinum catalyst used, high purity H2 required	Sensitive to CO_2 in fuel and air, Electrolyte management (aqueous), Electrolyte conductivity (polymer)	Low power output, Methanol is toxic and flammable	Expensive catalysts, Long start-up time, Sulfur sensitivity	High temperature corrosion and breakdown of cell components, Long start-up time, Low power density	Long start up time, issue on temperature stress during load following operation, expensive heat resistant material required

2.4.2 Heat-recovery units

Heat-recovery units work to recover thermal energy of gas streams exhausted from the prime mover to meet heating demands (Al Moussawi et al., 2016). The units can increase overall efficiency without additional fuels. It consists of heat exchangers with different specifications based on the requirements. In a CHP system, the units were divided by unfueled and fueled units. These units can be used concurrently or separately according to the design of the system (Oland, 2004).

Heat exchangers are the simplest heat recovery devices due to its flexible forms such as tube and shell, plate, fins and micro-channel. Those devices are slightly different with the heat recovery and steam generation (HRSG) which can produce heat and steam water from the rejected exhaust gases. The heat muffler is commonly used to recover the exhaust heat in reciprocating engines. The HRSG also generates pressured steam and hot water as it works in the range of 370°C to 540°C with less noise (Oland, 2002). However, the exhaust gas compositions affect the exit temperature of the mufflers and the amount of heat which can be recovered (Oland, 2004). Regular maintenance and cleaning are needed to keep up performance of the engine since the excessive back-pressure issue could reduce the capacity of the mufflers.

Another option for the heat recovery device is the thermoelectric generator (TEG). TEG components consist of materials that convert heat to electricity. The role of TEG is to increase the efficiency of the prime mover by recovering the exhaust heat into electricity. Using a temperature gradient across the TEG material, the electrons from n-type flow to p-type semiconductor and establish the voltage to drive the external load (Bensaid et al., 2012). The performance of TEG (ZT) is different based on the semiconductor types for p and n as well as the range of operating temperatures.

In its application, TEG has been widely used for heat recovery purpose in stationary and vehicle machines. By placing TEG in several parts of the heat recovery systems such as air and fuel preheaters, burner and exhaust heat, the overall efficiency can increase up to 5% from the base case (Terayama et al., 2013a). Currently, TEG has been commercialized as backup power of the prime mover in single and multi-power generation systems.

For trigeneration or polygeneration system, heating units have been implemented by few researchers in different applications. Dorer et al. (2005) assessed a micro-generation system in the residential area consisting SOFC and PEMFC in a separated system with gas boiler and solar collector as the heating units. Entchev et al. (2013) proposed a combined internal combustion engine (ICE) with the fired furnace as a heating unit for the residential house. Santo (2014) integrated HSRG and hot water circuit as the heating units for a trigeneration system using the ICE as a prime mover for hospital building applications. From the study, it showed that the steam engine contributes to the increase in the energy utilization factor (EUF) and exergy efficiency during part-load operation instead of the full-load operation.

Sadeghi et al. (2015) combined an SOFC and a heat exchanger as the heating and cooling units with added absorber for a standalone system. The study revealed that the heat exchanger gives significant effect to the destruction in exergy efficiency. Utilization of an absorption heat pump, solar thermal collector combined with a gas boiler was proposed by Anatone and Panone (2015) combining an ICE and photovoltaic (PV) as the prime movers. In another study, Entchev et al. (2014) conducted a performance analysis of a trigeneration system based on a combined ground source heat pump (GSHP) – photovoltaic thermal (PVT) to meet the power, heating and cooling demands in the residential and office buildings. It achieved the overall energy savings of 46% and 58.5%

respectively by implementing the GSHP and the integrated GSHP-PVT systems compared to the conventional system.

2.4.3 Cooling units

Instead of utilizing an extra fuel to meet the cooling demand, polygeneration system produces cooling from the exhaust heat of prime movers. The waste heat can be in the form of hot water, steam and exhaust gases that fall into different temperature ranges (Al Moussawi et al., 2016). Therefore, the best design of polygeneration system should consider the best combination between the prime mover, heating units and cooling units and other units based on their specifications to meet the power, heating, cooling and other demands.

Sorption cooling technologies (including absorption and adsorption) works with a thermal compression in producing cooling power instead of a mechanical compression which is adopted by refrigerator machines. An absorption cooling works with a pair of working fluids namely refrigerant and absorber, while an adsorption cooling produces chilled air or water based on a solid substance that adsorbs the refrigerant vapors (Sonar et al., 2014). A simple absorption cooling cycle consists of four main components; generator, absorber, evaporator and condenser. Typically working absorbent/ refrigerant pairs for an absorption cooling are lithium bromide-water ($LiBr/H_2O$) and water ammonia (H_2O/NH_3).

Numerous studies can be found regarding the cooling units used for power and heat generation systems. Cardona and Piacentino (2003) designed the size of a trigeneration system consisting of a power generation unit (PGU), boiler and absorption chiller in the Mediterranean areas. The study also analyzed the effect of part load operation of the absorption chiller with 70%, 85% and 100% of cooling load requirements. Utilization of an absorption chiller was also studied by Chen and Ni (2014) for commercial buildings in Hong Kong. The study conducted parameter analysis from an economic aspect regarding the cost variations for SOFC, absorption chiller and other auxiliary components in a cogeneration and trigeneration systems considering the pessimistic, optimistic cost scenario and the government subsidy scenario.

Arcuri et al. (2015) optimized the design of a tri-generation system for residential applications. Some aspects were considered including topologies, sizes, and operation strategies to increase the overall efficiency in the part-load operation. Some parameters such as inlet electrical power to compressor interval for cooling production, outlet cooling power interval from the compressor, outlet cooling power interval from the absorber and cooling power range for the absorption cooling were examined in details. Li et al. (2014) installed an air conditioning system as the backup for an absorption chiller used in a trigeneration system for an integrated residential and office buildings. The ratio of air conditioning to the cooling unit was examined with respect to the increase in the power energy saving (PES), annual total cost reduction (ATCR), and carbon dioxide emission reduction (CER). The study generated the best strategy using a combined air conditioning and heat storage topology with increased in energy saving of 12.9% and 23.68% for residential and office buildings respectively.

2.4.4 Hydrogen generation units

In reducing the utilization of primary energy sources such as oil, natural gas, electricity and renewable energy, some strategies have been made to produce a new type of fuel. Compared to petroleum and natural gas, the combustion process of hydrogen is much cleaner for the environment. However, due to its new technology, the prices of buying and selling the hydrogen are expensive. Therefore, the development in hydrogen production has been further studied, especially for fueling applications in the residential area (Siyal et al., 2015).

Establishment of hydrogen as fuel for the future is developed by the various hydrogen production systems using non-renewable and renewable energy sources. Several ways in producing hydrogen include steam methane reforming, gasification coal, biomass, nuclear and hydrolysis water (Sharma & Ghoshal, 2015). Amongst these, hydrogen formation from electrolysis of water is environmentally friendly. The advantages in producing extremely pure hydrogen using hydrolysis have been known since 1700, yet it was only used for small applications (Stojic et al., 2003). Currently, the hydrogen production from water electrolysis is about 4% of the world's hydrogen production. The large-scale applications of hydrogen production have been employed for private fueling stations, marines, rockets, spacecraft, electronic industries and food industries (Dunn, 2002).

2.4.5 Storage units

For the heat and power generation, fluctuation and asynchronicity in the power, heating and cooling supplies cause a decrease in the overall efficiency and an increase in energy cost. To address these issues, storage units are needed to store the excess energy when the demand is low and use the stored energies during peak hours. By utilizing storage units, the operating hour of the system will be increased. It will also minimize the fuel utilization and maximizing the overall efficiency. Moreover, the size of energy generation units should be optimized to minimize the energy loss and energy cost during its operation in the peak load hours.

In combined power, heat and cooling generation systems, two storages type are typically used namely electrical storage and heat storage. Electrical storage is used for saving the excess electricity from the prime mover, while heat storage is for saving the excess heat and the recovered heat from the prime mover and heat recovery units respectively. Although in many applications, the utilization of heat storage is more than electrical storage, the fluctuations in electrical demand can lead to be higher than the heat depending on the imported grid and its fluctuated prices. The electrical storage can reduce the dependence of the system to the grid source and recover the limitations of the prime mover in starting and in following the load (Napoli et al., 2015).

Utilization of electrical energy storage becomes more important to minimize electrical supply from the grid. It also improves working hours of the system during peak load period, when electrical tariff from the grid is high. Battery energy storage (BES) is considered as storage to store excess energy from the prime mover and other power sources. BES uses electrochemical reactions to convert the stored chemical energy into electricity by generating voltage between the terminals. Some recent technologies in BES have been implemented based on its chemical components, namely Lead-Acid (LA), Nickel (Ni), Sodium (Na), Lithium-Ion (Li) and metal-air batteries.

The BESs have become the most promising electrical energy storage device which have been implemented for hybrid and combined power generations. Napoli et al. (2015) studied the effect of utilizing a battery as the electrical storage for a combined SOFC and PEMFC cogeneration system in a residential house. The study revealed that the battery could reduce the independence of the system to the grid. It also could solve the issue for the high electricity price during peak load by connecting the system to the electrical storage. The study also conducted optimization on the design and structure of the cogeneration system using SOFC and PEMFC separately (Napoli et al., 2015). The increase of the primary energy saving (PES) was reached by adding a series of battery where decision-making and battery management were needed to increase the battery performance as backup power during peak load.

For trigeneration systems, Basrawi et al. (2014) added a battery for a combined photovoltaic-gas turbine (PV-GT) based trigeneration system and studied the economic and environmental effects of the proposed operation strategies considering base load, heat-match and power-match operations. In another study, similar proposed operation strategies as the combined gas turbine-battery trigeneration system considered the capacity of the battery, gas turbine, heat storage, chiller and the inlet precooling (Basrawi et al., 2016). The optimum design combined with the optimum strategy reduced the emission cost of the system about $92,407 per kg of carbon emissions.

Besides electricity, fluctuations in the heat and cooling demands also give significant effects in the reduction of the overall efficiency. For residential applications, heating and cooling demands are based on the occupant's behaviors where sometimes electricity is needed more than heating or cooling and vice versa. It increases the electricity requirement, hence making the exhaust heat from the prime mover become unusable at specific times. Therefore, thermal energy storage becomes just as essential as electrical storage in increasing the overall trigeneration efficiency.

Sensible heat storage (SHS) is a common type of heat storage used for combined heat and power generation systems. It works by adding energy to the material and increase its temperature without changing its phase (Mahlia et al., 2014). SHS capacity depends on the temperatures of the materials which are used for the heating or cooling transfers (usually solid or liquid materials), the changes of the temperature inside the storage and the amount of material stored. Water, sands, oils, and rock beds are commonly used as the materials to transfer heat for many applications. Water gives more advantage amongst other materials due to its low price and availability, yet utilization of solid materials such as metals, rocks concrete and bricks can also be used. Selection of the proper material to be used in the sensible heat storage has been conducted to minimize the initial and operational costs (New Mexico Environment Department, 2011). Availability and environmental effects such as the carbon footprint were also considered as part of the multi-objective optimization in the study.

For several fuel cell-based power generations, requirement of hydrogen as fuel can be met by using electrolyzer and stored in the hydrogen tank. Hydrogen-based energy storage (HES) has some advantages since its environmentally friendly component for stationary and vehicle applications. It also serves continuity in the electricity generation which cannot be provided from intermittent renewable energy sources such as photovoltaic and wind turbine generators. Applications of hydrogen-based storage are commonly coupled with a hybrid renewable energy system (HRES) (Ministry of Energy Green Technology and Water, 2015). The criteria such as safety, operational and the energy as well as its exergy performances are considered in the storage design. Furthermore, in line with the increasing attention in fuel cell-based heat and power generation, the utilization of hydrogen-based storage tanks is also increasing steadily. The use of employing an electrolyzer to convert available electricity into hydrogen which can be reused to feed fuel cells has also been actively studied. Akikur et al. (2014) conducted a performance analysis for combined power and heat generation system consisting of SOFC, photovoltaics and an electrolyzer. Sadeghi et al. (2015) performed optimization for the design of a combined photovoltaic, SOFC and an electrolyzer system to provide the optimal prime mover and storage capacities. Modeling and optimization of a combined SOFC-SOEC and hydrogen storage system were also performed by Shariatzadeh et al. (2015). Ozlu (2015) studied three configurations in a combined renewable energy and hydrogen storage system to provide electricity, domestic hot water, heating, cooling space and hydrogen. The increase in the exergy efficiency and the reduction in environmental emission were obtained by applying the proposed configurations.

2.5 SOFC based power generation system for residential applications

Fuel cells (FCs) has been identified as a promising future source in the recent development of renewable energy sources. There are six types of fuel cell as presented in Sub-section 2.4.1 based on the literature, where the existing studies classified PEMFC, DMFC, and PAFC as low-temperature operation cells, while MCFC and SOFC were classified as high-temperature operation cells. The low-temperature fuel cells are potential to be implemented in mobile applications as vehicle transportations, military and public facilities (Isa & Rahim, 2013; Ramadhani et al., 2017). On the other hand, the high-temperature fuel cells have higher temperature operation and higher efficiency that make them suitable for stationary applications such as the power generation systems (Choudhury et al., 2013; Mohamad et al., 2010).

SOFC has been developed for stationary power generations due to its advantages in its electrolyte material flexibility and versatility in the use of hydrocarbon fuels (Burer et al., 2003). Its high efficiency and its heat to power ratio make the SOFC useful to be integrated in the hybrid power generation to increase the electrical output and to be combined for the heat and power generation system. As depicted in Figure 2.5, the number of publications regarding the use of SOFC as a power generator has been increasing from year to year. Based on the type of power generated, the SOFC applications are divided into the single power generation, cogeneration, and trigeneration/polygeneration systems.

Researches use SOFC as a prime mover in the single power generation as early as 1992. Most of the studies concerned improving the performance of the stack SOFC to generate more electricity and to increase its electrical efficiency. From 1994 onwards, research in hybrid systems involving SOFC and gas turbines increased since the hybrid configuration gives significant effect to the increase in system efficiency. The investigation regarding the utilization of the exhaust heat from SOFC begun in 1995 and been increasing year to year drastically. Based on this data, it can be seen that the applications of cogeneration system were growing with the peak in 2014. However, in 2016 to 2017, the number of publications regarding cogeneration SOFC in residential was decreasing as many commercial products have been launched and more advanced systems were developed.

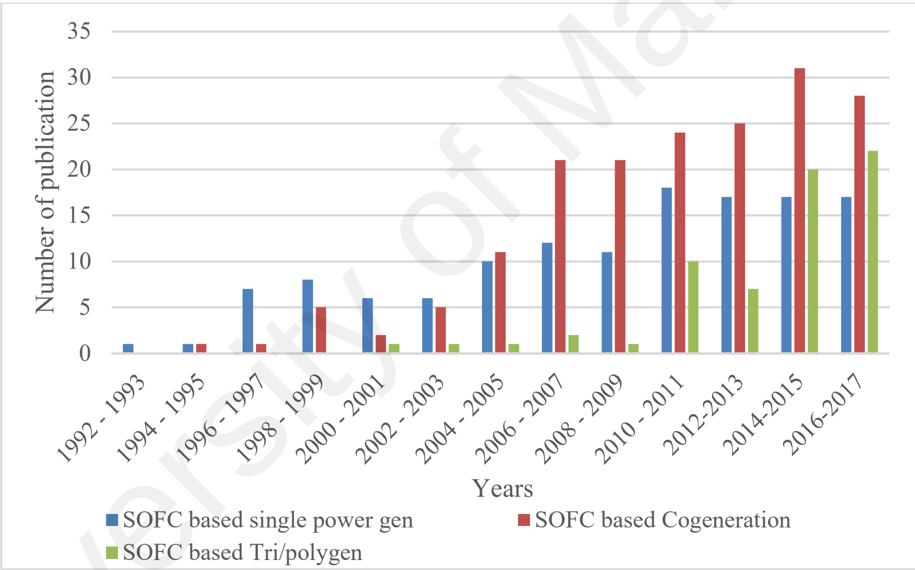

Figure 2.5: Double year-wise number of publications researching SOFC power generation in residential application

On the other hand, research topics in the trigeneration or polygeneration SOFC systems were increasing even though not as significant as the cogeneration system. Research in this area is categorized as a new topic which started in early 2000 and is still attractive for the next five to ten years. The increase in interest for applying SOFC in polygeneration systems is in line with the prediction of a price reduction in the SOFC investment cost for the next five to ten years (Akikur et al., 2015; Al Moussawi et al., 2017; Mahlia & Chan, 2011).

Moreover, the increase of polygeneration applications for residential buildings or areas has been caused by environmental issues along with non-renewable energy sources. As reported in the energy plan of the government, Malaysia targets to reduce emission carbon by 45% in 2030 (*Eleventh Malaysia Plan, Strategy Paper 17: Sustainable Usage of Energy to Support Growth*, 2017). Therefore, the applications of SOFC based polygeneration system could be promising in relation to the PES strategy and reducing carbon emissions in Malaysia.

Based on its design for residential energy planning, SOFC applications are divided into two configurations, i.e. integrated stationary power without and with vehicles power supply. The stationary power supply consists of varies forms of single power generation, cogeneration, and trigeneration/polygeneration systems. On the other hand, the integrated stationary power with vehicles power supply combines those stationary power systems with vehicles charging or refueling stations. An example is the single/multi-family house with an electric vehicle charging system or a small-scale fueling system placed in its residential area.

2.5.1 Integrated stationary power supply

At the end of 1989, research on the combined single-cell SOFC into the stack system was started by the new energy and industrial technology development organization (NEDO) of Japan. During the first period of the research, it had fabricated the 100W class of SOFC stack. From 1992, development of planar SOFC stack started to increase the power density of fuel cells and develop a larger active area of the cell and planned to manufacture several-kW class of SOFC stack. Until 2000, the investigation was focused on increasing the stability and reliability of the stack which initiated in the development of tubular SOFC cell.

In the USA, initiated by Siemens Westinghouse Power Corporation, the Department of Energy (DOE) National Energy Technology Laboratory (NTRL) developed a tubular SOFC power plant and commercialized the high efficiency, low cost and flexibility of the fuel types of an SOFC stack in the 3kW and 10kW powers. Moreover, Delphi Corporation also started to fabricate the stack SOFC for auxiliary power unit (APU) in a mobile application to supply a power engine-independent system that had high efficiency and low emissions. By taking the high efficiency of SOFC, the overall effectiveness of the APU was increased from 10 to 20% to up to 30 to 35% compared to the engineered-power generator. SOFC is an attractive power generator for APU since it does not have water management for the electrolyte. Also, it has compatibility in regards to the temperature between reformer and stack and it has a high tolerance for fuel impurities (Williams & Strakey, 2003). In its development, Delphi fabricated a 5 kW SOFC based APU system which had a compact design, fueled by gasoline and had a low mass system (Singhal et al., 1999).

Besides developing the stack and APU systems, the heat generation from the SOFC can be used to develop a hybrid system. The hybrid SOFC-heat generator came from the idea to optimize the utilization of exhaust heat. Siemens Westinghouse Power Corporation took the challenge to develop a hybrid project focused on the tubular SOFC stack after its achievement in successfully developing the SOFC stack project. It combined the fuel cell with the turbine to utilize its heat as byproduct. The increase in the power generation and the overall efficiency were achieved in line with the decrease in the energy cost since no extra fuel were consumed. With this hybrid project, related industries such as Rolls Royce and General Electric also developed a stack SOFC combined with

GT for the distributed generation following requirement of clean energy in "The Vision 21" energy plan (Singhal et al., 2003).

The development of the hybrid SOFC-turbine generator (SOFC-GT) have led to the other developments in combining SOFC with different heat generator types such as the stirling heat engine (SHE) and steam turbine (ST). Arsalis (2007) studied a hybrid SOFC-GT-ST model and conducted a parametric study of the system using thermo-economic analysis. The model was developed based on thermodynamic, kinetic, geometric and costing with sizes ranging from 1.5 MW to 10 MW. The study considered four different steam turbine cycles to design the hybrid system adequately. Implementation of regenerator for the hybrid SOFC-SHE system was performed by Chen et al. (2013). It acted as a counter-flow heat exchanger which absorbs the heat at high temperature to preheat the reactants in attaining the reaction temperature. Based on their study, the hybrid SOFC-SHE was considered as an efficient power generator and flexible fuel utilization.

Since the 1990s, the SOFC based cogeneration system has been studied by several researchers. Riensche et al. (1998) developed a 200kW SOFC based cogeneration system and studied its parameters such as air temperature, the degree of internal reforming, cell voltage and fuel utilization. According to the study, temperatures of the stack cooling and active cell area of the chimney were the two parameters affecting the cost of the cogeneration system. Adjusting the fuel utilization, increasing the air temperature and adapting an internal reforming system bought cost reductions about 5%, 20%, and 50%, respectively.

The study by Entchev (2003) optimized and managed a cogeneration system for the residential area using soft computing methods. The control mechanism was adopted for adjusting the water temperature according to the number of occupants. Two sensors were employed in the water storage tank and the thermostat was used to monitor the room temperatures. The advanced control revealed the increase in the efficiency by about 8 to 10% and pollutants reduction by 25 to 30%. In a recent development, the SOFC based cogeneration system focused on reducing the cost and unwanted gas emissions as well as commercializing the micro-rated power (1-50kW) to be implemented for office and residential buildings (Adam & Fraga, 2013; Napoli et al., 2015).

By using the SOFC as a prime mover, the trigeneration/polygeneration system have been implemented to supply energy for single and multi-family residential homes. Al Moussawi et al. (2017) designed an SOFC based trigeneration system by employing energy management for a multi-family residential building. Chitsaz et al. (2017) studied the effect of the recycling system in an SOFC based trigeneration system from the thermo-economic aspect. Moradi and Mehrpooya (2017) designed an optimal SOFC based trigeneration system and conducted an economic analysis. A multi-criteria evaluation has also been made by Jing et al. (2017) for an SOFC based trigeneration system for public buildings in China.

2.5.2 Integrated stationary power and vehicles power supply system

In line with the future of energy supply technology for residential applications, integrated systems for stationary and vehicle power supply have also been developed by researchers. By employing the SOFC as a prime mover, a combined heat and power generation coupled with an electric vehicles charging system has been developed in several research topics. Vialetto et al. (2017) analyzed a cogeneration system with an electric vehicle charging system designed for a single-family residential home. The analysis was conducted from the economic and energy aspects. Rosato et al. (2017) analyzed a micro combined heat and power system with electric cooling and electric vehicle charging systems for a residential house. The study performed energy, economic and environmental assessments to the system. Tanaka et al. (2014) designed and analyzed a micro-combined heat and power generation system employing SOFC as the prime mover and integrated it with an electric vehicle charger for a single-family application and analyzed its achievement for energy savings. Most of the existing research focused on the design and analysis of the integrated SOFC based stationary power and electric vehicles charging systems.

2.6 Energy planning for SOFC based polygeneration system in residential applications

Due to its high investment cost, energy planning should be designed for a polygeneration system efficiently. Three strategies were found in the literature regarding energy planning for residential applications, i.e. evaluation of configuration, operating strategy design and optimization of the system capacity as will be presented in the next sections.

2.6.1 Evaluation of configuration design

Structure evaluation or topology assessment is an important aspect in the design of polygeneration systems. Optimizing polygeneration structure begins from selecting the prime mover and components topology. Normally on SOFC based polygeneration, a stack SOFC is used as the prime mover using either standalone or hybrid configuration. In a standalone configuration, electricity generation and exhaust heat are generated from the single stack SOFC, while for hybrid configuration, SOFC is combined with other prime movers to increase the power generations. Combined prime movers between SOFC and renewable energy have also been studied including the organic rankine cycle (ORC), biomass and photovoltaic system. Moreover, evaluation of polygeneration could be conducted by choosing one or more than one prime movers as studied in the literature

(Wakui et al., 2016). The study did an optimization of the trigeneration structure based on the chosen prime mover between gas engine, PEMFC, and SOFC.

Structure evaluations are not only focused to choose the right prime mover, but also to design the proper heating, cooling, storage components and the connection to the grid. A study by Al Moussawi et al. (2016) provided a guideline in choosing the configuration of a trigeneration system based on energy, economic and environmental aspects. In particular, the study focused on the SOFC combined cooling, heating and power systems including the characteristics of heat to power ratio and the initial costs which were helpful in designing sufficient heating and cooling units.

Burners and heat exchanger are also commonly used for recovering the exhaust heat from the SOFC. Some studies recovered the exhaust gas from the SOFC using unfired heat recovery steam generator (HRSG) to provide hot water and space heating (Behbahani-nia et al., 2010; Takeshita et al., 2005; Zhang & Cai, 2002). For cooling units, due to the high temperature of the SOFC exhaust heat, a double or triple effect absorption chiller is most suitable to increase the overall efficiency. However, for unpredicted spikes in the peak load of heating and cooling, additional heating and cooling units such as an auxiliary boiler and an electric chiller can be used respectively.

Battery and sensible heat storages are also commonly used for electrical and heat storages due to having a direct power to capacity ratio. For the battery, the capacity which means the rates of charge and discharge are measured in voltage, while for sensible heat storage, the capacity is based on the temperature and pressure of the tank. Both electrical and heat storages give significant effect to the continuity of the system operations and reduce the dependence of the system from grid connectivity. However, the capacity and configuration of components should be evaluated to optimize its cost and efficiency.

Several studies have been done in evaluating the design and topology of combined cooling, heating and power systems based on energy, economic and environmental criteria (3E). Weber et al. (2006a) evaluated five configurations of the trigeneration system considering grid connected and standalone configurations. Their study simulated three configurations, i.e. the reference system, GSHP system and combined GSHP-SOFC system. Chitsaz et al. (2015) assessed four configurations of SOFC based power and heat generation system where the electrical power generator was used as the reference case, while cogeneration cooling, cogeneration heating and trigeneration were used as the proposed cases. Facci et al. (2016) conducted the technical and economical assessments for a trigeneration system with SOFC as the prime mover. The study considered boiler as an auxiliary heating unit and both absorption and electric chillers as the cooling units. It studied four configurations consisting of the prime mover, heating and cooling units and determined the optimum design which had minimum cost and lowest PEC.

Wakui et al. (2016) examined several configurations of the heat and power generation for residential houses considering the cogeneration, heating and storage components. The cogeneration candidates consisted of the gas-engine with constant power output, PEFC with the start-stop operation and SOFC with continuous operation at minimum power output. The candidates of the heating unit were the latent heat recovery type gas-fired boiler (LGB), electric heater, air-cooled heat exchanger and conventional type gas-fired boiler (CGB).

2.6.2 Operational strategy design

To reduce energy consumptions and increase the energy saving, optimization in the operating strategy has been conducted through several management approaches. Unlike the single power generation, managing the polygeneration system does not only consider electrical demand but also cooling, heating and other demands. Synergy in each component to meet all the requirements in the optimum energy flow has to the most considered as the main objective in the operational strategy. Based on the approach, the existing operation strategies which have been implemented for trigeneration or polygeneration systems can be divided into conventional, objective-based and intelligent-based approaches.

2.6.2.1 Conventional operating strategies

Conventional operational strategies work to manage the prime mover, cooling and heating units based on the required loads. For trigeneration or polygeneration system, electrical and thermal loads become the references in controlling the energy sources. Conventional operating strategies consider three approaches; following electrical load (FEL), following thermal load (FTL) and the combined FEL and FTL strategies.

Following electrical load (FEL) or electrical demand management (EDM) is an operational strategy to manage energy source in satisfying electrical load without considering the thermal load. In the applications, the prime mover is designed and operated optimally following the electrical load profile. In the FEL, the thermal requirement becomes the second priority to be satisfied by the prime mover. If the primary heating and cooling could not meet the demands, then an auxiliary boiler is used to generate additional heat. For dry and tropical countries, following electrical load strategy is more beneficial to increase the energy savings due to the fewer requirements for heating and cooling units (Wang et al., 2015a). The FEL strategy is also implemented for trigeneration system for heating, ventilation and air conditioning (HVAC) with an electrical heater, chiller, air conditioning and refrigeration units.

Conversely, following thermal load (FTL) or thermal demand management (TDM) is a strategy to fulfill the thermal demand firstly in designing and operating a polygeneration system. The prime mover capacity is designed to meet the thermal demand, while if the electrical demand could not be satisfied, extra electricity imported from the grid is required. The FTL strategy is usually implemented for countries which have high thermal demand such as the four-season countries. In summer, the prime mover generates more heat to be recovered by cooling units to satisfy the cooling requirement, while in the winter season, the exhaust heat is required for the space heating and domestic heat water system. During the peak load period, a heat storage unit can be used to increase the continuity of the trigeneration system and decrease its fuel utilization.

Operating the trigeneration system using both conventional strategies cause some issues on the energy saving and the overall efficiency as well as its operating cost. The excess energy from the electrical or thermal sources cannot be utilized and counted as an energy waste. Therefore, some studies considered in employing both of these strategies into a combined approach. Mago et al. (2009) analyzed both FEL and FTL strategies for a trigeneration system. In another study, authors proposed a combined FEL and FTL operating strategy to reduce the energy consumption, operation cost and carbon dioxide emission (Mago et al., 2010; Smith et al., 2010). Zheng et al. (2014) proposed a novel operating strategy called minimum distance (MD) and matching performance (MP) evaluations to optimize both the excess energy from the FEL and FTL.

2.6.2.2 Objective-based operating strategies

Intense developments on the optimization strategy for the combined heating and power system have resulted in several approaches such as the seasonal operation strategy, energy storage strategy, time-based, economic-based strategy and emission-based strategy. Seasonal operating strategy considers a climate change during a year to operate heat and cooling systems in satisfying both demands. The heating unit is intensively used during the winter season while the cooling unit is used thoroughly during the summer season.

During the peak load period, some options to utilize auxiliary heating or cooling units is considered. An auxiliary boiler and electric chiller could be an option as a power back up for a secondary heating and cooling units.

Kavvadias and Maroulis (2010) optimized a trigeneration system by applying two operation strategies based on climate changes in the summer and winter seasons. The study also considered an energy tariffs scenario to minimize the energy cost and maximize energy saving. The study proposed variable electricity to the cooling ratio based on the climate change to optimize the operating strategy of a trigeneration system. The study took into account three climate temperatures, i.e. hot, cool and moderate to define the variable electricity to the cooling ratio compared with the static electric to cooling ratio (SECR). Basrawi et al. (2014) considered three operation strategies for optimizing the design of an SOFC based trigeneration system operated in the baseload, thermal match and electrical match operations. Energy storages are considered in the supply performance enhancement and the energy saving. There were several studies which employed heat energy storage to increase the heat energy savings (Jiang et al., 2016; Kavvadias et al., 2010; Li et al., 2017b; Vögelin et al., 2017; Yao et al., 2017) while others preferred to utilize batteries as the electrical storage to increase the energy saving (Antonucci et al., 2017; Isa et al., 2016; Jabari et al., 2016; Misra et al., 2016; Vigneysh & Kumarappan, 2016).

Time-based operation or scheduling is a strategy to operate the system components for a defined time and period to satisfy the load demand. Operation of the prime mover, heating and cooling units are turned on and turned off in time specifically. Martínez-Lera et al. (2013) proposed a time-based operation to maximize energy saving and increase the coverage ratio of heat storage in the trigeneration system. Ondeck et al. (2015) carried out a scheduling strategy to improve the economic profit of a cogeneration system. The study proposed the selling electricity, cooling, and heat energies to the neighbors and selling electricity to the grid. Adam and Fraga (2013) also applied the strategy for designing the SOFC based heat and power generation. Three schedules proposed were for winter peak day, summer day and combined winter-summer day for two days.

In the economic-based strategy, energy tariffs scenario is mostly applied to reduce the energy cost of the system. Kavvadias et al. (2010) applied the energy tariffs scenario which were used for the electrical following, base, continuous operation and peak saving loads operating strategies. The study considered the tariffs for buying or selling from the grid. Several studies also implemented cost optimization to be compared with the FEL and FTL in reducing the system cost and the carbon emission (Hawkes & Leach, 2007; Hawkes et al., 2007).

2.6.2.3 Management-based operating strategies

To optimize the energy flow of the prime mover, the heating and cooling units, management in energy dispatch should be conducted. The objective is to satisfy the load demands and to increase profits from the system. Artificial neural network (ANN) is one of the methods that has been applied for energy management, modeling and predicting the loads. Taghavifar et al. (2015) developed an optimum design based on a predicted model using the Levenberg-Marquardt ANN method. The study implemented the intelligence technique in designing a trigeneration system and analyzed the energy destruction and the exergy efficiency from the optimum model. Anvari et al. (2015) carried out optimization in a trigeneration design using the ANN back propagation method considering energy and exergy analysis. The study claimed that the prediction model had an error of about 0.1% compared to the real model.

Fuzzy logic (FL) has been also implemented in several studies regarding power and heat generations. It determines the outputs from several fuzzy inputs which are regulated by several rules between the input and output. FL runs with multiple inputs and single or multiple outputs. Entchev (2003) employed the FL in controlling the energy output, temperature from the storage tank and the current room temperature. Linde (2016) applied a fuzzy selection to optimize the capacity and the operating strategy of a PGU unit in the trigeneration system. The study considered seven prime mover models, the operating strategy and three sub-models including energy-based, economic-based and environmental-based models. The fuzzy selection method analyzed the preferred optimum design based on an energy, economic and environmental criteria. Shaneb et al. (2012) performed an optimal operating strategy using FL-based energy management. The study considered thermal load, electrical load and storage temperature as the inputs to generate electricity from the prime mover and aim to reduce the energy cost and carbon emission.

2.6.3 Optimum size of polygeneration systems

Due to the fluctuations in the load pattern, climate condition, government regulations and other reasons, the design of the combined cooling, heating and power system should be well designed. The immature design leads to the decrease in the overall efficiency, extremely high investment cost and increases in the emission rate of the system. Moreover, overdesign the polygeneration system causes energy-wasting from the prime mover, while smaller design of the system leads to unreliable supply. The design of the polygeneration capacity are effluence by internal and external factors.

The internal factors such as specifications and capacity of the components cause different designs. For a polygeneration system, the prime mover capacity becomes the most crucial aspect of designing the overall system. The types of heating and cooling units and their efficiencies are also responsible for the increase in the overall efficiency. The size of storage units is also essential to the prime mover life cycle, continuity of the system and improve the system reliability during peaks hours.

As for external factors, some parameters such as the system applications, behavior of loads, climate conditions, regional conditions and government regulations become factors that influence the design of the polygeneration system. Based on its capacity, polygeneration can be categorized into the large, medium, small and micro-sizes. For industrial applications, the large-size and the medium-size are commonly used, while for office and academic buildings, the medium-size and the small-size are widely implemented. However, residential applications prefer to apply the small-size and the micro-size polygeneration systems which could be combined with a micro-grid power generation.

Different climates and regional conditions cause various heating and cooling requirements. For the four-season countries, heating units are highly required due to the cold weather during the fall and winter seasons, while cooling units are preferred during the spring and summer seasons. On the other hand, the countries in hot and tropical climates require higher cooling than heating for space and water. In several countries such as China and Japan, regulation does not allow exporting the excess electricity to the grid (Chen & Ni, 2014; Weber et al., 2006b), while some countries in UK and US allowed exporting electricity to the grid with feed-in tariffs regulation.

In the ASEAN countries, feed-in tariffs regulation for renewable energy sources such as solar and geothermal have been adopted in Thailand, Vietnam, Singapore, Indonesia and Malaysia (International Renewable Energy Agency, 2018). However, for other renewable energy types such as fuel cells, the regulation for exporting back to the grid has not been formalized yet. In practical, the government regulation that allows exporting the excess electricity from the user to the primary grid influence the operating strategy and design of the polygeneration system in decreasing its operating cost and increase the profits from the feed-in tariffs. For several applications in standalone configuration, utilization of battery as energy storage are essential in saving the excess energies and increasing its overall efficiency (Antonucci et al., 2015; Isa et al., 2016; Jabari et al., 2016; Misra et al., 2016; Nataf & Bradley, 2016).

After the optimal configuration is reached, sizing the components is needed to avoid discrepancies in the sources that occur during the operation. In a combined cooling, heating and power system, optimization of the capacity should be conducted for power, heat and cooling generators. Even though the prime mover is the main component influencing the heat and power generation, heating and cooling units should also be adequately designed in line with the load requirements. For a system with storage units, sizing the storages can reduce the energy cost of the system and increase its reliability in satisfying the load. An appropriate sizing is useful for auxiliary devices such as power electronic units (inverter and converter), BOP units (reformer, preheater, and combustor), boiler and electrical chiller as the secondary heating and cooling supplies. For the systems which combine the SOFC into a trigeneration system with renewable energies such as geothermal, wind and photovoltaic, sizing is needed to design the simultaneous energy generator which can meet the electrical load requirements.

Optimization in the polygeneration size has been attractive in recent years. The optimization strategy aims to design an efficient and compact system for research and commercial applications. Cardona and Piacentino (2003) optimized a trigeneration system for the Mediterranean area considering the prime mover size and absorption chiller partial load. Baghernejad et al. (2015) conducted optimization in sizing the SOFC capacity and SOFC power share for combined cooling, heating and power system. Some parameters such as electric-to-heat ratio and electric-to-cooling ratio were considered to determine the best combination between the SOFC and others prime movers. Arcuri et al. (2015) also optimized the cogeneration capacities in line with the topology evaluation. The study also considered an auxiliary boiler, selling and buying electricity scenario from the national grid. Elmer (2015) designed a trigeneration system consisting of SOFC, dehumidifier and cooling units to provide heat and power generation in a residential house. The study focused to size the SOFC capacity, dehumidifier and cooling capacity and increased its efficiency while decreasing the system cost, CO_2 emissions and primary energy demand. In another study, Wakui et al. (2016) also optimized the size of the prime mover, battery and hydrogen tank besides performing a topology evaluation.

For combined heat and power generation, the storage system is a crucial part which can affect the overall efficiency and energy saving in a trigeneration system. Martínez-Lera and Ballester (2010) proposed a novel method to design optimum heat storage system which considers heat storage volume and operation period to estimate the contribution of heat storage to maximize PES, the coverage ratio of heat load and estimated profit return. Hawkes et al. (2007) optimized the SOFC capacity and heat storage to proportionally meet the power and heat requirement of a residential home. It also analyzed the effect of utilizing a battery for energy savings in a heat and power generation system. The study considered four operating strategies and four combinations of the prime mover and heating units. Windeknecht and Tzscheutschler (2015) designed hot water storage with its operating temperature for optimizing the heat and power generation. The study focused on the effect of the operating temperature of the heat storage to the PES. Liso et al. (2015) modeled and optimized the heat storage capacity based on the input temperature of a power and heat generation system. The study was aimed to get an optimum heat accumulation during the night hours (approximately 8 hours).

Continually, many of previous studies considered the grid-connected configuration as the power back up when a polygeneration system could not fulfill the electric demand (Facci et al., 2016; Guo et al., 2013; Kavvadias et al., 2010; Wang et al., 2010a; Wang et al., 2010b, 2010c; Weber et al., 2006b). Sizing the prime mover is conducted for satisfying the load base requirement, while during the peak load duration electricity is imported from the grid. Import and export tariffs from the grid fluctuate based on the load requirements. Especially for a residential building, the rate of electricity consumption at night is frequently higher than in daylight. Regulations for the grid-connected and feed-in tariffs are not available in several countries. For example, China and Japan allow for importing electricity from the grid, yet the export regulation to the grid is still not defined (Chen & Ni, 2014). Therefore, further studies are needed to design, analyze and manage an integrated polygeneration system to be fully independent in the power source from the national grid.

2.7 Meta-heuristic-based optimization algorithms

Meta-heuristic algorithms are highly applicable in optimizing the design and operating strategy of a polygeneration system. Different from linear and non-linear programming, this method is more straightforward to define the solutions for multi-variable and non-linear problems. Meta-heuristic methods have also an excellent performance to reach the global optima instead of being trapped in the local optima. Another advantage of meta-heuristic methods over mathematical programming lies in its independence on mathematical equations to be solved. These methods use intelligence steps by generating a new, better and plenteous solutions to reach the global optimum. In conclusion, meta-heuristic methods can solve the multi-objective and multi-parameter problems and their complexities better than the mathematical programming although could take a longer time for the computation process.

Some meta-heuristic methods have been favored in optimizing the design and operating strategy of polygeneration systems including genetic algorithm (GA) and particle swarm optimization (PSO). Both methods have their advantages and disadvantages based on the applications. GA searches the solutions in a population-based searching method which is similar to PSO. However, GA can avoid a locally optimal solution by regenerating its previous solution to be a better solution for the next generation. It mimics a natural process in generating solutions with steps such as creating population, selection, mutation and crossover. Creating population and selection are natural habits to eliminate the weak candidates over the strong candidates.

Furthermore, mutation and crossover are performed to change the solutions (which are the best among others) to be better for the next generation. These two steps are the advantages of the GA to avoid from being trapped in a local optimum. However, using these methods could not guarantee that the next solutions (which have been changed) should be better than the previous. Therefore, an elitism process is applied to save the best solution and is compared to the next solution. Najafi et al. (2014) performed an analysis from exergetic, economic and environmental aspects to an SOFC based trigeneration system using multi-objective genetic algorithm method (MOGA). Li et al. (2014) carried out the optimization of power generation unit (PGU) and air conditioning unit (AC) to increase the PES of the system. Wang et al. (2015b) employed NSGA II to maximize the average useful output and minimize the heat transfer area by optimizing several operating parameters of the solar driven trigeneration system. Boyaghchi and Heidarnejad (2015) analyzed and optimized several operating conditions of a solar micro-trigeneration system to maximize its thermal and exergy efficiencies and to minimize the system cost.

On the other hand, PSO reaches solutions by generating better steps in each iteration. It mimics the social behavior of animals to catch prey in population. Without coordination, each particle will make a step to reach that prey in different step changes. Similar to this social behavior, PSO works with three levels: evaluation, update position and the best solution (global optima) and update the speed and location for each solution. The advantages of PSO is that it is more straightforward and takes less computational time. In PSO, the particle or solution movements can be tracked to control the particle step changes from being trapped into a stochastic searching. Therefore, in the optimization process, the particle velocity needs maximum and minimum constraint values to avoid the stochastic searching and enhance the overall performance of PSO.

2.8 Synthesis and analysis of the literature review

Based on the review regarding SOFC based polygeneration system, our study chooses an integrated supply for stationary power and vehicle applications to be optimized. This topic is new and beneficial for the future developments on the energy supply technology for residential applications. Based on the existing researches presented in Table 2.3, a comprehensive design which considers analysis for both electric vehicle (EV) and hydrogen vehicle (HV) has not been found yet. The existing research studies are mostly on the electric vehicles (EV) and few others focusing on hydrogen vehicles (HV) separately. Moreover, most of the existing studies only consider the heat demand. From the presented literature in Table 2.3, only one study considered both heat and cooling applications to be satisfied. However, since our study takes a tropical country such as Malaysia as the case study, cooling energy is also essential to be considered besides hot water. Therefore, a comprehensive energy supply is designed to satisfy the needs in a residential area.

In general, this study proposes an energy plan for a polygeneration system in the residential area. By using SOFC as the prime mover, the proposed system is evaluated, improved, managed and optimized based on the energy, economic and environmental aspects. Those aspects are considered to develop a comprehensive design and analysis study which is effective to be implemented into a real system. As presented in Table 2.3, none of the existing studies considered all these three aspects comprehensively. Most of the current studies considered efficiency and energy saving and some also discussed the economic criteria such as energy cost and payback period. However, there was no study considering the environmental criteria such as carbon emission and carbon savings. Therefore, to fill the gap in the system evaluation, this study considers all these criteria together.

As for improvement of the system, a renewable energy source such as photovoltaic thermal (PVT) is used as the backup for electricity and heat requirements. Compared to other types of renewable energy supply, the PVT is mostly suitable for heat and power generation (Calise et al., 2014). The combination between the PVT and low-temperature fuel cells has been studied for a polygeneration system (Awad et al., 2016; Calise et al., 2017c). From this point of view, integration between the PVT and the high-temperature fuel cells such as SOFC is also promising for the increase in the polygeneration performance.

Moreover, integrating the heat recovery with a thermoelectric generator has been shown to increase the prime mover efficiency (Zhang & Yamanis, 2007). A coupled system between the thermoelectric generator (TEG) and the SOFC has been studied by several researchers (Chen et al., 2010; Rosendahl et al., 2011; Terayama et al., 2013a; Terayama et al., 2013b; Yang et al., 2014; Zhang et al., 2017b). However, the existing studies combined the SOFC and TEG were only applied for single power generation where the thermoelectric generator could maximally recover the exhaust heat and increased in the system efficiency by about 2 to 5% (Zhang et al., 2017a). In this study, the heat recovery system utilizes the exhaust heat from the prime mover to generate cooling and hot water, which means the thermoelectric generator would be placed after or before the recovery system line. This improvement from the energy aspect will be analyzed in line with the economic and environmental criteria.

Table 2.3: SOFC application for stationary and vehicle power supply in residential area

Research topic	Objectives	Parameters studied	Methods used	Efficiency of overall system (%)	Energy criteria	Cost criteria ($)	Positive highlights	Limitations	References
Performance analysis of a SOFC based cogeneration system with electric vehicle charging	Grid-independent, decrease the thermal stress of SOFCs and to determine the nominal power of an integrated heating system	Three operation strategies studied: ELF, CEV and PS. Three configurations studied: traditional system (C1), cogeneration with traditional car (C2), cogeneration with electric car (C3)	MATLAB	-	PEC: 29,600 kWh (C1), 18,739 kWh (C2), 15,322 kWh (C3) PES: 37% (C2), 48% (C3)	Annual cost saving: 6.7% (C3)	Achieve a good energy and economic savings	Efficiency of each cases is not mentioned	Vialetto, G., 2017
Design and analysis of a SOFC based cogeneration with EV charging	Energy feasibility analysis	Two configurations studied: gas water heater and GSHP as water heater	Experimental study	60-80	PES: 16.2% (C1) 43.8 (C2)	-	The scenario was based on real profiles	EV charger is only run during night-time	Tanaka et al., 2017
Performance assessment of SOFC-based polygeneration system with hydrogen vehicle	Define the optimal configuration to minimize SOFC size	Configuration of plant (single power module and double power module)	Simulation with real input data	70.4 (conf. 1), 69.8 (conf. 2)	-	-	A simple but applicable system	The results are not complete	Perna, A., 2018
Evaluation of car parking lot supply design and operation modes for hydrogen car-comparison between catalyst reformer based and SOFC based H2 production	Energy and exergy efficiency	Car as Power Plant (CaPP) mode, corresponding to the open period of the facility which uses fuel cell electric vehicles (FCEVs) as energy and water producers while parked; and Pump mode	Simulation	-	Electric efficiency: 42.5% - 45% heat efficiency 4% - 4.5%	Exergy efficiency: 61% - 68%	The system was implemented for a rare application	Only focus on the hydrogen production	Fernandes, A., 2016

Table 2.3, continued

Research topic	Objectives	Parameters studied	Methods used	Efficiency of overall system (%)	Energy criteria	Cost criteria ($)	Positive highlights	Limitations	References
Design and analysis of a SOFC based cogeneration with EV charging	Energy feasibility analysis	SOFC size	Numerical simulation	77	PES: 30%	-	Achieved a good energy saving	EV charger is only run during night-time	Tanaka et al., 2014
Design and analysis of a SOFC based cogeneration with EV charging	Energy feasibility analysis	Electric and thermal efficiency	Numerical simulation	75	-	-	Achieved a fair efficiency for a cogeneration system	EV charger is only run during night-time	Hiroaki, K., 2013
Performance analysis of a SOFC based cogeneration system with electric vehicle charging	Energy assessment (energy saving)	Daily running distance, two configurations studied: conventional system and SOFC-CGS system	Simplex algorithm using GAMS and CPLEX	-	PES: 3.7%	-	Proposed a novel configuration	EV charger is only run during night-time Efficiency of the system is not mentioned	Wakui, T., 2012

In the existing literature, most of the studies only considered about either size optimization or operation optimization. Some studies focused on the size optimization with defined operating strategy of the system (Al-Zareer et al., 2018; Anvari et al., 2017; Bahlouli, 2018; Eveloy et al., 2017; Gimelli et al., 2017; Roshandel et al., 2018). Several other studies also considered sensitivity analysis based on single or multi-criteria to the parameters of the system design (Calise et al., 2017b; Moradi & Mehrpooya, 2017; Yao et al., 2017; Yin et al., 2018). On the other hand, the optimum operating strategy was conducted separately by other researchers based on defined sizes and design of the system (Ben Ali et al., 2018; Calise et al., 2017a; Hussain et al., 2017; Li et al., 2017a; Luo & Fong, 2017; Wakui et al., 2017).

Bi-level method optimizes the size and operation in the sequential process to reach the optimum design for single or multi-objective problems. It can be robust and comprehensive for complex system such the polygeneration. The optimization approaches method for the size optimization on the outer and the operation strategy in the inner of optimization cycle. With this approach, both size and operation points can be thoroughly optimized to reach the global optima and generate the best result to satisfy all the objectives. In several studies (Al Moussawi et al., 2017; Baky, 2010; Evins, 2015; Stojiljković et al., 2014; Stojiljković, 2017; Takama & Loucks, 1981) bi-level or multi-level optimization have proven to give performance better than the separated optimization in optimizing the design of the system. Therefore, by considering the complex components and operation in the polygeneration system, we propose to perform the design optimization using the bi-level optimization approach. The proposed optimization mechanism performs the operating strategy as the inner and the sizing as the outer layer in the optimization cycle.

From the previous studies, management-based operating strategy has been implemented for combined heat and power generation system. Compared to conventional operating strategies, the management-based operation has not been much explored to manage polygeneration system in real-time operation. Although this method is slightly complicated, management-based operating strategies can represent real-time operation strategy. It can also define the dynamic behavior of the system which can be implemented in simulation and real experimental models.

From the existing management-based methods, this study considers employing fuzzy logic (FL) due to its simplicity to be used for multi-input and multi-output (MIMO) parameters. Different from previous studies which considered multi-input and single-output parameters (MISO), this study does not only consider electricity and heat demand but also cooling demand. This study also includes the current condition of three energy storage devices, i.e. battery, heat storage, and hydrogen storage as the input management for multi-output parameters. The output parameters consist of fuel utilization and temperature of fuel cell that represent full load/part load condition of the prime mover. Moreover, charging or discharging rate for three types of storage and on/off control of electric chiller is also considered as the output of management. Due to the complexity of input and output, FL is the best management method to be applied in this study.

Due to the complexity of the design capacity and its operating strategy, the mathematical-based algorithms are not considered for solving this problem. The programming-based algorithms are also frequently trapped to local optima. Therefore, the metaheuristic-based algorithms are chosen due to its flexibility and ability to deal with the complex, multi-parameters, multi-objective problems.

Among the types of the evolutionary-based algorithm, GA and PSO are widely used to deal with the complex problems. In several cases, PSO could be suitable to solve certain problems compared to GA (Firozbakht et al., 2016; Martínez-Soto et al., 2014; Soheyli et al., 2016; Tafreshi & S.M.Hakimi, 2007). However, the performance of the algorithm depends on the complexity of the problem and parameters where any method could be suitable than others. Therefore, our study implements these two approaches for optimizing the size of a polygeneration system. The chosen method is based on the literature review done on the optimization topic in the polygeneration and tri-generation system. It is also found that this comparative study has never been conducted in previous works, especially for polygeneration systems.

2.9 Summary

Based on the review, SOFCs have been widely implemented for single and multi-power generation namely combined heat and power generation systems due to its high quality in the exhaust heat. In its application, the system also provides hydrogen and extra electricity for electric and hydrogen vehicles supply which is called the polygeneration system. Integration between a polygeneration system with automotive applications such as vehicle powers supply is a new topic which is interesting for future technology. As presented in Table 2.3, most of the existing studies considered particular cases, components, parameters and configurations of the system. However, due to its complexity in the design, as an emerging technology, this system should be configured and analyzed comprehensively to study the opportunity of this type of system to be developed for real applications.

Proposing a comprehensive energy planning for the polygeneration system is conducted through stages such as evaluating the configuration, improving the components, following by energy management strategy and finalizing by an optimally sizing. This chapter provided a literature survey on the way to optimize the design of a polygeneration system consisting of the evaluation of the structure before it is implemented. It also presented some previous works regarding the existing approaches in the operating strategy for a polygeneration system which had been implemented using conventional, simulation-based and management-based approaches. Several meta-heuristic algorithms which have been widely used for trigeneration and polygeneration systems were also discussed to gain information for researchers who interest in optimization topics, especially for the energy generations. Lastly, synthesis and analysis were presented as the critical review to analyze the gaps between this study with the previous works.

CHAPTER 3: METHODOLOGY

3.1 Introduction

This chapter discusses the methods of research conducted in this study. In Section 3.2, the explanation about the general method in conducting the research related to the optimization and management approaches for the polygeneration system is explained. The working principle of the SOFC based polygeneration system and several parameters influencing the performance of the overall system are discussed in Section 3.3. Section 3.4 provides information regarding the energy policy from the government and load profiles of residential areas in Malaysia as the case study. Evaluation criteria for the assessment of the design are presented in Section 3.5.

3.2 The general methodology of research

Collecting information from the literature was the first step to understand the state-of-art of this study. References gathered from research articles, conferences, books and electronic sources were extracted and synthesized related to the topics in the SOFC application, polygeneration, and tri-generation system as well as optimization and energy management. From the literature, analysis and synthesis of information were done regarding the highlights and limitations of existing studies to find gaps when initiated the proposed system in this study. Analysis of the previous studies was carried out firstly for the current topology of the polygeneration system.

For the SOFC application, this study focuses to explore the optimum configuration of polygeneration system which employs SOFC as the prime mover. In the literature review, the research gap regarding the objectives, criteria, and methods used in the topology evaluation was also analyzed to propose the relevant strategies for this study. Malaysia as a tropical country with the electrical, heat and cooling load requirements based on its climate and temperature changes was chosen as the case study to implement the proposed polygeneration system.

Load profiles were collected from the literature concerning the Malaysian residential and vehicle usage (Akikur et al., 2014; Mahlia & Chan, 2011). Based on the collected data, this study developed four topologies to be evaluated based on energy, economic and environmental criteria to analyze the performance of each polygeneration system. The proposed polygeneration design with the basic heat recovery system is referred to as system 1. Designing system 1 and evaluating the proposed topologies were the points in the first and second objectives of this study as given in Chapter 1 and depicted in Figure 3.1.

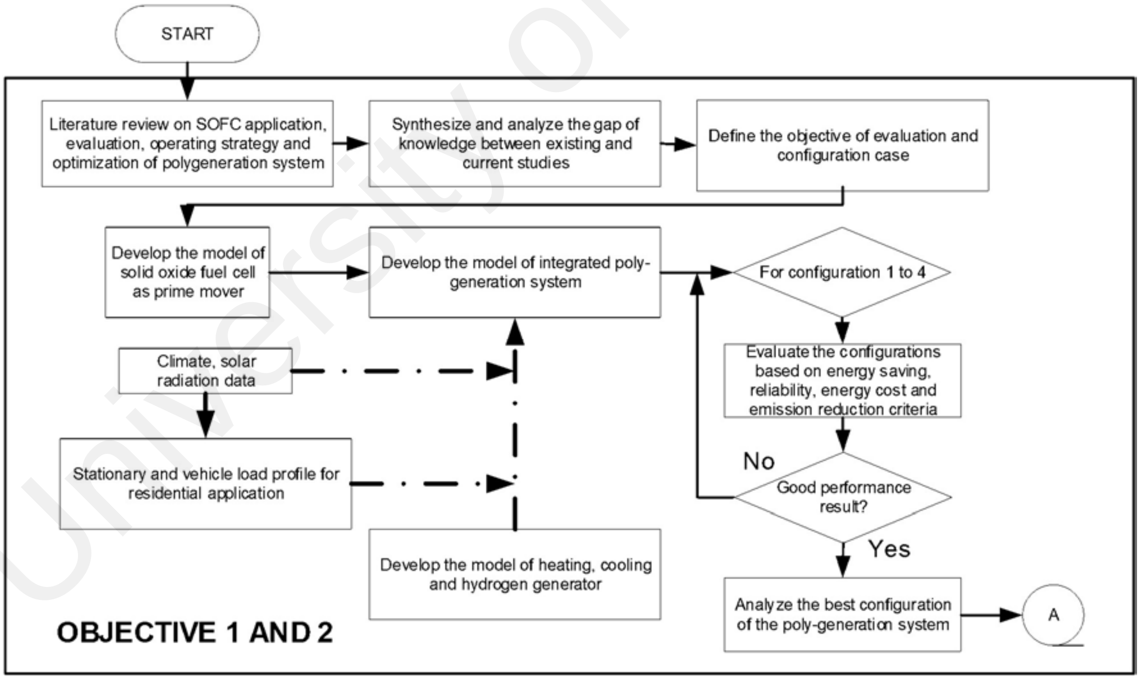

Figure 3.1: Research methodology of this study (Phase 1)

From the proposed system in Phase 1, several improvements were conducted to increase the performance of the polygeneration system. This study proposed integration between the SOFC and the renewable energy source such as the photovoltaic thermal. A thermoelectric generator was also employed to maximize utilization of the exhaust heat from the SOFC. Moreover, to prevent the system from higher supply losses, a series of battery is used as the storage. The improved system is referred as system 2. System 2 is compared to system 1 and the conventional separated system (CSS) to analyze the improvements in energy, economic and environmental aspects. The flow of methodology is depicted in Figure 3.2.

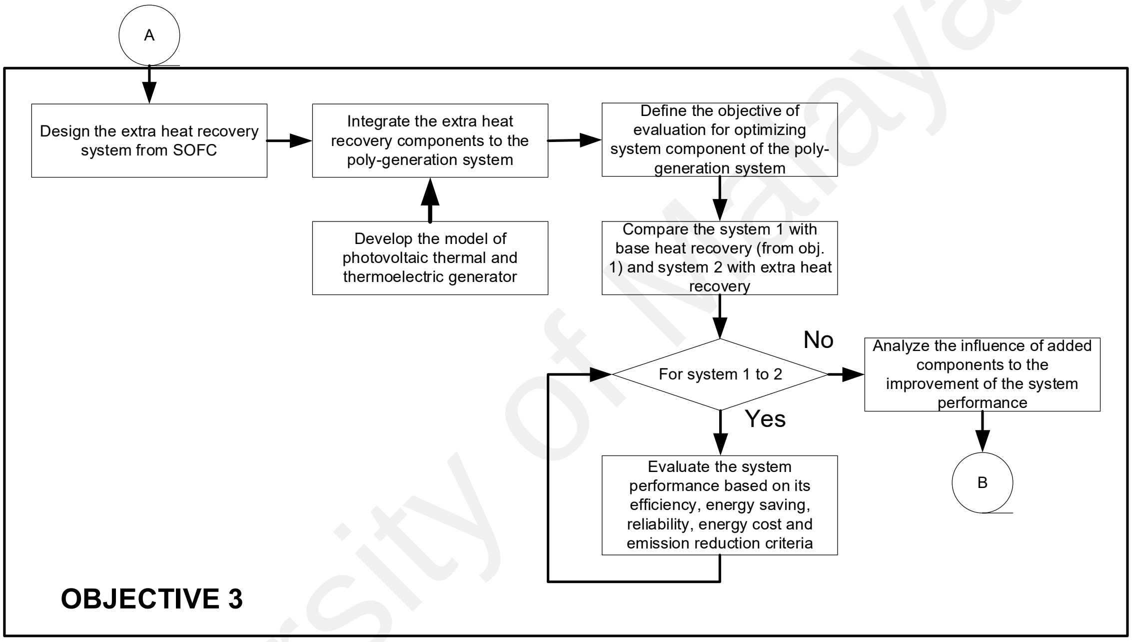

Figure 3.2: Research methodology of this study (Phase 2)

Furthermore, the improved polygeneration system will be enhanced by proposing an optimum operation strategy based on an intelligent energy management (IEM) approach. The objective of this management is to increase the PES and reduce the national grid dependence with good reliability in satisfying the electrical, cooling and heating requirements. The management is also applied to reduce the power loss of the system and improved the benefits in the economic aspect.

Since multi input and multi output parameters are included, the system is more difficult to be solved with conventional operation strategies. Therefore, fuzzy-based energy management system (FEMS) is chosen to manage the multi-level and multi-input-multi-output (MIMO) parameters of the system. Several inputs such as electrical, heat and cooling demands were considered in line with the condition of the battery. For 7860 hours, the operation strategy was simulated with several outputs, i.e. fuel utilization of SOFC, fuel temperature, chiller temperatures and electrolyzer power. Assessment of the FEMS was performed after the operation strategy was finished. Three types of fuzzy membership were also assessed to analyze the optimum operating strategy applied for the polygeneration system.

After the optimum configuration has been achieved, improvements of the system component and optimum operating strategy had been analyzed, the size of the polygeneration elements is optimized. Several decision variables regarding the SOFC, heating, cooling, storages, photovoltaic and thermoelectric generator capacities are included to satisfy the energy, economic and environmental criteria as the desired objectives. In this phase, two optimization methods based on the meta-heuristic approach namely GA and PSO were examined. Those methods were applied to analyze their performances in getting the best results for PES, the reliability of the system as well as reduction of system cost, and carbon emission as the objectives. This phase also performs analysis of several operating conditions in polygeneration which affect the overall performance of the system. The third phase of the research methodology from this study is to fulfill the fourth and fifth objectives is depicted in Figure 3.3.

3.3 SOFC based polygeneration system: working principle

Depicted in Figure 3.4, the polygeneration system consists of an SOFC stack as the prime mover, heat recovery system, hydrogen production system, storages and load demands. The SOFC operates by consuming fuel from natural gas and produces electricity and heat simultaneously. Electricity from the SOFC in the direct current (DC) form was used for the EV charging system and hydrogen production. The excess power was stored in a battery bank to reduce the supply loss during the peak load period.

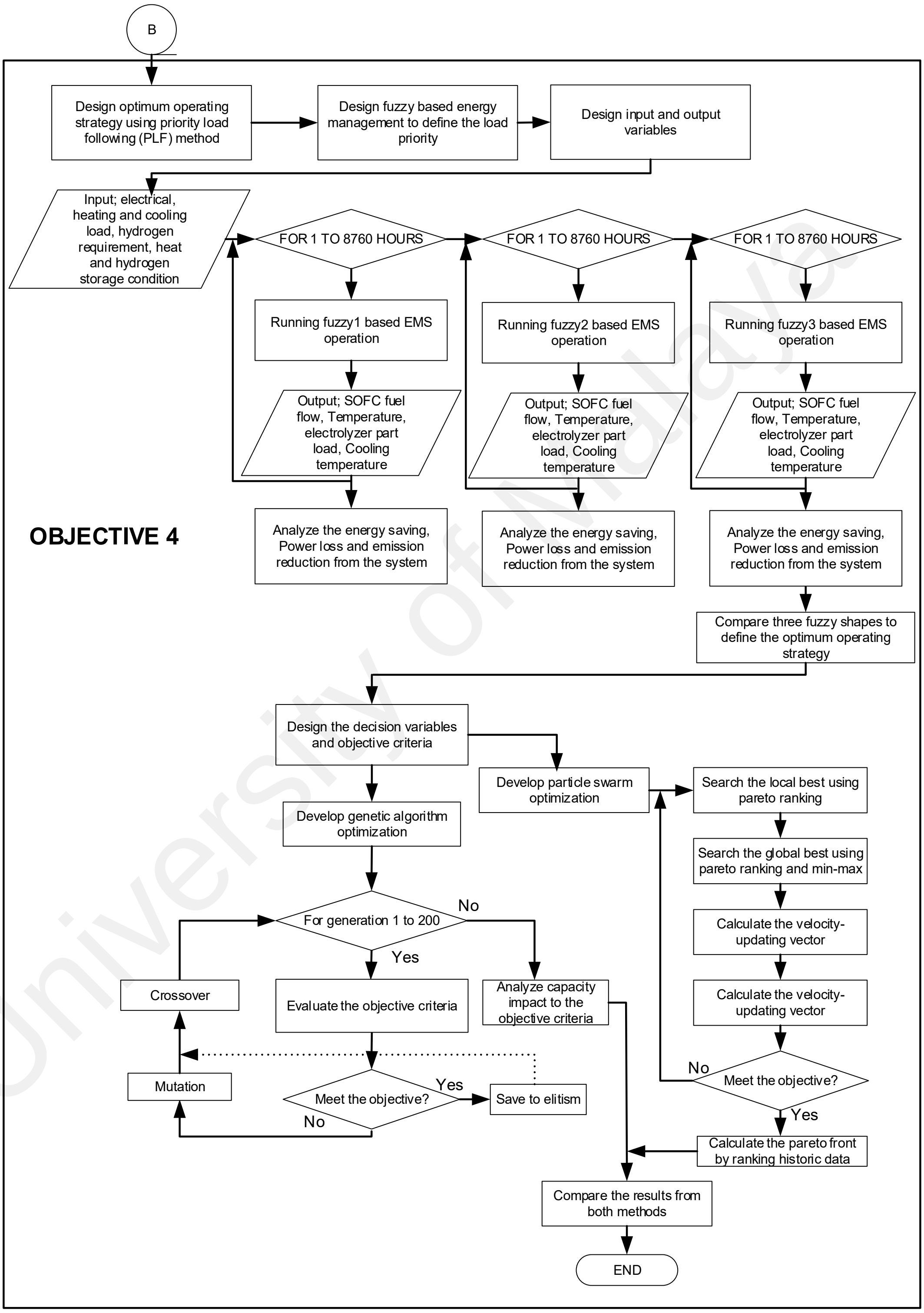

Figure 3.3: Research methodology of this study (Phase 3)

Furthermore, the generated electricity from the SOFC is also converted into alternate current (AC) and supplied to a residential area. For the hydrogen production system, electricity was consumed by the electrolyzer in generating hydrogen to supply the HV fueling station. The excess hydrogen is stored in the buffer tank, compressed and stored in the high-pressure and medium-pressure tanks or sold to gasoline retailers.

At the same time, the heat energy produced from the SOFC is used for the hot water supply as well as space and water cooling for residential users. The exhaust heat was processed in a heat recovery system consisting of the heat exchanger to produce hot water. Moreover, the exhaust heat energy is also absorbed using an absorption chiller to provide cooling space for the residential building. The unused heat from the absorption chiller was stored in a storage tank during the low consumption periods to avoid the heat loss.

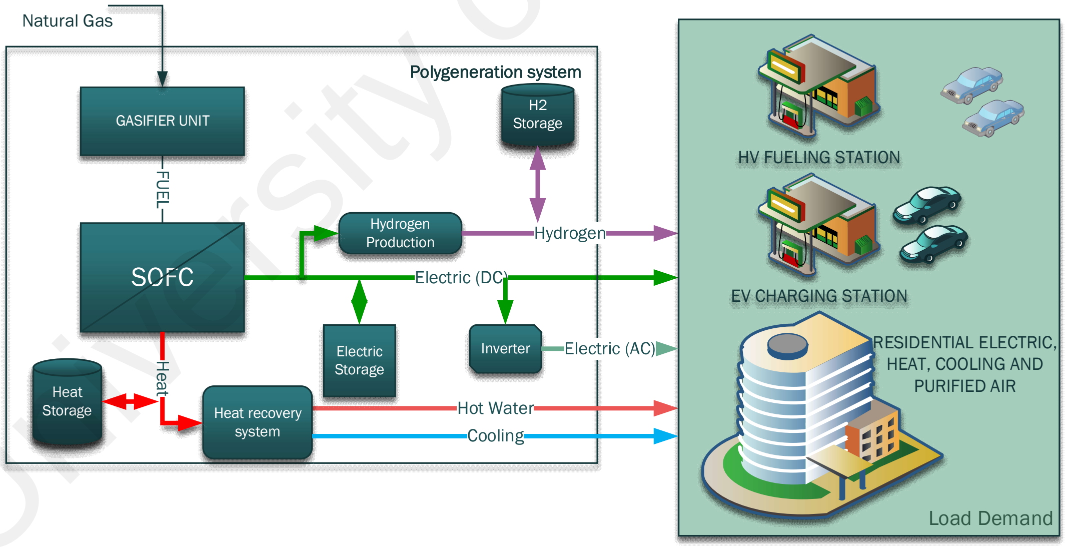

Figure 3.4: General design of SOFC based polygeneration system for the residential area

In this study, the evaluation of the performance from the system considered the continuous operation of the SOFC with full electrical power. To extend its life cycle, the continuous operation of SOFC was recommended rather than load-following operation as recommended by the company that produced the commercial SOFC for residential applications (Li et al., 2013). This operating strategy was combined with the on-off grid connection to analyze the performance of the prime mover such as the energy efficiency and PES from the system. Moreover, the evaluation also takes into account the optimal size of the prime mover to generate maximum energy and economic savings and to reduce the carbon emission from the system.

3.4 Residential load profile

3.4.1 Home load profile

This research considers Kuala Lumpur as a region for the case study. As one of the tropical countries in Asia, Malaysia has two seasons in a year, rainy and summer that makes the weather warm and humid throughout the year. It has an average rainfall of 250 centimeters a year with the average temperature of 27°C (Mahlia & Chan, 2011). It has the maximum and minimum high temperature with an average of about 33°C and 23°C, respectively starting from January until May. Meanwhile, the maximum and minimum low temperature average about 31°C and 22°C, respectively in August until December (Akikur et al., 2015; Mahlia & Chan, 2011). The details of the daily temperature during a year is depicted in Figure 3.5.

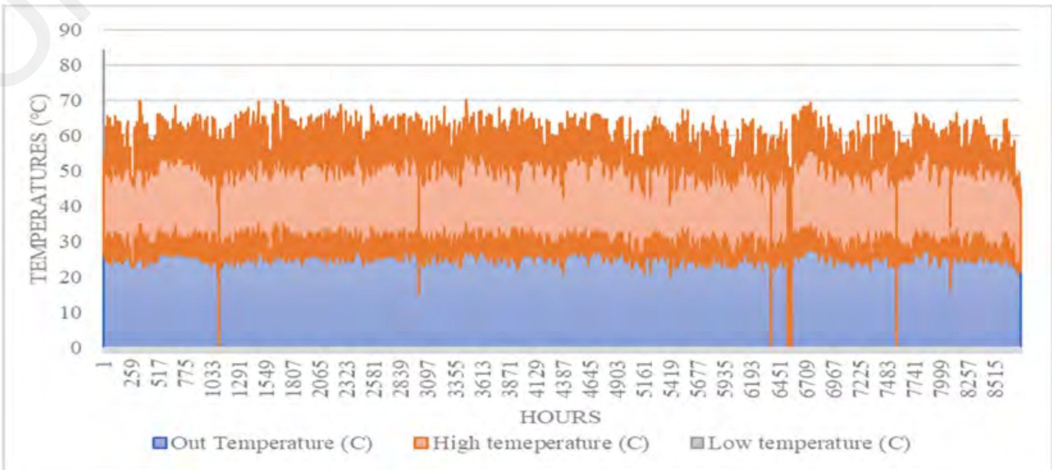

Figure 3.5: Hourly temperature in Kuala Lumpur (Akikur et al., 2015)

Moreover, the hourly solar radiation was also taken throughout the year to define the energy captured by the photovoltaic units (Isa & Rahim, 2013). From the data depicted in Figure 3.6, Malaysia has a solar radiation range of about 600 to 700 Wh/m^2 in the day which is mostly homogeneous throughout the year. This condition adds a value for implementing of the photovoltaic in generating electricity continuously.

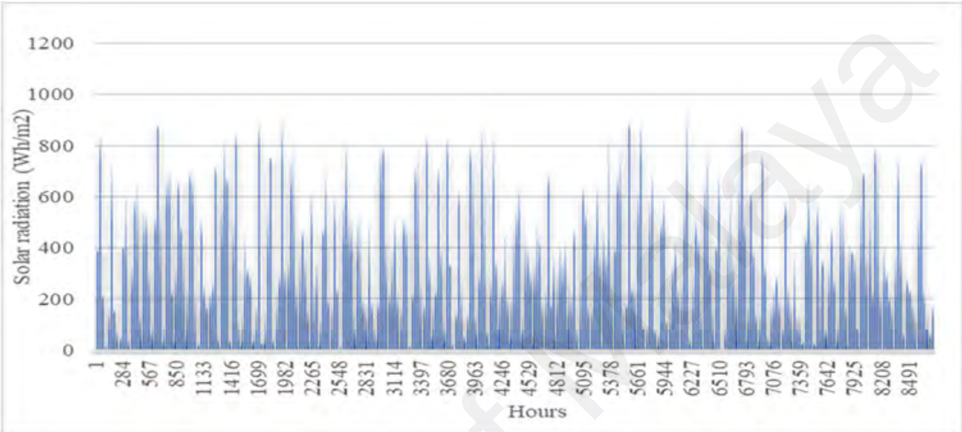

Figure 3.6: Hourly solar radiation in Kuala Lumpur (Khatib et al., 2011)

A residential area in Kuala Lumpur is considered as the case study to design the SOFC based polygeneration system consisting of 50 house units which consume electricity, cooling and heating energies. Based on a typical house in Malaysia, this study considers home with width ranging from 16' (5.48m) to 30' (7.32m) and length ranging from 50' (19.8m) to 85'(24.4m) (Abdul-Razak & Nair, 2015).

For a conventional separated system (CSS) as the reference, electricity consumption consists of heating and cooling for the electrical-based water heater and air conditioner. The amount of electricity consumed depends on the number of occupants, occupant's activity and climatic conditions in the area to determine the cooling and heating consumptions.

The annual electricity consumption is about 4387kWh per family with the yearly payment of $269 per year according to the electricity tariffs in Malaysia (TNB, 2016). Since Malaysia has a tropical season with high temperature and high humidity, water heating is considered in this study instead of room heating. Domestic water heating (DWH) is commonly used for cooking, bathing, dishwashing, face and hand washing (Mahlia & Chan, 2011). DWH consumed for a family is about 20 liter per month and the temperature of the hot water depends on the weather condition, air, water received and the ground temperature (Akikur et al., 2015).

Air conditioning normally consumes large energy which takes more than 20% of the total building energy usage in the residential house and has the highest energy cost among other appliances (Mahlia & Chan, 2011). Utilization period of the air conditioning dramatically increases from six hours to eight or ten hours per day. A high cooling profile considered in this study takes into account the utilization of ten hours per day for a single family. This scenario is considered in line with a survey mentioned that air conditioning is the highest electricity consumer for thermal comfort in residential building and 40% from occupants are willing to pay more to achieve comfort (Abdul-Razak & Nair, 2015). The cooling demand is calculated based on the outside temperature and the desired indoor temperature which is usually between 22 to 29°C, where, the data represent the thermal comfort range of the residential building in the tropical region (Tang & Chin, 2013). The profile of the air conditioning used for the Malaysian residential building is also taken from the literature (Ponniran et al., 2007). Based on these data, the cooling demand profile for a home is calculated by multiplying the electricity consumed with the coefficient of performance (COP) from a commercial air conditioning. The average COP for the commercial air conditioning is 3.0 to 3.5 and we consider the maximum COP (Koh, 2015) for this study. The hourly electricity, heat and cooling demands are depicted in Figure 3.7.

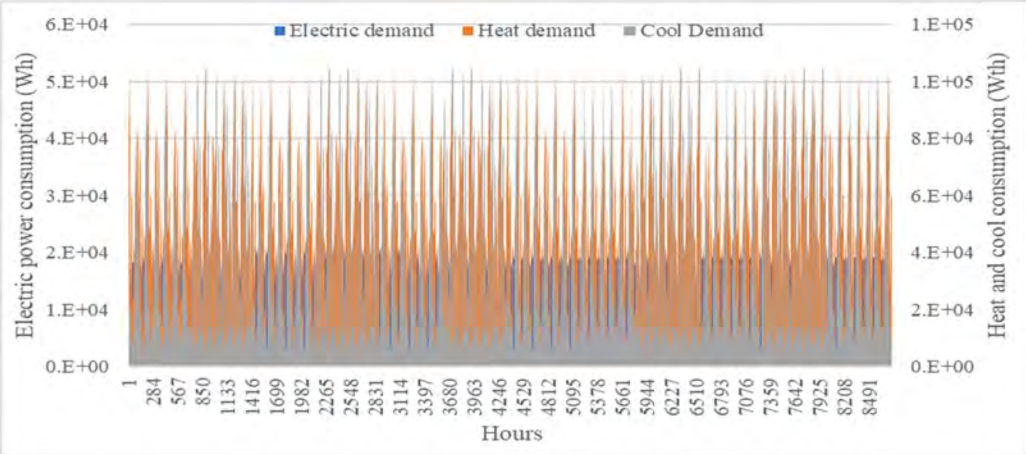

Figure 3.7: Hourly electric, heat and cool demand data of residential occupants (Akikur et al., 2015; Ponniran et al., 2007)

3.4.2 Vehicle load profile

The profile of the electric vehicles (EV) charging system and the hydrogen vehicles (HV) fueling system were calculated based on the driving distance per day. This study assumes that each family had an EV car for the polygeneration with EV charging and an HV car for the polygeneration with HV fueling in their house. The average driving distance in the city is about 15,600 km per year or 42.7 km per day (Vialetto et al., 2017). Due to the consideration of a real load profile for vehicle occupations, this study looked at three cases of driving distance based on the behavior of occupants (Tie et al., 2014). The average driving distance for the office-worker occupants (40% of the overall occupants) is approximately 36.75 km per day and for the business-worker is around 53.45 km per day (40% of the overall occupants), while for the housewife is about 36.75 km per day (20% of the overall occupants). The average driving distance per day was used to generate the hourly charging or fueling profile by multiplying with the efficiency of an electric vehicle which is about 0.2 kWh/km (Nansaia et al., 2002).

For each vehicle, it needs about 3.3 kWh per day with charging time of 2.1 hours for office-workers and housewife, while for business workers, it requires about 6.6 kWh of energy per day with charging time of about 1.5 hours. Based on the calculation of energy consumption each day, one plug-in charger can serve 9.9 kWh per day for each vehicle. The maximum demand load for ten plug-in chargers is about 39.6 kWh with the assumption that all the chargers are fully employed.

The profile of EV and HV consumption is depicted in Figures 3.8 (a) and 3.8 (b) respectively. Figure 3.8 (a) illustrates the charging pattern during weekdays, while Figure 3.8 (b) shows EV consumption during the weekends. In Figure 3.8 (a), distribution of charging time is maximum in the night from 16:00 to 23:00. with peak hour at 20:00. This study assumes that all the occupants charge their cars in private stations (outstation charger is not considered), while the workers and businesspeople charge their cars upon returning home or before they travel the office (in the forenoon). Housewives have a slightly flexible time to charge their vehicles, therefore the slot in the morning until noon is the best time to charge the car.

In Figure 3.8 (b), it is assumed that the consumption of electricity is spread evenly for each hour with an average consumption of 17 kWh per day. The occupants tend to charge their cars in the daylight between 12:00 to 20:00. Nonetheless, the plug-in charge is likewise employed in the morning for occupants who travel during the weekend. The residential charging station is assumed to be fully used during the weekend. The random data was generated from the ten charging stations in the residence with charging time of about 1 to 3.5 hours per vehicle per day.

3.5 Analysis criteria for optimum polygeneration design

3.5.1 Energy criteria

Performance evaluation based on energy criteria is an essential part of the system analysis, especially for a polygeneration system which generates more than one type of energy. This study considers three criteria for energy evaluation, i.e. efficiency, reliability and energy savings. Based on these criteria, the feasibility of the system was analyzed and compared to the conventional separated system (CSS) which consisted of grid supply (for the household electric device), natural gas fed to the boiler for heating and electrical air conditioning for the cooling system.

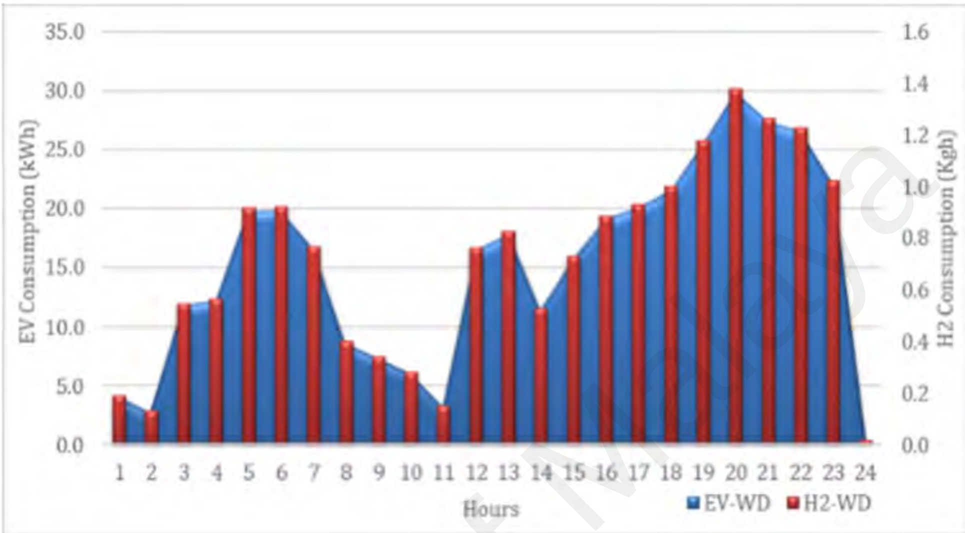

(a)

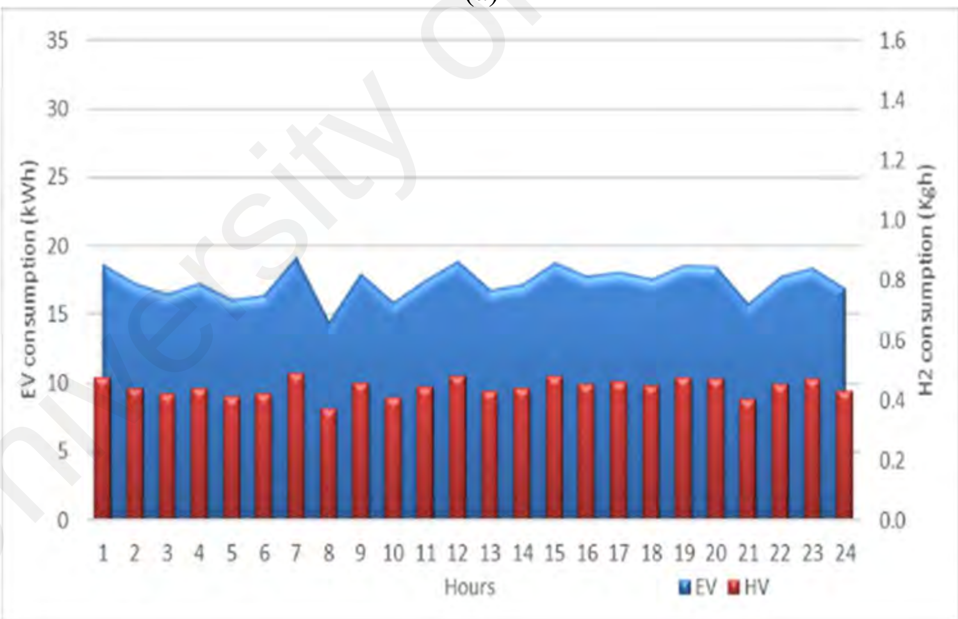

(b)

Figure 3.8: Electric and hydrogen consumption of vehicles for (a) weekday and (b) weekend

Efficiency of the polygeneration system was calculated based on the energy source from fuel and imported electricity from the grid for the grid-connected system. The outputs from the polygeneration system are electricity, hydrogen, domestic hot water and room cooling and the polygeneration efficiency is given by (Ramadhani et al., 2019)

$$\eta_{poly} = \begin{cases} \frac{E_{SOFC}+H_{hw}+H_{ac}+H_{H2}-H_{st}-H_{ex}}{H_{SOFC}+E_{H2}+{E_{add,g}}/{\eta_g}} & for\ grid-connected\ polygeneration \\ \frac{E_{SOFC}+H_{hw}+H_{ac}+H_{H2}-H_{st}-H_{ex}}{H_{SOFC}+E_{H2}} & for\ standalone\ polygeneration \end{cases} \quad (3.1)$$

Where $E_{SOFC}$is electric energy generated from the SOFC for households and EV charger (for EV connection), $E_{add,g}$ is electrical energy imported from the grid with efficiency, η_g and H_{hw} and H_{ac} are heat generated from hot water and cooling demand, respectively. H_{H2} and E_{H2} are the hydrogen energy generated by electrolyzer and the electric energy needed for running the electrolyzer, while H_{st} and H_{ex} are the energy stored in the heat storage tank and the exhaust heat energy from the polygeneration system. Since different systems had different performances, each of the configurations was analyzed compared to the CSS system.

Furthermore, the system reliability criterion was also applied for evaluating the performance in serving the loads. The reliability of the system expresses the capability of the system to satisfy the load demand without additional supply from the grid hourly throughout the year. Loss of power supply probability (LPSP) was applied as a criterion for the supply reliability to feed the demand (Ould Bilal et al., 2010; Ramadhani et al., 2013; Zhongshi et al., 2009). The LPSP calculated for electricity, heat, cooling and hydrogen demand is given as respectively

$$LPSP_e = \sum_{t=0}^{T} \frac{E_{DMN}-E_{SOFC}}{T} \qquad \text{for } E_{SOFC} < E_{DMN} \quad (3.2)$$

$$LPSP_H = \sum_{t=0}^{T} \frac{H_{HW}-H_{DHW}}{T} \qquad \text{for } H_{DHW} < H_{HW} \quad (3.3)$$

$$LPSP_c = \sum_{t=0}^{T} \frac{H_C-H_{AC}}{T} \qquad \text{for } H_{AC} < H_C \quad (3.4)$$

$$LPSP_{H2} = \sum_{t=0}^{T} \frac{Q_{HV,d} - Q_{H2}}{T} \qquad \text{for } Q_{H2} < Q_{HV,d} \tag{3.5}$$

To determine the overall reliability of the system with an EV charging station and HV fueling station, the following equations are used

$$LPSP_{poly,EV} = (LPSP_e + LPSP_H + LPSP_C)/3 \tag{3.6}$$

$$LPSP_{poly,HV} = (LPSP_e + LPSP_H + LPSP_C + LPSP_{H2})/4 \tag{3.7}$$

The LPSP value ranges between 0 and 1 to describe the reliability performance of the system. An LPSP of 1 identifies the lowest performance, which means the system had the highest losses throughout the year. On the other hand, an LPSP of 0 shows the highest performance, which means the system has no failures to satisfy the demand throughout the year. Since the grid-connected system always has available excess electricity, the criteria are calculated for heating, cooling and hydrogen demands. The calculation of LPSP in this study is presented in percentage from 0% to 100% referred from the LPSP 0 as the highest and the LPSP 1 as the lowest performance to define capability of the polygeneration supply.

The evaluation of energy saving was also considered to assess the configuration of the polygeneration system. PES is calculated to define the excess of energy from the integrated system as compared with the conventional system. Most of the PES evaluation only considers the primary energy used based on the nominal value of the supply without considering the fluctuated energy demand and energy allocated to the storage. This study considers a comprehensive approach in calculating the energy saving based on fuel consumption from the prime mover, for electricity, heating and cooling demand, imported electricity and gasoline demand profile as proposed from the previous literature (Pohl & Diarra, 2014; Pohl et al., 2016). For the conventional separated system, the PES is calculated based on the conventional power supply as well as traditional electric fuel using gasoline. The calculation of PEC of the conventional system is calculated as

$$PEC_{ref} = \frac{P_{el,d}}{\eta_g} + \frac{Q_{hw,d}}{\eta_b} + \frac{Q_c}{COP_c} + F_{car} \tag{3.8}$$

For each case, the PEC for the polygeneration systems can be calculated based on its configuration. When the electric is imported from the grid, the PES is calculated as

$$PEC_{poly,bl} = \frac{P_{poly}}{\eta_{el,poly}} + \frac{Q_{th,poly}}{\eta_{th,poly}} + \frac{Q_{c,poly}}{COP_{abs}} + \frac{P_{poly} - P_{el,d}}{\eta_g} \tag{3.9}$$

When $P_{poly} < P_{el,d}, Q_{th,poly} < Q_{hw,d}$ and $Q_{c,poly} < Q_{c,d}$, the operation of the electrolyzer is turned-off without production surplus, hence the hydrogen must be imported from retailers since it cannot support the hydrogen requirement by the vehicles fueling station. The PES is calculated as

$$PEC_{poly,se} = \frac{P_{poly}}{\eta_{el,poly}} + \frac{Q_{th,poly}}{\eta_{th,poly}} + \frac{Q_{c,poly}}{COP_{abs}} + \frac{W_{h2,elect} - W_{h2,d}}{\eta_{h2}} \tag{3.10}$$

$$PES_{sys} = 1 - \frac{PEC_{poly}}{PEC_{ref}} \tag{3.11}$$

3.5.2 Economic criteria

The economic evaluation of this system was conducted based on the energy unit cost and energy saving for each of the configurations. Energy per unit price was estimated based on annual operation and maintenance cost added to the investment cost. It can be calculated as follows

$$C_s = C_{inv} + C_{om} \tag{3.12}$$

Where C_{inv} refers to investment cost of polygeneration component and C_{om} refers the operation and maintenance cost. The investment cost of the component was calculated from the initial total purchased price multiplied by the individual replacement cost during its lifespan, given as

$$C_{inv} = C_{init} * CRF \tag{3.13}$$

Where capital recovery factor (CRF) is defined as the replacement cost of the component during its lifespan of n years with an interest rate of i% over a year, given by

$$CRF = \frac{i(1+i)^n}{(1+i)^n - 1} \tag{3.14}$$

Hence, the energy cost of i components is defined as

$$COE_i = \frac{C_{s,i}}{W_i} \tag{3.15}$$

Where COE_i is the energy cost of component i (SOFC, absorption chiller, electrolyzer) which was calculated based on the overall cost per unit energy generated from each of the components throughout the year. The system energy cost is estimated as

$$COE_{poly} = COE_{SOFC} + COE_{abs} + C_{electr} + C_{storage} + C_{grid} + C_{H2,buy} + C_{aux} - COE_{H2,Sold} \tag{3.16}$$

Apart from the energy cost, another criterion is used to evaluate the economic feasibility of the system is the cost saving ratio (CS) which is defined as the viability of the system to be implemented from the economic aspect compared to the conventional system. This criterion calculates the profit from cost saving of the proposed system compared to the conventional energy supply which is derived as

$$CS_S = \frac{COE_{ref} - COE_{poly}}{COE_{ref}} \tag{3.17}$$

Where COE_{ref} is the energy cost of the conventional separated system as the reference. Table 3.1 shows the overall component cost of the system which includes initial cost, maintenance cost, component lifetime and interest rate.

Table 3.1: Cost of polygeneration system components

Components	C_{init} ($)	C_{OM}	*n*	*i*	Reference
SOFC	2000/kW	4% of C_{init}	5 years	5%	(Akikur et al., 2015)
Absorption Chiller	576/kW	0.02% of C_{init}			(Bryant, 2011)
Electrolyzer	900/kW	2% of C_{init}	7 years	5%	(Saur & Ramsden, 2011)
Heat storage tank	135/m³	-			(Bryant, 2011)
BOP system	2% of SOFC C_{init}	-	20 years	5%	(Akikur et al., 2015)
Converter/Inverter	57.14/kW	-			(Akikur et al., 2015)
Heat exchanger	536/m²	-			(Akikur et al., 2015)
Hydrogen tank	160/Kg H_2	-	15 years	5%	(Nistor et al., 2016)
EV charger station	1800 for 2 plug-ins	3.5% of C_{init}	12 years	7%	(Madina et al., 2016)
HV fueling station	3600/Plug-in	2% of C_{init}	12 years	7%	(Nava et al., 2011)

The payback period analysis is also calculated to evaluate the potential of this system going to be implemented into the commercialized application. The calculation generates a period to earn the amount invested in the asset back from its present net cost as followed

$$PP_s = \frac{C_{s,ref}}{C_{s,ref},-C_{s,poly}} \tag{3.18}$$

Where $C_{s,ref}$ is the annual net present cost of the reference system, while $C_{s,poly}$ is the net present cost of the polygeneration system.

Moreover, electricity purchased price from the grid was based on the data given by the reference (TNB, 2016). The multi-level price scenario was considered based on the real price of electricity for residents in Malaysia. The price changes based on the rate of electricity consumption from the first 200 kWh to 901kWh onwards. The first 200 kWh of electricity purchased has a price of 0.051 $/kWh and with an increase of 100 kWh, the electricity price becomes 0.078 $/kWh and for the next 300kWh, it increases to 0.121$ per kWh. The next 300kWh purchased has a rate of 0.127 $/kWh and the last increase of 100kWh onwards has a price of 0.132$/kWh.

This scenario for the electricity price has a significant effect on the economic feasibility of the polygeneration implementation in Malaysia. Based on these tariffs, in general a family house in Malaysia spend on average of about $25 of electricity per month (Mahlia & Chan, 2011) (USD1 = MYR 4.27). The natural gas tariffs in Malaysia were referred from the data given by Malaysian government in January 2017 ("http://www.gasmalaysia.com/index.php/our-services/at-your-service/bills-payments/tariff-rates," 2017). Table 3.2 provides the electricity, natural gas, hydrogen and gasoline prices for this study (DEIA, 2016; MIDF, 2016; TNB, 2016).

Table 3.2: Cost of electricity and fuels bought from the supply

Items	Price	Units	Reference
Electricity	0.051 – 0.132	$/kWh	(TNB, 2016)
Hydrogen (buy/sell)	4.15/4.01	$/kg	(Seyezhai & Mathur, 2012)
Natural gas	0.202	$/Kg	(MIDF, 2016)
Gasoline	0.7	$/Kg	(Almeida et al., 2015)

3.5.3 Environmental criteria

Since this system utilizes natural gas as fuel for the SOFC, carbon emission from the refinement process in the fuel processor should be considered. Carbon (CO_2) emission equivalent is used as an indicator of environmental evaluation. For polygeneration systems with HV and EV fueling/charging stations, carbon emission can be calculated as follows (Sibilio et al., 2017)

$$CO_{2_{PS\_HV}} = E_{SOFC}\,\beta + E_{grid,buy}\,\alpha + F_{HV}\delta_{HV} \tag{3.19}$$

$$CO_{2_{PS\_EV}} = E_{SOFC}\,\beta + E_{grid,buy}\,\alpha \tag{3.20}$$

while for the CSS, carbon emission is calculated as

$$CO_{2\_ref} = Q_{hw}\beta + E_{grid}\,\alpha + F_{car}\gamma \tag{3.21}$$

then, carbon emission reduction (CO_2Red) and the percentage of reduction ($CO_2R\%$) are calculated as

$$CO_2Red = CO_{2\_ref} - CO_{2_{PS}} \tag{3.22}$$

$$CO_2R\% = {CO_2Red}/{CO_{2\_ref}} * 100\% \tag{3.23}$$

Where α, β and γ are emission factors associated with electricity consumption from the grid, SOFC and conventional car, respectively. For the grid consumption, the emission factor equals 573 gCO_2/kWh , while for natural gas equals 207 gCO_2/kWh (Rosato et al., 2017). The emission factor for the conventional car which equals 2343 gCO_2/Kg_g (Sullivan et al., 2004) where δ is an emission factor, according to the utilization of hydrogen from HV equal to 112 gCO_2/Kg_H (Granovskii et al., 2006).

3.6 Summary

The methodology to design an optimum polygeneration system using SOFC as the prime mover has been presented in this chapter. The flow chart of the research framework is explained and the general working principles of polygeneration system are presented. To optimize the polygeneration system, this study considers residential load profiles consisting of home and vehicle energy consumptions. Lastly, energy, economic and environmental criteria are described for the evaluation and optimization purposes.

CHAPTER 4: MATHEMATICAL MODELING OF THE SOFC BASED POLYGENERATION SYSTEM

4.1 Introduction

Development of SOFC based polygeneration system is the first step to design the optimal supply for residential energy needs. This chapter presents the mathematical modeling of the SOFC for generating electricity and heat. The heat recovery system is also modeled to provide hot water and cooling space for residential houses. Hydrogen production using electrolyzer is modeled based on electrochemical equations. Moreover, two types of storage are modeled using energy balance equations for saving electricity, heat and hydrogen. The last section presents the parameter analysis of the polygeneration components to study the performance of the prime mover, heat recovery system and hydrogen production.

4.2 Mathematical modeling of polygeneration system

The proposed polygeneration system consists of SOFC as the prime mover, absorption chiller (AC), heat exchanger (HEX) and storages as shown in Figure 4.1. In generating power, the stack SOFC system needed a balance of plant (BOP) to reform natural gas into pure hydrogen and preheated the hydrogen and air before injected into the cell. Moreover, PVT model was also integrated to increase the amount of electricity and heat generations, hence improving the system performance. An electrolyzer was included to the polygeneration system for hydrogen production purpose in the vehicle fueling station. TEG was also applied to the prime mover in maximizing the heat utilization, increasing the total efficiency of the polygeneration system. HEX was considered to provide hot water for residential houses, while the double-effect absorption chiller was employed in producing the cooling space for the homes.

The storages consist of a battery bank as the electrical storage, a hot water tank as the heat storage and a hydrogen tank as the hydrogen storage. The battery model was formulated to define the capacity of the storage for preserving the excess electricity from the prime mover, grid (for the grid-connected system) and thermoelectric generators. Sensible heat storage model was employed for saving the excess heat from the prime mover and PVT. Meanwhile, hydrogen storage was also modeled for storing the hydrogen production from the electrolyzer.

The design and evaluation of the proposed polygeneration systems were simulated by using MATLAB. There were several assumptions in the operation of the system which is described as follows:

1. All of the system components operate in steady state condition
2. All of the system capacities and operating conditions had been initially defined, any calculations for optimum size will be studied in Chapter 6
3. The auxiliary electrical components such as inverter and DC/DC converter has an efficiency of 95% based on the literature (Petrucci & Di Felice, 2009)
4. All the gas used in the stack SOFC were treated as ideal gases
5. The size of each component was based on the literature in (Akikur et al., 2015; Calise et al., 2017c; Napoli et al., 2015)
6. The specific design of the EV or HV supply station and the investment cost of the station were taken from the literature (Carr et al., 2014; Carr et al., 2016)

7. Greenhouse emission calculated in this study considered for vehicle fuel utilization stage.

4.2.1 SOFC stack system

a. SOFC cell

A stack tubular SOFC was used as the prime mover in the polygeneration system. It generates electricity and heat as the excess energy based on thermodynamic and electrochemical phenomena as depicted in Figure 4.1. This study developed a zero-dimension model of the SOFC for simplification to be integrated with other system components in developing a simulated polygeneration system.

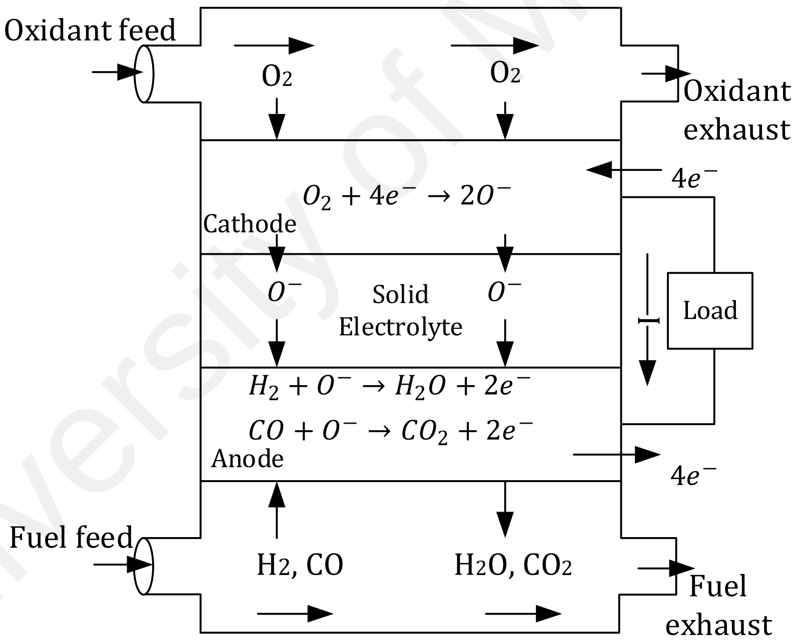

Figure 4.1: SOFC principles

From the thermodynamic principle in the gas inlet chamber, the movement of absorbed gas such as hydrogen, oxygen, and water change the partial pressure in the channel. The pressure change of the gas species in the channel could be calculated as follows (Gebregergis et al., 2009)

$$\frac{dP_{H_2}}{dt} = \frac{RT}{V_a}\left(N_{H_2}^{in} - K_{H_2}P_{H_2} - 2K_r I_{fc}\right) \tag{4.1}$$

$$\frac{dP_{H_2O}}{dt} = \frac{RT}{V_a}\left(N_{H_2O}^{in} - K_{H_2O}P_{H_2O} + 2K_r I_{fc}\right) \tag{4.2}$$

$$\frac{dP_{O_2}}{dt} = \frac{RT}{V_c}\left(N_{O_2}^{in} - K_{O_2}P_{O_2} - K_r I_{fc}\right) \tag{4.3}$$

Where $N_{H_2}^{in}, N_{H_2O}^{in}, N_{O_2}^{in}$ are the mole flow rate of the gases (H_2, H_2O, and O_2) entering the channel. The amount of hydrogen consumed is equal to the current input from the load I_{fc}. Based on the Equations. (4.1) to (4.3), the partial pressure of hydrogen and oxygen decreased in line with the increase in vapor water pressure.

Moreover, electrochemical equations were used to model the terminal voltage of fuel cell based on Nernst voltage and losses caused by activation, ohmic resistance, and concentration of gases in the fuel cell channel. The open voltage of the fuel cell was calculated as

$$E_{cl} = E_{0,cl} + N\frac{RT}{4F}ln\left[\frac{\left(P_{H_2}^{ch}\right)^2 P_{O_2}^{ch}}{\left(P_{H_2O}^{ch}\right)^2}\right] \tag{4.4}$$

Where $E_{0,cl}$ is a reference potential of the cell which depends on the operating temperature, while $P_{H_2}^{ch}$, $P_{H_2O}^{ch}, P_{O_2}^{ch}$ are the partial pressure of the gases in the channel. When the fuel cell was connected to the load, several losses occurred and decreased the output voltage given as

$$V_{cl} = E_{cl} - V_{act} - V_{ohm} - V_{con} \tag{4.5}$$

Where V_{act} is voltage loss caused during the activation moment before chemical reaction takes place. It depends on the current limit of the fuel cell (I_0) and current input from the load (I_{fc}). To calculate the activation losses, Butler-Vomer Equation was used as below

$$V_{act} = \frac{RT}{F} ln\left(\frac{I_{fc}}{I_0}\right) \tag{4.6}$$

The ohmic loss (V_{ohm}) was caused by the resistance of the electrolyte, electrodes, and interconnection between the fuel cell. The overall voltage drop could be calculated as

$$V_{ohm} = \acute{a} I_{fc} \exp\left(\varepsilon\left(\frac{1}{T_{in}} - \frac{1}{T_{fc}}\right)\right) \tag{4.7}$$

Where á and ε are ohmic resistant constant, T_{in} is temperature gas input and T_{fc} is fuel cell temperature. Voltage loss due to the increase of fuel concentration in line with the increase in load current (V_{con}) calculated as

$$V_{con} = \frac{RT}{2F} ln\left(1 - \frac{I_{fc}}{I_0}\right) \tag{4.8}$$

b. Fuel processor and air preheater

Since natural gas is used as the primary fuel for the SOFC stack, the BOP unit is needed to generate pure hydrogen from the natural gas. Fuel processor and air preheater consist of the reformer, water gas shifter and preheater. In the fuel reformer and water gas shifter, natural gas (CH_4) is converted into CO and then converted into CO_2 and H_2 through chemical reactions as follows:

$$Reforming: CH_4 + H_2O \rightarrow CO + 3H_2$$

$$Water\ gas\ shift: CO + H_2O \rightarrow CO_2 + H_2$$

The preheater is utilized to increase the temperature of inlet gases before being injected into the channel. In this work, the preheated chamber is considered to preheat the inlet gas from endotherm reactions. A burner generated the heat power with a temperature range of about 850℃ to 950℃ while the inlet gases entered the preheated chamber with a temperature of 25℃. The working temperature of the fuel cell is modeled based on the principles energy balance (Li et al., 2015) given as

$$m_s C_{ps} \frac{dT}{dt} = \sum q_x^{in}\left(h_x^{in} - h_x^{o}\right) + \sum q_x^{r} h_x^{o} - P \tag{4.9}$$

where $m_s C_{ps}$ is mass-specific heat product of the cell and h_x is the x^{th} gas per mole enthalpy written as:

$$h_x = h_{x,std} + C_{pi}\Delta T \tag{4.10}$$

where $h_{x,std}$ is the x^{th} gas per mole at the standard pressure of 0.1 MPa and the standard temperature of 283K, C_{pi} is the average constant-pressure of the gas specific heat and ΔT is the temperature change. By substituting Eq. (4.9) and Eq. (4.10) into Eq. (4.11), the temperature of the cell can be expressed as:

$$\frac{dT}{dt} = \frac{(A/B - T - P/B)}{\tau_T} \tag{4.11}$$

where

$$A = \left[\bar{C}_{pH2} q_{H2}^{in} + \left(\bar{C}_{pO2} + k_c \bar{C}_{pN2}\right) q_{02}^{in}\right] T_{in} - K_r I_{FC} T_{std}\left(2\bar{C}_{pH}\ q_{H2}^{in} + \bar{C}_{pO2} - 2\bar{C}_{pH2O}\right) - 2K_r I_{FC} H_{LHV} \tag{4.12}$$

$$\mathrm{B} = \bar{C}_{pH2}\left(q_{H2}^{in} - 2K_r I_{FC}\right) + \bar{C}_{pO2}\left(q_{02}^{in} - K_r I_{FC}\right) + 2K_r I_{FC} \bar{C}_{pH2O} + k_c \bar{C}_{pN2} q_{02}^{in} \tag{4.13}$$

$$\tau_T = {}^{m_s C_{ps}}\!/_{B} \tag{4.14}$$

The low heating value (H_{LHV}) is 241.83 kJ/mole at standard pressure and temperature. Table 4.1 demonstrates the input information for the SOFC model.

Table 4.1: Input data for SOFC model (Ramadhani et al., 2019)

Parameter	Value	Unit
Stack power nominal	100	(kW)
Operating temperature range	923 - 1123	(K)
Inlet gas pressure	1 - 3	(atm)
Hydrogen to air ratio	2.5 – 3	-
Current density	49	(A/m^2)
Cell active area	0.02	(m^2)
Fuel utilization	0.85	-
Number of cells	200	-

4.2.2 Heating unit

The heat exchanger is utilized to supply domestic hot water for multi-family homes from a water tank. Water input temperature depended on the soil temperature which is about 25°C to 30°C. Since this study considered Malaysia as the case study, the ground temperature was almost the same throughout the year. The heat exchanger model is given as

$$Q_{HEX} = m_{hex}C_p(T_{in} - T_{out}) \tag{4.15}$$

where m_{hex} and C_p express mass fluid flow rate (kg/s) and specific heat of fluid, T_{in} and T_{out} define input and output temperatures of fluid through the heat exchanger respectively. In this study, the fuel cell size is set to encompass the overall heat demand from the domestic heat water and the usage of a boiler is not considered.

4.2.3 Double effect absorption chiller

For the cooling unit, this study considered in employing a double-effect absorption chiller which generates cooling by recovering the exhaust heat from the fuel cell system. The absorption chiller had a higher coefficient of performance (COP) compared to the single-effect absorption chiller and a larger cooling capacity could be produced for the cooling space. The absorption chiller works with lithium-bromide/water as absorber/refrigerant with two generators attached, i.e. high and low-temperature generators. The model of the double effect absorption cooling was based to the literature (Lansing, 1976) by modifying the generator model from a single high-pressure to the double high and low-pressure generators. The equations of the absorption chiller model are given from Equations (4.16) to (4.34) as below:

$$\textit{Absorber concentration } (X_A) = \frac{49.04+1.125t_a-t_c}{134.65+0.47\ _a} \tag{4.16}$$

$$\textit{High temperature generator concentration } (X_{HG}) = \frac{49.04+\ .125t_{hg}-t_{lg}}{134.65+0.47t_{hg}} \tag{4.17}$$

$$\textit{Low temperature generator concentration } (X_{LG}) = \frac{49.04+1.125t_{lg}-t_e}{134.65+0.47t_{lg}} \quad (4.18)$$

$$\textit{Enthalpy of saturated liquid water } (H_l) = (t_c - 25) * 4184\ J/Kg \quad (4.19)$$

$$\textit{Enthalpy of saturated water vapors } (H_v) = (572.8 + 0.417t_e) * 4184\ J/Kg \quad (4.20)$$

$$\textit{Refrigerant flow rate } (m_r) = \frac{Q_e}{H_v - H_l} \quad (4.21)$$

$$\textit{Strong solution flow rate } (m_s) = m_r * \frac{X_{LG}}{X_A - X_{LG}} \quad (4.22)$$

$$\textit{Weak solution flow rate } (m_w) = m_r * \frac{X_A}{X_A - X_{LG}} \quad (4.23)$$

$$\textit{Medium solution flow rate } (m_m) = m_r * \frac{X_{HG}}{X_A - X_{LG}} \quad (4.24)$$

$$\textit{Liquid-liquid high-temperature heat exchanger} = \frac{t_{hg} - t_{in,lg}}{t_{hg} - t_{in,hex}} \quad (4.25)$$

$$\textit{Liquid-liquid low-temperature heat exchanger} = \frac{t_{lg} - t_{in,a}}{t_{lg} - t_a} \quad (4.26)$$

$$\textit{Specific heat of weak solution } (C_{xw}) = (1.01 - 1.23X_A + 0.48X_A^2) * 4184\ J/Kg \quad (4.27)$$

$$\textit{Specific heat of strong solution } (C_{xs}) = (1.01 - 1.23X_{LG} + 0.48X_{LG}^2) * 4184\ J/Kg \quad (4.28)$$

$$\textit{Enthalpy of superheated steam water } (H_{wv}) = 572.8 + 0.46t_{lg} - 0.043t_c \quad (4.29)$$

$$\textit{Heat balance of the condenser } (Q_c) = m_r(H_{ws} - H_l) \quad (4.30)$$

$$\textit{Heat balance of the high generator } (Q_{HG}) = m_m H_m + m_{wv} H_{wv} - m_w H_w \quad (4.31)$$

$$\textit{Heat balance of the low generator } (Q_{LG}) = m_s H_s + m_{wl} H_{wl} - m_m H_m - m_{wv} H_{wv} \quad (4.32)$$

$$\textit{Heat balance of the absorber } (Q_A) = m_w H_w - m_s H_s - m_v H_v \quad (4.33)$$

and the coefficient of performance (COP) could be calculated as

$$COP = \frac{Q_E}{Q_{HG} + W_p/\eta_p} \quad (4.34)$$

W_p and η_p are defined as the compressor consumption and efficiency which has values of 0.1 and 0.33 respectively (Huicochea et al., 2011). The input data of the model is shown in Table 4.2

Table 4.2: Input data for heating and cooling units

Parameter	Value	Unit
Domestic hot water		
Temperature of hot water	333	(K)
Double-effect Absorption Chiller		
Cooling capacity	70	(kWth)
Generator high temperature	454	(K)
Generator low temperature	414	(K)
Condenser temperature	309	(K)
Absorber temperature	304	(K)
Evaporator temperature	277	(K)
High-temperature heat exchanger effectiveness	0.7	-
Low-temperature heat exchanger effectiveness	0.7	-

4.2.4 Electrolyzer

In this study, the electrolyzer is used to produce hydrogen from the electrolysis process. A high-pressure alkaline/water electrolyzer is modeled using electrochemical equations to develop the cell model. The stack electrolyzer consisted of 45 cells linked in series with a total capacity of hydrogen producing about 1.9 Kg/h. The amount of hydrogen produced was calculated as (Calise et al., 2017c)

$$V_{cell} = V_{ref} + r' \frac{i_{EL}}{A_{cell}} + S' log \left[\frac{t' i_{EL}}{A_{cell}} + 1\right] \tag{4.35}$$

where

$$r' = r_1 + r_2 T_{EL}$$

$$S' = S_1 + S_2 T_{EL} + S_3 T_{EL}^2$$

$$t' = t_1 + \frac{t_2}{T_{EL}} + \frac{t_3}{T_{EL}^2}$$

where the hydrogen production rate is proportional to the input current and number of the electrolyzer cell. Therefore, the total hydrogen production could be calculated as

$$n_{H_2} = \eta_f N_{cell} \frac{i_{EL}}{nF} \tag{4.36}$$

where η_f is the Faraday efficiency that takes into account the parasitic current phenomena calculated as

$$\eta_f = \left[\frac{i_{dens}^2}{a_1 + i_{dens}^2}\right] a_2 \tag{4.37}$$

The electrolyzer efficiency is calculated based on its thermoneutral voltage (U_{tn}) and actual cell voltage. The thermoneutral voltage occurs due to heat generated during the electrolysis process which decreases the efficiency of the electrical consumption. Table 4.3 describes the input data of the stack electrolyzer. All the equations of the electrolyzer are adopted from the previous study (Pino et al., 2011).

Table 4.3: data for electrolyzer

Parameter	Value	Unit
Stack power	90	(kW)
Operating temperature	423	(K)
Cell area	0.1	(m^2)
Number of cells	45	

4.2.5 Storage units

The storage units consist of two tanks which are used for relieving the excess heat and the hydrogen as presented in Table 4.4. The heat storage is used to save the latent thermal from the fuel cell heat power. The storage has a maximum temperature of 80°C where the size is estimated based on the requirement of domestic hot water (DHW) for the multi-family houses. The modeling of heat storage tank is calculated as (Vögelin et al., 2017)

$$m_s C_p \frac{dT}{dt} = Q_{FC}\eta_{th,FC} - Q_{HG}\eta_{loss} - Q_{DHW} \tag{4.38}$$

Where the heat storage temperature T depends on the heat generated by the SOFC Q_{FC} and its temperature $\eta_{th,FC}$. The heat generated is diminished by self-loss in the tank η_{loss} and heat reduction Q_{HG} as well as hot water consumption by users Q_{DHW}. Heat capacity of the tank depends on the mass fluid m_s and heat capacity of water C_p. The volume of heat storage depends on its capacity (Q_{TES}), the density of fluid inside the storage (ρ_w), the specific heat of fluid (C_{pw}) and temperature difference $(T_{in,TES} - T_{out,TES})$ in the storage which is calculated as

$$V_{TES} = \frac{Q_{TES}}{\rho_w C_{pw}(T_{in,TES} - T_{out,TES})} \tag{4.39}$$

The hydrogen tank is likewise utilized to store the hydrogen production from the electrolyzer. Since this study analyzes both electrical charging and hydrogen usage of the vehicle, the hydrogen tank is an essential component to the fueling vehicle station. The high-pressure hydrogen storage is considered due to its wide usage and low investment cost based on reference (Carr et al., 2016). Three types of hydrogen tank were considered in this study which are buffer hydrogen tank, middle-pressure hydrogen tank, and high-pressure hydrogen tanks. The buffer tank operated with an operating pressure of 200 bar, while the middle and the high-pressure tanks operated at 350 bar and 700 bar, respectively (Nistor et al., 2016). The buffer tank was integrated with the electrolyzer to store the hydrogen before being compressed and transferred to the high-pressure and the middle-pressure tank. The stored amount of hydrogen can be calculated as

$$M_{H2\_Stored} = \int_0^t (M_{H2\_produced} - M_{H2\_consumed})dt \tag{4.40}$$

Table 4.4: Input data for storage units

Parameter	Value	Unit
<u>Heat storage</u>		
Capacity	453	(kWth)
Temperature of storage	353	(K)
Volume of tank	10	(m^3)
<u>Hydrogen storage</u>		
Volume of tank	20	(m^3)
Temperature of storage	353	(K)

Where the size of hydrogen can be determined by calculating the volume of the tank using the ideal gas law equation and considering the amount of hydrogen stored throughout the year (Assaf & Shabani, 2016).

4.3 Mathematical modeling of extra heat recovery system

4.3.1 Photovoltaic thermal collector (PVT)

In this study, a series of PVT panel was used to generate electricity as well as heat for the users. The model considered in this study was based on the literature (Amrizal et al., 2013), consisting electrical and heat generation models. The electrical power generation (P_{el}) considers the depletion zone in the single diode (I_d), ideal current source (I_{ph}) and current losses (I_{sh}) governed as

$$P_{el} = {}^{N_P N_S}\!/_{A_{col}} V_C\left(I_{ph} + I_d + I_{sh}\right) \tag{4.41}$$

Where N_P and N_S are the numbers of PVT panel and A_{col} is the area of the collector. The diode current is modeled as

$$I_d = I_0\left[exp\left({}^{V}\!/_{nV_T}\right) - 1\right] \tag{4.42}$$

The electrical characteristic of the diode is influenced by the potential of photovoltaic (V) as well as thermal potential (V_T). I_0 is thermal dependence diode current from $\varphi(T)$, where $\varphi(T) = T_c^3 exp\left(-\frac{E_g}{K_B}T_C\right)$ is the thermal dependence factor of the band gap energy (E_g) from the cell which is considered as a constant value. T_C is the junction temperature (K), while k_B is the Boltzmann-constant. By modifying Equation (5.2) with the temperature dependence factor, it can be written as

$$I_d = d_1\varphi(T)\left[exp\left({}^{V + r_s I_C}\!/_{nV_T}\right) - 1\right] \tag{4.43}$$

Where d_1 is the temperature dependence of the saturation diode current. For ideal current source current losses, the equation is written as

$$I_{ph} = d_2 k_\theta(\theta)(\tau\alpha)_{gen}G \tag{4.44}$$

$$I_{sh} = d_3(V_c + r_s I_c) \tag{4.45}$$

Where V_c and I_c are the potential voltage and current from the photovoltaic thermal cell. On the other hand, the thermal generation of the PVT was calculated using the following equation as

$$P_{th} = mc_P(T_{out} - T_{in})/A_{col} \tag{4.46}$$

Where m is the mass flow rate of the fluid, c_p is the fluid heat capacity, $(T_{out} - T_{in})$ is a temperature difference between the inlet and outlet of the PVT pipeline and A_{col} is the absorber area of the photovoltaic-thermal plate. In this study, the PVT cell temperature was assumed homogenous throughout the absorber plate area. Therefore, the cell temperature from the collector plate is calculated as

$$T_c = T_{in} + {}^{P_{th}}/_{F'U_L}(1 - F') \tag{4.47}$$

Where F' and U_L are the collector efficiency factor and overall convective heat loss of the PVT collector respectively.

4.3.2 Thermoelectric generator

To maximize utilization of the exhaust heat from the SOFC, a coupled thermoelectric device was used in the heat recovery system which converts the heat into electricity. There were two types of TEG used in this system namely high and low-temperatures TEG. The high-temperature TEG was placed on the air preheater and fuel processor pipes while the low-temperature TEG was located on the generators of the absorption chiller. Both of the TEGs generated electricity which was stored in the battery and was used as backup to the prime mover during the high period of electricity consumption.

The model of the TEG is based on the literature (Terayama et al., 2013a; Terayama et al., 2013b; Terayama et al., 2013c). For the high-temperature TEG, the inlet flow changed based on the exhaust heat from the SOFC stack system with temperature of 181°C flows to the high temperature side of the TEG. For the low temperature side, the inlet flows temperature changed based on the output flow temperature from the heat exchanger with temperature of 100°C. For the low-temperature TEG, the temperature of about 141°C flows to the high-temperature of TEG from the high-pressure generator of the absorption chiller. Meanwhile, the cooling side temperature was based on the exhaust flow from the photovoltaic thermal fluid. The heat transfer at the high temperature side is calculated as

$$Q_{in} = h_{ex} A_{pl} \left(T_h - T_{hj}\right)$$
$$= \alpha T_{hj} I_{TEG} - {}^{1}\!/_{2}\, R_{TEG} I_{TEG}^{2} + K\left(T_{hj} - T_{cj}\right) \qquad (4.48)$$

while the heat transfer for the low temperature side is governed as

$$Q_{out} = h_w A_{pl} \left(T_{cj} - T_c\right)$$
$$= \alpha T_{cj} I_{TEG} - {}^{1}\!/_{2}\, R_{TEG} I_{TEG}^{2} + K\left(T_{hj} - T_{cj}\right) \qquad (4.49)$$

the TEG power is calculated as

$$P_{TEG} = R_L I_{TEG}^{2}$$
$$I_{TEG} = {}^{\alpha\left(T_{hj} - T_{cj}\right)}\!\big/_{\left(R_{TEG} + R_L\right)} \qquad (4.50)$$

Where h_{ex} *and* h_w are the heat transfer coefficient between the exhaust gas and the TEG modules and between the TEG modules and the water respectively. T_h *and* T_{hj} are the temperatures from the exhaust gas and the TEG module in the high temperature side. T_{cj} *and* T_c are the TEG and water temperatures at the low temperature side respectively. K is the thermal conductance (W/K), calculated as $K = \lambda\, {}^{A_{el}}\!/_{t}$, where t is the module height (m), A_{el} is the element cross-sectional area (m^2) of the TEG module, α is the Seebeck coefficient (V/K), while λ and ρ are the thermal conductivity (W/mK) and resistivity ($\mu\Omega m$) of the thermoelectric material, respectively.

4.3.3 Electric storage

The battery is used as an electrical storage to store the excess electricity from the SOFC, TEG and PVT. The battery model was based on the literature (Brahman & Jadid, 2014; Soheyli et al., 2016; Vigneysh & Kumarappan, 2016). The state of charge (SOC) is an indicator for charging and discharging rate from the sources. The battery was also used to reduce the grid utilization and increased the efficiency of the polygeneration system. The energy flow equations for charging and discharging states are calculated as

$$E_{bat_{charg}} = E_{bat\_now} + (E_{PVT} + E_{TEG} + E_{SOFC})/\eta_{ch} - E_{demand} \quad (4.51)$$

$$E_{bat_{discharg}} = (E_{bat\_now} - E_{demand})/\eta_{dch} \quad (4.52)$$

and the SOC was calculated as

$$SOC_{bat} = {}^{E_{bat\_now}}/_{C_{bat}V_{bat}} \quad (4.53)$$

Where $C_{bat}\, and\, V_{bat}$ are the capacity of the battery (Ah) and battery voltage (V) respectively. As a power backup, the battery is operated under some constraints of SOC to increase the life cycle of the battery. The constraint of battery operation is determined as

$$SOC_{min} < SOC_{bat} < SOC_{max} \quad (4.54)$$

The maximum and the minimum SOC values affect the size and the operation of the battery (Brahman & Jadid, 2014). For evaluation purpose, the value of SOC_{min} and SOC_{max} were chosen to be 0.4 and 0.9 respectively.

4.4 Parameter analysis of the components in the polygeneration system

In this study, parameter analysis of the components in the polygeneration system was conducted for prime mover power generations, cooling and hydrogen production. As a prime mover, the SOFC behavior is essential to be studied. Therefore, the current study analyzed both thermodynamic and electrochemical phenomena and the fluctuated temperature during the production process. Moreover, performance analysis for the double-effect absorption chiller is also necessary to be studied due to the high consumption of cooling from the residential building. Furthermore, the hydrogen production system using electrolyzer was also analyzed based on the working conditions of the cells.

4.4.1 Model validation of the SOFC with single cell

Validation of the modeling SOFC model was carried out by comparing the developed model with previous studies (Gebregergis et al., 2009; Lakshmi et al., 2013; Ullah et al., 2015) using simulated and experimental data. Due to the limitation in obtaining exhaustive data for all outputs, the validation process took into account several essential output variables such as cell voltage, electrical power and electrical efficiency, heat power and heat efficiency.

The I-V characteristic of the standard operating temperature is depicted in Figures 4.2(a) to (d) based on the literature (Gebregergis et al., 2009; Lakshmi et al., 2013). From these results, it can be seen that the changes in the cell voltage depend on the working temperature and hydrogen flow rate. The increase in temperature and the flow rate simultaneously increased the cell voltage and vice versa.

In Figures 4.1(a) and (b), validation of the current model was conducted by using the model taken from the literature based on an experimental study (Gebregergis et al., 2009). Meanwhile, Figures 4.1(c) and (d) showed validation between the current model and the literature from Lakshmi et al. (2013). Comparisons between the proposed model and the previous studies in Figure 4.2(a) shows that the I-V curves between the proposed model and the real data at temperature points of 1073K and 1123K have similarities better than the curves at temperatures of 973K and 1023K. The relative error between the proposed model and the experimental data from Gebregergis et al. (2009) at the temperature of 1073K and 1123K was about 0.061.

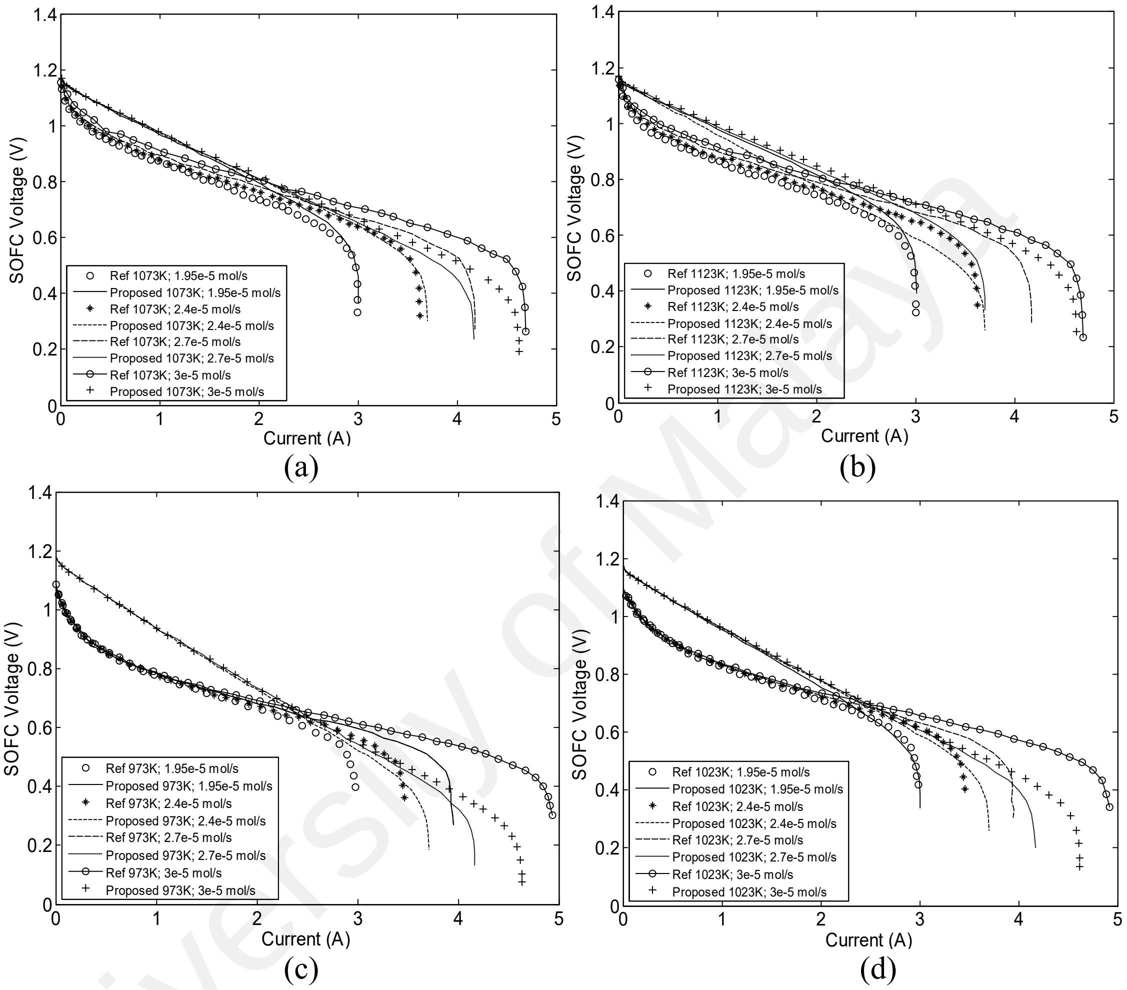

Figure 4.2: I-V curves for different input of hydrogen flows at (a) temperature 1073K; (b) temperature 1123K; (c) temperature 973K and (d) temperature 1023K

On the other hand, the relative error between the proposed model and the simulated data from Lakshmi et al. (2013) showed a higher value compared to the experimental data from Gebregergis et al. (2009). At a temperature of 973K, the relative error was about 0.102 while at the temperature of 1023K the error was approximately 0.0802. Based on the figures, the proposed model had higher voltage slope when the load current was increased due to the steep increase of ohmic losses.

Furthermore, the experimental data from Ullah et al. (2015) was also used as the validation for the electrical power, electrical efficiency, heat power and heat efficiency. Experiments were carried out in the laboratory using a single SOFC cell (Ullah et al., 2015). Table 4.5 presents the validation data where the proposed model was closely similar to the experimental data. For the electrical power based on the changes of fuel flow rate, this study showed a lower power generation compared to the reference as well as for the electrical efficiency. The differences were possibly caused by the activation and ohmic losses that affect the voltage and power loses. Moreover, the specific heat enthalpy of the gas species might be different since this study defined the coefficients by the specific values which may not match with the real experimental measurements. However, all these results confirmed that a good level of accuracy and reliability can be achieved in using our proposed SOFC model.

Table 4.5: Validation of electrical and heat for power and efficiency

Temp (K)	Fuel flow rate (mol/s)	Maximum electrical power (W)		Maximum electrical efficiency (%)		Maximum thermal power (W)		Maximum thermal efficiency (%)		Maximum overall efficiency (%)	
		Ref[1]	This study	Ref[1]	This study	Ref[1]	This study	Ref[1]	This study	Ref[1]	This study
923	9.0e-05	0.96	1.01	25.19	23.53	2.06	2.13	55.23	55.13	80.42	78.66
	1.1e-05	1.33	1.31	24.41	22.03	2.79	2.61	53.08	45.26	77.49	67.29
	1.2e-05	1.38	1.4	19.57	21.23	2.83	2.84	41.16	41.29	60.73	62.52
1023	1.1e-05	1.58	1.41	24.72	25.61	3.72	3.15	58.66	54.29	83.38	79.9

Ref[1]: Data were taken from Ullah et al. (2015)

4.4.2 Electrochemical behavior of SOFC

We analyzed six parameters of the operating point of the SOFC model, i.e. fuel utilization (FU), current limiter (I_{lim}), air to fuel ratio (AFR), pressure (P_{FC}), fuel temperature (T_{FC}) and air temperature (T_A). Analysis of these parameters are presented as follows:

a. Fuel utilization

At constant utilization, FU represents the utilization factor of continuous fuel flow rate. Referring to Figures 4.3(a) to (c), the increase in fuel utilization reduced the output power, voltage and electrical efficiency. The changes in the fuel utilization from 0.7 to 0.9 decreased the maximum point of output power by about 0.25W. As the operating fuel utilization is increased, the electrical efficiency increased and at the same time the voltage dropped drastically, and the load current limit decreased. On the other hand, the increase of fuel utilization gave a significant effect on the rise of temperature, heat generation and efficiency where the heat efficiency escalated by about 0.3 and fuel utilization increases from 0.7 to 0.9.

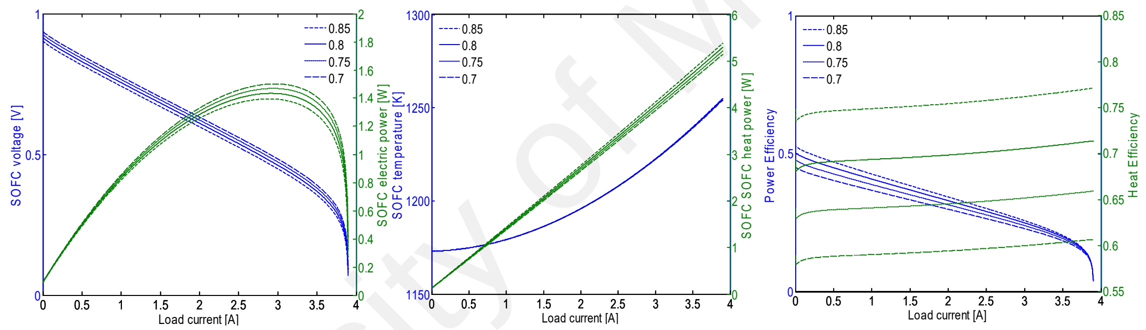

(a) (b) (c)

Figure 4.3: (a) V-P-I characteristic; (b) T-Q-I characteristic; (c) $n_{real} - \eta_{tfc}$-I characteristic of SOFC at the different fuel utilization variations

b. Current limit

This study also analyzed the effect of current limiter to the output parameters of the SOFC cell as depicted in Figures 4.4(a) to (c). By increasing the current limit of the cell from 3A to 5.5A, the output voltage, electrical power and electrical efficiency increased. However, the current limit did not give any effects on the temperature, heat power and heat efficiency. The increase in electrical power was about 0.3 W when increasing the current limit from 3 A to 5.5 A.

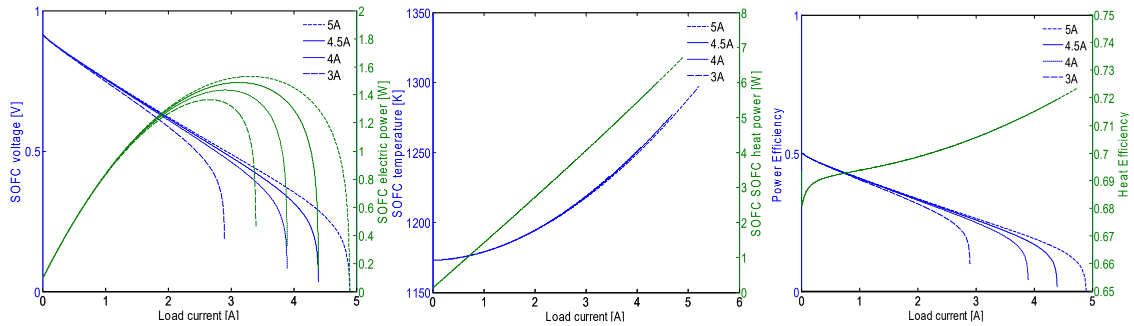

(a) (b) (c)

Figure 4.4: (a) V-P-I characteristic; (b) T-Q-I characteristic; (c) $n_{real} - \eta_{tfc}$-I characteristic of SOFC at the different current limit variations

c. Air to fuel ratio

AFR is the ratio between the molar flow rate of air to fuel particularly in combusting processes. The low AFR affected SOFC temperature which would increase and could cause material damage while the high AFR caused low heat generation and heat efficiency. This study analyzed six points of AFR value in ranges of 0.5 to 3.5. It was found that the parameter affected mostly the SOFC output performances. The higher value of AFR impacted the increase in output voltage, power and electrical efficiency due to the reduction in the over-potential loss. However, the output temperature decreased and affected in the reduction of heat generation and heat efficiency as depicted in Figures 4.5(a) to (c).

d. Fuel pressure

The pressure effects as shown in Figures 4.6(a) to (c) caused the increase in cell voltage and power drop. The maximum power generated was about 1.5 W per cell. The increase in the cell pressure affected all output performances which increased the voltage and output power and decreased the heat generation and heat efficiency.

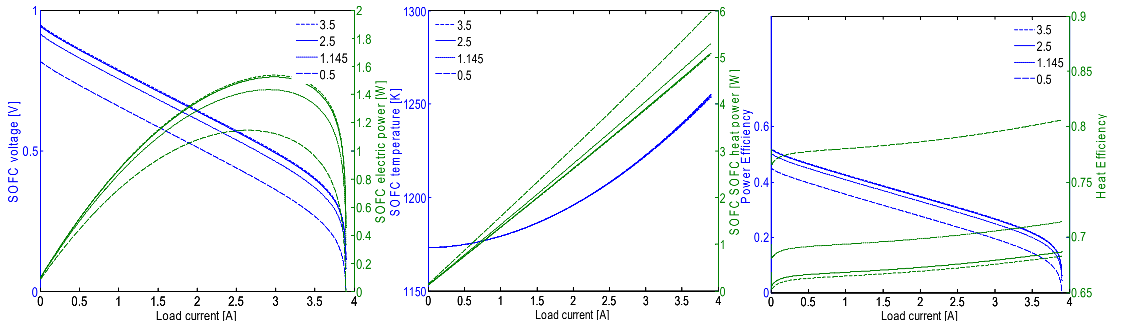

(a) (b) (c)

Figure 4.5: (a) V-P-I characteristic; (b) T-Q-I characteristic; (c) $n_{real} - \eta_{tfc}$-I characteristic of SOFC at the different air to fuel ratio variations

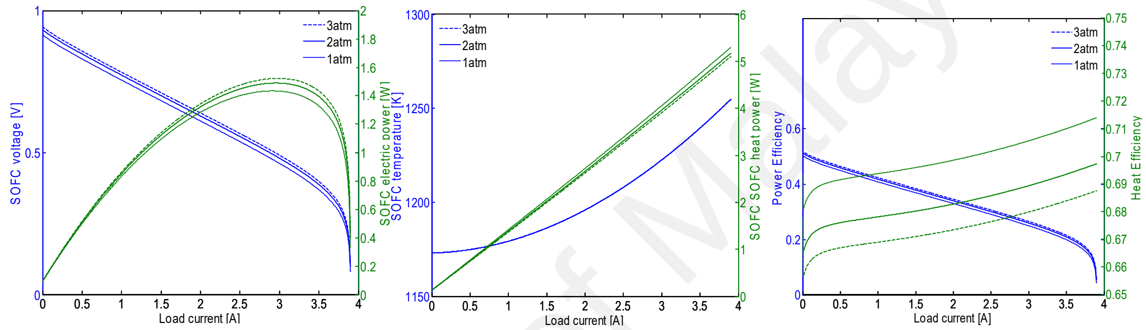

(a) (b) (c)

Figure 4.6: (a) V-P-I characteristic; (b) T-Q-I characteristic; (c) $n_{real} - \eta_{tfc}$-I characteristic of SOFC at the different pressure variations

e. Fuel temperature

The fuel temperature had significant effects on the increase of electrical voltage, power and electrical efficiency, which at the same time decreased the output temperature, heat generation and heat efficiency. As depicted in Figures 4.7(a) to (c), the lowest point of temperature in this study (973K) increased the maximum power from 1W to 1.5W and maximum efficiency by about 10%, while it also decreased the voltage drop by 0.1V. The reduction of fuel temperature from 1373K to 973K causes depletion of the heat generation and efficiency by about 1W and 10%, respectively.

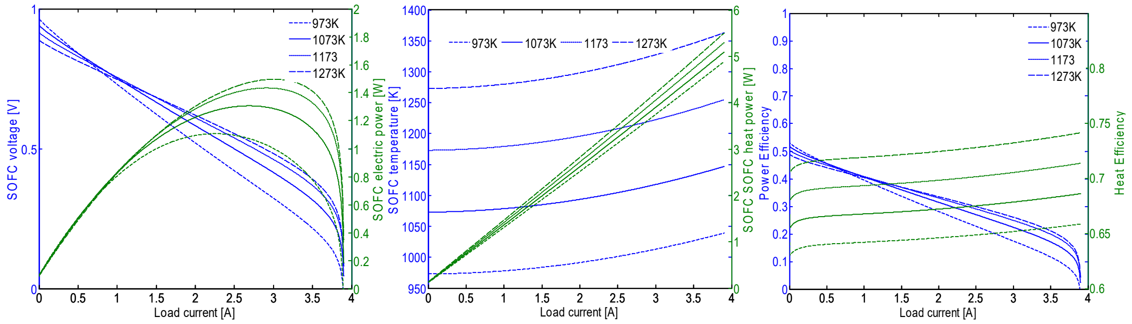

(a) (b) (c)

Figure 4.7: (a) V-P-I characteristic; (b) T-Q-I characteristic (c) $n_{real} - \eta_{tfc}$-I characteristic of SOFC at the different fuel temperature variations

f. Air temperature

The air temperature parameter did not have any significant effects on the output parameters for the single cell SOFC as depicted in Figures 4.8(a) to (c). The output patterns of the six SOFC parameters were almost similar for the changes of air temperature because the air temperature was not used as the reference temperature in SOFC operation. Therefore, this study considered using similar temperature for the fuel and the air in the fuel cell operations.

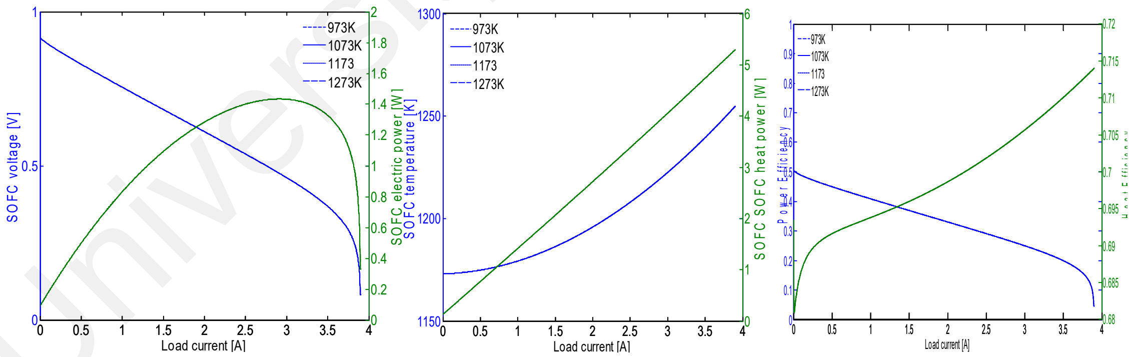

(a) (b) (c)

Figure 4.8: (a) V-P-I characteristic; (b) T-Q-I characteristic; (c) $n_{real} - \eta_{tfc}$-I characteristic of SOFC at the different air temperature variations

4.4.3 Double-effect absorption chiller

The COP and the temperature of the high-pressure generator from a double-effect absorption chiller were analyzed based on the changes in the input temperature of the high-pressure generator, low-pressure generator, condenser, evaporator and absorber.

Furthermore, the coefficient of the heat exchangers at the high-temperature and low-temperature generators effects to the COP of the absorption chiller were also analyzed.

a. High-pressure generator

The COP for the absorption chiller was analyzed based on the high-pressure generator temperature. As depicted in Figures 4.9(a) to (f), the range of temperature for the high-pressure generator has to be in the range of 150℃ to 175℃ to get the desired COP. Beyond this range, COP could not be calculated due to crystallization effects. From the figures, the COP increased in line with the increase in generator temperature. At the temperature difference of 70℃ between the high and low-pressure generators, it achieved the highest COP compared to the different in value of 75℃ and 80℃. The increase in the evaporator temperature could decrease the absorption chiller performance which was similar to the condenser temperature effect. However, absorber temperature has a different effect compared to others. With the decrease in the absorber temperature, the absorption chiller performance increased significantly. In conclusion, low-pressure generator and absorber temperature have a significant effect on the increase in the absorption chiller performance compared to other parameters due to the generator and absorber temperatures effect on the Li-Br concentration as the solution and the water as the refrigerant.

b. Absorber temperature

The effect of absorber temperature to the absorption chiller performance is depicted in Figures 4.10(a) to (f). In this study, the temperature of the absorber was set at 15℃ to 40℃ as per the literature (Wakui & Yokoyama, 2015). The increase in the absorber temperature and heat exchanger coefficient gave significant effect to the absorption chiller performance. However, the coefficient decreased significantly in line with the escalation in the absorber temperature by more than 30°C. As the high and low-pressure generator temperatures increased, the absorption chiller performance increased, while this increase in the evaporator and condenser temperatures decreased the coefficient of performance.

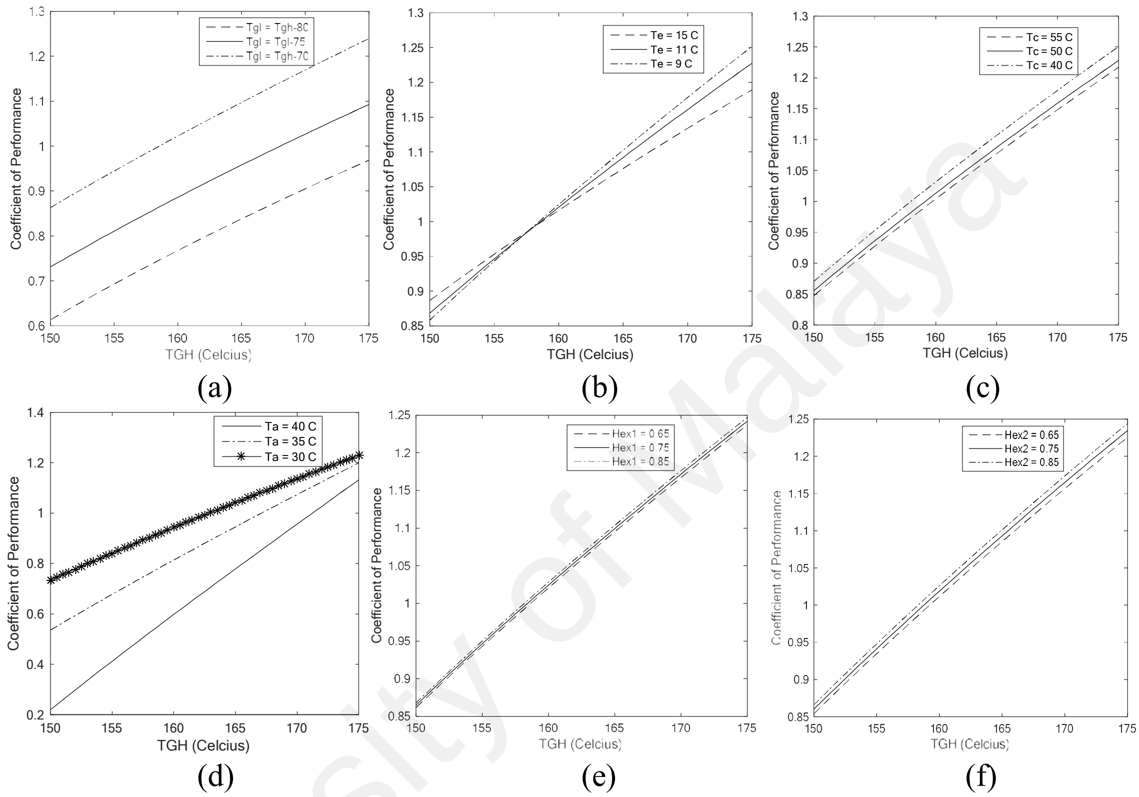

Figure 4.9: Coefficient of performance regarding the high-pressure generator temperature at the differences of (a) low-pressure generator, (b) evaporator, (c)condenser, (d) absorber temperatures and (e) low-temperature and (f) high-temperature heat exchanger coefficients

4.4.4 Electrolyzer

The analysis of electrolyzer parameters was conducted with respect to the power consumed by the cells. The output parameters studied were electrical efficiency, hydrogen generation, heat consumption and output voltage. The input and output parameters were analyzed based on the difference in the cell area, the number of cells and temperature of the cell.

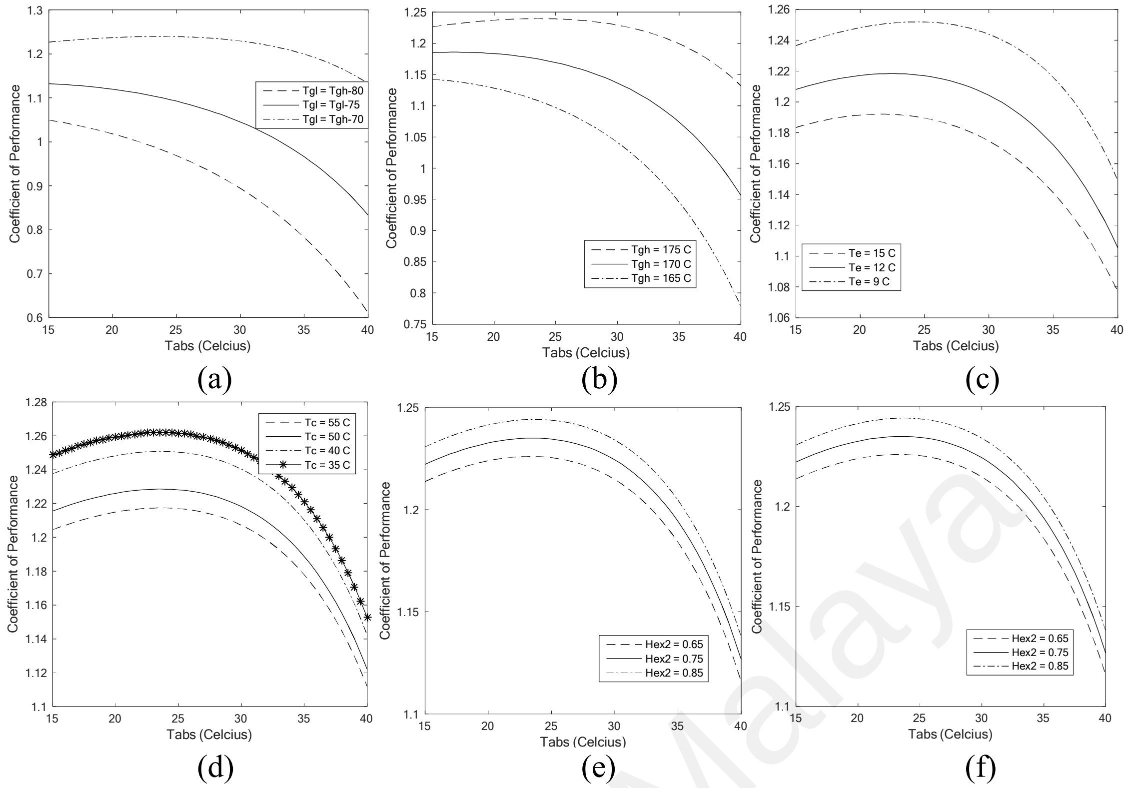

Figure 4.10: Coefficient of performance in regard to the absorber temperature at the differences of (a) low-pressure generator, (b) high-pressure generator, (c) evaporator, (d) condenser temperatures and (e) low-temperature and (f) high-temperature heat exchanger coefficients

a. Cell area

The effect of the cell area which influences electricity consumed was analyzed based four output parameters as depicted in Figures 4.11(a) to (d). As the ell area is increased, the efficiency escalates at a lower slope, while the smaller cell area makes the slope in the electrolyzer efficiency sharper at the input power from 0.1 kW to 0.5kW and after that, the efficiency decreased gradually. The increase in power consumed also escalated the hydrogen generation and the smaller the cell area the higher the hydrogen production. However, the decrease in the cell area caused lower hydrogen production below 70% of the maximum electrolyzer power rate. As the cell area was increased, the heat consumption also increased. The electrolyzer cell voltage also increased in line with the increase in the cell area with the maximum value of about 9V per cell at full load operation.

b. Number of cells

For similar cell area, the increase in the cell number gave different effects to the electrolyzer performances as depicted in Figure 4.12(a) to (d). The increase in the cell number gave a fast rise of efficiency at below 50% of the part-load operation. However, above 50% of the electrolyzer power rate, the efficiency starts to decrease in line with the increase in cell number. The hydrogen production for the 3 cells had an optimal value with a linear slope and highest hydrogen production compared to the other cell amounts. From the heat consumption patterns, the increase of cell number would reduce the consumed heat which affect to the rise in the cell efficiency. The increase in the cell number also increases the generated cell voltage, hence its efficiency increased as well. From these figures, it can be concluded that the cell number gives better improvement on the voltage generated compared to the cell area.

c. Cell temperature

The effect of cell temperature was not too significant as compared to the cell number and cell area. As depicted in Figures 4.13(a) to (d), the increase in the cell temperature improved its efficiency and hydrogen generation and at the same time reduced the heat consumption and the output voltage. This happened due to the temperature effects on the reaction rate, hence increasing the hydrogen production and the cell efficiency.

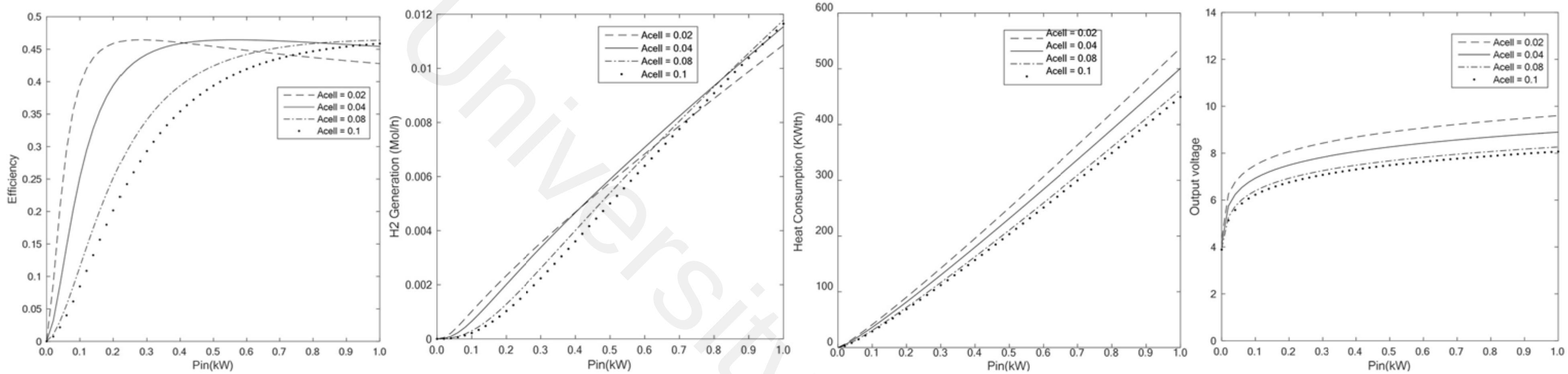

(a) (b) (c) (d)

Figure 4.11: (a) electrical efficiency, (b) H_2 generation, (c) heat consumption and (d) output voltage against power input electrolyzer at the cell area differences

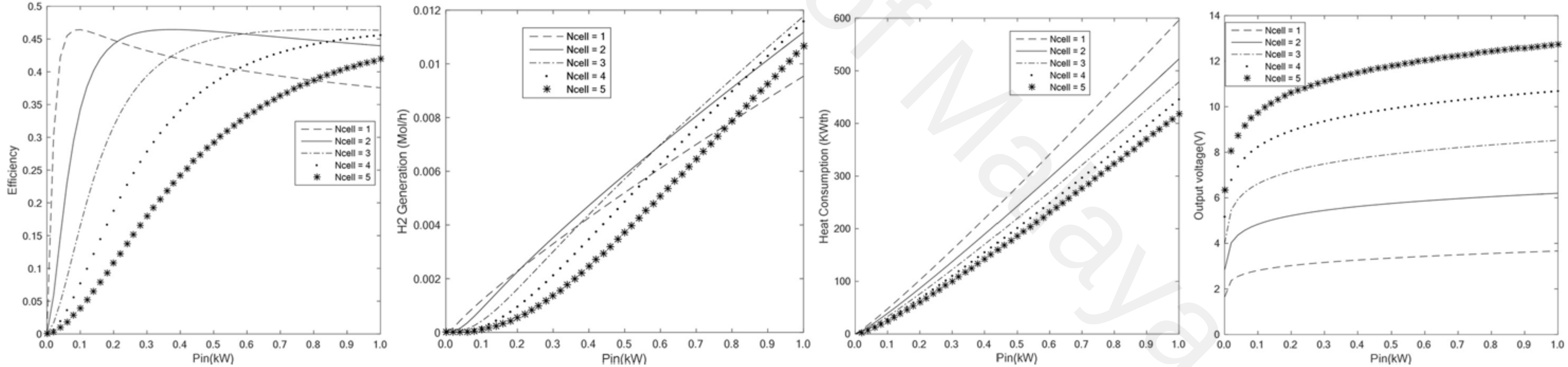

(a) (b) (c) (d)

Figure 4.12: (a) electrical efficiency, (b) H_2 generation, (c) heat consumption and (d) output voltage against power input electrolyzer at the cell number differences

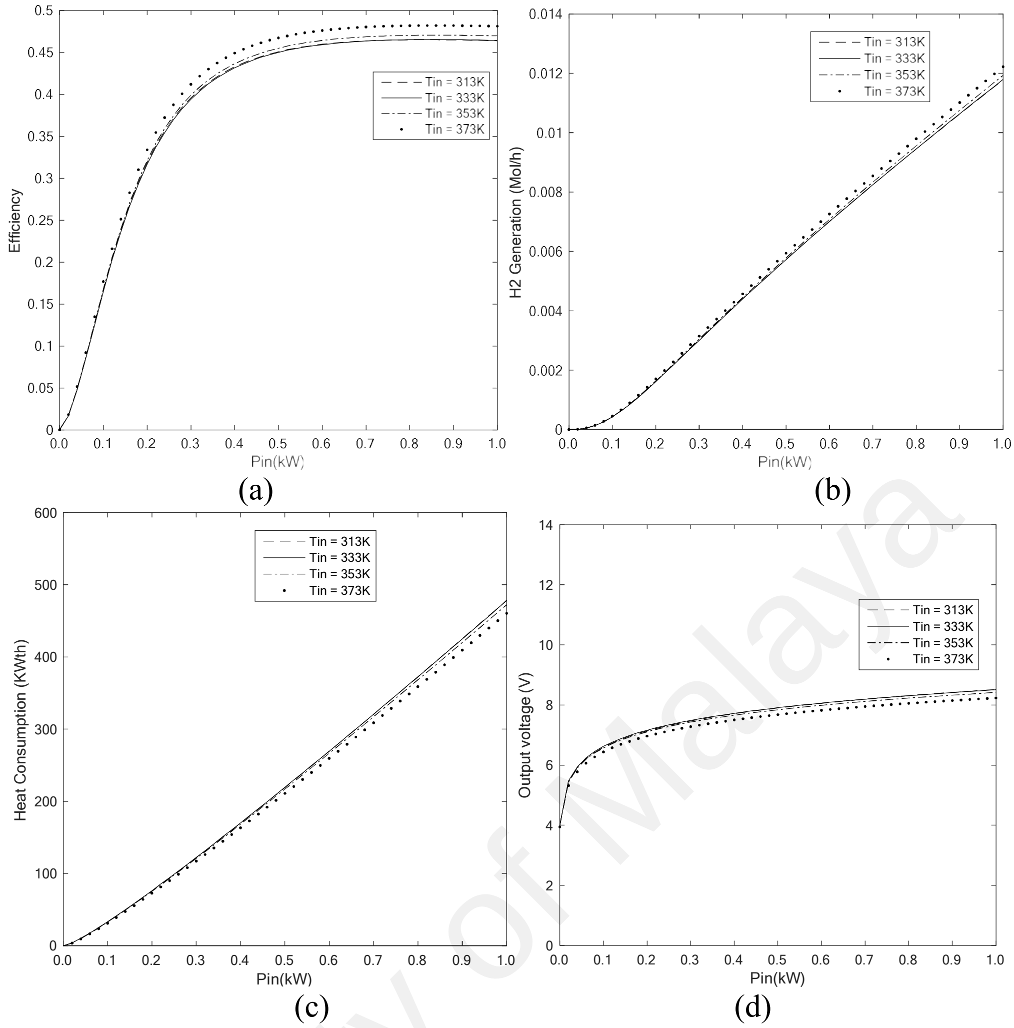

Figure 4.13: (a) electrical efficiency, (b) H_2 generation, (c) heat consumption and (d) output voltage against power input electrolyzer at the input temperature differences

4.5 Parameter analysis of extra heat recovery system

4.5.1 Photovoltaic thermal

a. Solar radiation

The correlations between solar radiation intensity and the output current, power and efficiency of the PVT are depicted in Figures 4.14(a) to (e). Solar radiation gives significant effect to the change of PVT current, electrical efficiency, heat power and heat efficiency. As the increase in solar radiation, the current and power of the PVT also increased. However, heat efficiency of the PVT did not change significantly compared to the electrical power for the increase in the solar radiation by about 500W/m^2. On the other hand, the increase in the solar radiation intensity decreased electrical efficiency significantly. This happens due to the temperature effect which causes degradation in the PVT efficiency.

b. Ambient temperature

The temperature of air also gives effects to the performance of the PVT as depicted in Figure 4.15(a) to (e). The PVT current increased slightly over the increase of ambient temperature, yet having a higher current drop compared to the lower temperatures. Similar result is seen for the electrical output and electrical efficiency which dropped in line with the increase of ambient temperature. The heat efficiency increased significantly in line with the increase of ambient temperature, while the heat power increased slightly compared to the electrical power.

The temperature of inlet fluid does not give significant improvement to the PVT output as depicted in Figure 4.16(a) and (b). It only affected the heat power and heat efficiency with insignificant enhancement in the decrease of inlet fluid temperature. It is similar to the efficiency which increased in the low temperature of the inlet fluid.

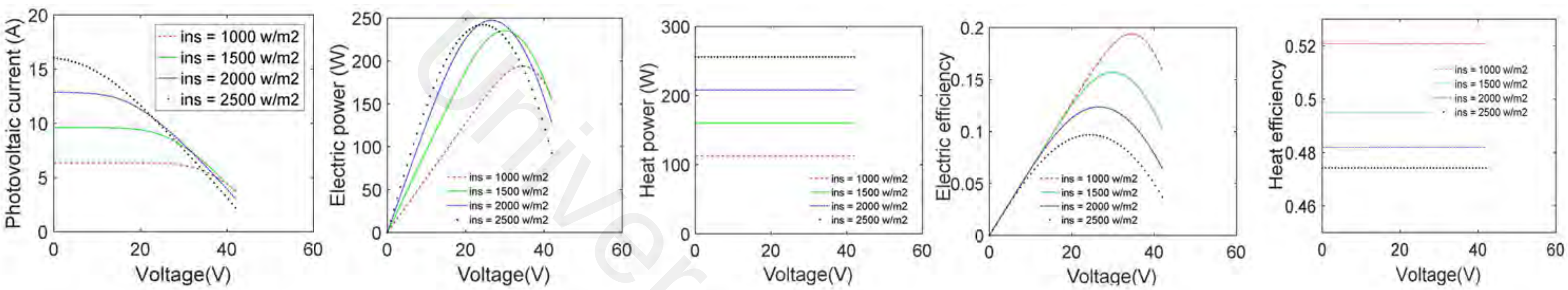

(a) (b) (c) (d) (e)

Figure 4.14: (a) PVT current, (b) electric power, (c) heat power, (d) electric efficiency, and (e) heat efficiency against photovoltaic voltage at the differences of solar radiation

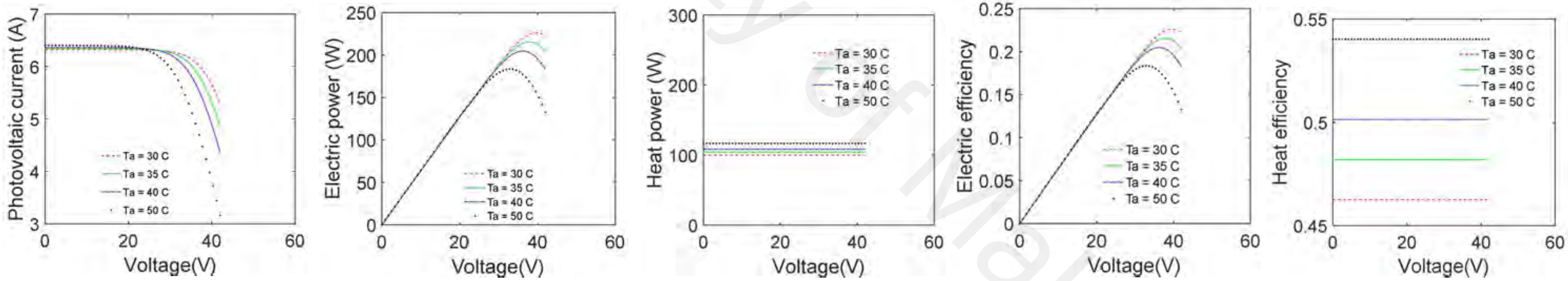

(a) (b) (c) (d) (e)

Figure 4.15: (a) PVT current, (b) electric power, (c) heat power, (d) electric efficiency, and (e) heat efficiency against photovoltaic voltage at the differences of ambient temperature

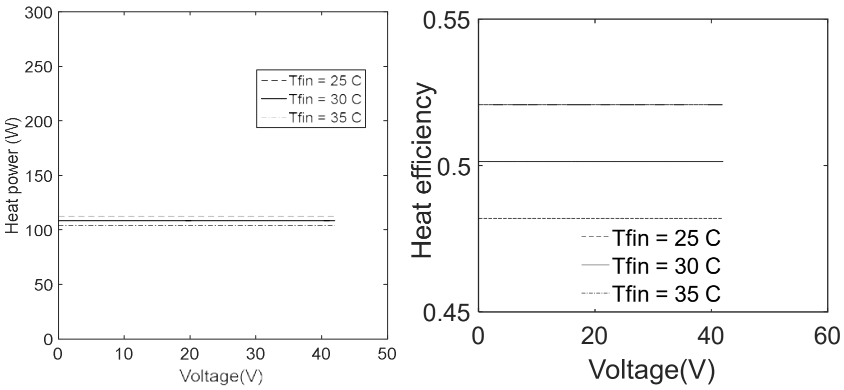

(a) (b)

Figure 4.16: (a) heat power and (b) heat efficiency against photovoltaic voltage at the differences of fluid input temperature

4.5.2 Thermoelectric generator

a. Low temperature side

The analysis of TEG power and heat was conducted by changing the fluid temperature in the low temperature side from 338K to 358K. The output power and efficiency of TEG were calculated over the resistance of the TEG load. As depicted in Figure 4.17(a) to (c), the increase of low side temperature improved the output power of TEG, yet it also decreased due to the increase in the load resistance. On the other hand, the heat power of TEG increased in line with the increase in the load resistance and decreased over the temperature increments. The electrical efficiency increased slightly for the cooling temperature rise of about 20K.

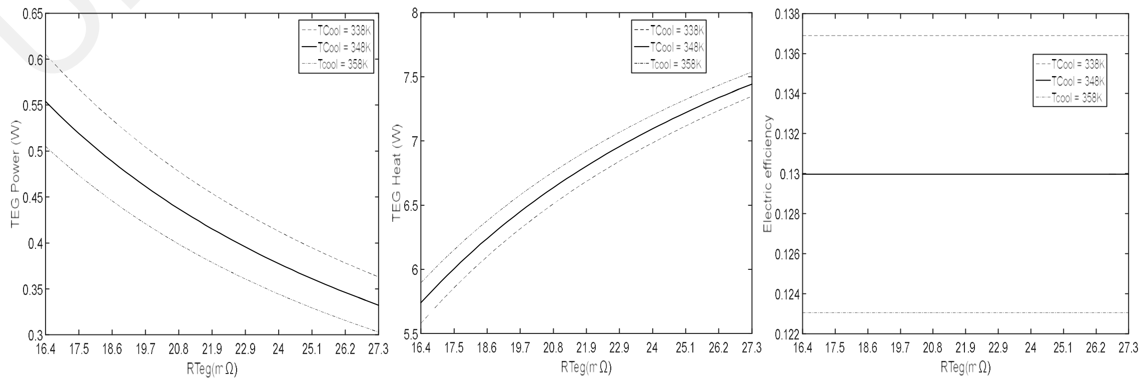

(a) (b) (c)

Figure 4.17: (a) TEG power, (d) TEG heat, and (c) TEG efficiency against thermoelectric resistance at the differences of cooling side temperature

b. High temperature side

The high inlet temperature also gave effects to the performances of TEG. By increasing the high side inlet temperature by 850K to 950K, the power of TEG decreased by 0.15 W per cell and it continuously decreased in line with the increase in load resistance. The TEG heat consumed raises with the increase in the high side temperature by about 0.2 W per cell and it continuously increased with the increase in the load resistance. The power efficiency of the TEG showed a linear pattern with the changes in the high temperature side. For the increase by about 10K, the efficiency of TEG decreased by about 0.4% but the increase in the load resistance did not affect its efficiency.

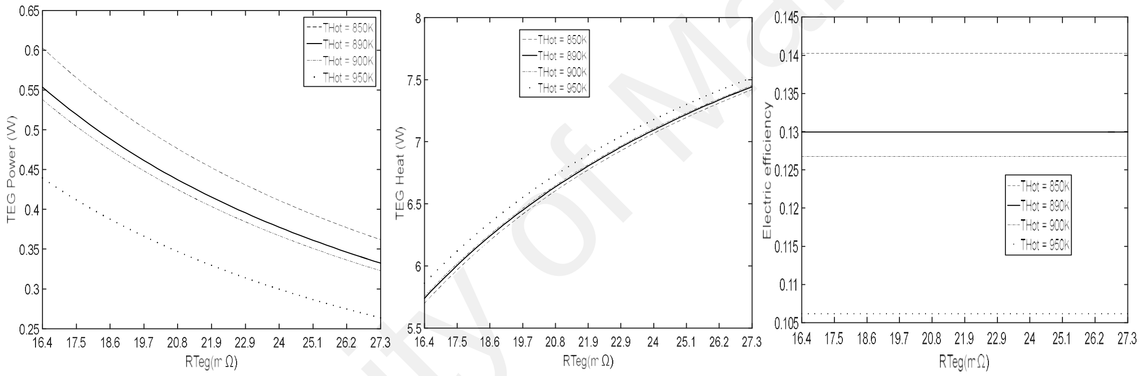

(a) (b) (c)

Figure 4.18: (a) TEG power, (d) TEG heat, and (c) TEG efficiency against thermoelectric resistance at the differences of high temperature side

4.6 Overall findings

From these parameter analyses for the SOFC, fuel utilization and fuel temperature had the most significant impact to the output performance of the SOFC whereas air temperature could be neglected due to its less impact to the SOFC performances. Fuel utilization gave significant effect to the decrease in the output voltage and power and the increases in the electrical efficiency, heat generation and heat efficiency. The increase in the air-to-fuel ratio improved the output voltage, electrical power and electrical efficiency. At the same time, it also decreased the temperature, heat generation and heat efficiency. The increase in the fuel pressure raised the output voltage, power and electrical efficiency, yet dropped its heat power and heat efficiency. The increase of fuel temperature decreased both output voltage and power, electrical efficiency, temperature, heat generation and heat efficiency.

For the double-effect absorption chiller, the temperature of generators and absorber have significant impact on the coefficient of performance. The increase in the generator temperatures improved the coefficient of performance linearly for the different values of absorption, condenser and evaporator temperatures. Similarly, the increase in the absorption temperature also increased the coefficient of performance within a certain range but would decrease gradually beyond that range. Both heat exchangers gave similar effects to the coefficient of performance at the different generator and absorption temperatures. The higher the heat exchanger coefficient value, the higher the value of the coefficient of performance.

The analysis for the electrolyzer revealed that all of parameters studied gave better effects to the efficiency, hydrogen generation, heat consumption and the voltage generation from the cell. However, cell number and cell area gave more significant impacts as compared to the cell temperature. As the increase of the cell number, the efficiency and voltage would increase. However, it also decreased the heat consumption and hydrogen production. Similar effect occurred to the cell area which increased the efficiency of electrolyzer at certain part load points. Therefore, it is suggested that the power input for the electrolyzer should be controlled at the optimum efficiency value to increase the performance of the polygeneration system.

4.7 Summary

In this chapter, a polygeneration system had been modeled using SOFC as the prime mover. The modeling process was conducted based on mathematical equations and was simulated using MATLAB. Furthermore, parameter analysis was also conducted for the SOFC, absorption chiller and electrolyzer to study the effect of several parameters on the performances related to operation and optimization of the polygeneration system. From the results, it reveals several important parameters that affect the performance of each components in the polygeneration system. Moreover, these analyses are essential technically to validate the polygeneration performances based on the behavior of each component in the system.

CHAPTER 5: EVALUATION OF CONFIGURATION AND IMPROVEMENT OF POLYGENERATION SYSTEM

5.1 Introduction

In this chapter, both the phase 2 and phase 3 of the research framework are presented. Firstly, four configurations of polygeneration are proposed based on grid connectivity and type of vehicles used as the load. Evaluation of the configuration is conducted based on energy, economic and environmental criteria. Furthermore, several improvements are made by adding renewable energy and thermoelectric devices to increase the performance of the polygeneration system. The improved system is compared to the polygeneration system with the basic heat recovery. Finally, the performances of both systems are analyzed to study the improvements in the system efficiency, energy saving, reliability, cost saving and carbon reduction.

5.2 Evaluation of polygeneration topologies

Different load patterns have different requirements of supply which lead to the specific design of supply. The requirements of electricity, heating, cooling, hydrogen and other energy types depend on its regions, applications, number of energy user and their activities. For countries with four seasons, the requirement of heating and cooling is almost balanced throughout the year. Heating is required during winter and cooling during summer while hot-climate countries require more cooling energy than heating. For tropical countries, the users need cooling instead of heating for the room, yet hot water is still required in a small quantity especially in the night and rainy season. This study chooses a tropical region as the case study since it has potential to be implemented in the residential areas. Most tropical countries in the South-east Asia such as Thailand, Indonesia and Malaysia still implement the conventional system in providing electricity, heating and cooling in residential applications. In the conventional system, utilization of electricity, heating and cooling is provided by a separated system which combines electricity from the national grid with auxiliary boiler and air conditioning to provide heating and cooling space. Furthermore, the advanced power generations such as polygeneration system have not been much studied further in those countries compared to developed countries such as the United States (US), United Kingdom (UK), Japan and China which have four seasons during a year. Therefore, analyzing and optimizing the design of polygeneration system in the tropical country such as Malaysia should be an interesting topic to be studied to highlight the possibility in developing this system for residential usages.

As explained in the first paragraph, applications and behaviors of the users affect the requirement of electricity, heating and cooling. For commercial applications such as office buildings, supermarkets and industries, the implementation of polygeneration system employing SOFC as the prime mover is not favorable unless the initial cost of SOFC could be decreased as predicted in 10 to 15 years later (Akikur et al., 2015). However, increase in attention comes from applications for residential use in form of a single home and apartments in developed countries (Kyriakarakos & Papadakis, 2015). This trend could be followed by developing countries such as Malaysia which has regulations regarding renewable energy utilization and feed-in-tariffs to be a potential market in commercializing this system.

Performance evaluation is the first step in this study in optimally designing a polygeneration system applying SOFC as the prime mover. In this phase, four proposed designs were studied and evaluated as per the energy, economic and environmental aspects. The optimum configuration of the polygeneration system is implemented for a

Malaysian residential area. The performance evaluations were designed based on four configurations as shown in Table 5.1. The evaluated configurations consist of four cases where Case 1 represents the grid-connected polygeneration system with EV charging and Case 2 represent the standalone polygeneration system with EV charging. Meanwhile Case 3 defines the grid-connected polygeneration with HV fueling supply and Case 4 represent the standalone polygeneration with HV fueling supply.

Table 5.1: Configurations proposed for evaluation purpose

Configurations	Grid connection		Vehicles power supply	
	Grid-connected	Standalone	EV charging	HV fueling
Case 1	√		√	
Case 2		√	√	
Case 3	√			√
Case 4		√		√

Moreover, the size of SOFC was also analyzed to determine the capacity requirement of the prime mover to satisfy the residential homes and vehicles energy consumptions. In these studies, the SOFC acting as the prime mover operated at the full load continuous operation, yet the electrolyzer operation depends on the available electricity. For the systems which were connected to the national grid, the electrolyzer operated at full load continuously. When there is lack of electricity, the excess was imported from the national grid and maximizing the hydrogen production. On the other hand, the standalone systems must be operated based on the availability of electricity from the prime mover. Therefore, the operation of the electrolyzer was controlled based on the excess electricity from the prime mover without any support from the national grid.

Although the grid-connected systems could import electricity from the national grid, the polygeneration system was assumed not to export the excess of electricity to the grid. This operating strategy is based on the government regulations in Malaysia and due to grid stability issues (Akikur et al., 2015; Tie et al., 2014). Therefore, excess electricity should be minimized during the operation.

5.3 Improvement of system components

The third phase in the energy planning for the residential polygeneration system focuses on the improvements for the system components. In this phase, two types of heat recovery system were compared to analyze the performance of heat recovery to improve the system efficiency. The heat recovery system studied for the first and second systems will be explained in the next sub-sections.

5.3.1 SOFC with the basic heat recovery (system 1)

The polygeneration with the basic heat recovery is depicted in Figure 5.1. The SOFC based polygeneration system was integrated with electrical or hydrogen vehicles charging or fueling stations. The fuel processor and air preheater were used to convert the natural gas through steam reforming and water gas shift reactions and preheated up to 650°C before injecting to the cells tube. The fuel from the processor moved to the anode side, while the air stream was injected to the cathode side of the cells. Electricity generated from the fuel cell was converted to alternate current (AC) power supplying the residential area, while direct current (DC) power was used for supplying electric vehicles station and electrolyzer to generate hydrogen. For polygeneration with the electric vehicles charging station, the unused hydrogen generated by the electrolyzer was sold to the gasoline retailers. On the other hand, for the polygeneration with the hydrogen vehicles fueling station, the hydrogen was stored in the buffer tank, compressed to a high-pressure gas and stored in the high-pressure tanks as fuel for hydrogen vehicles and the excess hydrogen could be sold.

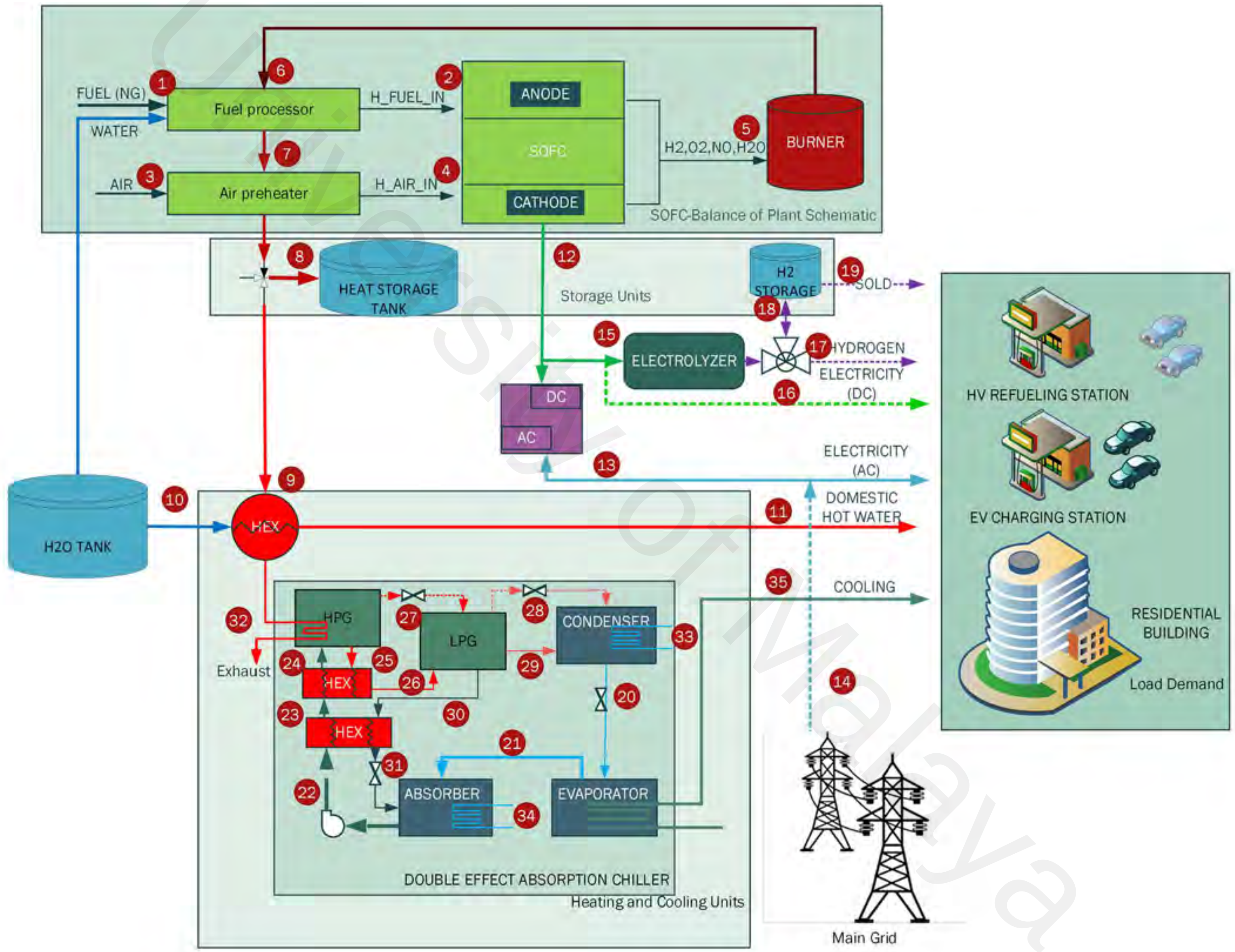

Figure 5.1: SOFC based polygeneration with the basic heat recovery system (system 1)

The exhaust gases from the fuel cell was heated until 900°C to increase the outer temperature and preheated fuel, air and water. A heat exchanger (HEX) was applied to supply hot water for residential families from the groundwater with the temperature of between 25°C to 28°C based on the ambient temperature (Mahlia & Chan, 2011). A double-effect absorption chiller provides primary space cooling for the houses by utilizing the excess heat from the fuel cell with an inlet temperature of 185°C, while the excess heat from the absorption chiller is released into the air.

The basic heat recovery configuration consists of the heat exchanger for hot water supply and double-effect absorption chiller for the cooling supply. The exhaust heat from the high-temperature generator was released into the air with the temperature of 130°C. This heat could be useful for heating or energy conversion purposes to increase the heat efficiency of the SOFC, hence the system was improved by adding a renewable energy source and energy conversion device.

5.3.2 SOFC with the extra heat recovery (system 2)

The improved heat recovery system is depicted in Figure 5.2 by adding photovoltaic thermal (PVT) panels and thermoelectric generators (TEG). The working principle of system 2 was different regarding the heat utilization and conversion mechanisms. The exhaust heat from the prime mover and balance of plant (BOP) was converted into electricity by the high-temperature TEG (HT-TEG) through fuel processor and air preheater pipelines. The stream of gases flow through the high temperature side of TEG, while the water flowed through the low temperature side. The temperature of the HT-TEG which was about 180°C and 90°C in the high and low temperature sides respectively generated electricity as the back-up power of the prime mover during high-consumption periods.

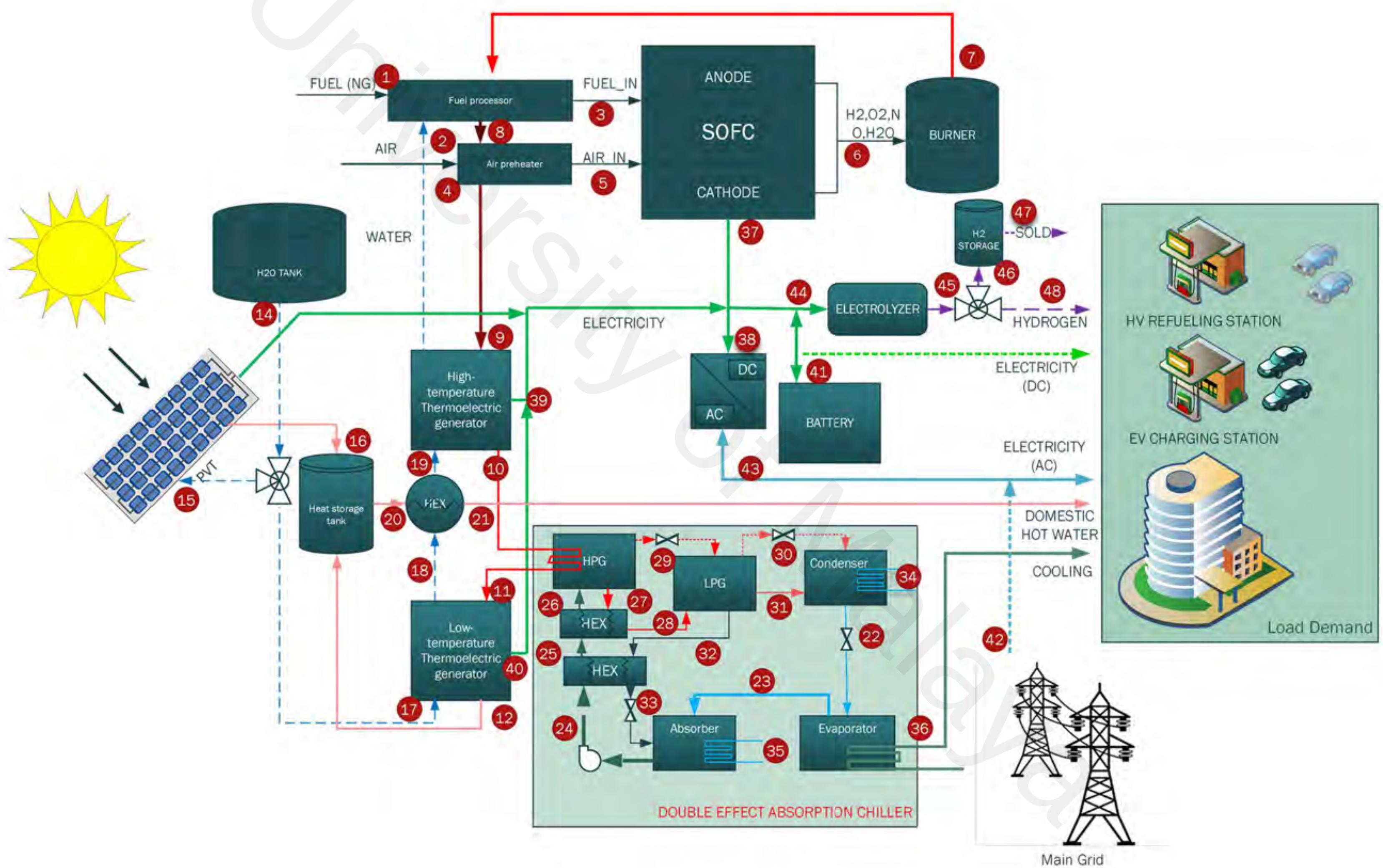

Figure 5.2: SOFC based polygeneration with extra exhaust heat recovery (system 2)

Moreover, a low-temperature TEG (LT-TEG) was also integrated through the pipeline in the low-pressure generator of the absorption chiller to optimize the utilization of exhaust heat. The outer temperature from the generator of about 140℃ was utilized to preheat the water fluid from the photovoltaic thermal collector. The outer temperature in the cool side of LT-TEG of about 50℃ was injected to the cooling side of the HT-TEG.

With the additional PVT and TEG components, this configuration has several advantages in optimizing the heat utilization from the SOFC, the fuel processor and the air preheater. Firstly, the preheated water from the PVT was utilized for hot water supply and flows to the cooling side of the TEG. In the water preheating process from the PVT to the HT-TEG, the steamed water was injected to the processor without adding burner to increase the water temperature. Furthermore, the conversion process in the TEG generated more electricity for the peak load period to minimize power consumption from the grid.

5.4 Configuration analysis of polygeneration system

The aim of this study is to evaluate the performance of the SOFC based polygeneration system. The evaluation takes into account four configurations as the case study with five criteria of assessment based on energy, economic and environmental aspects. Moreover, as the prime mover in the polygeneration system, SOFC plays an essential role on energy saving, cost and the reduction of carbon emission. Therefore, based on four configurations as mentioned in Section 5.2, the analysis for the SOFC capacity from 40kW to 160kW is also analyzed.

5.4.1 Annual consumption

The performance of the system is directly related to the profile of demand. From the case study proposed, Malaysia as a tropical country has a higher cooling demand compared to heating. Based on Figure 5.3, the annual cooling consumption of the multi-family residential houses is about 321 MWhth per year with an average consumption of about 6.42 MWhth per-family.

The second highest rate of energy consumption in the residential area is from hydrogen consumption. The hydrogen demand plotted is based on hydrogen consumption from vehicles only. The annual hydrogen consumption obtained per year is 252 MWh for multi-family and average consumption of 5.03 MWh per year for single-family. On the other hand, it is interesting to note that the energy consumption of an electric vehicle (EV) is much less than hydrogen vehicle (HV). Compared to other loads, electricity consumption of the vehicle is the second lowest rate of annual consumption at 139 MWh per year with an average consumption of 2.79 MWh per family. This analysis is almost similar to the literature (Carr et al., 2016) which revealed that the energy consumption of hydrogen fuel vehicle is 28% higher than the electric vehicle based on the load profiles in the U.K.

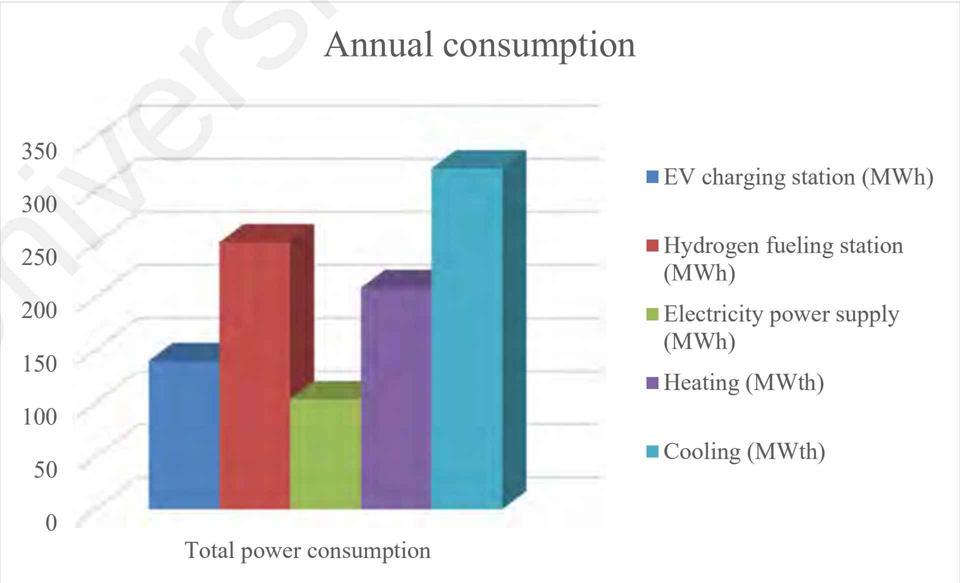

Figure 5.3: Yearly energy use of residential demand

The annual heat consumption of multi-family houses is about 208 MWhth per year with an average of 4.17MWhth per-family. On the other hand, the annual electricity consumption is at a lower rate than others since cooling and heating power generation of the electronic devices (air conditioner and water heater) have been converted into an integrated supply in this polygeneration system. The annual electric consumption for a multi-family is about 103 MWh per year with average consumption of 2.07 MWh per family.

5.4.2 Energy analysis

In this study, the prime mover capacity is defined based on the requirement for a single family where the average size of SOFC that can be installed is about 2 kW (Akikur et al., 2014). However, this capacity was excluded from the electricity consumption of the electric vehicle and electrolyzer which respectively consumed 16 kWh and 90 kWh of energy on average basis. Therefore, the increase in size and the addition of electricity from the grid are needed to overcome the lack of energy from the prime mover power generation.

For this study, all cases have similar SOFC capacity as the prime mover with the full load under continuous operation with maximum power reaching about 102.7 kW during peak load. With the current technology in fuel cell material, the SOFC can operate for 40,000 hours which is equivalent to 4.5 years (McPhail et al., 2017). This operation influences the efficiency of fuel usage when the consumed energy is lower than the output power in the SOFC.

The results of the energy evaluation for all cases are depicted in Figure 5.4. Case 1, 3 and 4 have similar reliability, higher compared to case 2. In case 1, the full coverage electricity was provided by the main grid, while in case 3 and 4, the electricity demand for the resident can be fully recovered by the SOFC. From this result, case 1 had a higher imported grid of 6.426 MWh in a year compared to case 3 which had grid consumption of about 1.853 kWh per year. Meanwhile, the highest electricity loss occurred in case 3. When electricity consumption from the residential home is much lower than the electric vehicle, the full load operation of the SOFC caused an excess of electricity which cannot be stored or sold to the grid.

On the other hand, the reliability of the system of case 2 is the lowest of all the cases. It is caused by an off-grid configuration which failed to serve the electricity demand from the resident home as well as the electric vehicle. In case 2, 9.85% of electricity demand cannot be covered by the prime mover only, however, due to the controlled operation of the electrolyzer, the power loss is not as huge as expected (73.52% in full load operation of electrolyzer).

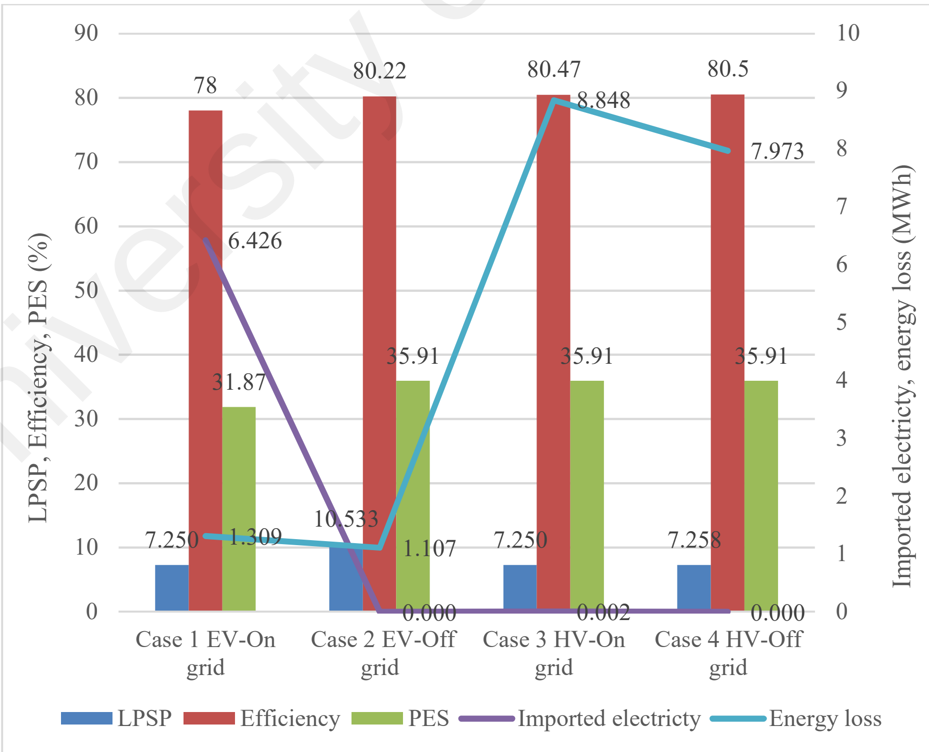

Figure 5.4: Energy evaluation for all cases

Regarding efficiency, the efficiency of the system in case 4 is the highest compared to case 2 and 3. The standalone system configuration and minimum electricity consumptions increased the overall efficiency of the system. On the other hand, Case 1 has the lowest efficiency compared to others. Due to the high consumption of electricity from the house and vehicle as well as the electrolyzer, imported electricity from the grid becomes high priority which decrease the efficiency of the system. It is similar to the PES value which shows that case 1 has the highest electricity consumption from the main grid where the PES is lower by 4% as compared to other cases. This shows that grid consumption can decrease both efficiency and PES from the polygeneration system.

Figure 5.5 depicts the evaluation of SOFC capacity with respect to the reliability of the system, energy savings and overall efficiency. The increase in the SOFC size decreases the LPSP value which means that the reliability performance of the system to serve demand increases. For the size under 100 kW, the reliability performance of the system increases dramatically, while if the size is above 100 kW, the reliability is stable at 7.25%. Case 2 has the highest LPSP value compared to others when the reliability reaches its stable value of 120 kW. The reliability of the polygeneration system can be enhanced by increasing the cooling capacity since cooling has the highest demand and losses occurred compared to electricity and hot water.

On the other hand, overall efficiency and energy saving decrease in line with the increase in SOFC size as shown by the dashed lines in Figure 5.5. For the SOFC size of 120 kW and above, both efficiency and PES are not changing significantly for the overall case. The highest value for system efficiency and PES is for case 2. It reveals that the utilization of electric vehicle in a standalone system brings improvements to energy saving and efficiency of the system. On the other hand, Case 1 has the lowest efficiency and PES due to its high consumption of grid electricity. Since the grid has low efficiency, the more the electricity is consumed from the grid, the lower the efficiency of the system and energy savings.

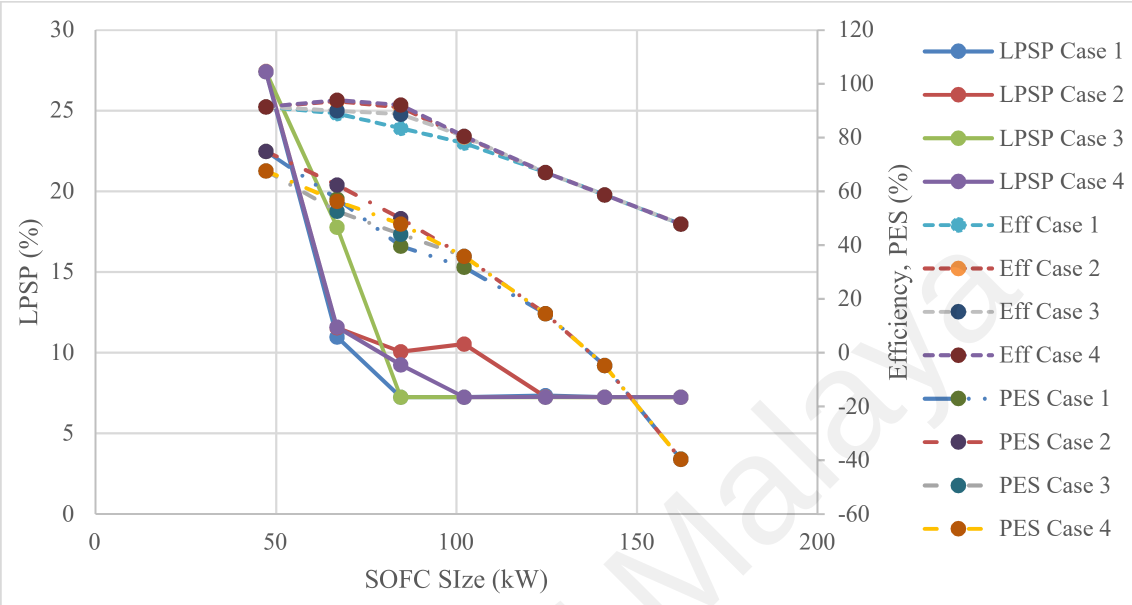

Figure 5.5: Reliability, efficiency, and energy saving from case 1 to case 4 in relation to the size of SOFC

For the analysis on grid consumption and energy loss, Figure 5.6 shows the result for all cases. The amount of electricity imported from the grid was analyzed for case 1 and case 3 only since case 2 and 4 are standalone systems. An unusual trend occured for the imported electricity in case 1 where the value decreases for the SOFC size of 80 kW, but it suddenly increases for the SOFC size of 100 kW as shown from the dashed line. It occurs due to the operation of the electrolyzer which is employed as long as the system has sufficient exhaust heat (it operates at a temperature of 80°C). When the size of SOFC was increased, the exhaust heat also increased, and the electrolyzer operated normally. Otherwise, the electrolyzer turned off when there is no sufficient heat. Therefore, the amount of electricity needed should be higher than 80kW SOFC to run the electrolyzer as well as serving the demand. On the other hand, different results are achieved for case 3 where the imported grid increases in line with the rise of SOFC size yet decreases for the size of 100 kW. The size of 100 kW is sufficient to supply the residential area without any imported electricity from the grid since case 3 uses less electricity compared to case 1 and case 2.

The minimum energy loss occurs with the SOFC size of 100 kW for all cases. Both case 1 and case 2 have lower energy loss compared to case 3 and case 4. Due to the high rate of electricity consumption for stationary and vehicles, case 3 and case 4 have maximum power consumption compared to case 1 and case 2. It is interesting to analyze the energy loss in case 3 and case 4 when the SOFC size is 160 kW. While in case 1 and case 2 the energy loss is slightly different, case 3 and case 4 have a significant difference in energy loss with similar SOFC size at 160 kW. It is due to the operation of the electrolyzer affecting the system. This considerable energy loss could be saved by adding a storage device or by controlling the prime mover operation. Due to temperature stress issues in SOFC operation, load following control cannot be applied to the prime mover operation. Thus, some storage devices must be used to reduce the power loss and imported electricity from the grid.

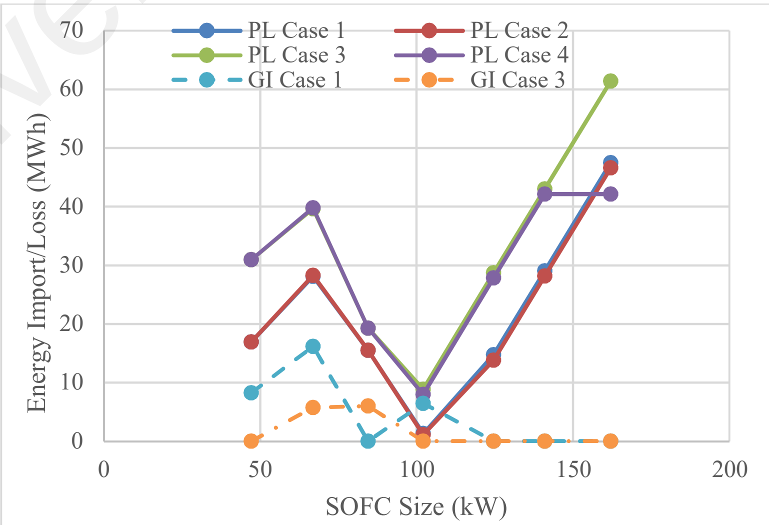

Figure 5.6: Grid import/system loss from case 1 to case 4 in relation to the size of SOFC

5.4.3 Economic analysis

Economic evaluation of the polygeneration performance was conducted using energy cost and energy saving criteria and compared with the conventional system using Equations (3.12) to (3.18). As depicted in Figure 5.7, this study evaluated the system considering the hydrogen selling strategy to analyze the effect of hydrogen production on the system cost reduction. Mostly, the electrolyzer is always attached to the system even when not used in the hydrogen fueling station. Therefore, the hydrogen can be sold at an affordable price to cover the investment cost of the polygeneration system.

Even though the grid-connected system with EV does not have high energy savings, it has lower energy cost compared to other configurations. From Figure 5.7, Case 1 has an energy cost of about 6 cents per kWh, which is the lowest cost rate using the hydrogen selling strategy. The cost saving is more than 50% compared to the CSS which consumes grid electric and boiler for heat generation. Meanwhile, if the selling-hydrogen strategy is not applied, the cost increases to 10.53 cents per kWh with cost savings of about 24%. The low energy cost is caused by cost saving from the electric vehicle compared to the conventional vehicle using gasoline. It also shows that case 3 and case 4 have the highest energy cost of about 8.6 cents per kWh and 10.88 cents per kWh with and without the hydrogen selling strategy, respectively. These results show that the electric vehicle is economically more beneficial to be used in residential areas compared to using the hydrogen vehicle. However, if the hydrogen selling strategy is not applied, all the cases have different energy costs. Therefore, this strategy can be implemented in the residential areas to decrease energy cost as well as reduce the payback cost period.

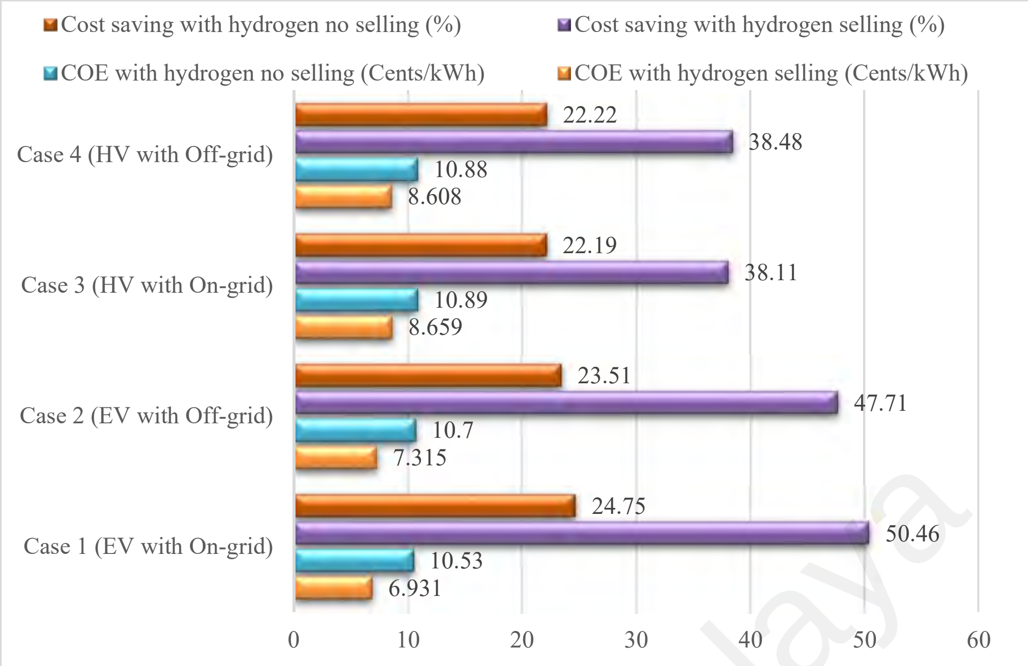

Figure 5.7: Economic analysis for case 1 to case 4

Besides the analysis of energy cost and energy saving, distribution of system cost has also been analyzed as shown in Figure 5.8. Distribution of annualized cost is dominated by the cost of SOFC which has the highest investment cost against other components. Hence it can be seen that the SOFC and other fuel cell types are new technologies which needs more expensive material compared to other prime mover types. However, a positive trend for the future energy cost of fuel cell especially the SOFC is that its cost would be reduced by up to 50% in 2020 (Akikur et al., 2014; Akikur et al., 2015). Therefore, the increase in SOFC utilization in the market leads to the reduction of the investment cost of the component. The second and the third highest investment costs are the absorption chiller and electrolyzer respectively. Therefore, further development of the combined fuel cell-electrolyzer system is expected to reduce these investment costs, hence decrease the energy cost of the proposed polygeneration system.

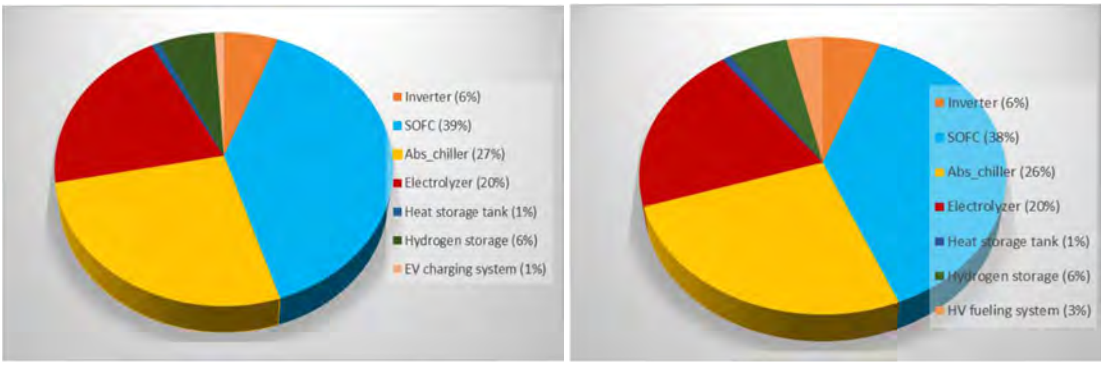

(a) (b)

Figure 5.8: Distribution of annualized costs for the main component of polygeneration system with (a) EV charging system and (b) HV fueling system

The consumable energy cost distribution is presented in Table 5.2. The trend of cost distribution is different for each configuration. Natural gas consumption contributes the highest consumable energy cost for the polygeneration system which cannot be avoided since the fuel cell operates under full load operation as the prime mover. The value of hydrogen sold is more than the consumed natural gas, and then it can be profitable for the system. However, for the configuration with the integrated hydrogen fuel vehicle, the selling-hydrogen strategy has lesser effect to the energy cost reduction due to the lower amount of hydrogen that can be sold.

Table 5.2: Distribution of consumable component costs in the polygeneration system

Components (Thousand $)	*Case 1 (EV & On-grid)*	*Case 2 (EV & Off-grid)*	*Case 3 (HV & On-grid)*	*Case 4 (HV & Off-grid)*
Imported electricity from grid	3793	0	0	0
Hydrogen sold	66.63	60.24	39.76	40.63
Hydrogen bought	0	0	1.018	1.018
Natural gas	29.05	29.05	29.05	29.05

Economic evaluation was also taken into account for the four cases with different sizes of the SOFC as depicted in Figure 5.9. From the aspect of the cost of energy (COE), the

100 kW SOFC size has the minimum energy cost for all cases. Case 1 has the lowest energy cost compared to others for the selling and without the hydrogen selling strategies. The trend of energy cost was drastically decreased from the size of 40 kW to 100 kW, while gradually increased for size above 100 kW. The hydrogen selling strategy plays an important role to decrease energy costs of the system by up to 34.17%. The energy cost of 6.9 cents/kWh achieved by the proposed system is still lower than the values found in the literature (Al Moussawi et al., 2017). This could be due to the integration of electrical and hydrogen vehicles to the residential areas which decrease the fuel cost compared to the conventional gasoline vehicle in this proposed system.

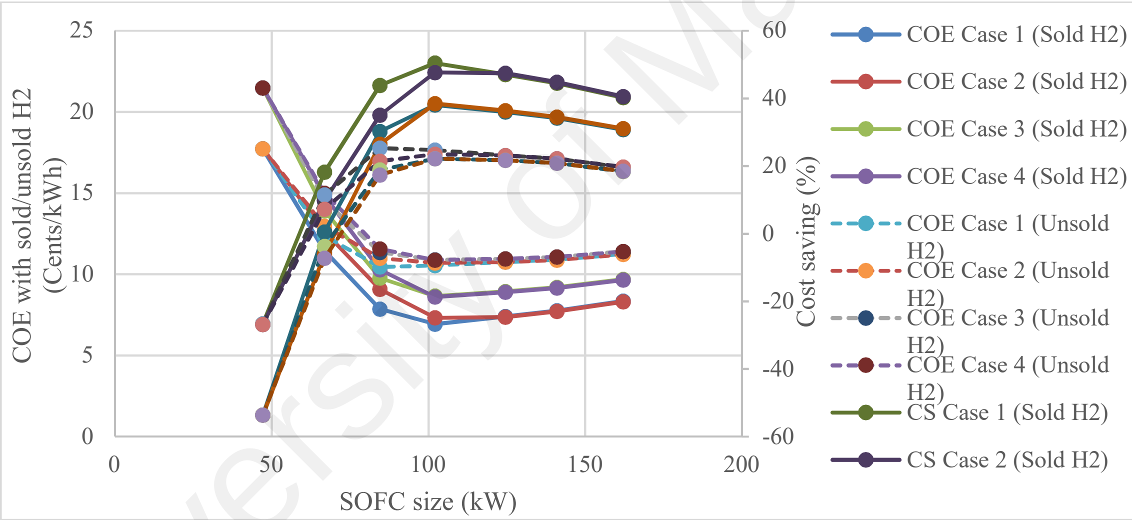

Figure 5.9: COE and cost saving (CS) from case 1 to 4 with and without the hydrogen selling strategy

Compared to the conventional separated system which has an energy cost of about 10 cents/kWh, the proposed system has the maximum cost savings for the SOFC capacity of 100kW. The negative value of cost-saving means that the energy cost is higher than the conventional system which occurs for the size of 40 kW in case 1 and 2. Case 3 and 4 have lower cost savings, especially when the hydrogen is not sold. The hydrogen selling strategy gives a significant effect on the energy cost saving compared to the conventional system with the SOFC size of 160kW for case 2. About 51.37% of energy cost saving was achieved for the hydrogen selling strategy in case 2 compared to the system without the hydrogen selling strategy. For future applications which allow own retail setups to have charging/fueling station in a small community, the hydrogen selling strategy seems promising to reduce the energy cost for the user.

5.4.4 Environmental analysis

Reduction of carbon emission is achieved for all the configurations in the proposed system as calculated using Equations (3.19) to (3.21). Based on the results in Table 5.3, it reveals that the proposed system is environmentally friendly compared to the conventional grid consumption with conventional gasoline for cars with similar average driving distance profile. It is due to the natural gas consumption by system which has lower carbon emission and electric and hydrogen supply instead of gasoline for the vehicles. Due to the higher consumption of grid electricity, case 1 has the highest carbon emission production compared to other configurations. As the emission factor of the natural gas is lower than the grid, case 2 has 36.18 % of emission lower compared to case 1.

Table 5.3: Emission reduction rate and percentage for the proposed polygeneration system

Parameters/ configurations	*Case 1 (EV with On-grid)*	*Case 2 (EV with Off grid)*	*Case 3 (HV with On-grid)*	*Case 4 (HV with Off grid)*
Emission carbon proposed system (Ton/year)	594.3	506.1	506.2	506.1
Emission reduction percentage (%)	20.74	32.5	32.5	32.5

As depicted in Figure 5.10, the increase in the emission is in line with the increase in SOFC size. Since the SOFC is fueled by natural gas, the amount of carbon emission for the SOFC operation affects the environment. For SOFC size above 120 kW, the carbon emission is higher than the conventional system by up to 47%. Therefore, to reduce carbon emission, the size of SOFC should be at the maximum of 120 kW. It related to case 1 and 2, case 3 and 4 have lower carbon emission rates, which shows that hydrogen vehicle has a significant effect in reducing the carbon emission compared to the electric vehicle. The standalone configuration also plays a role in environmental savings due to the reduction of the imported electric from the grid, which has a high carbon emission factor. This can be seen for case 2 which has similar environment saving trends with case 4.

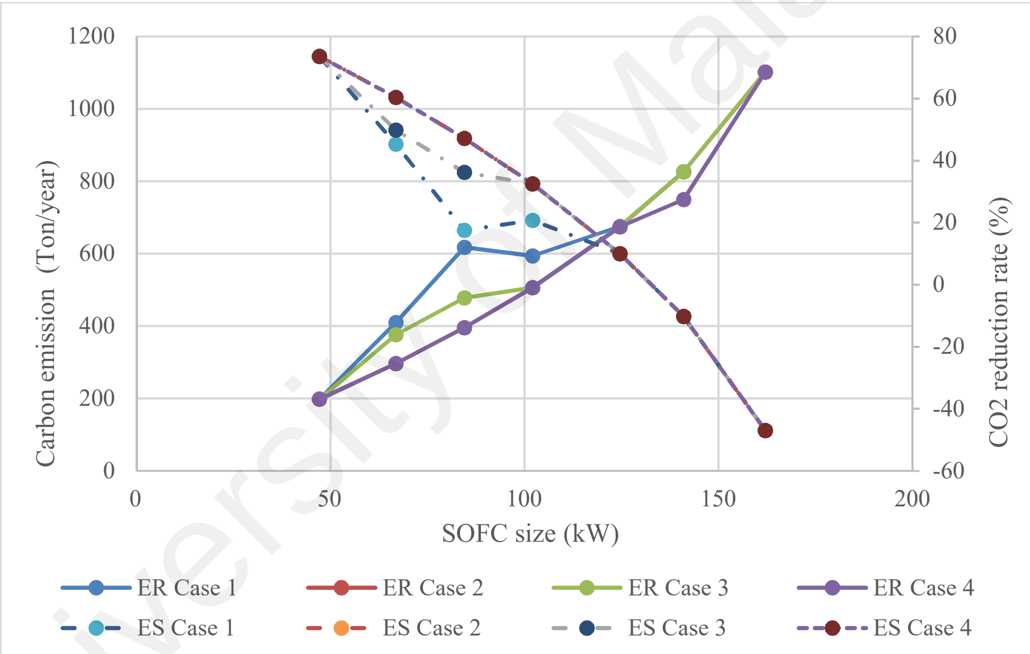

Figure 5.10: Emission reduction (ER) and environment saving (ES) from case 1 to case 4

5.5 Comparison between the basic heat recovery and the extra heat recovery systems

5.5.1 Energy analysis

As depicted in Figure 5.11 (a), system 2 has several improvements achieved in terms of efficiency and PES and reliability. The efficiency of system 2 increases approximately by 10.57% compared to system 1. In addition, The PVT and TEG increase the electricity generation as well as heat without causing any losses in the heat recovery system. Case 1 in system 2 has the largest difference in efficiency by about 14.36% compared to system 1, while case 3 has the highest efficiency value of 89.45%. Case 4 gives the smallest improvement of efficiency compared to other cases. Due to the high consumption of hydrogen and no consumption of electricity from the grid, hence it is no effect on upgrading the heat recovery system. This can be concluded that the additional heat recovery affects the consumption of electricity from the grid. The higher the grid consumption is reduced, the higher the increase in the overall polygeneration efficiency.

Furthermore, PES increases as expected for case 1 only, while does not have any effect on other cases. The energy saving enhanced for Case 1 in system 2 of about 11.58% compared to system 1. This could be caused due to massive electricity consumption for stationary power and electric vehicle supply from that is covered the polygeneration system instead of the grid.

On the other hand, the reliability of system 2 is slightly higher than system 1 for case 1. It is different for the other cases where a significant improvement is achieved for the reliability marked with the lower value of LPSP. The highest improvement of reliability is achieved in case 2 by 99% compared to case 1 and the second is for case 4 which achieves 37.24% higher than system 1. It can be concluded that the extra heat recovery is suitable to be implemented for the standalone system (case 2 and case 4 are standalone), which deals with lower reliability without support from the grid.

The power imported from the grid and the power loss from the system can be analyzed through Figure 5.11(b). The improvement of polygeneration in system 2 can reduce grid consumption by up to 12.85% for case 1 and 100% for case 3. This means that the proposed heat recovery system can improve the performance of the polygeneration by being independent over the grid connectivity. Furthermore, due to the high electricity generation, the power loss of the polygeneration in system 2 is higher compared to system 1. This excess of power can be reduced by properly sizing and optimizing the operation of polygeneration system. Otherwise, the power excess can be saved by proper sizing the storage device such as using battery or converting the power to hydrogen by the electrolyzer.

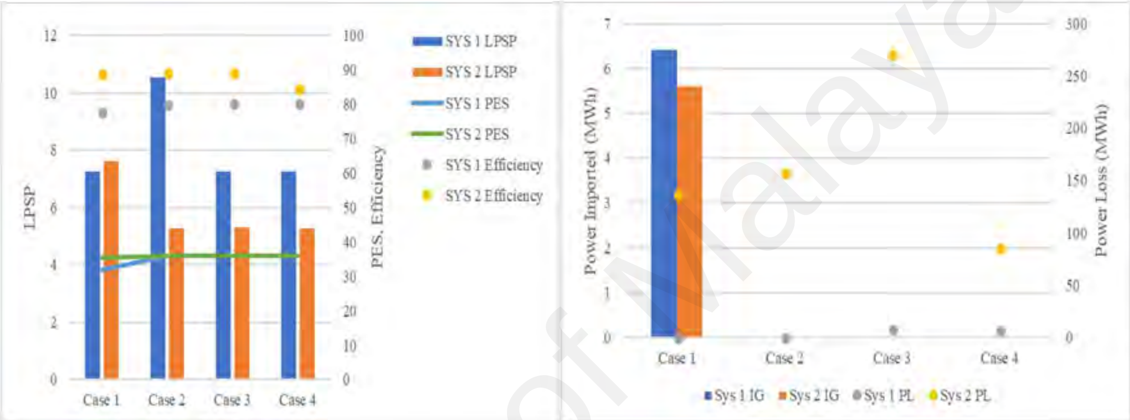

(a) (b)

Figure 5.11: (a) LPSP, PES, and efficiency; (b) power imported/loss for the proposed system

Sensitivity analysis was also conducted for the efficiency, PES, LPSP and power import/loss from the system with respect to the size of SOFC. In Figure 5.12(a), the efficiency of the system decreases in line with the increase in SOFC size. Both systems follow similar linear trends. Furthermore, the PES pattern for system 1 is different from the system for case 2 and 4. The polygeneration with extra heat recovery can deal with deprivation of energy saving compared to system 1. Depicted in red and yellow lines, the higher SOFC size in system 2 does not affect the energy saving which appears in system 1. The LPSP for system 2 is higher than system 1 for the SOFC size of 80 kW as well as its imported electric from the grid as depicted in Figure 5.12(c). However, the reliability of the polygeneration system increases for the size of SOFC at 100 kW or more, even the grid consumption reduced. This can be used as considerations in sizing the optimum SOFC capacity. Below 100 kW, the size of SOFC affects the reduced reliability and increased of imported power which can lessen the performance of the polygeneration system.

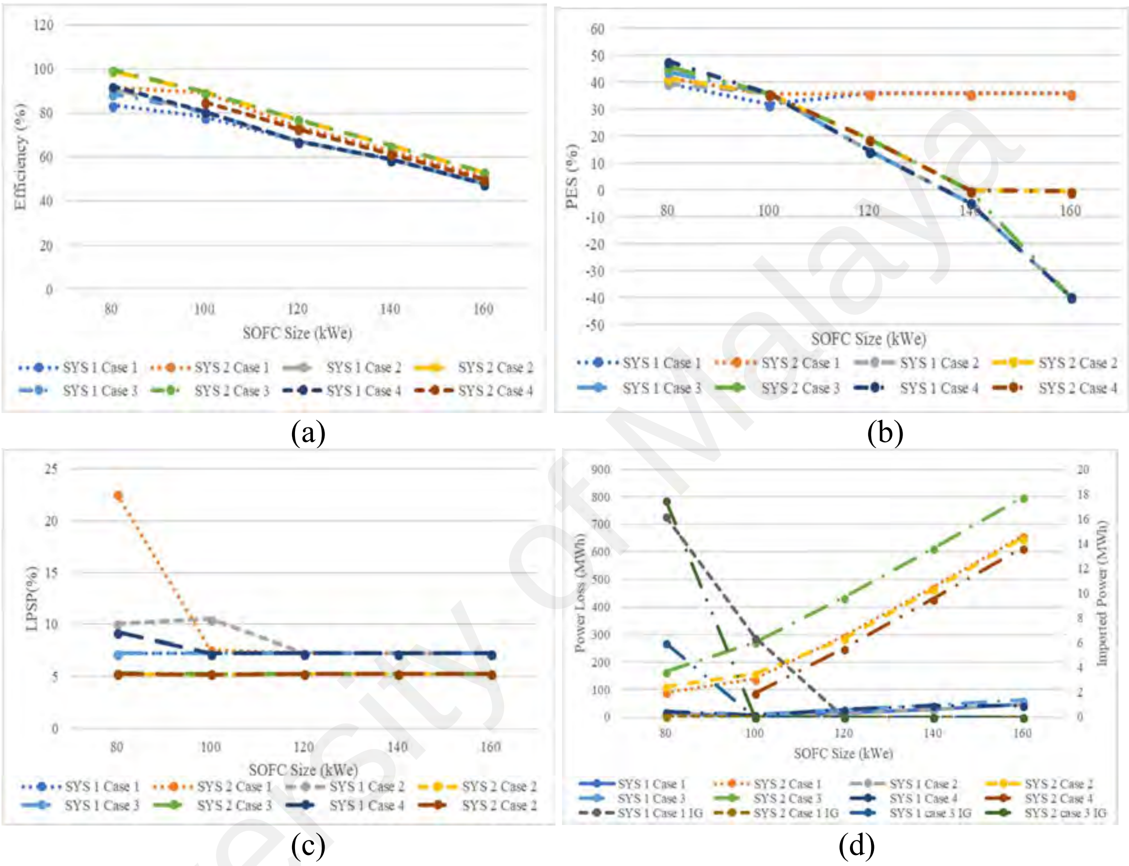

Figure 5.12: (a) efficiency; (b) PES; (c) LPSP, and (d) power loss/imported over the size of SOFC

5.5.2 Economic analysis

From the economic aspect, the polygeneration using extra heat recovery can be affordable compared to the reference system which uses separated energy supply for homes and vehicles. The system 2 achieves the energy cost of 9.97 cents/kWh with sold hydrogen scenario, which is lower than the reference system by about 28.78%. However, compared to system 1, the extra heat recovery system takes a higher price especially for the photovoltaic part which has high investment costs. The cost saving achieved by system 2 is as high as 31.44% and 23.89% for sold and unsold hydrogen scenario respectively.

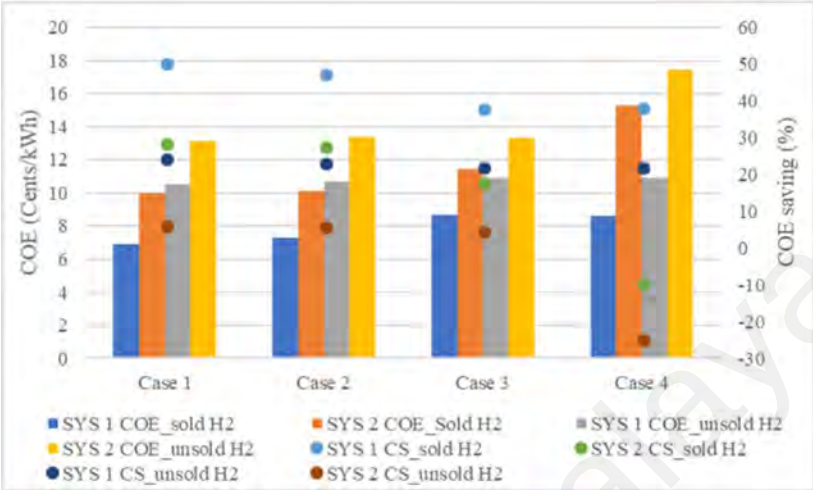

Figure 5.13: COE and COE saving of the polygeneration system over the proposed configuration

The analysis for the cost of energy (COE) and the cost of energy savings (CS) relative to the size of SOFC is depicted in Figure 5.14(a) and (b). Case 4 in system 2 has the highest energy cost as well as the lowest cost saving compared to other cases. On the other hand, the lowest energy cost is achieved by System 1 with case 1 and 2 configurations. The higher the SOFC size, the lower the gap of differences in energy cost as well as cost saving between system 1 and 2. The highest difference in energy cost is achieved by case 4, which is about 37%. Sold and unsold hydrogen scenario still affects the energy cost as well as the cost saving for both of systems. By applying the hydrogen selling scenario, the energy cost can be decreased to about 21% for each case in system 2. Case 1 has the highest energy cost reduction compared to other cases due to the high excess of hydrogen sold.

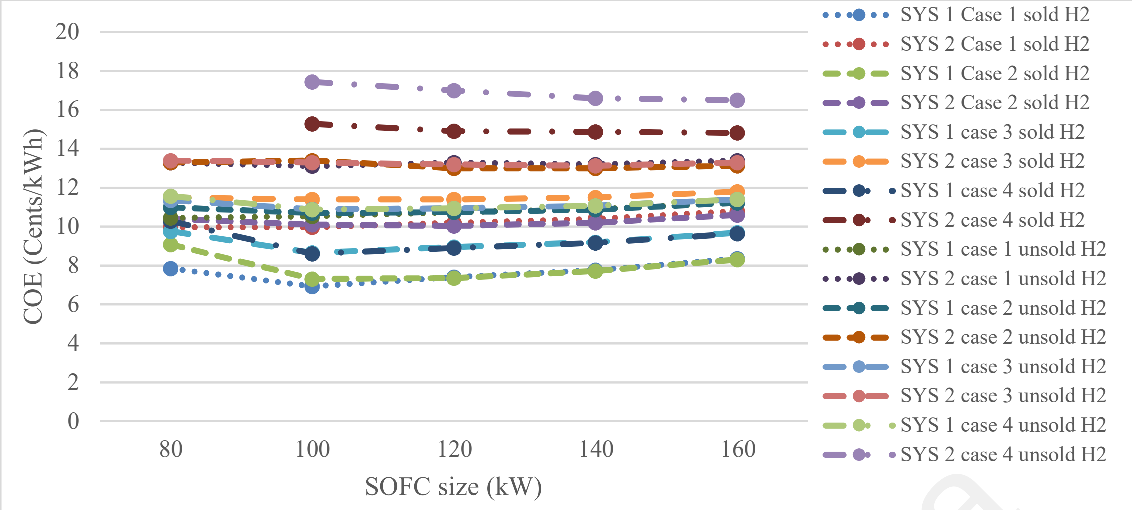

(a)

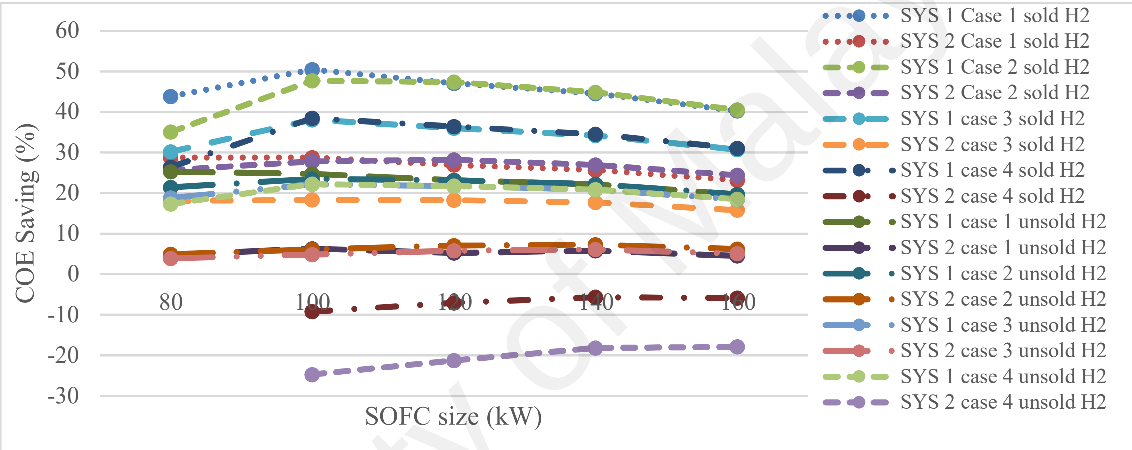

(b)

Figure 5.14: (a) COE, and (b) COE saving over the size of SOFC for polygeneration system with the basic heat (system 1) and extra heat recoveries (system 2)

5.5.3 Environmental analysis

Carbon emission production and CO_2 reduction are used as the basis to evaluate the polygeneration with basic heat and extra heat recovery systems as presented in Figures 5.15 and 5.16 respectively. From these figures, system 2 has a lower emission compared to system 1. The polygeneration with extra heat recovery system reduces the carbon production of 13.63% for case 1, while for case 2 and 3, it slightly increases by about 1%. This is due to the photovoltaic utilization, which reduces carbon emission, yet the value is not too significant compared with emission from grid utilization. For case 4, the carbon production is almost similar between system 1 and system 2.

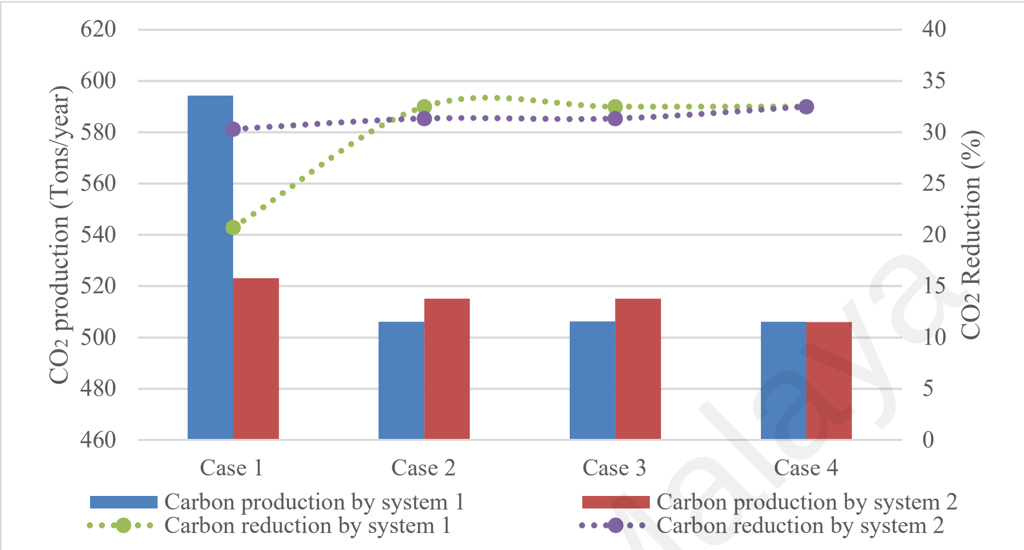

Figure 5.15: CO_2 production and reduction of polygeneration system with the basic heat and extra heat recovery

Furthermore, Figure 5.16 also depicts trends for CO_2 production and reduction over the size of SOFC. It is almost similar for system 1 and system 2 where the CO_2 production increases in line with the increase of SOFC size and vice versa for the CO_2 reduction rate. The trend of CO_2 production is not linear for system 2 case 4, which has a higher gap of differences for SOFC sizes of 140 kW and 160 kW. Thus, it can be concluded that system 2 can be considered a more environmentally friendly system with lower emission production compared to system 1.

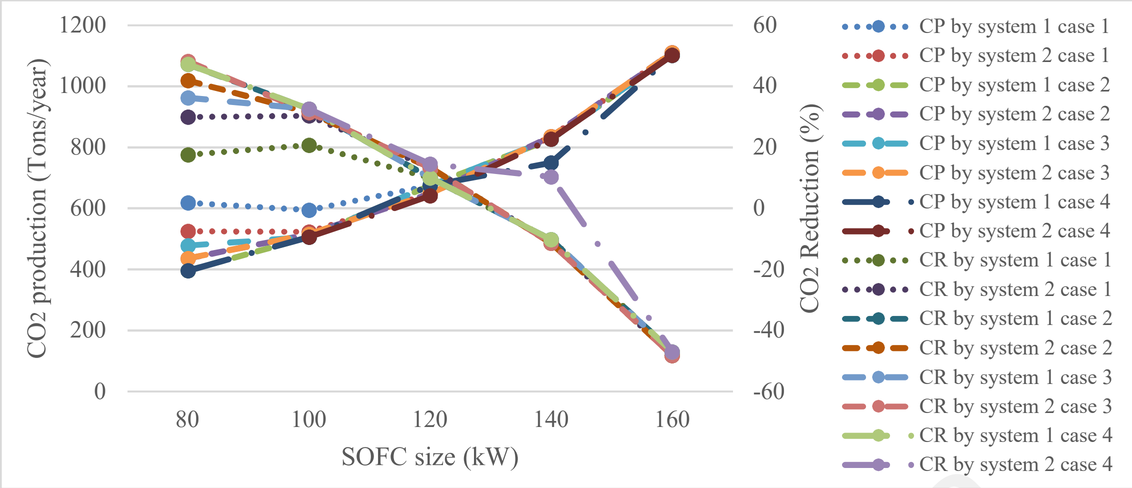

note: CP = carbon production; CR = carbon reduction

Figure 5.16: CO_2 production and reduction of polygeneration system over the size of SOFC

5.6 Discussions

Based on these results, the proposed configuration achieved a maximum energy saving of about 70% compared to the conventional system. While for the energy cost saving, the proposed system reached 50.46% and 25.29% of the maximum energy cost savings in the case with and without hydrogen selling strategy respectively. With respect to the environmental aspect, reduction of carbon emission from the proposed system is much lower than the conventional system by about 70% at the maximum rate.

The hydrogen selling strategy has a significant effect on the reduction of the energy cost by about 51% for the configuration which attaches electric vehicle station. Meanwhile, this strategy does not influence the configuration with hydrogen vehicle since the hydrogen consumed is more than or equal to its production. Also, the grid connection has reduced the probability of the supply loss (LPSP) by about 45.25% for configuration with the attached electric vehicle, while it does not affect the system with an attached hydrogen vehicle. The strategy also affects the payback period of the polygeneration system. The lowest payback period was achieved by case 1 and followed by case 2 (about 3.3 years and 3.4 years respectively). On the other hand, case 3 and 4 attained payback period of 6.4 years and 6.2 years respectively. These results showed good agreement with the previous study concerning application of fuel cell-based energy generation system for clinic and supermarket buildings (Facci & Ubertini, 2018). It exhibits promising potential of fuel cell-based energy generation system to be implemented for small and medium scale applications.

Compared to the other configurations, case 1 has the most promising energy and cost saving values compared to the other cases. However, it has an issue on environment due to highest carbon emission than other cases. On the other hand, case 2 can be considered as the optimum configuration which has high efficiency and energy saving as well as has a minimum of energy cost and carbon emission. However, it needs auxiliary storages to avoid the power loss issue. Lastly, case 3 and case 4 still have a higher energy cost compared to case 1 and case 2 due to the high cost of hydrogen. The system with hydrogen fueling configuration becomes viable in terms of energy cost when the price of hydrogen reduces, or the amount of selling hydrogen increases.

The improvement of the heat recovery system in polygeneration affects the increase of system reliability. The polygeneration with extra heat recovery system achieves a higher reliability of about 35.91% for Case 2, 3 and 4 and 4.83% for the polygeneration with extra heat recovery, EV supply and on-grid system for Case 1 in system 2. The improved system also enhances the energy saving of about 11. 58% compared to the polygeneration with basic heat recovery. The efficiency also increases by about 14.36%, 11.38%, 11.16% and 5.37% for the polygeneration with extra heat recovery in Case 1, 2, 3, and 4, respectively. Therefore, the polygeneration system can suffice the load independently without the imported power from the grid.

In terms of the environmental aspect, the polygeneration system is more environmentally friendly with emission reductions of about 31.60% and 30.32% compared to system 1 and the conventional separated system respectively. Based on the analyses between system 1 and system 2 with four cases, it can be concluded that case 2 in system has the most significant improvements compared to other cases and systems. It has high efficiency, reliability and energy cost saving and also high reduction of emission carbon. However, a huge excess of electricity still has to be optimized due to the decreased power loss of the system. Moreover, the additional components such as the photovoltaic cells increase the initial cost of the system, therefore, optimizing the operation and the size of the polygeneration are solutions to deal with the high energy cost of the system.

5.7 Summary

This chapter has presented the second and third phases of the research framework from this study. Four configurations i.e. the on-grid polygeneration with EV, off-grid polygeneration with EV, on-grid polygeneration with HV and off-grid polygeneration with HV are proposed to evaluate the optimum system performance based on energy, economic and environmental criteria. Evaluation of SOFC size has also been conducted for initial analysis to the optimization of system capacity from the polygeneration system. The third phase of this study has also been conducted for improving the energy generation from the system. Performance analysis for the improved system has been simulated and the result is compared to the system with the basic heat recovery system. Lastly, several important points are discussed regarding the improvement of polygeneration system from the configuration and system component aspects.

CHAPTER 6: OPTIMUM OPERATING STRATEGY AND SIZE OF SOFC BASED POLYGENERATION SYSTEM

6.1 Introduction

This chapter discusses the optimization process of SOFC based polygeneration system to obtain its operating strategy and component size. This step is essential in developing the optimum design of polygeneration for residential application. Section 6.2 presents the optimization process while Section 6.3 provides information on proposed fuzzy design for optimizing its operation such as input variables, objective, and constraints of operation. Section 6.4 introduces metaheuristic methods for optimum sizing of the polygeneration capacity. Furthermore, the performance of the proposed optimization methods and discussion of results are presented in Section 6.5 and Section 6.6, respectively.

6.2 Design optimization of polygeneration system

After evaluating the configuration and improving the recovery system of polygeneration, optimization of its design should be considered to improve the system performance. The optimum design of polygeneration system can be achieved using two approaches; operation optimization (OO) and size optimization (SO). The OO optimizes the operation of polygeneration system to maximize or minimize single or multiple objectives. The optimum operation can be applied in scheduling, on/off or any management strategies for the polygeneration components. On the other hand, size optimization is to find the optimal size of the polygeneration system components based on single or multiple objectives. The components including prime mover, heating and cooling units, hydrogen generation unit and storages.

6.3 Fuzzy logic for the operating strategy

Fuzzy logic (FL) method is employed to manage the polygeneration components in the operation optimization (OO) stage. The strategy works with fuzzy set and rules which drive the logic of the fuzzy output. It has several advantages in defining vagueness and imprecision of constraints, multi-objective problems and complex parameters through human communication language (Stojiljković, 2017). In this study, fuzzy sets are generated for five input and five output parameters using the multi-input-multi-output (MIMO) fuzzy approach. Two fuzzy rules are executed sequentially to control the SOFC and absorption cooling with different inputs, outputs and rules. Furthermore, as depicted in Figure 6.1, the bi-level fuzzy operation is also applied to control the operation of SOFC power and heat generation based on the fuel input, fuel to air and fluid temperature. For the absorption chiller, the generator and absorber temperature are controlled to optimize its coefficient of performance.

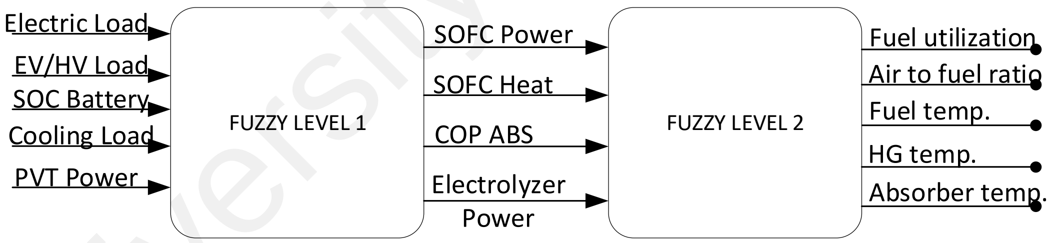

Figure 6.1: Fuzzy design for optimum energy management strategy

The management process using the Fuzzy algorithm is depicted in Figure 6.2. The process starts to initialize input of Simulink data i.e. solar radiation, electric load, vehicle load, cooling load, and heat load. Furthermore, input variables of fuzzy management are also initialized consisting variables such as electric load (*el*), electric vehicle load (*evl*), hydrogen vehicle load (*hvl*), photovoltaic thermal power (*pvt*), and SOC of the battery (*socb*) and their bounds are defined. As for the outputs, the fuel cell output power (*sofc_p*), fuel cell output thermal power (*sofc_q*), consumed power by the electrolyzer (*elect_p*), and coefficient of performance of the absorption chiller (*cop_abs*) variables are initialized, and their bounds are defined as well. All inputs and outputs have to be normalized into the range [0,1] from the real values. Then, the fuzzification process converts all input variables into fuzzy linguistic values and their respect to membership degrees. Each input variables represents one or two linguistic value with the associated membership degree.

Weight calculation is used to calculate the membership degree of output before it is converted into the normalized values through the defuzzification process. For the electrolyzer power output, the fuzzy value is converted into the real value, while for *sofc_p*, *sofc_q* and *cop*, the fuzzy values of these variables are converted into fuzzification level 2. Similar to level 1, fuzzy management in level 2 aims to manage the SOFC and absorption coefficient by using several variables. These variables act as the output of fuzzy management from the fuzzy rules with three linguistic values i.e. LOW, MED, and HIGH. The process of converting the input to the output continues with defuzzification and normalization of the output to the real values.

6.3.1 Input-output variables

In the first level of fuzzy, two fuzzy inference systems are used to operate the SOFC and electrolyzer on the one side and operate the absorption chiller on the other side. In the first level of fuzzy, the management actuators consist of three variables, i.e. SOFC power, SOFC heat, and electrolyzer power, while the second fuzzy generates a coefficient of performance (COP) of the absorption chiller.

Furthermore, the second level of fuzzy also employs two fuzzy inference systems to manage SOFC power and heat and COP absorption chiller. In the first fuzzy, SOFC power and heat are controlled by changing three variables i.e. fuel utilization *(FU)*, fuel temperature *(FT)*, and air to fuel ratio *(AFR)*, while the second fuzzy controls COP by changing temperatures of the high-pressure generator *(HG)* and absorber temperatures *(ABS)*.

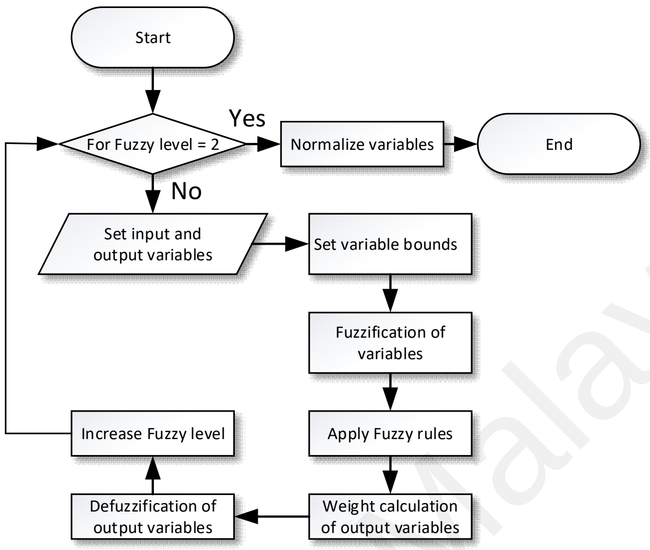

Figure 6.2: Fuzzy-based algorithm of multi-level management for polygeneration system

Firstly, input variables should be fuzzified to get number between 0 and 1 to simplify the fuzzy calculation. The linear fuzzy membership used is the triangle and trapezoid forms as the linear form is more accurate to generate satisfied solutions and simple to be applied (Stojiljković, 2017). This study adopts linear membership fuzzy for input variables *el*, *evl* or *hvl, socb*, *pvt* and *cl* represented as $\mu_{el}, \mu_{evl}\ or\ \mu_{hv}\ , \mu_{socb}, \mu_{cl}, \mu_{pvt}$. The function to define fuzzification uses the triangle shape given as

$$\mu_{el}(el_x) = \begin{cases} el_x - el_{x\_s} \Big/ el_{x\_m} - el_{x\_s}, & el_x > el_{x\_s} \quad and \quad el_x \leq el_{x\_m} \\ el_{x\_l} - el_x \Big/ el_{x\_l} - el_{x\_m}, & el_x > el_{x\_m} \quad and \quad el_x \leq el_{x\_l} \\ 0, otherwise & \end{cases} \tag{6.1}$$

while for trapezoid membership shape, it is defined as

$$\mu_{el}(el_x) = \begin{cases} el_x - el_{x\_s} \big/ el_{x\_ms} - el_{x\_s}, \; el_x > el_{x\_s} \quad and \quad el_x \leq el_{x\_ms} \\ el_{x\_l} - el_x \big/ el_{x\_l} - el_{x\_ml}, el_x > \; el_{x\_ml} \quad and \quad el_x \leq \; el_{x\_l} \\ 1, \; el_x > \; el_{x_{ms}} \; and \; el_x \leq el_{x\_ml} \end{cases} \tag{6.2}$$

Where $el_{x\_s}, el_{x\_m}, el_{x\_l}$ are real numbers corresponding to fuzzy value small, medium and large, respectively, while el_{x_ms} and el_{x_ml} are real numbers of the fuzzy value of medium-small and medium-large. Each variable is fuzzified to get the normalized value of fuzzy and converted into linguistic value. In this study, three types of fuzzy membership shapes are studied to optimize the fuzzy operating strategy as depicted in Figure 6.3.

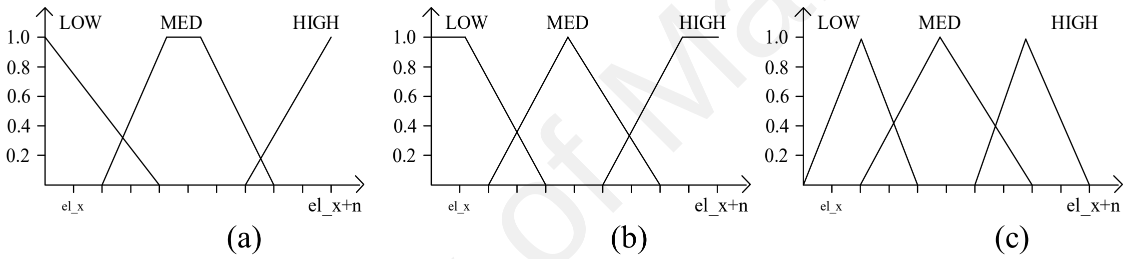

Figure 6.3: Three types of fuzzy membership used in this study i.e. (a) fuzzy type 1; (b) fuzzy type 2; and (c) fuzzy type 3

Each fuzzy type represents three levels of linguistic value of input i.e. LOW, MED and HIGH in fuzzy value [0,1]. To reduce the complexity of this system, the fuzzy type 1, 2 and 3 is adopted for fuzzy level 1, while fuzzy level 2 uses fuzzy type 1. All figures for membership fuzzy are presented in Appendix A. At the output, the defuzzification process is conducted based on a Sugeno approach using three to five fuzzy degrees. As for the output power and heat of SOFC, four linguistic values are used to represent the fuzzy degrees, i.e. LOW, MED, HIGH, and VERY HIGH.

In the second level of fuzzy management, output variables related to the SOFC and absorption coefficient are taken as the input variables (see Appendix A). The input variable degrees are similar to the output variables in the first fuzzy level. Real values of input are normalized from the maximum and minimum bound into the range [0.1]. This normalization is applied to easily calculate the input which has different ranges of value. Furthermore, the output value is also normalized from the range [0,1] to the maximum and minimum range of SOFC power, heat, and electrolyzer. The maximum and minimum bound of input and output variables are presented in Table 6.1.

Table 6.1: Variable bound of input and output of fuzzy management

Variables (in/out)	Units	Upper bound	Lower bound	Fuzzified equations
El load (in)	kWh	21.086	1.251	$el_x = 0.05042x - 0.0630$
EV load (in)	kWh	31.004	0	$evl_x = 0.0323x$
HV load (in)	Kgh	1.431	0	$hvl_x = 0.68812x$
SOC battery (in)	%	0	100	$socb_x = 0.01x$
Cool load (in)	kWh	4.98	107	$cl_x = 0.009802x - 0.0488$
Electrolyzer power (out)	Kgh	0	1.854	$y_{ep} = 0.539374ep_y$
SOFC power (out/in)	kWh	76.81	111.3	$y_{sofcp} = 37.5sofcp_y + 75$
				$sofcp_{x2} = \frac{x_2}{37} - \frac{75}{37}$
SOFC heat (out/in)	kWh	90.66	233.4	$y_{sofch} = 144sofch_y + 90$
				$sofch_{x2} = \frac{x_2}{144} - \frac{5}{8}$
COP absorption (out/in)	-	0.5	1.0	$y_{cop} = 0.8cop_y + 0.5$ $cop_{x2} = 1.25x_2 - 0.625$
O_2 to H_2 ratio (out)	-	2	5	$y2_{otoh} = 3otoh_{y2} + 2$
SOFC temperature (out)	K	923	1173	$y2_{sofct} = 250sofct_{y2} + 923$

6.3.2 Fuzzy rules

In the first level of fuzzy, the rules are to minimize output SOFC and maximize consumption electricity from the electrolyzer when the load is LOW, and the battery level is HIGH. On the other hand, maximizing the SOFC power and the electrolyzer consumption is prioritized when the loads are HIGH and battery level is LOW. The detail rules of fuzzy level 1 by using different vehicle load are presented in Table 6.2 and Table 6.3, respectively.

Furthermore, fuzzy level 2 focuses on controlling the SOFC power using several input parameters such as fuel temperature, fuel utilization, and air to fuel ratio, while also control coefficient of performance (COP) of absorption chiller using high-pressure generator and absorption temperatures as the parameters. To generate precise value of the SOFC power and heat, three levels and five levels of linguistic value are used for the first fuzzy, while the second fuzzy uses three levels of linguistic values for the inputs and outputs. The detail rules for fuzzy level 2 is presented in Table 6.4.

6.4 Metaheuristic method for optimizing polygeneration size

Besides optimizing operation using Fuzzy method, size optimization is also conducted using metaheuristic and bio-inspired approach based on evolutionary and swarm particle methods. GA is chosen as an evolutionary-based method, while PSO is considered for the swarm-based method. Both methods utilize powerful algorithms to optimize multi-objectives and multi-modal problems giving the high performance of global optimizing search (Martínez-Soto et al., 2014).

Table 6.2: Fuzzy rules level 1 for load management with electric vehicle demand

Variables		Rules																																						
Input	E load	L	L	L	L	L	L	L	L	L	M	M	M	M	M	M	M	M	M	H	H	H	H	H	H	H	H	H	-	-	-	-	-	-	-	-	-	-	-	-
	EV load	L	L	L	M	M	M	H	H	H	L	L	L	M	M	M	H	H	H	L	L	L	M	M	M	H	H	H	-	-	-	-	-	-	-	-	-	-	-	-
	SOC bat	L	M	H	L	M	H	L	M	H	L	M	H	L	M	H	L	M	H	L	M	H	L	M	H	L	M	H	-	-	-	-	-	-	-	-	-	-	-	-
	PVT	-	-	-	-	-	-	-	-	-	-	-	-	-	-	-	-	-	-	-	-	-	-	-	-	-	-	-	L	M	H	-	-	-	-	-	-	-	-	-
	Cool load	-	-	-	-	-	-	-	-	-	-	-	-	-	-	-	-	-	-	-	-	-	-	-	-	-	-	-	-	-	-	L	L	L	M	M	M	H	H	H
	Pre-cool	-	-	-	-	-	-	-	-	-	-	-	-	-	-	-	-	-	-	-	-	-	-	-	-	-	-	-	-	-	-	L	M	H	L	M	H	L	M	H
Output	Sofc_P	M	L	L	M	L	L	M	L	L	M	L	L	M	M	L	M	M	L	M	M	L	M	M	L	M	L	L	M	L	L	-	-	-	-	-	-	-	-	-
	Sofc_Q	VH	VH	VH	VH	VH	VH	VH	VH	VH	VH	VH	VH	VH	VH	VH	VH	VH	VH	VH	VH	VH	VH	H	VH	VH	VH	VH	VH	VH	VH	-	-	-	-	-	-	-	-	-
	Elect_P	H	H	H	M	H	H	M	H	H	M	H	H	M	H	H	M	H	H	M	H	H	M	H	H	M	H	H	M	H	H	-	-	-	-	-	-	-	-	-
	COP_Abs	-	-	-	-	-	-	-	-	-	-	-	-	-	-	-	-	-	-	-	-	-	-	-	-	-	-	-	-	-	-	L	M	M	L	M	M	M	M	H

**L=Low; M=Medium; H=High; VH=Very High*

Table 6.3: Fuzzy rules level 1 for load management with hydrogen vehicle demand

Variables		Rules																																						
Input	E load	L	L	L	L	L	L	L	L	L	M	M	M	M	M	M	M	M	M	H	H	H	H	H	H	H	H	H	-	-	-	-	-	-	-	-	-	-	-	-
	HV load	L	L	L	M	M	M	H	H	H	L	L	L	M	M	M	H	H	H	L	L	L	M	M	M	H	H	H	-	-	-	-	-	-	-	-	-	-	-	-
	SOC bat	L	M	H	L	M	H	L	M	H	L	M	H	L	M	H	L	M	H	L	M	H	L	M	H	L	M	H	-	-	-	-	-	-	-	-	-	-	-	-
	PVT	-	-	-	-	-	-	-	-	-	-	-	-	-	-	-	-	-	-	-	-	-	-	-	-	-	-	-	L	M	H	-	-	-	-	-	-	-	-	-
	Cool load	-	-	-	-	-	-	-	-	-	-	-	-	-	-	-	-	-	-	-	-	-	-	-	-	-	-	-	-	-	-	L	L	L	M	M	M	H	H	H
	Pre-cool	-	-	-	-	-	-	-	-	-	-	-	-	-	-	-	-	-	-	-	-	-	-	-	-	-	-	-	-	-	-	L	M	H	L	M	H	L	M	H
Output	SOFC_P	M	L	L	M	L	L	M	L	L	M	L	L	M	M	L	M	M	L	M	M	L	M	M	L	M	L	L	M	L	L	-	-	-	-	-	-	-	-	-
	SOFC_Q	VH	VH	VH	VH	VH	VH	VH	VH	VH	VH	VH	VH	VH	VH	VH	VH	VH	VH	VH	VH	VH	VH	H	VH	VH	VH	VH	VH	VH	VH	-	-	-	-	-	-	-	-	-
	Elect_P	H	H	H	H	H	H	H	H	H	H	H	H	H	H	H	H	H	H	H	H	H	H	H	H	H	H	H	H	H	H	-	-	-	-	-	-	-	-	-
	COP_Abs	-	-	-	-	-	-	-	-	-	-	-	-	-	-	-	-	-	-	-	-	-	-	-	-	-	-	-	-	-	-	L	M	M	L	M	M	M	M	H

**L=Low; M=Medium; H=High; VH=Very High*

Table 6.4: Fuzzy rules level 2 for SOFC and absorption chiller management

Variables		Rules																									
Input	SOFC_P	L	M	H	L	M	VL	VH	H	L	M	VH	H	VL	L	M	VH	H	M	H	L	-	-	-	-	-	-
	SOFC_Q	VL	VL	VL	L	L	L	L	L	M	M	M	M	M	H	H	H	H	VH	VH	VH	-	-	-	-	-	-
	COP_Abs	-	-	-	-	-	-	-	-	-	-	-	-	-	-	-	-	-	-	-	-	VL	L	M	H	VH	EH
Output	FUSOFC	H	H	H	M	M	L	H	H	M	M	H	H	L	M	M	H	L	M	L	L	-	-	-	-	-	-
	O2TOH2	VH	VH	VH	VH	VH	VH	H	H	H	H	M	M	H	M	M	L	M	L	L	L	-	-	-	-	-	-
	TSOFC	H	M	L	M	L	H	L	M	H	M	L	M	H	H	M	L	L	H	L	H	-	-	-	-	-	-
	TGH	-	-	-	-	-	-	-	-	-	-	-	-	-	-	-	-	-	-	-	-	L	L	L	H	M	H
	TGL	-	-	-	-	-	-	-	-	-	-	-	-	-	-	-	-	-	-	-	-	L	L	M	H	H	H
	TA	-	-	-	-	-	-	-	-	-	-	-	-	-	-	-	-	-	-	-	-	M	M	M	M	L	L

6.4.1 Optimization variables and objectives

There are seven components of the polygeneration system which have to be sized well, thus giving the whole system better energy savings, lessen cost and power loss. SOFC size is the most important part since it is a prime mover of the polygeneration, while cooling capacity is also important to maximize energy saving from the heat utilization part. PVT panels which consist of parallel and series configurations are also considered as an auxiliary source of electric and heat for the polygeneration system. Since it has a high initial price, the units must be optimized to increase energy saving as well as reduce power loss. Moreover, electrolyzer size, TEG module which consumes heat and battery as power storage are also important to be considered in increasing the performance of polygeneration system.

In order to speed up in searching the optimum size for each component, this study considers defining the search space as presented in Table 6.5. These values are also converted into integers to simplify the searching process and defining the near real component size to the commercialized version.

There are six criteria of objectives used for the polygeneration in the standalone polygeneration system with extra heat recovery and electric vehicle supply, i.e. polygeneration efficiency (n_poly), primary energy saving (pes), cost of energy saving

(cs), carbon reduction (CO_2R), power loss (P_{loss}), and loss of supply probability $(lpsp)$. Since the system adopts a standalone configuration with electric vehicle (EV) as the load, there is no imported grid considered as the objective of optimization. The fitness value of to be achieved is calculated as

$$fit = a_1 * n_{poly} + a_2 * pes + a_3 * coe + a_4 * CO2_{red} + a_5 * \left(1 - \frac{P_{loss}}{5.0e8}\right) + a_6 * lpsp \qquad (6.3)$$

Where $a_1 to\ a_6$ are the weight values of each objective criterion. Since other criteria except P_{loss} are normalized into the range $[0,1]$, then the additional calculation is needed to convert power loss value into a similar range.

Table 6.5: Variable constraints of optimization of polygeneration components

Variables	Units	Upper bound	Lower bound
SOFC size	kW_e	58.4	140.9
Cooling capacity	kW_{th}	70	120
PVT series number	-	2	10
PVT parallel number	-	10	100
Electrolyzer size	kW_e	80	120
TEG module number	-	20	100
Battery size	AH	500	3000

6.4.2 Genetic algorithm method

Optimization of polygeneration design using the GA method starts by initializing the input variables and their constraints. There are seven variables of polygeneration component to be optimized as presented in Table 6.5. Initial GA properties such as population, generation number, variable number, mutation and crossover coefficients are presented in Table 6.6. As the objective has multi-variables, inertia weights of objective variables have to be initialized as well. Some external variables are initialized as the input of simulation such as fuzzy management using the optimal shape of fuzzy membership.

For the first generation, the variable of polygeneration size (*poly_size*) is generated with matrix data representing a number of population and number of variables. In this study, the populations consisting seven variables are generated for evaluation. Since all individuals in the population are evaluated, *maxfit* representing the best individual with the best fitness value can be defined by comparing the fitness value of each individual in the population. Moreover, *minfit* as the worst individual, *bestobj* as the best fitness value and *best_size* as the best individual are also defined. The best individual in the population is saved by the elitism process to keep the best solution in the population for the next generation.

Furthermore, ranking the fitness value and selection process are also conducted to remove bad solutions with low fitness values, while keeping the good solutions with high fitness values. The individual with the higher fitness value has the higher chance to be chosen as the parents in the next process. In the crossover process, the parents generate a child by changing the DNA of parents representing the variables of the solution. In the mutation process, the children generated from the crossover mutate their DNA to generate better individuals.

Lastly, new individuals generated replace the old individuals in the population for the next generation. All processes are iterating until the last generation is reached. The algorithm of optimization using the GA method is depicted in Figure 6.4.

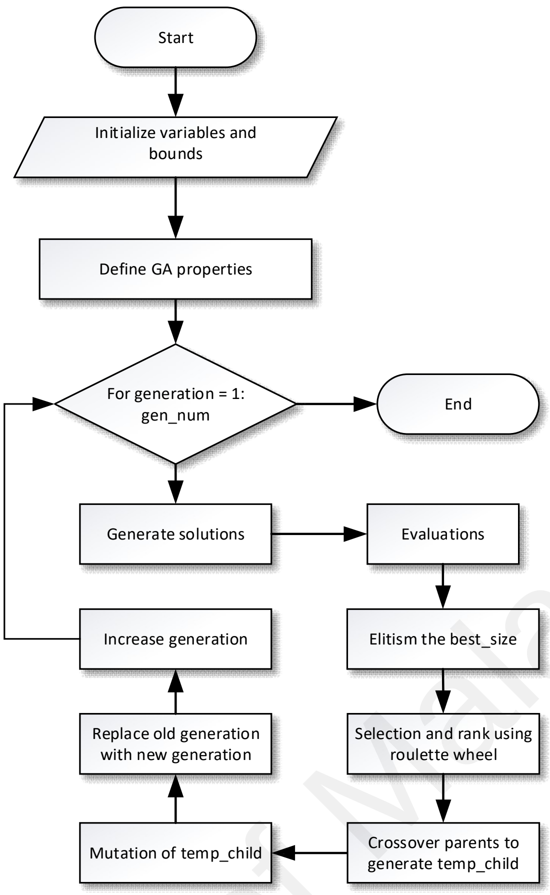

Figure 6.4: Optimization algorithm using the GA method

6.4.3 Particle swarm optimization method

PSO inherits the habit of swarm population of bird in reaching the prey. As depicted in Figure 6.5., the algorithm of PSO is quite similar to GA in terms of its evaluation and generating the population. Initialization of PSO properties consisting of several variables namely iteration number, velocity of a particle with maximum and minimum bounds, inertia of swarm with maximum and minimum bounds, and also coefficient of c1 and c2 representing cognitive and social learnings from the swarm.

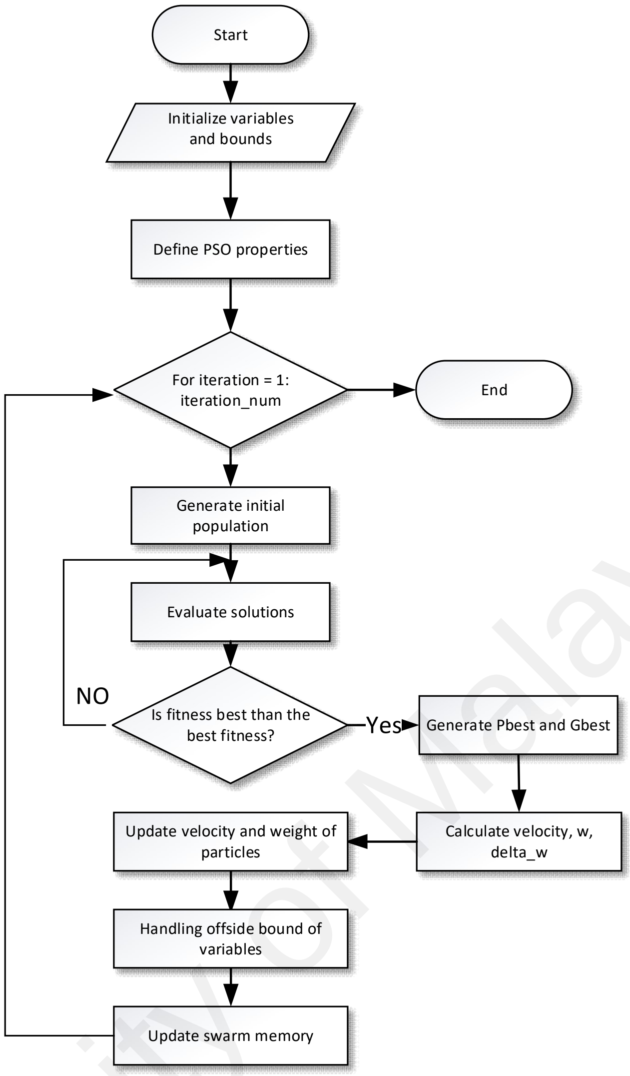

Figure 6.5: Optimization algorithm using PSO method

The process starts to generate the initial population consisting number of population and number of variables representing the particles. Evaluation of particles is done by simulating the polygeneration system to get several outputs of objective variables. All variables are calculated based on their inertia values to generate the fitness value. All particles in the swarm population are evaluated to identify the best particle representing by *pbest*. On the other hand, the global best particle (*gbest*) is also calculated as the same as the population best particle (*pbest*) for the initial population. These values are the reference values to evaluate the particles in the next iteration.

Table 6.6: Optimization properties for GA and PSO

Properties	GA	PSO
Generation/iteration	30	30
Mutation	0.2	-
Crossover	0.9	-
Maximum velocity	-	100
Minimum velocity	-	-100
Population	10-30	10-30
Constriction factor (kf)	-	0.7
Cognitive learning (c1)	-	2.1
Social learning (c2)	-	2.1
Initial inertia coefficient (w_init)	-	0.9
End inertia coefficient (w_end)	-	0.4

As the *pbest* and *gbest* are defined, initial velocity, initial *delta_w* and *w* representing inertia weight of particle velocity are also calculated. When the iteration started, velocity and inertia weight of each particle in the population is calculated. The new particles generated from the updated velocity and inertia weight must be evaluated to assure the particle value is in their bounds. Furthermore, the new particles are evaluated to get the objective value represented as the fitness and compared to get the best particle with the best fitness value. Moreover, the *gbest* is also searched to represent the best particle with the best fitness in all the iteration number. The new swarm replaces the old swarm memory to be updated again to the next iteration. The processes are repeated until the last iteration number is reached.

6.5 Analytic Hierarchy Process (AHP) for optimizing objective weight

Optimizing the solution using either evolutionary or swarm-based methods are robust for solving complicated problems. However, with multi-objective and multi-criteria to be considered, it is difficult to determine which objective criteria is more preferred than others. In this study, AHP for decision making is used to prioritize the objective criteria and optimize the fitness value of the searching process.

As depicted in Figure 6.6, the process of decision making in determining the priority of objective criteria starts with the first phase to generate a pairwise matrix A and define the weight of each matrix cell. The number of pairwise generated is based on the number of criteria decided n. In this study, six criteria are used which is defined as the weight of the pairwise matrix. Since our study analyzes all possibilities of criteria to be evaluated, there are two cases considered. The detail explanation of each case will be presented in Section 6.6.

$$A = \begin{bmatrix} a_{11} & \cdots & a_{16} \\ \vdots & \ddots & \vdots \\ a_{61} & \cdots & a_{66} \end{bmatrix} \tag{6.4}$$

Where $a_{ii} = 1, a_{ji} = {}^{1}/_{a_{ij}}$. Since pairwise matrix contained priority weight of each criterion over other criteria (*a_norm*), each matrix column is summed up to calculate the weighted priority (*a_prior*). Each of matrixes at the same column is divided by the sum of matrix column for weighted priority, and then the value of matrix in the same row is summed up and multiplied by a number of criteria considered to calculate the priority of each criterion.

$$a\_norm[i][i] = {}^{a_{ii}}/_{sum(a_{ii}: a_{ji})} \tag{6.5}$$

$$a\_prior[i][i] = a_{ii} * sum(a\_norm_{ii}: a\_norm_{ij}) \tag{6.6}$$

One thing that has to be considered is the consistency of the judgment to prioritize one criterion over others. The allowed consistency value for the judgment is 0.1 that means lessen the value the better the judgment. Furthermore, the second phase is to derive local priority for the alternatives. In this study, ten individuals (in GA terms) or particles (in

PSO terms) are used as the alternatives of multi-criteria decision making after optimizing the size. From the alternatives, local priority is calculated based on its preferences from the case. As an example, Case 1 which has equal-weighted objective generates ten alternative solutions based on the different preference values. The alternatives generated based on those individuals were compared to each other into pairwise matrixes based on the referenced criteria. Each alternative objective value containing six criteria is compared over the maximum value of each criterion amongst the ten alternatives to get the normalized value of objective. The matrixes containing the weighted value of each alternative are summed up and divided by the number of criteria to generate a local priority of each alternative. Performance sensitivity can be done based on the preference of each case to get a robust judgment for each alternative. Lastly, both the priority of criteria and the local priority are multiplied to making a final decision for each alternative based on the referenced criteria.

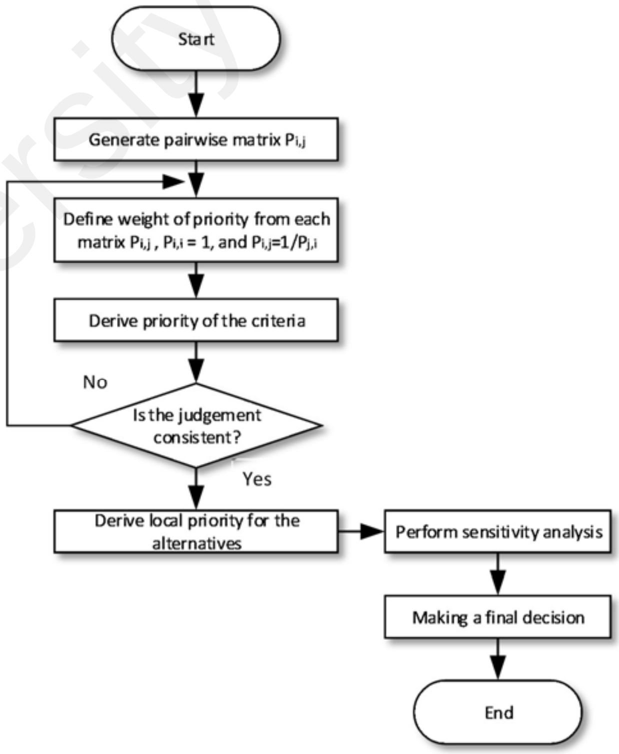

Figure 6.6: Algorithm of decision-making process for objective criteria using AHP

6.6 Analysis of design optimization (DO) of polygeneration system

For this section, analysis of the optimization process is divided into single-level operating optimization and bi-level OO and SO optimization. The single level only considers the operating process to be optimized using FEMS. Meanwhile, this bi-level optimization procedure considers employing FEMS in line with GA and PSO as a meta-heuristic searching method. Lastly, an improvement on deciding the optimum size of polygeneration based on the certain preference considers using AHP method which is applied with the meta-heuristic searching.

(a) *Single-level operating optimization using fuzzy ems*

In analyzing the importance of each optimization process, this study firstly starts to optimize the operation of polygeneration using FEMS. By considering three types of fuzzy shape as presented in Figure 6.3, the optimum fuzzy operation is chosen considering six criteria of performance mentioned in Sub-section 6.4.1. This phase is referred as a single-level operating optimization (OO) consisting analysis from energy, economic, and environment criteria. Moreover, energy flow analysis is also conducted for the optimum fuzzy daily and weekly. The optimum fuzzy will be used as the operation in the bi-level optimization process.

(b) *Bi-level OO and SO using Fuzzy-GA-AHP and Fuzzy-PSO-AHP multi-objective*

There are two cases studied for bi-level optimization regarding with multi-criteria decision-making method using AHP. In case 1, optimum design with equal weighted objective criteria was carried out. This case places all six criteria in similar priority to generate optimum size of the polygeneration components. Thereafter, the optimization process begins to search the best solution regarding the objective of generating the lowest fitness value amongst the population. This optimization process was run ten times in simulation and generates ten best individuals. All these individuals are analyzed for their preferences using the AHP decision-making method to get the local priority based on their chromosome values. Moreover, criteria priority is also determined using the AHP based on six preferences considered. Sensitivity analysis of each preference is done to get the initial optimum design of polygeneration from the different preference criteria.

In case 2 and 3, the weighted objective was developed based on combinations of multi-objective criteria i.e. PES, CS, CO_2R, and power loss. In case 2, combinations based on two criteria are used while in case 3 the objective is developed based on three criteria. Based on the mentioned objective, optimizations are run using GA and PSO for. After the solutions and their fitness values are generated, all solutions are evaluated compared to others in getting the local priority.

The local priority of each alternative is then multiplied to the criteria priority used in the weighted objective to generate overall priority. The prioritized alternative in case 1, case 2 and case 3 are compared to get the best solution of the polygeneration size.

6.6.1 Single-level operating optimization (OO) analysis

Analysis of single-level operating optimization is conducted for two best configurations chosen from objective 3 of this study. The off-grid polygeneration with electric vehicle charging and the on-grid polygeneration with hydrogen vehicle (case 2 and case 3 in system 2) are chosen as these two cases represent different configurations in terms of grid connectivity and vehicle load used. Therefore, these cases are analyzed over three types of fuzzy shape proposed for the optimum operation. Analysis of operation is conducted based on the energy, economic and environmental criteria compared to the system with no management strategy. For further analyses, these two configurations will be mentioned as the polygeneration with EV and off-grid connection (case 1) and the polygeneration system with HV and on-grid configuration (case 2).

(a) *Energy analysis*

Analysis of FEMS performance in terms of energy criteria improves the reliability of polygeneration by about 52% compared to the system without applying fuzzy. The highest enhancement occurs in fuzzy shape 1 compared to other types for polygeneration with EV and off-grid connection. Fuzzy shape 3 also reduces the supply probability loss (LPSP) by 22.05% and 53.46% compared to case 1 and case 2 with no FEMS, respectively. As depicted in Figure 6.7, even fuzzy shape 3 has higher LPSP over the others, it can maintain to have higher efficiency and PES of about 1.75% and 4.97%, respectively compared other fuzzy types, especially for case 1.

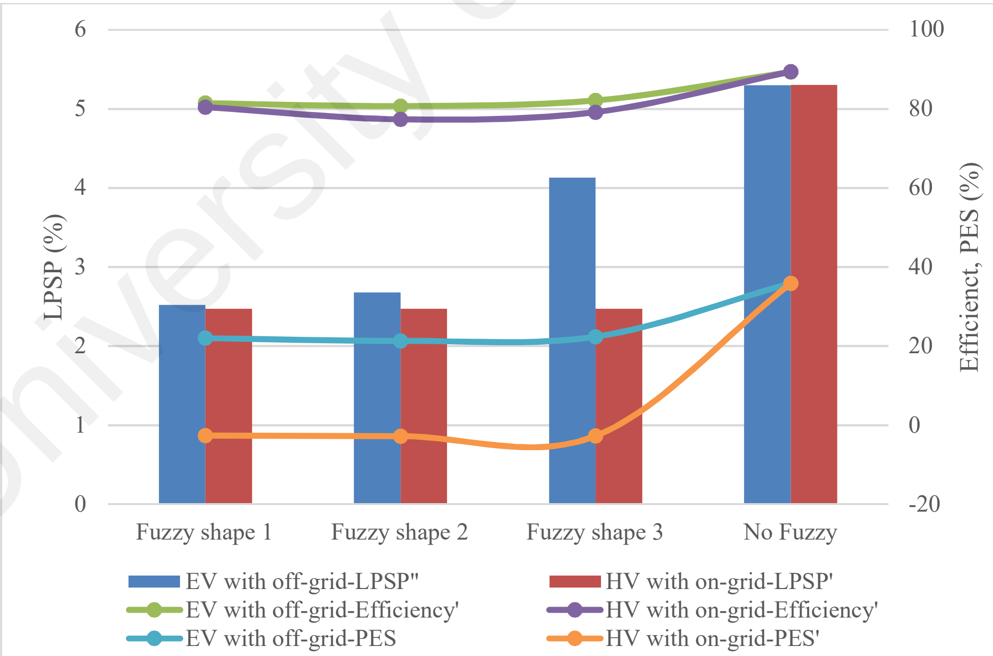

Figure 6.7: Energy analysis of polygeneration system based on three fuzzy shapes

This result also reveals the superior enhancement in the energy saving for case 1. Compared to case 2, case 1 has higher energy savings and efficiency of about 112% and

3.71%, respectively. It can also be seen that the management gives poor impact on energy saving in case 2 where it becomes negative compared to not using FEMS. It can be analyzed as the impact of controlling SOFC as the prime mover and electrolyzer which produce electricity and hydrogen. As those two devices being controlled, the system prioritizes utilization of grid instead of the prime mover to supply the loads which can lessen the PES.

In Figure 6.8, enhancement in energy loss reduction occurs for all fuzzy shapes compared to the system with no FEMS. The management using fuzzy shape 3 has higher reduction compared to other types by about 48.82% and 49.26% for case 1 and case 2, respectively. This result fulfills the requirement of this study though there are still energy losses occurred in those systems. The result also proofs that the polygeneration in case 1 having lower energy loss compared to case 2 by about 41.41%.

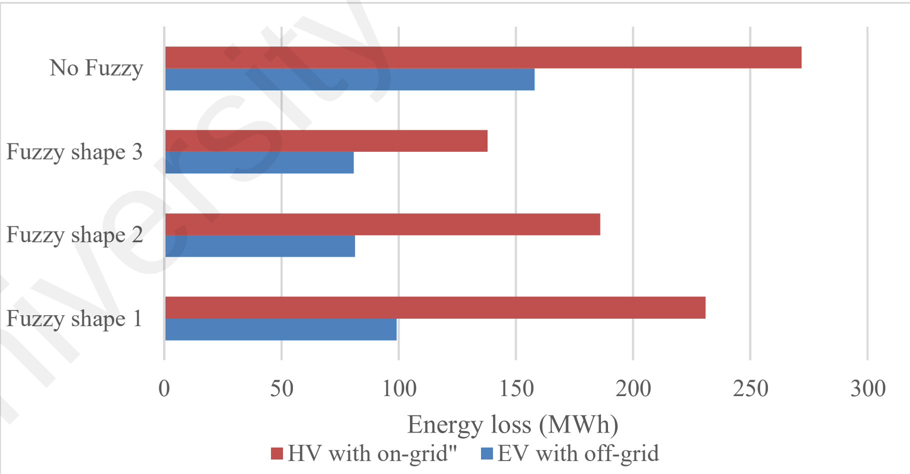

Figure 6.8: Power loss reduction of polygeneration system with and without FEMS

(b) *Economic analysis*

Energy management also affects the energy cost of polygeneration system since the fluctuation operation of power generation utilizing different fuel cost and grid consumption cost. This analysis is taken for the polygeneration with EV and off-grid connection (case 1) having improvement of energy saving compared to the system without FEMS. As depicted in Figure 6.9, the polygeneration in case 1 that employs fuzzy shape 3 has cost saving of 32.58% which is higher than employing fuzzy shape 1 and 2. This increase is about 2% and 0.7% compared to fuzzy 1 and 2, respectively. As compared to the system without employing FEMS, the increase of cost saving is more significant by 17% for case 1.

However, this management could not bring any improvement on the polygeneration with HV and off grid system since the cost saving of the system worsens. As seen in the figure, after employing FEMS, energy cost saving in case 2 becomes negative which means the cost of energy is higher than the separated system as reference. This happens due to the high consumption of hydrogen utilized for HV on one side, and limited electric from the prime mover to be harvested for running the electrolyzer on the other hand. The scenario results in the large amount of imported hydrogen that must be used to fulfill the vehicle's requirement which rapidly increases the energy cost of the polygeneration system.

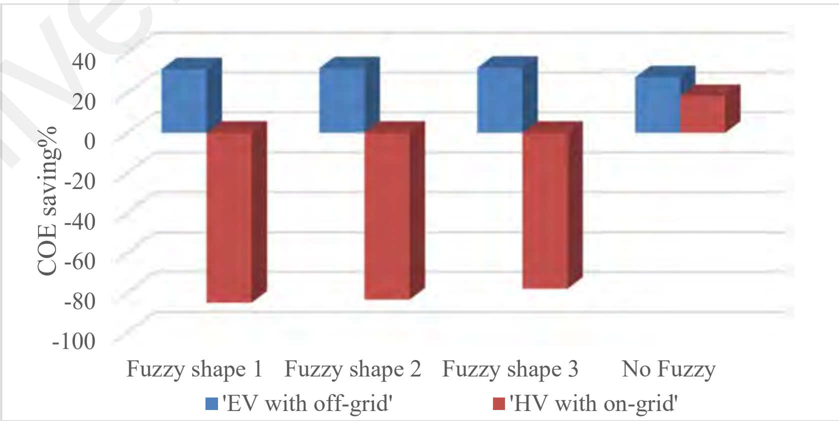

Figure 6.9: Energy cost saving of polygeneration with and without FEMS

(c) *Environmental analysis*

The effect of FEMS on the reduction of carbon emission for both case 1 and case 2 seems not too significant as compared to the polygeneration without FEMS. The polygeneration has a CO_2 reduction of about 17% in case 1 while having a reduction of about 14% in case 2 by employing FEMS. This reveals the improvement in terms of environmental health, the polygeneration with EV and off-grid connection has better performance compared to the system with HV and on-grid configuration. This is due to the effect of high-power loss that occurs which increases the carbon emission more than the hydrogen used for the vehicle. As depicted in Figure 6.8, case 2 has much power loss occurred compared to case 1 by about 41.41%. The losses are caused by the PVT, SOFC and grid consumption. The result proves that maximizing the electric utilities and lessen the power loss will affect the system against environmental health issue.

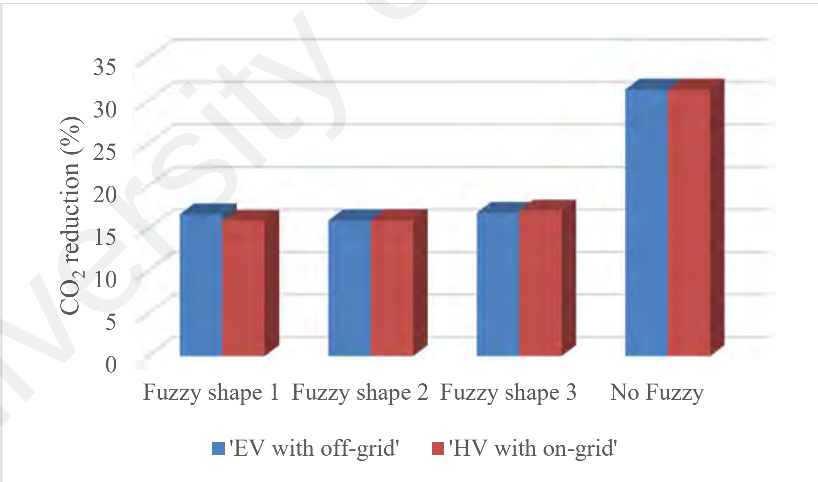

Figure 6.10: Carbon emission reduction of polygeneration system with and without FEMS

(d) *Energy flow analysis of optimum energy management*

Besides evaluating the effect of the FEMS to the polygeneration system, analysis of energy flow after managed by the FEMS is also presented in this study. The energy flow analysis presents the delivered, consumed and saved power between the sources, demands and the storage. In this study, energy flow analysis is conducted for case 1 with fuzzy shape 3 as the configuration and the optimum FEMS were chosen over the others. The analysis consists of a daily and weekly analysis of energy flow to study the effect of optimum FEMS to the optimum configuration in the energy way.

Electric power flow through the supplies to the demands and storages is depicted in Figure 6.11. and 6.12. SOFC as the prime mover becomes the highest power generator supplying electric house and vehicle loads. It can be seen from the figure that SOFC generates electricity in the range of 80 to 90 kW hourly to suffice the demands. Moreover, depicted in a green line, PVT also generates power to back up the prime mover in supplying demands based on sunlight intensity. In the daylight, PVT generation rises significantly higher than SOFC at peak power of about 90 kW hourly.

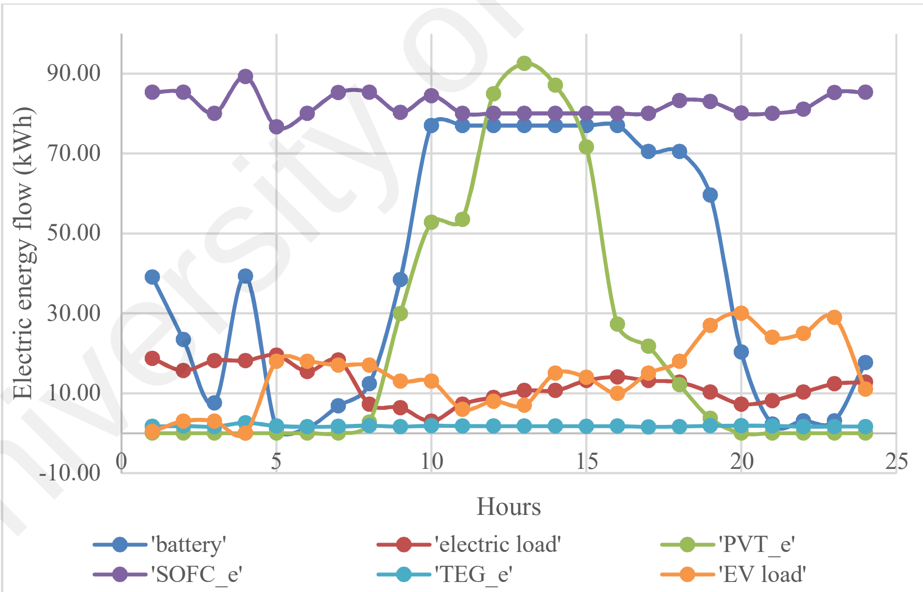

Figure 6.11: Daily analysis of polygeneration electric energy flow

The auxiliary backup power is generated by TEG to support the prime mover by utilizing excess heat from SOFC and converting it into electricity. From the figure, the gap between suppliers and demands are huge, then more energy exceeded. Fortunately, the battery can be used to store the excess power from the sources and minimize power loss. However, since the sources generate power out of requirement, there is power loss occurred at about 220 kWh per day which can lessen the performance of the polygeneration energy saving and its efficiency.

In terms of heat energy flow, Figure 6.12 depicts daily analysis based on six components i.e. heat and cooling loads, PVT heat, SOFC heat, absorption chiller, and heat storage. Heat generated by SOFC is the highest energy source amongst other suppliers in this system. Since this management controls the SOFC to generate very high heat power, there is no significant fluctuated power in the SOFC. Furthermore, cooling energy from absorption chiller becomes the second highest source generated in the polygeneration system. The cooling energy generated fluctuates in the range of 100 and 150 kWhth per day following the cooling load requirement depicted by the blue line. Since the heat storage tank cannot store much of exceeded heat energy, there is still heat loss which is consumed by some components such as electrolyzer and TEG.

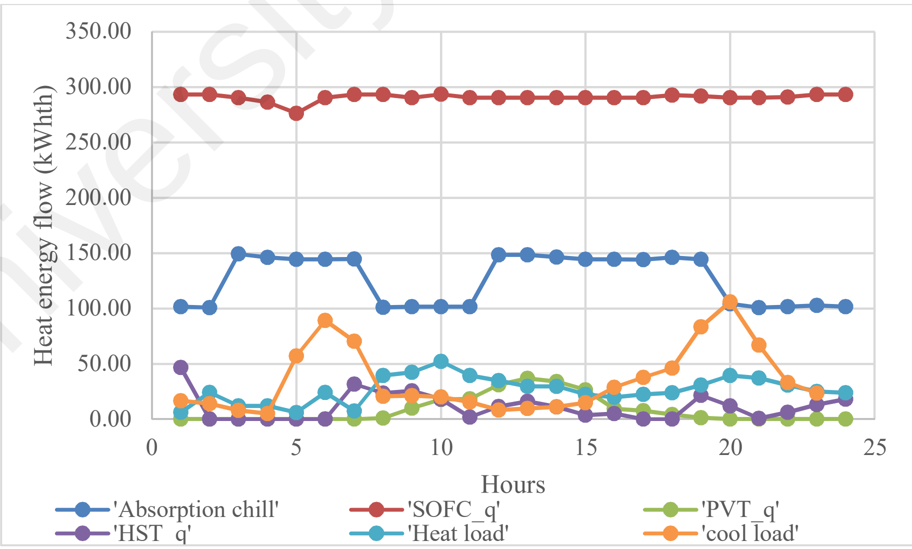

Figure 6.12: Daily analysis of polygeneration heat energy flow

Weekly analysis is taken from the first hour on Monday until the last hour on Sunday from 1 to 164 hours' time simulation. As depicted in Figure 6.13, fluctuation of electric energy occurs in several of the polygeneration components such as battery, PVT, and SOFC. SOFC energy fluctuates from 70 to 90 kWh and at several times PVT generates more than 90 kW per hour. The energy stored in the battery reaches the highest rate on Thursday and the lowest is on Day 1 and Day 2. A little bit of electric energy comes from TEG depicted in the purple diagram. From this figure, in several times PVT and SOFC generate power higher than the demand, then high energy loss occurred. This proves the need for the optimum size of each polygeneration component to reduce the possibility of power loss and improve the performance of the system.

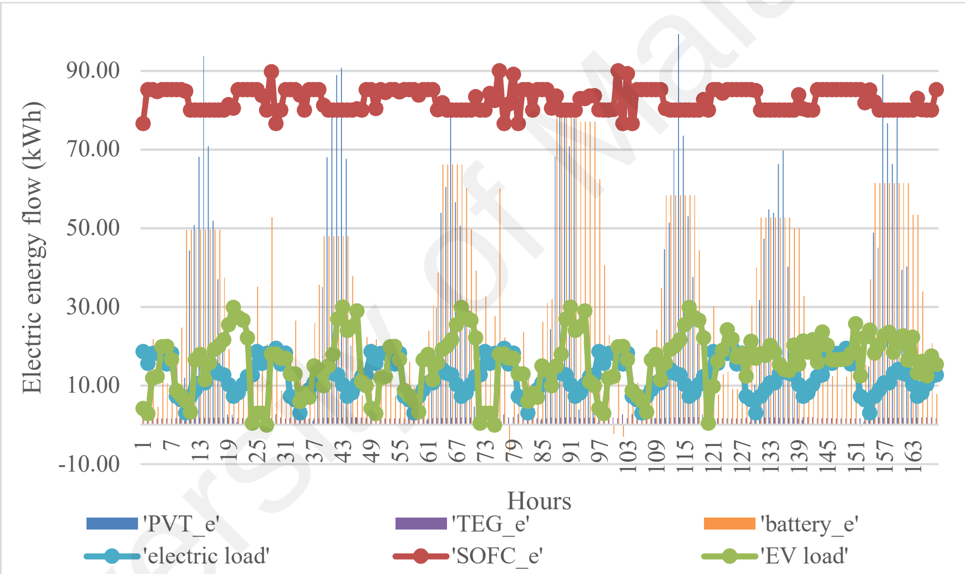

Figure 6.13: Weekly analysis of polygeneration electric energy flow

The same condition goes for the heat flow analysis depicted in Figure 6.14. On the daily analysis, SOFC takes more portion to generate heat compared to other components. Since the heat and cooling load is mostly similar throughout the week, no significant changes in cooling generation from the absorption chiller occurs either stored heat in the hot tank. For some hours there are cases that cooling demand is higher than its generation, then some load losses occur. However, this loss is less than the polygeneration without

FEMS which is proven by the decreased in the number of loss probability as presented in Figure 6.7.

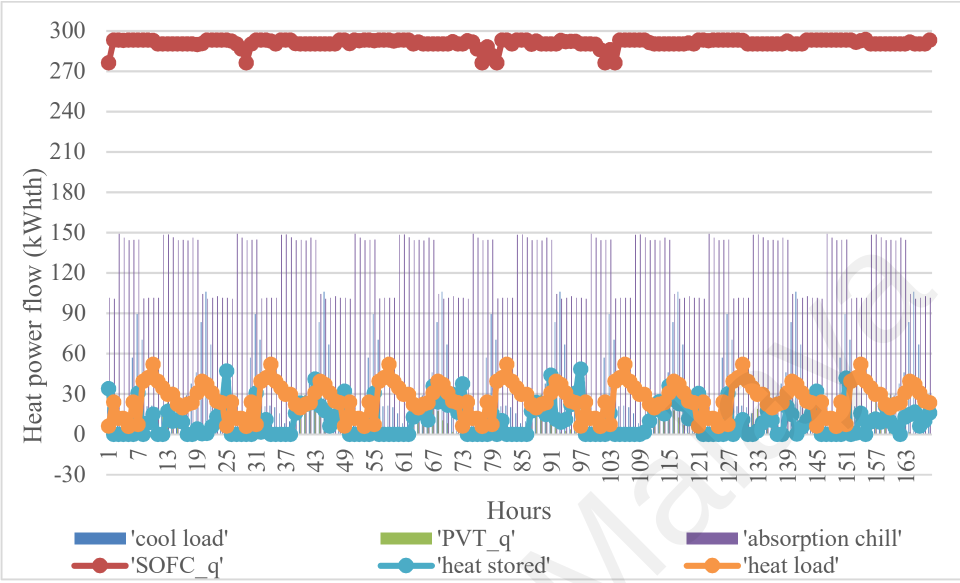

Figure 6.14: Weekly analysis of polygeneration electric power flow

6.6.2 AHP for prioritizing the best fitness weight inertia

In order to make a priority of each criterion in the objective function, the decision-making process is conducted using the AHP method. Based on the objective function in Eq. (6.1), there are six criteria considered in optimizing the polygeneration size. Due to the restriction to consider all criteria at the same time, overall priorities have to be defined for each solution as the subject. The priority is defined from the criteria and local priority values. As mentioned in section 6.6 b, case 1 considers equal weights to optimize the polygeneration size, while case 2 considers three criteria with different priority values in the optimization process. As solutions have generated from the different weighted objective value, local priority should be obtained amongst the solution to get the overall priority. The overall priority is calculated by multiplying the criteria and local priorities together using the referred preferences as explained detail in Appendix C.

Table 6.7 presents the weighted objective criteria, preferences, and consistency of the judgment. As this study has a restriction to simulate all possibilities of the weighted objective criteria, this study chooses six possibilities of objective weight for each optimization method. Case 1 employs equal weighted values for each criterion while Case 2 and Case 3 uses combinations of two and three criteria as the objective, respectively. After the solutions are gathered for both these cases, the decision-making process is conducted to choose the best solution.

As the essential parameter to examine the judgment of priority for all criteria, consistency index (RI) is used as an indicator. This value represents the consistency of defining the priority value of one criterion over the others to calculate its weighted value. The index value of 0.1 or less means the judgments are consistent. As presented in the table, all possibilities of judged criteria based on their preferences are acceptable since they have less of consistency index. The detail calculation of weighted objective criteria is presented in Appendix C.

Table 6.7: Weighted objective criteria, preferences, and consistency of judgment

Weighted objective	Preference	a1 (poly)	a2 (pes)	a3 (cs)	a4 (CO_2)	a5 (ploss)	a6 (lpsp)	Consistency (RI)
Equal (case 1)	EQUAL	0.167	0.167	0.167	0.167	0.167	0.167	0.000
Multi-objective 2 criteria (case 2)	PES_PLOSS	0.132	0.263	0.058	0.039	0.413	0.095	0.026
	PES_COES	0.089	0.312	0.323	0.051	0.142	0.083	0.083
	PLOSS_COES	0.095	0.147	0.233	0.050	0.394	0.081	0.059
	PES_CO2R	0.073	0.287	0.138	0.335	0.110	0.056	0.056
Multi-objective 3 criteria (case 3)	PES_PLOSS_COES	0.089	0.253	0.271	0.046	0.263	0.077	0.058

6.6.3 Bi-level OO and SO analysis for multi-objective problem

After the optimal operating strategy has been generated, optimization of the polygeneration design continues to search the best size of polygeneration components using meta-heuristic approaches based on evolutionary and swarm methods. Furthermore, to define the weighted objective criteria and decides the best candidate of solution based on the referred preference, AHP decision-making method is used.

(a) *Sensitivity analysis of GA and PSO optimization*

Before conducting optimization and prioritizing process for the polygeneration size, sensitivity analysis is conducted for both the GA and PSO methods. Since we are applying population-based optimization, the amount of population in the searching process will affect the optimum fitness value for both methods. In this study, three values of population are tried to determine the optimum parameters for GA and PSO. As presented in Table 6.8, the population number is evaluated in terms of fitness value, objective criteria values and its simulation time.

Table 6.8: Sensitivity analysis of the optimum population for GA and PSO methods

Method	Population	Fitness	fa1 (poly)	fa2 (pes)	fa3 (cs)	fa4 (co2r)	fb1 (ploss)	fb3 (lpsp)
GA	10	0.342	0.790	0.150	-0.396	0.102	5.146E+08	5.600E-03
GA	20	0.463	0.527	0.212	0.446	0.166	5.083E+08	1.029E-01
GA	30	0.441	1.230	0.594	-0.706	0.572	2.032E+08	3.060E-02
PSO	10	0.222	0.769	0.111	-0.389	0.063	4.987E+08	5.600E-03
PSO	20	0.237	0.995	0.390	-0.476	0.349	4.589E+08	1.110E-02
PSO	30	0.427	1.316	0.574	-0.559	0.543	3.246E+08	1.107E-02

Based on the results, it can be seen that the higher the population, the higher the fitness value. Optimization using 30 populations give the best fitness value, however the improvement is not equal to the simulation time required. For GA, improvement of the polygeneration performance appeared in reduction of energy loss, carbon emission, polygeneration efficiency, and PES. However, it reduced its cost saving more than 50% compared to the reference system. On the other hand, PSO optimization using 30 populations generated higher values of efficiency, PES, CO_2R and energy loss, yet increase its energy cost. Moreover, using 30 populations takes about 13 days to finish the computation process which is time consuming compared to 20 populations.

The best solution generated for each generation using GA is depicted in Figure 6.15. The optimum value reached by GA optimization is faster with a population of 20 compared to population 10 and 30. The best fitness in population 30 does not change until reached the last generation. It can also be observed that population of 20 reaches the minimum fitness better than population of 30 and population of 10.

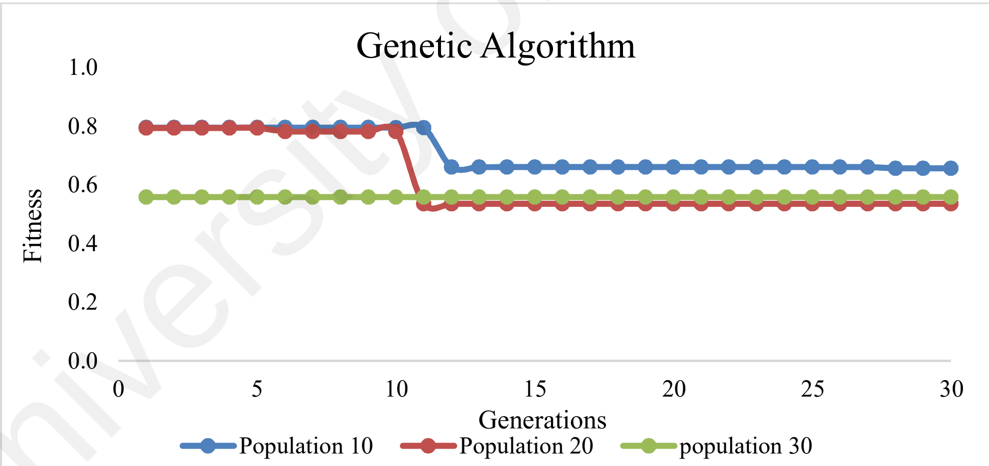

Figure 6.15: The best solution generated for each generation using GA

Figure 6.16 shows the best solution for the optimization using PSO for each of the iteration number. In contrast to the GA, optimization using PSO does not provide better solutions for each iteration. A small change is reached with population of 20, yet the value is not as good as the solution achieved using the GA. Although iteration with 30 populations gives the best solution compared to 10 and 20 populations, it takes longer time to reach the last iteration. In order to minimize the simulation time and get fair solution, this study considers applying the population of 20.

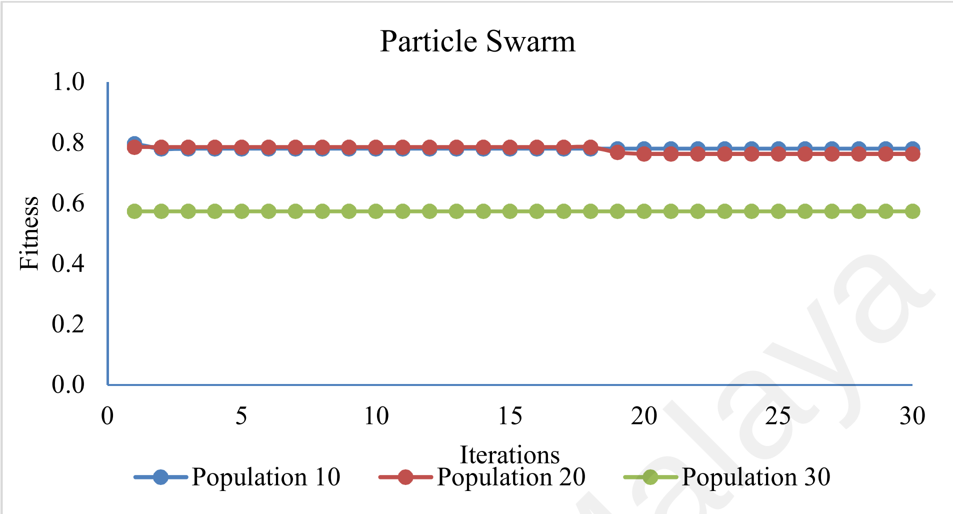

Figure 6.16: The best solution generated for each iteration using PSO algorithm

(b) ***Single objective optimization using GA and PSO***

Optimization of polygeneration design is conducted using GA and PSO with single-objective criterion. This study takes important criteria as the objectives, energy loss, CS, PES, and CO_2R. In line with the fourth objective of this study, the optimum design is expected to maximize energy saving, energy cost saving, and carbon emission reduction as well as minimize energy loss of the polygeneration system. For the optimization results, six performance parameters are presented such as polygeneration efficiency, primary energy saving, energy cost saving, carbon emission reduction, energy loss, and reliability of the system.

The results of the optimization are presented in Table 6.9 for GA and PSO with four important criteria as the single objective. From the fitness value of the GA-based optimization, PES as the optimum design criterion has the highest value compared to other criteria of about 0.694. Moreover, the highest polygeneration efficiency and reliability is achieved by power loss (PLOSS) based optimization with the value of 0.795 and 0.006 respectively, yet the energy loss of the design is still high compared to the PES based design. The PES based design attains the lowest energy loss of about 235 MWh per year besides having the highest energy saving of about 0.648 compared to the conventional separated system.

The PSO-based optimization attains an optimal design using the PES as the reference. With fitness value of 0.261, the PES design achieves the efficiency and PES by 77.1% and 22.5% respectively. The second-best design is achieved by the CO2R as the preference with the fitness value by 0.217. The PES and CO2R preferences have the most similar criteria values except for the LPSP. The CO2R design has a slightly better reliability compared to the PES design. Although it has the lowest fitness value amongst other designs, the COES design has the best reliability with loss probability by about 0.6%. Compared to others which have an average loss probability by about 3%, the COES design is categorized as a reliable system. Moreover, the COES design also has the highest cost saving compared to others with the value of about -36%. In general, the results of PSO-based optimization achieve performances lower than the GA-based optimization regarding its efficiency, PES and PLOSS criteria. However, it has better cost saving, carbon reduction and reliability compared to the GA results.

(c) ***Multi-objective optimization using GA-AHP and PSO-AHP***

Furthermore, this study also conducted optimization for the polygeneration size using GA and PSO with multi-objective criteria. Six preferences are used as presented in Table 6.10 in line with the GA and PSO based optimization results. Four criteria are used as the objectives namely PES, PLOSS, COES and CO_2R. Based on the criteria, the preferences are determined in different weighted value of each criterion as the optimization objective.

The GA-based optimization result can be seen in Table 6.10. The PES_CO2R based design achieves highest fitness value opposed to other preferences of about 0.512. The PES_PLOSS_COES-based design attains highest PES and CO2R and polygeneration efficiency of about 0.668, 0.636, and 0.847, respectively. The PLOSS_COES-based design reaches the best energy cost saving compared to others of about 0.424. This value is the best energy cost saving achieved by the polygeneration system with extra heat recovery system and almost as high as the polygeneration with the basic heat recovery system. The design also accomplishes the lowest energy loss of about 238 MWh per year. The highest reliability is achieved by the EQUAL and PES_PLOSS-based designs with the supply loss probability of about 8.6%.

For the PSO-based optimization, the multi-objective results have better performances compared to single-objective. The EQUAL design achieved the highest fitness value by 0.237. With this high fitness value, the design also attained the highest efficiency, energy savings and carbon reduction compared to others. Meanwhile, the lowest energy loss was achieved by the PES_COES design with value of 55 kWh per year. The PES_CO2R and PES_PLOSS designs are the best in reliability with probability of supply loss by about 6%. The significant drawback occurred in these designs are they having minus values of the cost saving. It means that none of these designs is profitable to be implemented economically. This also reveals the weaknesses of searching process in PSO over the GA where the optimal design cannot cover all criteria required especially for the cost saving criteria. All these results are gathered into ten solutions which is ranked by the AHP decision-making method. The process of prioritizing the optimum design considers both local priority of each solution to the others and the overall priority calculation by considering the judgment value presented in Table 6.7. The decision-making process is explained in Appendix C.

Table 6.9: Optimization results for single objective design using GA and PSO

Criteria	Preferences	GA							PSO						
		Fitness	fa1 (poly)	fa2 (pes)	fa3 (cs)	fa4 (co2r)	fb1 (ploss)	fb3 (lpsp)	Fitness	fa1 (poly)	fa2 (pes)	fa3 (cs)	fa4 (co2r)	fb1(ploss)	fb3 (lpsp)
SO	COES	-0.226	0.660	0.203	-0.355	0.152	5.766E+08	0.072	-0.326	0.804	0.114	-0.363	0.062	5.540E+08	0.006
	PES	0.694	0.725	0.648	-1.844	0.623	2.358E+08	0.197	0.261	0.771	0.225	-0.606	0.177	5.267E+08	0.036
	PLOSS	0.005	0.795	0.118	-0.395	0.068	5.198E+08	0.006	0.002	0.771	0.225	-0.606	0.177	5.267E+08	0.036
	CO2R	0.603	0.775	0.630	-1.509	0.597	3.476E+08	0.183	0.217	0.771	0.225	-0.606	0.177	5.267E+08	0.031

Table 6.10: Optimization results for multi-objective design using GA and PSO

Criteria	Preferences	GA							PSO						
		Fitness	fa1 (poly)	fa2 (pes)	fa3 (cs)	fa4 (co2r)	fb1 (ploss)	fb3 (lpsp)	Fitness	fa1 (poly)	fa2 (pes)	fa3 (cs)	fa4 (co2r)	fb1(ploss)	fb3(lpsp)
MO	EQUAL	0.385	0.602	0.204	-0.893	0.150	5.898E+08	0.086	0.237	0.995	0.390	-0.476	0.349	2.369E+08	0.237
	PES_PLOSS	0.228	0.611	0.208	-0.824	0.162	4.993E+08	0.086	0.191	0.892	0.204	-0.380	0.150	5.936E+08	0.006
	PES_COES	0.449	0.850	0.650	0.299	0.618	3.280E+08	0.145	0.071	0.669	0.113	-0.620	0.061	5.595E+04	0.036
	PLOSS_ COES	0.334	0.797	0.651	0.424	0.626	2.382E+08	0.153	0.073	0.669	0.113	-0.620	0.061	5.595E+08	0.036
	PES_ CO2R	0.512	0.805	0.632	0.391	0.596	3.776E+08	0.153	0.145	0.892	0.204	-0.380	0.150	5.936E+08	0.006
	PES_PLOSS_ COES	0.333	0.847	0.668	0.115	0.636	3.197E+08	0.153	0.072	0.669	0.113	-0.620	0.061	5.595E+08	0.036

Table 6.11 presents the GA-AHP result for the prioritized optimum design. The results are arranged from the highest to the lowest priority value. The best solution is reached by the PLOSS_COES-based design with the priority value of 0.124. This result is in accordance with the multi-objective design of polygeneration in Table 6.10. The design achieves several improvements in the PES, COES, CO_2R as well as a reasonable polygeneration efficiency and the lowest energy loss compared to other solutions.

Table 6.11: GA-AHP results for prioritized optimum design

Alternatives	Preferences	poly	pes	cs	co2r	ploss	lpsp	priority
Solution 1	PLOSS_COES	0.797	0.651	0.424	0.626	2.382E+08	0.153	0.124
Solution 2	PES_COES	0.850	0.650	0.299	0.618	3.280E+08	0.145	0.118
Solution 3	PES_PLOSS_COES	0.847	0.668	0.115	0.636	3.197E+08	0.153	0.117
Solution 4	PES_CO2R	0.805	0.632	0.391	0.596	3.776E+08	0.153	0.114
Solution 5	PES	0.725	0.648	-1.844	0.623	2.358E+08	0.197	0.103
Solution 6	CO2R	0.775	0.630	-1.509	0.597	3.476E+08	0.183	0.098
Solution 7	PLOSS	0.795	0.118	-0.395	0.068	5.198E+08	0.006	0.088
Solution 8	COES	0.660	0.203	-0.355	0.152	5.766E+08	0.072	0.082
Solution 9	PES_PLOSS	0.611	0.208	-0.824	0.162	4.993E+08	0.086	0.080
Solution 10	EQUAL	0.602	0.204	-0.893	0.150	5.898E+08	0.086	0.076

On the other hand, the EQUAL-based design gives the worst solution with the lowest priority value. This result reveals the advantage of using the process of prioritizing to determine the best weight value of each criteria to generate multi-objective solution which is non-dominated in reaching the required performances. The EQUAL-based preference approaches for all the criteria evenly, despite one criterion can be superior than others. This affects the searching process and the result of the design as well.

The results for the prioritized optimum design using PSO-AHP is presented in Table 6.12. The best design with the highest priority value was achieved by the EQUAL as the preference. Also, the EQUAL design attains the highest efficiency by 99.5% and the highest primary energy saving by 39% compared to others. Moreover, the EQUAL design turn to be the most environmentally friendly system compared to other designs with the highest emission saving by about 35%. The EQUAL design also has the best performance regarding the system loss with achieving less in the energy loss by about 237 MWh per year. However, the second-best design achieved by the PES_PLOSS gets better reliability than the EQUAL design with the LPSP value by about 6% as the lowest power loss probability.

Table 6.12: PSO-AHP results for prioritized optimum design

Alternatives	Preferences	poly	pes	cs	co2r	ploss	lpsp	priority
Solution 1	EQUAL	0.995	0.390	-0.476	0.349	2.369E+08	0.237	0.144
Solution 2	PES_PLOSS	0.892	0.204	-0.380	0.150	5.936E+08	0.006	0.115
Solution 3	COES	0.804	0.114	-0.363	0.062	5.540E+08	0.006	0.109
Solution 4	PES	0.771	0.225	-0.606	0.177	5.267E+08	0.031	0.098
Solution 5	CO2R	0.771	0.225	-0.606	0.177	5.267E+08	0.031	0.098
Solution 6	PLOSS	0.771	0.225	-0.606	0.177	5.267E+08	0.036	0.097
Solution 7	PES_COES	0.795	0.118	-0.395	0.068	5.198E+08	0.006	0.088
Solution 8	PLOSS_COES	0.660	0.203	-0.355	0.152	5.766E+08	0.072	0.082
Solution 9	PES_CO2R	0.611	0.208	-0.824	0.162	4.993E+08	0.086	0.080
Solution 10	PES_PLOSS_COES	0.602	0.204	-0.893	0.150	5.898E+08	0.086	0.076

6.7 Discussions

Analysis of Fuzzy logic method as the optimal operation strategy reveals its effect on the improvement of polygeneration system with standalone system and electric vehicle power supply as well as with grid-connection and hydrogen vehicle power supply. The FEMS provides positive enhancements on the standalone polygeneration system with electric supply, yet negative degradations on the grid-connected polygeneration with hydrogen vehicle power supply system. The improvement of the reliability of the polygeneration system achieved by the standalone polygeneration using optimal operating strategy is about 53% compared to the system with no fuzzy-based operating strategy. It is also confirmed the enhancement of energy saving and efficiency are 112%

and 4% respectively for the standalone polygeneration system compared to grid-connected polygeneration system applying the optimal FEMS. The operation strategy reveals its impact on reducing grid energy loss in both systems by 48.82% and 49.26% for the standalone and grid-connected polygeneration systems, respectively. The result also proves the advantage of the standalone polygeneration system with electric vehicle power supply economically with achieving energy cost saving of about 32.58% which is higher than the system with no fuzzy-based operation.

Moreover, from the daily and weekly analysis, it concludes that the supply sources can satisfy the demands very well for both electricity and thermal loads. However, optimization of polygeneration size must be conducted to design the best component capacity in reducing power loss and increasing its energy performance.

The comparison between the results achieved by the GA-AHP and the PSO-AHP is presented in Table 6.13. The comparison was conducted by calculating the priority for each solution based on their assessment criteria, i.e. polygeneration efficiency, PES, COES, CO_2R, PLOSS and reliability of the system. Based on the results, it can be seen that the GA-AHP optimization achieves better solution in the first, second and third places. The first place is achieved by the power loss-energy cost saving as the preference using the GA-AHP optimization. The design has the best in cost savings as well as a fair energy saving, carbon reduction, energy loss and reliability. In the second place, the PES-COES design attains the higher efficiency compared to the PLOSS-COES design while it has lower cost savings, energy saving and emission reduction. The design also has more energy loss and highest reliability compared to the first design.

The PSO-AHP designs achieve the fourth and the fifth places as the best design. Compared to the GA-AHP, the PSO-AHP designs has a drawback in the cost saving even though it has better efficiency and reliability. It causes the design having lower priority compared to the GA-AHP. The best efficiency of the system is achieved by using PSO in the EQUAL design by about 99.5% while for the best PES and emission reduction, it is attained by using GA in the PES-PLOSS-COES design by about 66.8% and 63.6% respectively. The EQUAL design using PSO is at the fourth place achieves the lowest energy loss, however it also has the worst reliability compared to other designs. In conclusion, the best design achieved by its priority is not considered for single criterion only but also multi-criteria. Therefore, in the results, one design could be better than other for a specific criterion. However, the highest priority achieved by the GA-AHP optimization using the power loss-energy cost saving as the preferences means that the design is best in accommodating all criteria with non-dominated solution.

Table 6.13: GA-AHP compared to PSO-AHP results for the best design

Alternatives	Preferences	poly	pes	cs	co2r	ploss	lpsp	priority
Solution 1	GA-PLOSS_COES	0.797	0.651	0.424	0.626	2.382E+08	0.153	0.188
Solution 2	GA-PES_COES	0.850	0.650	0.299	0.618	3.280E+08	0.145	0.180
Solution 3	GA-PES_PLOSS_COES	0.847	0.668	0.115	0.636	3.197E+08	0.153	0.175
Solution 4	PSO-EQUAL	0.995	0.390	-0.476	0.349	2.369E+08	0.237	0.162
Solution 5	PSO-PES_PLOSS	0.892	0.204	-0.380	0.150	5.936E+08	0.006	0.128

After the best design was achieved, the best optimization preference was run for ten times to analyze the stability of the result through deviation and average analyses. The results for the power loss-energy cost saving using GA run in ten times optimization cycles is presented in Table 6.14. From the results, it can be seen that the results have a good stability in achieving the optimum performance with errors by about 2%. The results also confirm the average value of each criteria is not too different than achieved by the optimal value. The high stability of result is due to the search space in searching the optimum design and the combination of criteria and preferences used. It makes the optimization searching process reach the convergence at the same solutions in every iteration run.

As the optimal capacity achieved by the polygeneration components, the SOFC as the prime mover has the size of 38kW while the absorption chiller capacity of about 16kWth. With 10 panels and 28 panels in series and parallel respectively, the optimal energy generated from the photovoltaic thermal achieved. Moreover, 100 kW of electrolyzer is sufficient to generate hydrogen in covering the load requirement or profitably to be sold. The 63 modules of thermoelectric generator are optimal in converting the excess heat from the prime mover while the battery capacity 1.7 kWh is sufficient to store the excess electricity without increase the system cost significantly.

Table 6.14: The best design from GA-AHP running for 10 times

Solution name	Simulation times	Fitness	fa1 (poly)	fa2 (pes)	fa3 (cs)	fa4 (co2r)	fb1(ploss)	fb3(lpsp)
GA-PLOSS_COES	1	0.330	0.750	0.651	0.428	0.626	2.382E+08	0.183
	2	0.330	0.750	0.651	0.428	0.626	2.382E+08	0.183
	3	0.330	0.750	0.651	0.428	0.626	2.382E+08	0.183
	4	0.334	0.797	0.651	0.424	0.626	2.382E+08	0.153
	5	0.330	0.750	0.651	0.428	0.626	2.382E+08	0.183
	6	0.330	0.750	0.651	0.428	0.626	2.382E+08	0.183
	7	0.334	0.797	0.651	0.424	0.626	2.382E+08	0.153
	8	0.330	0.750	0.651	0.428	0.626	2.382E+08	0.183
	9	0.330	0.750	0.651	0.428	0.626	2.382E+08	0.183
	10	0.334	0.797	0.651	0.424	0.626	2.382E+08	0.153
Deviation		0.002	0.021	0.000	0.002	0.000	0.000	0.014
Average		0.331	0.764	0.651	0.427	0.626	2.382E+08	0.174

Moreover, the optimized polygeneration achieves several improvements in the energy saving, cost saving and the percentage of carbon emission. The PES from the optimized polygeneration has increased by 81.29% compared to the unoptimized polygeneration system. The energy cost savings and carbon reduction are also increase by about 54% and 99% respectively. These results prove the effect of optimization on the polygeneration system from energy, economic and environmental aspects. Due to the solution given is a non-dominated that would be better for several criteria, other criteria such as efficiency and reliability show results that is not better than before optimization. However, since the energy saving, cost saving and carbon emission are the priority criteria, this optimized polygeneration can be adopted as the optimal system.

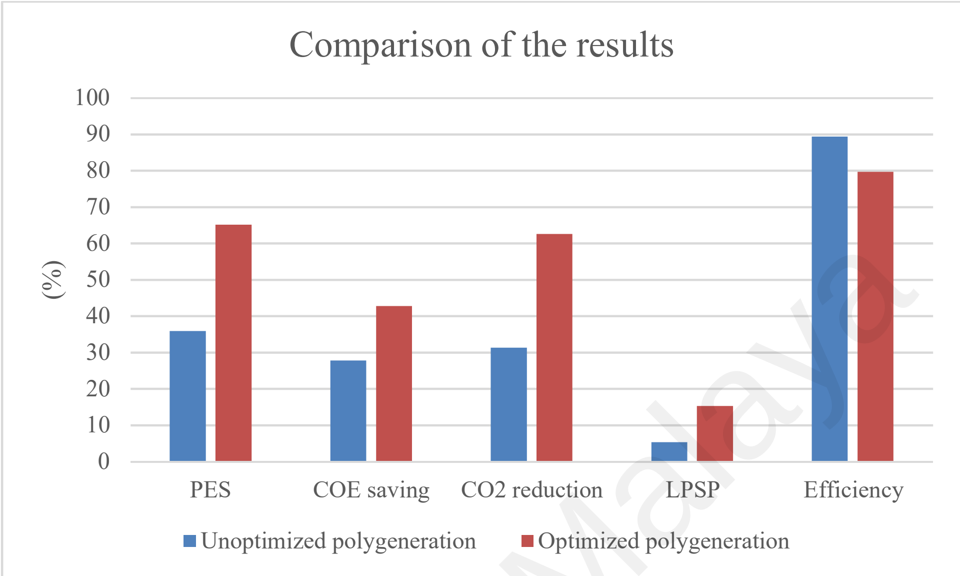

Figure 6.17: Comparison of results between unoptimized and optimized polygeneration systems

Based on the optimization process using GA and PSO methods, it can be concluded that the optimization performances are variative based on their problems, criteria combinations, parameters and their preferences. This study achieves the best optimal design using GA method while for other problems and preferences, the results could be different.

6.8 Summary

This chapter has presented the fourth objective of this study to optimizing the operating strategy and size of the polygeneration system. In optimizing the operating strategy, fuzzy energy management strategy has been applied with different shapes of fuzzy membership. It reveals that the better performance has been achieved by managing the power and heat from the SOFC, electrolyzer and absorption chiller temperature in satisfying loads and reduce the energy loss. Moreover, optimization of the polygeneration size has been conducted using GA and PSO methods. By considering six criteria based on energy, economic and environmental aspects, optimizations were developed using single-objective and multi-objective approaches. In multi-objective approach, analytical hierarchy programming has been considered to define the preference based on the combinations between two and three criteria considered. The results reveal that the preference using energy loss and cost saving as the combined criteria achieve the highest priority as the best design of polygeneration system. This study also proves the superior of the GA performance in optimizing the polygeneration size better than the PSO method for this problem and objective.

CHAPTER 7: CONCLUSIONS AND FUTURE WORKS

7.1 Conclusions

Based on the results from the first to fourth objective, there are several achievements reached on the optimum design of polygeneration system. Firstly, as the initial step in analyzing and optimizing the SOFC based polygeneration design, a simulation-based modeling was conducted using MATLAB software. The simulation developed presented in Chapter 4 consists mathematical model of SOFC in thermodynamic and electrochemical equations, heat exchanger and absorption chiller models, as well as energy storage models including battery, sensible heat, and hydrogen. The model of polygeneration components was demonstrated its performance in the different changes of operating conditions which satisfied the first objective of this study. This model was an integrated and simplified model which could be used for further process systems such as management and optimization purposes. The model of polygeneration was run in the hourly-based period throughout 8760 hours or a year.

Moreover, amongst four scenarios evaluated in this study, the polygeneration with electric vehicle scenario had the best performance and was competitive compared to hydrogen vehicle (HV) scenario as the HV seemed to have a higher cost due to the highly fueling price of hydrogen. However, since the polygeneration with HV scenario did not consume electricity as high as the EV scenario, penetration of the main grid could be avoided, and the system had better performance in a standalone configuration. The scenario of hydrogen selling to retailers in this study gave a significant effect to the reduction of the energy cost of polygeneration system. The hydrogen selling strategy reduced almost a quarter of energy cost, hence increased the cost saving compared to the polygeneration with no chance to sell hydrogen due to high consumption of hydrogen in the fueling station. However, consuming hydrogen instead of electricity from the grid has given a better effect on the environmental aspect as the emission carbon reduced significantly.

The additional heat recovery system seems to increase the efficiency of the overall system, PES, cost saving, carbon reduction as well and decrease the penetration effect of the grid by reducing its imported electricity to the system. The chosen PVT and TEG as the extra energy generation and heat recovery of the prime mover increase the reliability of supply in serving loads. Not only in electricity, but also in heat and cooling demands. Another improvement was reached for imported energy from the grid which was significantly reduced when extra heat recovery is applied. The high initial cost of PVT could be balanced with the energy generated both electricity and heat, hence increase cost saving of polygeneration system. In conclusion, the extra heat recovery system is suitable to be employed in the polygeneration system where the electric demands are higher than heating, cooling, and hydrogen. Moreover, the possibility to implement the polygeneration in a standalone system is higher by applying this recovery system due to its better reliability in serving the loads. The comparative study conducted between polygeneration with the basic heat recovery and extra-heat recovery has been performed in fulfilling the third objective.

In line with satisfying the fourth objective, the optimum operating strategy was performed in the first phase. An artificial intelligence (AI)-based energy management was proposed using fuzzy logic programming (FLP) namely fuzzy energy management system (FEMS). In handling either SOFC, absorption chiller, and electrolyzer operations, the FEMS was designed in multi-variables and multi-level management mechanism. The first level dealt with power, heat and cooling managements considering electric and hydrogen loads, PVT power at the time as well as the power level stored in the battery.

Meanwhile, the second level of management feedbacked the power and heat of SOFC as well as the COP of the chiller to control several operating points including temperature, fuel utilization, and air to fuel ratio for SOFC, while generator and absorber temperature for the chiller. As the results presented in Chapter 6, fuzzy operating strategy exhibited its capability in handling various load patterns between electricity, heat, cooling, and hydrogen and served in better reliability. The reliability of the polygeneration system was increasing in line with the decrease of power loss using the operating strategy. Amongst three proposed fuzzy memberships, the triangle membership produced better results in increasing the reliability and reducing the power loss. However, the optimum operation should be combined with an optimum size of polygeneration components to increase its PES and COES, as well as reduce the power loss as the point in the fourth objective.

The further study conducted in optimizing the design of polygeneration and combined to the optimum operation of components employed meta-heuristic optimization using evolutionary-based and swarm-based algorithms. This study considered six variables as the decision and six criteria applied to search the best component capacity of polygeneration system. In optimizing the polygeneration size, both population-based methods are efficient to optimize the capacity of SOFC, cooling chiller, TEG, PVT and the electrolyzer. Moreover, to optimize the objective criteria and generate non-dominated solutions in optimizing the polygeneration size, a decision-making method was applied using analytic hierarchical process (AHP). The AHP was used to determine the best weighted objective values of each criterion based on the proposed preferences. In this study, three cases consisting six combinations of criteria were adopted at this decision-making process to fulfill the fourth objective. As for multi-objective including two or more criteria to be considered, this AHP was used also for determining the best solution generated based on the desired preference. As stated in the results, the AHP decision-making method reveals to have better performance on optimizing the objective weight criteria and generates a non-dominated solution which can deal with the multi-objective and multi-criteria requirements.

7.2 Future works

As this system is a novel SOFC based polygeneration with integrated vehicle power supply system, several future directions can be considered for future works:

1. Firstly, it is challenging to conduct both optimum operating strategy and searching the best capacity of polygeneration with HV fueling system. Since this study considered the best configuration as the case in conducting optimization for the operation and the size, the polygeneration with HV was not considered at this time. However, by applying both optimization approaches, it is expected to generate a polygeneration with better energy saving and cost saving while having the lowest power lost in the HV scenario.

2. Since the obstacle is the hydrogen price, an economic scenario such as feed-in tariffs or incentives from the government can be applied to analyze how competitive the system to be implemented in a real application.

3. Moreover, since the cases comparatively distinguished between the polygeneration with EV and HV, further study should be conducted to search the best design of polygeneration which includes both vehicles power supply systems. Optimization of operation and size could be performed to search the best shares of supply for both EV and HV to be included in the polygeneration.

REFERENCES

Abdul-Razak, A.H.N., Leardini, P., , & Nair, N.K.C. (2015). *Adapting Malaysian housing for smart grid deployment based on the first nationwide energy consumption survey of terrace houses*. Paper presented at the Living and Learning: Research for a Better Built Environment: 49th International Conference of the Architectural Science Association 2015.

Adam, A., & Fraga, E.S. (2013). Modelling and optimisation in terms of CO2 emissions of a solid oxide fuel cell based micro-CHP system in a four bedroom house in London. *Energy Procedia, 42*, 201-209.

Ahmadi, P. (2013). *Modeling, Analysis and Optimization of Integrated Energy Systems for Multigeneration Purposes.* (Doctor of Philosophy), University of Ontario Institute of Technology, Oshawa, Ontario, Canada.

Akikur, R.K., Saidur, R., Ping, H.W., & Ullah, K.R. (2014). Performance analysis of a co-generation system using solar energy and SOFC technology. *Energy Conversion and Management, 79*, 415-430.

Akikur, R.K., Saidur, R., Ullah, K.R., Hajimolana, S.A., Ping, H.W., & Hussain, M.A. (2015). Economic feasibility analysis of a solar energy and solid oxide fuel cell-based cogeneration system in Malaysia. *Clean Technologies and Environmental Policy, 18*(3), 669-687.

Al-Zareer, M., Dincer, I., & Rosen, M.A. (2018). Multi-objective optimization of an integrated gasification combined cycle for hydrogen and electricity production. *Computers & Chemical Engineering, 117*, 256-267.

Al Moussawi, H., Fardoun, F., & Louahlia-Gualous, H. (2016). Review of tri-generation technologies: Design evaluation, optimization, decision-making, and selection approach. *Energy Conversion and Management, 120*, 157-196.

Al Moussawi, H., Fardoun, F., & Louahlia, H. (2017). 4-E based optimal management of a SOFC-CCHP system model for residential applications. *Energy Conversion and Management, 151*, 607-629.

Almansa, X.F. (2010). *Innovative biomass fuelled SOFC's for polygeneration.* (Master of Science Thesis), KTH School of Chemical Science and Engineering,

Almeida, L.Q.d., Sales, L.C.M., & Sodré, J.R. (2015). Fuel consumption and emissions from a vehicle operating with ethanol, gasoline and hydrogen produced on-board. *International Journal of Hydrogen Energy, 40*(21), 6988-6994.

Ameri, M., & Besharati, Z. (2016). Optimal design and operation of district heating and cooling networks with CCHP systems in a residential complex. *Energy and Buildings, 110*, 135-148.

Amrizal, N., Chemisana, D., & Rosell, J.I. (2013). Hybrid photovoltaic–thermal solar collectors dynamic modeling. *Applied Energy, 101*, 797-807.

Anatone, M., & Panone, V. (2015). A Model for the Optimal Management of a CCHP Plant. *Energy Procedia, 81*, 399-411.

Antonucci, V., Branchini, L., Brunaccini, G., De Pascale, A., Ferraro, M., Melino, F., . . . Sergi, F. (2017). Thermal integration of a SOFC power generator and a Na–NiCl2 battery for CHP domestic application. *Applied Energy, 185*, 1256-1267.

Antonucci, V., Brunaccini, G., De Pascale, A., Ferraro, M., Melino, F., Orlandini, V., & Sergi, F. (2015). Integration of μ-SOFC Generator and ZEBRA Batteries for Domestic Application and Comparison with other μ-CHP Technologies. *Energy Procedia, 75*, 999-1004.

Anvari, S., Khoshbakhti Saray, R., & Bahlouli, K. (2017). Employing a new optimization strategy based on advanced exergy concept for improvement of a tri-generation system. *Applied Thermal Engineering, 113*, 1452-1463.

Anvari, S., Taghavifar, H., Saray, R.K., Khalilarya, S., & Jafarmadar, S. (2015). Implementation of ANN on CCHP system to predict trigeneration performance with consideration of various operative factors. *Energy Conversion and Management, 101*, 503-514.

Arcuri, P., Beraldi, P., Florio, G., & Fragiacomo, P. (2015). Optimal design of a small size trigeneration plant in civil users: A MINLP (Mixed Integer Non Linear Programming Model). *Energy, 80*, 628-641.

Arsalis, A. (2007). *Thermoeconomic Modeling and Parametric Study Hybrid Solid Oxide Fuel Cell – Gas Turbine – Steam Turbine Power Plants Ranging from 1.5 MWe to 10 MWe.* (Master of Science), Virginia Polytechnic Institute and State University, Blacksburg, Virginia.

Arteconi, A., Brandoni, C., & Polonara, F. (2009). Distributed generation and trigeneration: Energy saving opportunities in Italian supermarket sector. *Applied Thermal Engineering, 29*(8-9), 1735-1743.

Assaf, J., & Shabani, B. (2016). Transient simulation modelling and energy performance of a standalone solar-hydrogen combined heat and power system integrated with solar-thermal collectors. *Applied Energy, 178*, 66-77.

Awad, A., Bazan, P., & German, R. (2016). Optimized Operation of PV/T and Micro-CHP Hybrid Power Systems. *Technology and Economics of Smart Grids and Sustainable Energy, 1*(1).

Badami, M., Mura, M., Campanile, P., & Anzioso, F. (2008). Design and performance evaluation of an innovative small scale combined cycle cogeneration system. *Energy, 33*(8), 1264-1276.

Badea, N., Cazacu, N., Voncila, I., Paraschiv, I., & Oanca, M. (2008). Strategies Used for Developing Micro-CCHP Structures in Residential and Public Buildings. *The annals of "dunarea de jos" university of galati fascicle III, 31*(1), 43-48.

Baghernejad, A., Yaghoubi, M., & Jafarpur, K. (2015). Optimum power performance of a new integrated SOFC-trigeneration system by multi-objective exergoeconomic optimization. *International Journal of Electrical Power & Energy Systems, 73*, 899-912.

Bahlouli, K. (2018). Multi-objective optimization of a combined cycle using exergetic and exergoeconomic approaches. *Energy Conversion and Management, 171*, 1761-1772.

Baky, I.A. (2010). Solving multi-level multi-objective linear programming problems through fuzzy goal programming approach. *Applied Mathematical Modelling, 34*(9), 2377-2387.

Basrawi, F., Ibrahim, T.K., Habib, K., & Yamada, T. (2016). Effect of operation strategies on the economic and environmental performance of a micro gas turbine trigeneration system in a tropical region. *Energy, 97*, 262-272.

Basrawi, F., Yamada, T., & Obara, S.y. (2014). Economic and environmental based operation strategies of a hybrid photovoltaic–microgas turbine trigeneration system. *Applied Energy, 121*, 174-183.

Behbahani-nia, A., Bagheri, M., & Bahrampoury, R. (2010). Optimization of fire tube heat recovery steam generators for cogeneration plants through genetic algorithm. *Applied Thermal Engineering, 30*(16), 2378-2385.

Ben Ali, I., Turki, M., Belhadj, J., & Roboam, X. (2018). Optimized fuzzy rule-based energy management for a battery-less PV/wind-BWRO desalination system. *Energy, 159*, 216-228.

Bensaid, S., Brignone, M., Ziggiotti, A., & Specchia, S. (2012). High efficiency Thermo-Electric power generator. *International Journal of Hydrogen Energy, 37*(2), 1385-1398.

Bernard, A. (2008). Micro combined heat and power operating on renewable energy for residential building. *PhD, CEP-Centre Energétique et Procédés*.

Boyaghchi, F.A., & Heidarnejad, P. (2015). Thermoeconomic assessment and multi objective optimization of a solar micro CCHP based on Organic Rankine Cycle for domestic application. *Energy Conversion and Management, 97*, 224-234.

Brahman, F., & Jadid, S. (2014). *Optimal Energy Management of Hybrid CCHP and PV in a Residential Building*. Paper presented at the Electrical Power Distribution Networks (EPDC), 2014 19th Conference on, Niroo Research Institute.

Bryant, S.M. (2011). *Techno-economic Feasibility of CHP Plants Equipped With Thermal Storage in Ontario, Canada and their Conversion to Trigeneration Plants Using Absorption Chillers.* (Master of Science), Aalborg University,,

Burer, M., Tanaka, K., Favrat, D., & Yamada, K. (2003). Multi-criteria optimization of a district cogeneration plant integrating a solid oxide fuel cell–gas turbine combined cycle, heat pumps and chillers. *Energy, 28*(6), 497-518.

Calise, F. (2011). Design of a hybrid polygeneration system with solar collectors and a Solid Oxide Fuel Cell: Dynamic simulation and economic assessment. *International Journal of Hydrogen Energy, 36*(10), 6128-6150.

Calise, F., Dentice d'Accadia, M., Libertini, L., Quiriti, E., Vanoli, R., & Vicidomini, M. (2017a). Optimal operating strategies of combined cooling, heating and power systems: A case study for an engine manufacturing facility. *Energy Conversion and Management*.

Calise, F., Dentice d'Accadia, M., Libertini, L., Quiriti, E., & Vicidomini, M. (2017b). A novel tool for thermoeconomic analysis and optimization of trigeneration systems: A case study for a hospital building in Italy. *Energy, 126*, 64-87.

Calise, F., Dentice d'Accadia, M., & Piacentino, A. (2014). A novel solar trigeneration system integrating PVT (photovoltaic/thermal collectors) and SW (seawater) desalination: Dynamic simulation and economic assessment. *Energy, 67*, 129-148.

Calise, F., Figaj, R.D., Massarotti, N., Mauro, A., & Vanoli, L. (2017c). Polygeneration system based on PEMFC, CPVT and electrolyzer: Dynamic simulation and energetic and economic analysis. *Applied Energy, 192*, 530-542.

Calise, F., Figaj, R.D., & Vanoli, L. (2017d). A novel polygeneration system integrating photovoltaic/thermal collectors, solar assisted heat pump, adsorption chiller and electrical energy storage: Dynamic and energy-economic analysis. *Energy Conversion and Management*.

Cardona, E., & Piacentino, A. (2003). A methodology for sizing a trigeneration plant in mediterranean areas. *Applied Thermal Engineering, 23*(13), 1665-1680.

Carr, S., Premier, G.C., Guwy, A.J., Dinsdale, R.M., & Maddy, J. (2014). Hydrogen storage and demand to increase wind power onto electricity distribution networks. *International Journal of Hydrogen Energy, 39*(19), 10195-10207.

Carr, S., Zhang, F., Liu, F., Du, Z., & Maddy, J. (2016). Optimal operation of a hydrogen refuelling station combined with wind power in the electricity market. *International Journal of Hydrogen Energy, 41*(46), 21057-21066.

Chachuat, B., Mitsos, A., & Barton, P.I. (2005). Optimal design and steady-state operation of micro power generation employing fuel cells. *Chemical Engineering Science, 60*(16), 4535-4556.

Chen, J.M.P., & Ni, M. (2014). Economic analysis of a solid oxide fuel cell cogeneration/trigeneration system for hotels in Hong Kong. *Energy and Buildings, 75*, 160-169.

Chen, L., Gao, S., & Zhang, H. (2013). Performance Analysis and Multi-Objective Optimization of an Irreversible Solid Oxide Fuel Cell-Stirling Heat Engine Hybrid System. *Int. J. Electrochem. Sci., 8*, 10772 - 10787.

Chen, X., Pan, Y., & Chen, J. (2010). Performance and Evaluation of a Fuel Cell-Thermoelectric Generator Hybrid System. *Fuel Cells, 10*(6), 1164-1170.

Chitsaz, A., Hosseinpour, J., & Assadi, M. (2017). Effect of recycling on the thermodynamic and thermoeconomic performances of SOFC based on trigeneration systems; A comparative study. *Energy, 124*, 613-624.

Chitsaz, A., S. Mahmoudi, S.M., & Rosen, M.A. (2015). Greenhouse gas emission and exergy analyses of an integrated trigeneration system driven by a solid oxide fuel cell. *Applied Thermal Engineering, 86*, 81-90.

Choudhury, A., Chandra, H., & Arora, A. (2013). Application of solid oxide fuel cell technology for power generation—A review. *Renewable and Sustainable Energy Reviews, 20*, 430-442.

Ciampi, G., Rosato, A., Scorpio, M., & Sibilio, S. (2014). Experimental analysis of a micro-trigeneration system composed of a micro-cogenerator coupled with an electric chiller. *Applied Thermal Engineering, 73*(1), 1309-1322.

DEIA, U.S. (2016). Hydrogen Fuel Cost vs Gasoline. Retrieved from http://heshydrogen.com/hydrogen-fuel-cost-vs-gasoline/

Dennehy, E.R., Brian, P., & Gallachóir, O. (2018). Ex-post decomposition analysis of passenger car energy demand and associated CO2 emissions. *Transportation research part D, 59*, 400-416.

Department of Energy, U.S. (2015). *Chapter 5: Increasing Efficiency of Building Systems and Technologies*. Retrieved from United States of America:

Dicks, A.L., Fellows, R., Mescal, C.M., & Seymour, C. (2000). A study of SOFC–PEM hybrid systems. *Journal of Power Sources, 86*(1), 501-506.

Dorer, V., Weber, R., & Weber, A. (2005). Performance assessment of fuel cell micro-cogeneration systems for residential buildings. *Energy and Buildings, 37*(11), 1132-1146.

Dunn, S. (2002). Hydrogen futures: toward a sustainable energy system. *International Journal of Hydrogen Energy, 27*, 235-264.

Eberle, U., Muller, B., & von Helmolt, R. (2012). Fuel cell electric vehicles and hydrogen infrastructure: status 2012. *Energy & Environmental Science, 5*(10), 8780-8798.

Eleventh Malaysia Plan, Strategy Paper 17: Sustainable Usage of Energy to Support Growth. (2017). Retrieved from Putrajaya, Malaysia:

Ellamla, H.R., Staffell, I., Bujlo, P., Pollet, B.G., & Pasupathi, S. (2015). Current status of fuel cell based combined heat and power systems for residential sector. *Journal of Power Sources, 293*, 312-328.

Elmer, T. (2015). *A novel SOFC tri-generation system for building applications.* (Doctor of Philoshopy), University of Nottingham,

Elmer, T., Worall, M., Wu, S., & Riffat, S.B. (2015). Fuel cell technology for domestic built environment applications: State of-the-art review. *Renewable and Sustainable Energy Reviews, 42*, 913-931.

Entchev, E. (2003). Residential fuel cell energy systems performance optimization using “soft computing” techniques. *Journal of Power Sources, 118*(1-2), 212-217.

Entchev, E., Yang, L., Ghorab, M., & Lee, E.J. (2014). Performance analysis of a hybrid renewable microgeneration system in load sharing applications. *Applied Thermal Engineering, 71*(2), 697-704.

Entchev, E., Yang, L., Szadkowski, F., Armstrong, M., & Swinton, M. (2013). Application of hybrid micro-cogeneration system—Thermal and power energy solutions for Canadian residences. *Energy and Buildings, 60*, 345-354.

Eveloy, V., Rodgers, P., & Al Alili, A. (2017). Multi-objective optimization of a pressurized solid oxide fuel cell – gas turbine hybrid system integrated with seawater reverse osmosis. *Energy, 123*, 594-614.

Evins, R. (2015). Multi-level optimization of building design, energy system sizing and operation. *Energy, 90*, 1775-1789.

Facci, A.L., Cigolotti, V., Jannelli, E., & Ubertini, S. (2016). Technical and economic assessment of a SOFC-based energy system for combined cooling, heating and power. *Applied Energy*.

Facci, A.L., & Ubertini, S. (2018). Analysis of a fuel cell combined heat and power plant under realistic smart management scenarios. *Applied Energy, 216*, 60-72.

Fernandes, A., Woudstra, T., van Wijk, A., Verhoef, L., & Aravind, P.V. (2016). Fuel cell electric vehicle as a power plant and SOFC as a natural gas reformer: An exergy analysis of different system designs. *Applied Energy, 173*, 13-28.

Firozbakht, N., Ahmadi, A., & Mahmoudpour, E. (2016). *Optimization of capacity and operation for CCHP system by PSO algorithm*. Paper presented at the International conference of Innovation in Science & Technology, Barcelona, Spain.

Franco, A., & Versace, M. (2017). Multi-objective optimization for the maximization of the operating share of cogeneration system in District Heating Network. *Energy Conversion and Management, 139*, 33-44.

Gebregergis, A., Pillay, P., Bhattacharyya, D., & Rengaswemy, R. (2009). Solid Oxide Fuel Cell Modeling *Ieee Transactions on Industrial Electronics, 56*(1), 139-148.

Ghaem Sigarchian, S., Malmquist, A., & Martin, V. (2018). The choice of operating strategy for a complex polygeneration system: A case study for a residential building in Italy. *Energy Conversion and Management, 163*, 278-291.

Gimelli, A., Muccillo, M., & Sannino, R. (2017). Optimal design of modular cogeneration plants for hospital facilities and robustness evaluation of the results. *Energy Conversion and Management, 134*, 20-31.

Gładysz, P., & Ziębik, A. (2013). Complex analysis of the optimal coefficient of the share of cogeneration in district heating systems. *Energy, 62*, 12-22.

Granovskii, M., Dincer, I., & Rosen, M.A. (2006). Economic and environmental comparison of conventional, hybrid, electric and hydrogen fuel cell vehicles. *Journal of Power Sources, 159*(2), 1186-1193.

Guo, L., Liu, W., Cai, J., Hong, B., & Wang, C. (2013). A two-stage optimal planning and design method for combined cooling, heat and power microgrid system. *Energy Conversion and Management, 74*, 433-445.

Hajabdollahi, Z., & Fu, P.-F. (2017). Multi-objective based configuration optimization of SOFC-GT cogeneration plant. *Applied Thermal Engineering, 112*, 549-559.

Hawkes, A., & Leach, M. (2007). Cost-effective operating strategy for residential micro-combined heat and power. *Energy, 32*(5), 711-723.

Hawkes, A.D., Aguiar, P., Croxford, B., Leach, M.A., Adjiman, C.S., & Brandon, N.P. (2007). Solid oxide fuel cell micro combined heat and power system operating strategy: Options for provision of residential space and water heating. *Journal of Power Sources, 164*(1), 260-271.

Hiroaki, K.T., T. Toshiya, B. Ayshah, Z. Naoto, K. Yoshitaka, I. . (2013). *Energetic Analysis of SOFC Co-generation System Integrating with Charging Stand for Electric Vehicle*. Paper presented at the PowerTech (POWERTECH), 2013 IEEE Grenoble

http://www.gasmalaysia.com/index.php/our-services/at-your-service/bills-payments/tariff-rates. (2017).

Huicochea, A., Rivera, W., Gutiérrez-Urueta, G., Bruno, J.C., & Coronas, A. (2011). Thermodynamic analysis of a trigeneration system consisting of a micro gas turbine and a double effect absorption chiller. *Applied Thermal Engineering, 31*(16), 3347-3353.

Hussain, A., Bui, V.-H., Kim, H.-M., Im, Y.-H., & Lee, J.-Y. (2017). Optimal Energy Management of Combined Cooling, Heat and Power in Different Demand Type Buildings Considering Seasonal Demand Variations. *Energies, 10*(6), 789.

ICF International Company. (2008). *Technology Characterization: Steam Turbines*. Retrieved from

Im-orb, K., Visitdumrongkul, N., Saebea, D., Patcharavorachot, Y., & Arpornwichanop, A. (2018). Flowsheet-based model and exergy analysis of solid oxide electrolysis cells for clean hydrogen production. *Journal of Cleaner Production, 170*, 1-13.

International Energy Agency, I. (2011). *Energy-efficient Buildings: Heating and Cooling Equipment*. Retrieved from France:

International Renewable Energy Agency, I. (2018). *Renewable energy market analysis: Southeast Asia*. Retrieved from

Irvine, J.T.S., & Connor, P. (2012). *Solid Oxide Fuels Cells: Facts and Figures: Past Present and Future Perspectives for SOFC Technologies*: Springer London.

Isa, N.M., Das, H.S., Tan, C.W., Yatim, A.H.M., & Lau, K.Y. (2016). A techno-economic assessment of a combined heat and power photovoltaic/fuel cell/battery energy system in Malaysia hospital. *Energy, 112*, 75-90.

Isa, Z.M., & Rahim, N.A. (2013, 2013). *PEM fuel cell model parameters optimization using modified particle swarm optimization algorithm.* Paper presented at the IEEE Conference on Clean Energy and Technology (CEAT).

Islam, S., Dincer, I., & Yilbas, B.S. (2017). Analysis and Assessment of A Biomass Energy-Based Multigeneration System with Thermoelectric Generators. *Energy & Fuels, 31*(10), 10901-10915.

Islam, S., Dincer, I., & Yilbas, B.S. (2018). Development, analysis and assessment of solar energy-based multigeneration system with thermoelectric generator. *Energy Conversion and Management, 156*, 746-756.

Jabari, F., Nojavan, S., Mohammadi Ivatloo, B., & Sharifian, M.B.B. (2016). Optimal short-term scheduling of a novel tri-generation system in the presence of demand response programs and battery storage system. *Energy Conversion and Management, 122*, 95-108.

Jana, K., Ray, A., Majoumerd, M.M., Assadi, M., & De, S. (2017). Polygeneration as a future sustainable energy solution – A comprehensive review. *Applied Energy, 202*, 88-111.

Jens Palsson, A.S., Lars Sjunnesson. (2000). Combined solid oxide fuel cell and gas turbine systems for efficient. *Journal of Power Sources, 86*, 442-448.

Jiang, X.Z., Zeng, G., Li, M., & Shi, L. (2016). Evaluation of combined cooling, heating and power (CCHP) systems with energy storage units at different locations. *Applied Thermal Engineering, 95*, 204-210.

Jing, R., Wang, M., Brandon, N., & Zhao, Y. (2017). Multi-criteria evaluation of solid oxide fuel cell based combined cooling heating and power (SOFC-CCHP) applications for public buildings in China. *Energy*.

Jradi, M., & Riffat, S. (2014). Tri-generation systems: Energy policies, prime movers, cooling technologies, configurations and operation strategies. *Renewable and Sustainable Energy Reviews, 32*, 396-415.

Kavvadias, K.C., & Maroulis, Z.B. (2010). Multi-objective optimization of a trigeneration plant. *Energy Policy, 38*(2), 945-954.

Kavvadias, K.C., Tosios, A.P., & Maroulis, Z.B. (2010). Design of a combined heating, cooling and power system: Sizing, operation strategy selection and parametric analysis. *Energy Conversion and Management, 51*(4), 833-845.

Kazempoor, P., Dorer, V., & Weber, A. (2011). Modelling and evaluation of building integrated SOFC systems. *International Journal of Hydrogen Energy, 36*(20), 13241-13249.

Khatib, T., Mohamed, A., Mahmoud, M., & Sopian, K. (2011). Modeling of Daily Solar Energy on a Horizontal Surface for Five Main Sites in Malaysia. *International Journal of Green Energy, 8*(8), 795-819.

Koh, S.L. (2015). Viability of Distributed Generation in Single Family Houses Using Solid Oxide Fuel Cells in Tropical Climate. *Journal of Clean Energy Technologies, 3*(5), 345-350.

Kubota, T., Jeong, S., & Toe, D.H.C. (2011). Energy Consumption and Air-Conditioning Usage in Residential Buildings of Malaysia (Renewable Energy). *国際協力研究誌, 17*(3), 61-69.

Kyriakarakos, G., & Papadakis, G. (2015). Polygeneration Microgrids for Residential Applications. 1-12.

Lakshmi, T.V.V.S., Geethanjali, P., & Krishna, P.S. (2013). *Mathematical modelling of solid oxide fuel cell using Matlab/Simulink.* Paper presented at the International Conference on Microelectronics, Communication and Renewable Energy (ICMiCR-2013).

Lansing, F.L. (1976). *Computer modeling of a single-stage lithium bromide/water absorption refrigeration unit*. Retrieved from Pasadena, CA:

Li, G., Zhang, R., Jiang, T., Chen, H., Bai, L., Cui, H., & Li, X. (2017a). Optimal dispatch strategy for integrated energy systems with CCHP and wind power. *Applied Energy, 192*, 408-419.

Li, L., Mu, H., Gao, W., & Li, M. (2014). Optimization and analysis of CCHP system based on energy loads coupling of residential and office buildings. *Applied Energy, 136*, 206-216.

Li, X., Ogden, J., & Yang, C. (2013). Analysis of the design and economics of molten carbonate fuel cell tri-generation systems providing heat and power for commercial buildings and H2 for FC vehicles. *Journal of Power Sources, 241*, 668-679.

Li, Y., Rezgui, Y., & Zhu, H. (2017b). District heating and cooling optimization and enhancement – Towards integration of renewables, storage and smart grid. *Renewable and Sustainable Energy Reviews, 72*, 281-294.

Li, Y., Wu, Q., & Zhu, H. (2015). Hierarchical Load Tracking Control of a Grid-Connected Solid Oxide Fuel Cell for Maximum Electrical Efficiency Operation. *Energies, 8*(3), 1896-1916.

Linde, L. (2016). *Implementation of BECCS in a polygeneration system - A techno-economic feasibility study in the district heating network of Stockholm.* (Master of Science), KTH Industrial Engineering and Management,

Liso, V., Zhao, Y., Yang, W., & Nielsen, M. (2015). Modelling of a Solid Oxide Fuel Cell CHP System Coupled with a Hot Water Storage Tank for a Single Household. *Energies, 8*(3), 2211-2229.

Liu, M., Shi, Y., & Fang, F. (2014). Combined cooling, heating and power systems: A survey. *Renewable and Sustainable Energy Reviews, 35*, 1-22.

Liu, Y., & Leong, K.C. (2006). Numerical study of an internal-reforming solid oxide fuel cell and adsorption chiller co-generation system. *Journal of Power Sources, 159*(1), 501-508.

Luo, X.J., & Fong, K.F. (2017). Control Optimization of Combined Cooling and Power System with Prime Mover of Solid Oxide Fuel Cell-gas Turbine for Building Application. *Energy Procedia, 105*, 1883-1888.

Madina, C., Zamora, I., & Zabala, E. (2016). Methodology for assessing electric vehicle charging infrastructure business models. *Energy Policy, 89*, 284-293.

Mago, P.J., Chamra, L.M., & Ramsay, J. (2010). Micro-combined cooling, heating and power systems hybrid electric-thermal load following operation. *Applied Thermal Engineering, 30*(8-9), 800-806.

Mago, P.J., Fumo, N., & Chamra, L.M. (2009). Performance analysis of CCHP and CHP systems operating following the thermal and electric load. *International Journal of Energy Research, 33*(9), 852-864.

Mahlia, T.M.I., & Chan, P.L. (2011). Life cycle cost analysis of fuel cell based cogeneration system for residential application in Malaysia. *Renewable and Sustainable Energy Reviews, 15*(1), 416-426.

Mahlia, T.M.I., Saktisahdan, T.J., Jannifar, A., Hasan, M.H., & Matseelar, H.S.C. (2014). A review of available methods and development on energy storage; technology update. *Renewable and Sustainable Energy Reviews, 33*, 532-545.

Malico, I., Carvalhinho, A.P., & Tenreiro, J. (2009). Design of a trigeneration system using a high‐temperature fuel cell. *International Journal of Energy Research, 33*(2), 144-151.

Martínez-Lera, S., & Ballester, J. (2010). A novel method for the design of CHCP (combined heat, cooling and power) systems for buildings. *Energy, 35*(7), 2972-2984.

Martínez-Lera, S., Ballester, J., & Martínez-Lera, J. (2013). Analysis and sizing of thermal energy storage in combined heating, cooling and power plants for buildings. *Applied Energy, 106*, 127-142.

Martínez-Soto, R., Castillo, O., & Aguilar, L.T. (2014). Type-1 and Type-2 fuzzy logic controller design using a Hybrid PSO–GA optimization method. *Information Sciences, 285*, 35-49.

McPhail, S.J., Kiviaho, J., & Conti, B. (2017). *The yellow pages of sofc technology 2017*. Retrieved from

MIDF, M. (2016). *Gas Malaysia Berhad: IBR for period 2017 to 2019*. MIDF Amanah Investment Bank Berhad

Ministry of Energy Green Technology and Water. (2015). *Power Policy & National Development Plan*.

Misra, S., Satyaprasad, G., Mahapatra, S.S., Mohanty, A., Biswal, S.R., & Dora, A. (2016). Design of Fuel cell based Co-generation systems: An approach for battery less Solar PV system.

Mohamad, H., Abu Bakar, A.H., Ping, H.W., & Mokhlis, H. (2010). An adaptive controller of hydro generators for smart grid application in Malaysia. *2010 International Conference on Power System Technology*, 1-6.

Moradi, M., & Mehrpooya, M. (2017). Optimal design and economic analysis of a hybrid solid oxide fuel cell and parabolic solar dish collector, combined cooling, heating and power (CCHP) system used for a large commercial tower. *Energy, 130*, 530-543.

Najafi, B., Shirazi, A., Aminyavari, M., Rinaldi, F., & Taylor, R.A. (2014). Exergetic, economic and environmental analyses and multi-objective optimization of an SOFC-gas turbine hybrid cycle coupled with an MSF desalination system. *Desalination, 334*(1), 46-59.

Nansaia, K., Tohnob, S., Konoc, M., & Kasaharab, M. (2002). Effects of electric vehicles (EV) on environmental loads with consideration of regional differences of electric power generation and charging characteristic of EV users in Japan. *Applied Energy, 71*, 111-125.

Napoli, R., Gandiglio, M., Lanzini, A., & Santarelli, M. (2015). Techno-economic analysis of PEMFC and SOFC micro-CHP fuel cell systems for the residential sector. *Energy and Buildings, 103*, 131-146.

Nataf, K., & Bradley, T.H. (2016). An economic comparison of battery energy storage to conventional energy efficiency technologies in Colorado manufacturing facilities. *Applied Energy, 164*, 133-139.

Nava, H., Padilla, J., Chimn, D., Aguilar, M.A., Green, P., Shawaludin, F., . . . Castro, C. (2011). *Hydrogen home fueling station*. Lons angeles.

New Mexico Environment Department. (2011). *Air-water temperature correlation*. Retrieved from

NewEnCo. (2017). Organic rankine cycle systems convert thermal energy to electrical energy. Retrieved from http://www.newenco.co.uk/organic-rankine-cycle/what-is-the-organic-rankine-cycle

Nistor, S., Dave, S., Fan, Z., & Sooriyabandara, M. (2016). Technical and economic analysis of hydrogen refuelling. *Applied Energy, 167*, 211-220.

Oland, C.e.a. (2002). *Guide to low-emission boiler and combustion equipment selection*. Retrieved from

Oland, C.e.a. (2004). *Guide to combined heat and power systems for boiler owners and operators*. Retrieved from

Ondeck, A.D., Edgar, T.F., & Baldea, M. (2015). Optimal operation of a residential district-level combined photovoltaic/natural gas power and cooling system. *Applied Energy, 156*, 593-606.

Ould Bilal, B., Sambou, V., Ndiaye, P.a., Kébé, C.M.F., & Ndongo, M. (2010). Optimal design of a hybrid solar–wind-battery system using the minimization of the annualized cost system and the minimization of the loss of power supply probability (LPSP). *Renewable Energy, 35*(10), 2388-2390.

Ozlu, S. (2015). *Development and analysis of solar energy based multigeneration systems.* (Doctor of Philosophy), University of Ontario Institute of Technology (UOIT), Oshawa, Ontario, Canada.

Palmero-Marrero, A.I., & Oliveira, A.C. (2011). Performance simulation of a solar-assisted micro-tri-generation system: hotel case study. *International Journal of Low-Carbon Technologies, 6*(4), 309-317.

Perdikaris, N., Panopoulos, K.D., Hofmann, P., Spyrakis, S., & Kakaras, E. (2010). Design and exergetic analysis of a novel carbon free tri-generation system for hydrogen, power and heat production from natural gas, based on combined solid oxide fuel and electrolyser cells. *International Journal of Hydrogen Energy, 35*(6), 2446-2456.

Petrucci, L.B., C. Francois, B., & Di Felice, P. (2009). *Hybrid trigeneration system management with a double DC-bus configuration on the electrical side*. Paper presented at the Advanced Electromechanical Motion Systems & Electric Drives Joint Symposium, 2009. ELECTROMOTION 2009. 8th International Symposium on.

Pino, F.J., Valverde, L., & Rosa, F. (2011). Influence of wind turbine power curve and electrolyzer operating temperature on hydrogen production in wind–hydrogen systems. *Journal of Power Sources, 196*(9), 4418-4426.

Pohl, E., & Diarra, D. (2014). A method to determine primary energy savings of CHP plants considering plant-side and demand-side characteristics. *Applied Energy, 113*, 287-293.

Pohl, E., Meier, P., Maximini, M., & Schloß, J.v. (2016). Primary energy savings of a modular combined heat and power plant based on high temperature proton exchange membrane fuel cells. *Applied Thermal Engineering, 104*, 54-63.

Ponniran, A., Sulaiman, E., Jumaat, S.A., Ishak, M., Chulan, M.A., & Saiman, S. (2007). *A study on electric energy usage at the residential area.* Paper presented at the 1st Engineering Conference on Energy & Environment.

Ramadhani, F., Bakar, K.A., Hussain, M.A., Erixno, O., & Nazir, R. (2017). Optimization with traffic-based control for designing standalone streetlight system: A case study. *Renewable Energy, 105*, 149-159.

Ramadhani, F., Bakar, K.A., & Shafer, M.G. (2013, 2013). *Optimization of standalone street light system with consideration of lighting control.* Paper presented at the

Technological Advances in Electrical, Electronics and Computer Engineering (TAEECE), 2013 International Conference on.

Ramadhani, F., Hussain, M.A., Mokhlis, H., Fazly, M., & Ali, J.M. (2019). Evaluation of solid oxide fuel cell based polygeneration system in residential areas integrating with electric charging and hydrogen fueling stations for vehicles. *Applied Energy, 238*, 1373-1388.

Riensche, E., Stimming, U., & Unverzagt, G. (1998). Optimization of a 200 kW SOFC cogeneration power plant Part I: Variation of process parameters. *Journal of Power Sources, 73*, 251-256.

Rokni, M. (2018). Analysis of a polygeneration plant based on solar energy, dual mode solid oxide cells and desalination. *International Journal of Hydrogen Energy*.

Rosato, A., Sibilio, S., Ciampi, G., Entchev, E., & Ribberink, H. (2017). Energy, Environmental and Economic Effects of Electric Vehicle Charging on the Performance of a Residential Building-integrated Micro-trigeneration System. *Energy Procedia, 111*, 699-709.

Rosendahl, L.A., Mortensen, P.V., & Enkeshafi, A.A. (2011). Hybrid Solid Oxide Fuel Cell and Thermoelectric Generator for Maximum Power Output in Micro-CHP Systems. *Journal of Electronic Materials, 40*(5), 1111-1114.

Roshandel, R., Golzar, F., & Astaneh, M. (2018). Technical, economic and environmental optimization of combined heat and power systems based on solid oxide fuel cell for a greenhouse case study. *Energy Conversion and Management, 164*, 144-156.

Sadeghi, M., Chitsaz, A., Mahmoudi, S.M.S., & Rosen, M.A. (2015). Thermoeconomic optimization using an evolutionary algorithm of a trigeneration system driven by a solid oxide fuel cell. *Energy, 89*, 191-204.

Saidur, R., Masjuki, H.H., Jamaluddin, M.Y., & Yap, F.C. (2006). Actual Usage Conditions, Energy Savings and Associated Emission Reductions of Washing Machines. *HKIE Transactions, 13*(2), 16-23.

Santo, D.B.d.E. (2014). An energy and exergy analysis of a high-efficiency engine trigeneration system for a hospital: A case study methodology based on annual energy demand profiles. *Energy and Buildings, 76*, 185-198.

Saur, G., & Ramsden, T. (2011). *Wind Electrolysis: Hydrogen Cost Optimization*. Retrieved from

Seyezhai, R., & Mathur, B.L. (2012). Design and implementation of interleaved boost converter for fuel cell systems. *International Journal of Hydrogen Energy, 37*(4), 3897-3903.

Shaneb, O.A., Taylor, P.C., & Coates, G. (2012). Real time operation of μCHP systems using fuzzy logic. *Energy and Buildings, 55*, 141-150.

Shariatzadeh, J.O., Refahi, A.H., Abolhassani, S.S., & Rahmani, M. (2015). Modeling and optimization of a novel solar chimney cogeneration power plant combined with solid oxide electrolysis/fuel cell. *Energy Conversion and Management, 105*, 423-432.

Sharma, S., & Ghoshal, S.K. (2015). Hydrogen the future transportation fuel: From production to applications. *Renewable and Sustainable Energy Reviews, 43*, 1151-1158.

Sibilio, S., Rosato, A., Ciampi, G., Scorpio, M., & Akisawa, A. (2017). Building-integrated trigeneration system: Energy, environmental and economic dynamic performance assessment for Italian residential applications. *Renewable and Sustainable Energy Reviews, 68*, 920-933.

Sigurjonsson, H.Æ., & Clausen, L.R. (2018). Solution for the future smart energy system: A polygeneration plant based on reversible solid oxide cells and biomass gasification producing either electrofuel or power. *Applied Energy, 216*, 323-337.

Singhal, S.C., Dokiya, M., Division, E.S.H.T.M., Division, E.S.B., Division, E.S.E.T., & Japan, S.S.o. (2003). *Solid Oxide Fuel Cells VIII: (SOFC VIII) : Proceedings of the International Symposium*: Electrochemical Society.

Singhal, S.C., Dokiya, M., Division, E.S.H.T.M., Division, E.S.B., & Japan, S.S.o. (1999). *Solid Oxide Fuel Cells (SOFC VI): Proceedings of the Sixth International Symposium*: Electrochemical Society.

Siyal, S.H., Mentis, D., & Howells, M. (2015). Economic analysis of standalone wind-powered hydrogen refueling stations for road transport at selected sites in Sweden. *International Journal of Hydrogen Energy, 40*(32), 9855-9865.

Smith, A., Luck, R., & Mago, P.J. (2010). Analysis of a combined cooling, heating, and power system model under different operating strategies with input and model data uncertainty. *Energy and Buildings, 42*(11), 2231-2240.

Soheyli, S., Shafiei Mayam, M.H., & Mehrjoo, M. (2016). Modeling a novel CCHP system including solar and wind renewable energy resources and sizing by a CC-MOPSO algorithm. *Applied Energy, 184*, 375-395.

Sonar, D., Soni, S.L., & Sharma, D. (2014). Micro-trigeneration for energy sustainability: Technologies, tools and trends. *Applied Thermal Engineering, 71*(2), 790-796.

Stojic, D., Marceta, M., Sovilj, S., & Miljanic, S. (2003). Hydrogen generation fromwater electrolysis—possibilities of energy saving. *Journal of Power Sources, 118*, 315.

Stojiljković, M., Stojiljković, M., & Blagojević, B. (2014). Multi-Objective Combinatorial Optimization of Trigeneration Plants Based on Metaheuristics. *Energies, 7*(12), 8554-8581.

Stojiljković, M.M. (2017). Bi-level multi-objective fuzzy design optimization of energy supply systems aided by problem-specific heuristics. *Energy*.

Sullivan, J.L., Baker, R.E., Boyer, B.A., Hammerle, R.H., Kenney, T.E., Muniz, L., & Wallington, T.J. (2004). CO2 emission benefit of diesel (versus gasoline) powered vehicles. *Environmental Science & Technology, 38*(12), 3217-3223.

Suruhanjaya Tenaga, e.c. (2016). *National energy balance 2016*. Retrieved from Malaysia:

Szega, M., & Zymelka, P. (2017). Thermodynamic and Economic Analysis of the Production of Electricity, Heat And Cold in the CHP Unit with the Absorption Chillers. *Journal of Energy Resources Technology*.

Tafreshi, S.M.M., & S.M.Hakimi. (2007). *Optimal sizing of a stand alone hybrid power system via particle swarm optimization (PSO)*. Paper presented at the International Power Engineering Conference (IPEC 2007).

Taghavifar, H., Anvari, S., Saray, R.K., Khalilarya, S., Jafarmadar, S., & Taghavifar, H. (2015). Towards modeling of combined cooling, heating and power system with artificial neural network for exergy destruction and exergy efficiency prognostication of tri-generation components. *Applied Thermal Engineering, 89*, 156-168.

Takama, N., & Loucks, D.P. (1981). Multi-level optimization for multi-objective problems. *Applied Mathematical Modelling, 5*(3), 173-178.

Takeshita, K., Amano, Y., & Hashizume, T. (2005). Experimental study of advanced cogeneration system with ammonia–water mixture cycles at bottoming. *Energy, 30*(2–4), 247-260.

Tanaka, T., Kamiko, H., Bando, T., Zaffirah, A., Kakimoto, N., Inui, Y., & Maeda, T. (2014). Energetic analysis of SOFC co-generation system integrated with EV charging station installed in multifamily apartment. *International Journal of Hydrogen Energy, 39*(10), 5097-5104.

Tang, C., & Chin, N. (2013). Building energy efficiency technical guideline for passive design. *Public Works Department Malaysia, Kuala Lumpur*.

Terayama, T., Nagata, S., Tanaka, K., Momma, A., Kato, T., & Yamamoto, A. (2013a). Improvement of SOFC System Efficiency by Incorporating Thermoelectric Power Generation Heat Exchanger. *ECS Transactions, 57*(1), 2627-2636.

Terayama, T., Nagata, S., Tanaka, Y., Momma, A., Kato, T., Kunii, M., & Yamamoto, A. (2013b). Numerical simulation for thermoelectric generator with optimized design for compact SOFC co-generation system. *Trans. Mat. Res. Soc. Japan, 38*(4), 659-662.

Terayama, T., Nagata, S., Tanaka, Y., Momma, A., Kato, T., Kunii, M., & Yamamoto, A. (2013c). Studies on Effective Utilization of SOFC Exhaust Heat Using Thermoelectric Power Generation Technology. *Journal of Electronic Materials, 42*(7), 2306-2313.

Tie, C.H., Gan, C.K., & Ibrahim, K.A. (2014). *The impact of electric vehicle charging on a residential low voltage distribution network in Malaysia.* Paper presented at the Innovative Smart Grid Technologies-Asia (ISGT Asia), 2014 IEEE.

TNB, M. (2016). Tariff Rates of domestic consumer in Malaysia. Retrieved from https://www.tnb.com.my/residential/pricing-tariffs

Tonekabonimoghadam, S., Akikur, R.K., Hussain, M.A., Hajimolana, S., Saidur, R., Ping, H.W., . . . Hashim, M.A. (2015). Mathematical modelling and experimental validation of an anode-supported tubular solid oxide fuel cell for heat and power generation. *Energy, 90*, 1759-1768.

Udomsri, S., Bales, C., Martin, A.R., & Martin, V. (2012). Decentralized cooling in district heating network: System simulation and parametric study. *Applied Energy, 92*, 175-184.

Ullah, K.R., Akikur, R.K., Ping, H.W., Saidur, R., Hajimolana, S.A., & Hussain, M.A. (2015). An experimental investigation on a single tubular SOFC for renewable energy based cogeneration system. *Energy Conversion and Management, 94*, 139-149.

Ullvius, N.C., & Rokni, M. (2018). A study on a polygeneration plant based on solar power and solid oxide cells. *International Journal of Hydrogen Energy*.

US DOE Energy Efficiency and Renewable Energy, E. (2007).

Verrilli, F., Parisio, A., & Glielmo, L. (2016). *Stochastic model predictive control for optimal energy management of district heating power plants*. Paper presented at the Decision and Control (CDC), 2016 IEEE 55th Conference on.

Vialetto, G., Noro, M., & Rokni, M. (2017). Combined micro-cogeneration and electric vehicle system for household application: An energy and economic analysis in a Northern European climate. *International Journal of Hydrogen Energy*.

Vigneysh, T., & Kumarappan, N. (2016). Autonomous operation and control of photovoltaic/solid oxide fuel cell/battery energy storage based microgrid using fuzzy logic controller. *International Journal of Hydrogen Energy, 41*(3), 1877-1891.

Vögelin, P., Koch, B., Georges, G., & Boulouchos, K. (2017). Heuristic approach for the economic optimisation of combined heat and power (CHP) plants: Operating strategy, heat storage and power. *Energy, 121*, 66-77.

Wakui, T., Kawayoshi, H., & Yokoyama, R. (2016). Optimal structural design of residential power and heat supply devices in consideration of operational and capital recovery constraints. *Applied Energy, 163*, 118-133.

Wakui, T., Sawada, K., Kawayoshi, H., Yokoyama, R., Iitaka, H., & Aki, H. (2017). Optimal operations management of residential energy supply networks with power and heat interchanges. *Energy and Buildings, 151*, 167-186.

Wakui, T., Wada, N., & Yokoyama, R. (2012). Feasibility study on combined use of residential SOFC cogeneration system and plug-in hybrid electric vehicle from energy-saving viewpoint. *Energy Conversion and Management, 60*, 170-179.

Wakui, T., & Yokoyama, R. (2012). Optimal sizing of residential SOFC cogeneration system for power interchange operation in housing complex from energy-saving viewpoint. *Energy, 41*(1), 65-74.

Wakui, T., & Yokoyama, R. (2015). Optimal structural design of residential cogeneration systems with battery based on improved solution method for mixed-integer linear programming. *Energy, 84*, 106-120.

Wang, J.-J., Jing, Y.-Y., & Zhang, C.-F. (2010a). Optimization of capacity and operation for CCHP system by genetic algorithm. *Applied Energy, 87*(4), 1325-1335.

Wang, J., Yang, Y., Mao, T., Sui, J., & Jin, H. (2015a). Life cycle assessment (LCA) optimization of solar-assisted hybrid CCHP system. *Applied Energy, 146*, 38-52.

Wang, J., Zhai, Z., Jing, Y., & Zhang, C. (2010b). Optimization design of BCHP system to maximize to save energy and reduce environmental impact. *Energy, 35*(8), 3388-3398.

Wang, J., Zhai, Z., Jing, Y., & Zhang, C. (2010c). Particle swarm optimization for redundant building cooling heating and power system. *Applied Energy, 87*(12), 3668-3679.

Wang, M., Wang, J., Zhao, P., & Dai, Y. (2015b). Multi-objective optimization of a combined cooling, heating and power system driven by solar energy. *Energy Conversion and Management, 89*, 289-297.

Weber, C., Koyama, M., & Kraines, S. (2006a). CO2-emissions reduction potential and costs of a decentralized energy system for providing electricity, cooling and heating in an office-building in Tokyo. *Energy, 31*(14), 3041-3061.

Weber, C., Maréchal, F., Favrat, D., & Kraines, S. (2006b). Optimization of an SOFC-based decentralized polygeneration system for providing energy services in an office-building in Tōkyō. *Applied Thermal Engineering, 26*(13), 1409-1419.

Williams, M.C., & Strakey, J.P. (2003). *U.S. DOE Office of fossil energy's solid oxide fuel cell programs*.

Windeknecht, M., & Tzscheutschler, P. (2015). Optimization of the Heat Output of High Temperature Fuel Cell Micro-CHP in Single Family Homes. *Energy Procedia, 78*, 2160-2165.

Yang, Z., Liao, T., & Lin, B. (2014). The optimal performance of solid oxide fuel cell-thermoelectric generator hybrid system. *Scientia Sinica Physica, Mechanica & Astronomica, 44*(6), 569.

Yao, E., Wang, H., Wang, L., Xi, G., & Maréchal, F. (2017). Multi-objective optimization and exergoeconomic analysis of a combined cooling, heating and power based compressed air energy storage system. *Energy Conversion and Management, 138*, 199-209.

Yin, J., Yu, Z., Zhang, C., Tian, M., & Han, J. (2018). Thermodynamic analysis and multi-objective optimization of a novel power/cooling cogeneration system for low-grade heat sources. *Energy Conversion and Management, 166*, 64-73.

Zaid, S.M., Myeda, N.E., Mahyuddin, N., & Sulaiman, R. (2013). *The Need for Energy Efficiency Legislation in the Malaysian Building Sector*. Paper presented at the The 3rd International Building Control Conference.

Zhang, H., Kong, W., Dong, F., Xu, H., Chen, B., & Ni, M. (2017a). Application of cascading thermoelectric generator and cooler for waste heat recovery from solid oxide fuel cells. *Energy Conversion and Management, 148*, 1382-1390.

Zhang, H., Xu, H., Chen, B., Dong, F., & Ni, M. (2017b). Two-stage thermoelectric generators for waste heat recovery from solid oxide fuel cells. *Energy, 132*, 280-288.

Zhang, J., & Yamanis, J. (2007). *Techno-Economic Feasibility of Highly Efficient Cost-Effective Thermoelectric-SOFC Hybrid Power Generation Systems*. Retrieved from

Zhang, N., & Cai, R. (2002). Analytical solutions and typical characteristics of part-load performances of single shaft gas turbine and its cogeneration. *Energy Conversion and Management, 43*(9–12), 1323-1337.

Zhao, H., Jiang, T., & Hou, H. (2015). Performance analysis of the SOFC–CCHP system based on H2O/Li–Br absorption refrigeration cycle fueled by coke oven gas. *Energy, 91*, 983-993.

Zheng, C.Y., Wu, J.Y., & Zhai, X.Q. (2014). A novel operation strategy for CCHP systems based on minimum distance. *Applied Energy, 128*, 325-335.

Zhongshi, L., Wei, Z., & Hongxing, Y. (2009). One Novel Optimum Sizing Method for Solar Lighting System by Using Genetic Algorithm. *2009 International Conference on Energy and Environment Technology*, 225-228.

LIST OF PUBLICATIONS AND PAPERS PRESENTED

Ramadhani, F., et al. (2017). "Optimization strategies for Solid Oxide Fuel Cell (SOFC) application: A literature survey." Renewable and Sustainable Energy Reviews 76: 460-484. (Q1)

Ramadhani, F., et al. (2019). “Evaluation of solid oxide fuel cell based polygeneration system in residential with electric/hydrogen vehicle charging/fueling station”. Applied Energy, Elsevier (Q1).

Ramadhani, F., et al. (2018). “Modeling and Parameter Analysis of Solid Oxide Fuel Cell (SOFC) for power and heat generation based on Different Fuel Operating”. *In review, submitted to Journal of Renewable and Sustainable Energy - AIP (Q3).*

Ramadhani, F., et al. (2019). “A techno-economic-environmental assessment of polygeneration systems with vehicles energy supply in the residential application”. *In review, submitted to Renewable Energy, Elsevier (Q1).*

Ramadhani, F., et al. (2019). “Fuzzy-based optimal energy management strategy for solid oxide fuel cell combined with photovoltaic thermal and thermoelectric generators in a polygeneration system with electric and hydrogen vehicles station supply”. *In second review, submitted to Energy, Elsevier (Q1).*